DYNAMIC ANALYSIS
OF SINGLE SPAN CABLES

by

Antoine Bliek

Burgerlijk Ingenieur
K.U.L. Belgium (1979)
S.M. in Nav. Arch. and Mar. Eng.
S.M. in Ocean Engineering
M.I.T. (1982)

SUBMITTED TO THE DEPARTMENT OF OCEAN ENGINEERING IN PARTIAL FULFILLMENT OF THE REQUIREMENTS FOR THE DEGREE OF

DOCTOR OF PHILOSOPHY

at the

MASSACHUSETTS INSTITUTE OF TECHNOLOGY

July 1984

Signature of Author _____
Department of Ocean Engineering
July 12, 1984

Certified by _____
Michael S. Triantafyllou
Thesis Supervisor

Accepted by _____
A. Douglas Carmichael
Chairman, Department Committee

DYNAMIC ANALYSIS OF SINGLE SPAN CABLES

by

Antoine Bliek

Submitted to the Department of Ocean Engineering on July 12, 1984 in partial fulfillment of the requirements for the degree of Doctor of Philosophy.

Abstract

The linear and non-linear dynamics of single span cables are studied in this thesis. First, the equations of motion and the compatibility relations for a three-dimensional single span cable are derived in vectorial form. The two-dimensional equations are obtained from the general equations as a special case. For small motions, the linearized three-dimensional equations of motion are formulated.

Subsequently, new perturbation solutions are derived for both inextensible and extensible linear, two-dimensional cable dynamics. The perturbation solutions contribute significantly to a better understanding of the effect of the principal cable parameters on the linear dynamics. The solutions are compared with previously obtained approximations and numerical results, and it is found that they can predict very accurately the linear dynamic behavior of a cable. The orthogonality of the modes for the extensible and inextensible cases is also discussed.

Finally, the effect of non-linearities is studied, which are known to play a significant role in the dynamic behavior of a marine cable. The use of modal expansions for a non-linear analysis is first illustrated by studying the non-linear string, for which known analytic solutions exist. In the more general case of a cable with sag, the modal expansions lead to a new method for the time simulation of dynamic mooring problems. The numerical scheme is very compact and is used extensively to identify the effect of the various non-linearities involved. Both the linear and non-linear theories are illustrated by a number of applications, including comparisons with experimental data.

Acknowledgments

I would like to express my special appreciation to Professor Michael S. Triantafyllou, my thesis supervisor. His in-depth knowledge, enthusiasm and patience were very inspiring. I also thank the other members of my thesis committee; Professor M.A. Abkowitz, Professor J.K. Vandiver and Professor D.K. Yue. Their comments and advice were greatly appreciated.

I wish to express my gratitude to the Belgian American Educational Foundation, which supported my first year at M.I.T. Without the encouragements of my parents this thesis would never have seen its completion. Finally I want to thank my friends Henk, Karl and Michiko for their help and social support during the moments of the hardship.

Table of Contents

List of Figures

List of Tables

Nomenclature

A_o	Area of the cable in unstretched condition
C_{Dt}	Tangential drag coefficient
C_{Dn}	Normal drag coefficient
C_i	Modal generalized displacement
D_o	Diameter of the cable in unstretched condition
D_w	Waterdepth
E	Young's modulus
F	Force per unit length
H	Horizontal Tension
H_*	Horizontal Tension projected on the chord ($H/\cos\phi_a$)
[H(s,r)]	Matrix influence function
L	Length of the unstretched cable
M	Mass plus the added mass per unit unstretched length
Q	Quantity governing slow dynamics $Q(\sigma)=-h(\phi_{o\sigma}^2 - M\omega^2L^2/(EA))$
T	Tension
T_e	Effective tension
T_o	Effective static tension
T_1	Effective dynamic tension

U	Current velocity
S	Impedance transfer function
b	Sag of the cable
b_d	Damping constant $0.5\ \rho_w C_D D_o$
$\vec{b}$	Bi-normal vector
c_{tr}	Transverse wavespeed
c_{el}	Elastic wavespeed
c_H	Transverse wavespeed projected on the horizontal direction
e	Strain
e_o	Static strain
e_1	Dynamic strain
g	Gravity constant
h	Ratio of the mass and the mass plus the added mass
k	Wavenumber
$\vec{k}$	Vertical unit vector
l	Length of the span of the cable
m	Mass per unit unstretched length
m_a	Added mass per unit unstretched length
$\vec{n}$	Normal unit vector
p	Tangential displacement [except in chapter 1 where it is the stretched Lagrangian coordinate along the cable]

q	Normal displacement
r	Bi-normal displacement
s	Unstretched Lagrangian coordinate along the cable
t	Time
$\vec{v}$	Velocity
$\vec{v}_r$	Relative velocity in the water
w_o	Net weight per unit unstretched length
$\mathcal{A}_i$	Airy function
$\mathcal{B}_i$	Bairy function
J_o	Zeroth order Bessel function of the first kind
Y_o	Zeroth order Bessel function of the second kind
W_o	Parabolic cylinder function
$\vec{\Omega}$ $(\Omega_1,0,\Omega_3)$	Darboux vector
$\vec{\Omega}_o(\Omega_{1o},0,\Omega_{3o})$	Static component of the Darboux vector
$\vec{\Omega}_1(\Omega_{11},0,\Omega_{31})$	Dynamic component of the Darboux vector
α	Ratio of the total weight and the horizontal tension (W_oL/H) [except in chapter 2, where it is the angle between the current velocity and the (x,y) plane)
α_*	Ratio of the total weight and the projected horizontal tension (W_oL/H_*)
β	Projected elastic strain ($H_*/(EA)$)
ϵ	Small perturbation quantity

η	Non-dimensional normal displacement
θ	Euler angle around vertical axis
θ_o	Static component of θ
θ_1	Dynamic component of θ
λ	Ratio of the elastic stiffness and the catenary stiffness for horizontal cables [except in 3.6 where λ is a non-dimensional frequency parameter]
λ_*	Ratio of the elastic stiffness and the catenary stiffness for inclined cables
ξ	Non-dimensional tangential displacement
ρ	Density of the cable material [except in chapter 1 where it is the curvature]
ρ_w	Density of the water
σ	Non-dimensional unstretched length parameter
τ	Geometric stiffness parameter [except in chapter 1 where it is the torsion]
ϕ	Angle between the cable and the horizontal
ϕ_o	Static component of the ϕ
ϕ_1	Dynamic component of the ϕ
ϕ_a	Angle of the chord of the cable and the horizontal
ψ	Euler angle around the tangential direction of the cable
ψ_o	Static component of ψ

ψ_1	Dynamic component of ψ
ω	Circular frequency
$\vec{\omega}$	Rotation vector

Introduction

In recent years exploration and production of oil in deep water has become increasingly important. Semi-submersibles operating at greater depths are normally positioned with a multi-leg mooring system. The deployment and adequate control of the mooring lines is one of the most critical factors in the overall success of the operation. The challenge of production at greater depths was met with a generation of innovative platform designs. The common feature of these designs is a certain amount of compliancy, because the construction of a rigid structure proved to be too costly for deep water. Among the most well known deep water designs are the tension leg platform and the guyed tower. Here, again, the mooring system is a critical part of the design. Failure of the mooring lines can cause significant economic losses and even loss of life.

The study of the behavior of the mooring system is, therefore, an integrated part of most deep water offshore projects.

The first step in the design of a mooring system is a static analysis, where the dynamics of the line are completely ignored. The statics of the mooring lines is a well understood problem. Analytic and numerical tools, which provide reliable estimates of the static behavior of the system are available in the design process. Still, some improvement in the efficiency could be made using special purpose iteration procedures to solve multi-leg systems.

The analysis of the dynamic behavior of a mooring system is much more complex than the static analysis. The major parameters of interest in the design of a mooring system are:

- The dynamic tension response of the cable at the top point due to the motions of the offshore stucture and subsequently the effect of the forces of the mooring system on the motions of the platform.

- The accurate prediction of the motions and the dynamic tension along the mooring line. This is essential for predicting structural failure, or the fatigue life of the lines.

Since Walton and Polachek [Walton 60] studied in 1960 the transient motions of cables using a finite difference scheme, several numerical tools have been proposed to analyse the dynamic behavior of cables. The finite element method was applied to cables in the beginning of the 70's and is at present the most widely used numerical tool for dynamic analysis, besides finite difference methods. For an overview, see [Leonard 81]. Several special purpose finite element codes are commercially available.

The dynamics of cables constitute, under very weak restrictions, a hyperbolic system and can, therefore, be studied using the method of characteristics. This method is certainly better suited to analyse the phenomena of elastic waves on the cable (see [Critescu 67]), but it is not, to the author's knowledge, used to solve mooring problems. Although all of the above methods provide quantative solutions to the problem, they provide relatively little information about the effect of the parameters, which govern the dynamics of the problem.

Only recently, significant progress has been made in the understanding of the dynamic cable behavior. Simpson [Simpson 66] and Irvine and Caughey [Irvine 74] formulated analytic solutions for shallow sag cable

dynamics. Several interesting phenomena, such as the completely different behavior of extensible and inextensible cables and the cross-over of the modes could finally be explained in a consistent way.

This thesis can be divided in three major parts: the formulation of the governing equations, the analysis of linear, two-dimensional cable dynamics and the analysis of non-linear, two-dimensional cable dynamics.

In chapter 1, the complete non-linear governing equations in three dimensions are derived using vector calculus. The equations are expressed completely in the so-called natural coordinates of the cable. This has significant advantages when the dynamic properties of the cable are investigated.

The linearised dynamic equations are obtained in chapter 2. The important case of a cable whose static configuration lies in one plane is obtained from the more general equations.

Although a casual observer might think that linear cable dynamics are a trivial matter, THEY ARE NOT. In the opinion of the author this can be attributed to the interaction of two physical mechanisms.

- The dynamics of a cable can be seen as the interaction of three different types of forces, which are: the inertia forces, the elastic stretching forces and the gravity forces. The possible interaction between gravity restoring forces and elastic stretching forces is a phenomenon rarely found in conventional dynamic systems.

- In the cable system two different types of waves are present: elastic waves and transverse waves. The elastic waves are travelling at

least 15 to 20 times faster than the transverse waves. This causes the system to be very stiff in the tangential direction. In the case of inextensible cables, a readjustment to tangential disturbances of the cable occurs immediately over the total cable length.

Using perturbation techniques, an extensive study of the solution of the in-plane dynamics of a two dimensional hanging cable is made in chapter 3. Purely analytic, approximate solutions are derived and their physical significance is discussed.

The WKB solution for a taut string with variable tension, which forms one of the bases for the cable solutions, is derived and different assumptions involved are analysed in detail.

For inextensible cables, the orthogonality of the modes is proved analytically. A new first and second order perturbation theory is proposed. The first order perturbation theory gives significantly better results than the one previously derived by Saxon and Cahn [Saxon 53]. The limiting case of a vertically hanging chain is discussed.

In the case of extensible cables, the governing equations can be reduced asymptotically to two second order equations. The first governs the transverse waves of the cable, and is completely similar to the transverse solution derived for an inextensible cable, while the second equation governs the slow (in space) varying dynamics of the cable. Various approximate solutions for the slow equations are proposed and analysed.

A numerical solution, using central differences is also proposed in chapter 3. This scheme has been used to make comparisons of the accuracy of the various schemes.

In chapter 4, some application examples are given. The main purpose of these examples is to illustrate the significant power of the approximate solutions in predicting the dynamic behavior of cables. This could lead to an improved capability for designing mooring systems.

Non-linear effects play a dominant role in the dynamic response of a mooring line. The understanding of the basic characteristics of these non-linearities and their influence on the overall dynamic behavior of a mooring line is, therefore, very important. The four sources of non-linearities are: the non-linear hydrodynamic loading, the geometric non-linearity due to the overall change in configuration of the cable, the non-linear boundary conditions, especially when the cable lays partially on the ocean bottom, and the non-linear material behavior. In this thesis, we will restrict ourselves to the two first types of non-linearities. The major source of excitation of a cable are clearly the motions at the top end of the cable. The effects of the non-linearities are examined using non-linear modal expansion techniques.

In chapter 5, the case of a non-linear string subject to fluid damping and geometric non-linearities is studied, using modal expansions.

In chapter 6, the use of modal expansions in cable dynamic problems is demonstrated. The case of an imposed top motion excitation is examined in detail. Finally, the full incremental solution of the problem, using modal expansions is formulated for the two dimensional problem.

The illustration of the effect of non-linearities is given in chapter 7. Time simulations of the non-linear string and the non-linear cable are discussed.

In the last appendix, a fairly complete bibliography of reported research

on cables, which was collected during the thesis, is given. It may form a good start for the reader who wants to broaden his perspective on the fascinating subject of cables.

1 References

[Critescu 67] Critescu, N.
Dynamic Plasticity.
North Holland Publishing Company, Amsterdam, Holland, 1967, chapter Extensible Strings.

[Irvine 74] Irvine, H. M. and Caughey, T. K.
The Linear Theory of Free Vibrations of a Suspended Cable.
Proceedings of the Royal Society Series A 341:299-315, 1974.

[Leonard 81] Leonard, J. W. and Nath, J. H.
Comparison of Finite Element and Lumped Parameter Methods for Oceanic Cables.
Engineering Structures 3(3):153-167, July, 1981.

[Saxon 53] Saxon, D. S. and Cahn, A. S. .
Modes of Vibration of Suspension Chain.
Quarterly Journal of Mechanics and Applied Mathematics 6:273-285, 1953.

[Simpson 66] Simpson, A.
Determination of the In-Plane Natural Frequencies of Multispan Transmission Lines by a Transfer Matrix Method.
Proceedings IEE 113(5), May, 1966.

[Walton 60] Walton, T. S. and Polachek, H.
Calculation of Transient Motion of Submerged Cables.
Mathematical Tables and Aids to Computation 14:27-60, 1960.

Chapter 1

THREE DIMENSIONAL EQUATIONS OF CABLE DYNAMICS

1.1 Introduction

Three dimensional cable dynamics can be studied in several coordinate systems. Critescu used a Cartesian coordinate system to study the motions of extensible cables [Critescu 67]. The fundamental dynamic properties of cables are better analysed in the so called natural coordinates of a cable, which are fixed on the cable. The cable coordinate system is, therefore, varying both in time and space. Another advantage of this system is that the fluid forces can be described easily. In chapter 3, we will show that this description leads to analytical solutions of the linearised cable dynamic equations.

A derivation of the three dimensional equations in natural coordinates has been done by Lenskii [Lenskii 78]. Cannon and Genin [Cannon 72a] derive the equations directly in terms of the velocities and angular rotations. Barr [Barr 74] obtained equations of motion in two dimensions, starting from a more general formulation, which includes bending effects. A study on the treatment of the hydrodynamic forces on cables can be found in [Breslin 74] and [Goodman 76].

1.2 Kinematics in Three Dimensions

We consider the cable idealized as a single curvilinear line. We define a certain material point on the cable as the origin and a certain direction as positive along the cable. For example, we will usually fix the origin at the lower end of a marine cable and the positive direction will be from the lower towards the upper cable end.

The cable is made of an elastic material, so it is extensible. As a result, the distance between two material points will vary depending on the state of stretching. Let s denote the unstretched distance of a material point from the origin and p(s,t) the stretched distance of the same point at a certain time, t. Both s and p are Langrangian coordinates of the material point.

The cable configuration, i.e. the shape of the idealized line is a continuous function of time and of the coordinates s (or p). Each material point can be described by its distance from the origin of a cartesian system (x, y, z), i.e.

$$x(s,t)$$

$$y(s,t)$$

$$z(s,t)$$

In order to account properly for the fluid forces, though, we will employ a different description system, which introduces a certain degree of complexity, so it is worthwhile establishing a few basic properties, which we can recall systematically in subsequent sections.

The system $\vec{t}$, $\vec{n}$, $\vec{b}$: We define a tangential unit vector $\vec{t}$, at a certain

point A of the cable configuration. The vector AC, where C is another point on the cable, has a limiting position as C tends towards A, which is the tangent direction (provided the cable configuration does not form an angle at the point A, in which case there are two tangents, one from the left and one from the right).

Next we define a normal unit vector $\vec{n}$ at point A: We pick a point B to the left of A and a point C to the right of A (both B and C lie on the cable configuration). We form two planes, one perpendicular to AC and passing through the middle point of AC, and a similar plane for AB. The two planes cross along a line whose shortest distance from A is AM. The limit position of AM, as B and C tend to A, define the normal direction (see figure 1-1), which is perpendicular to the tangential direction. The limit distance AM denoted by ρ is called the radius of curvature.

Finally, we define the binormal unit vector $\vec{b}$ such that the system of vectors $(\vec{t}, \vec{n}, \vec{b})$ is orthogonal and right-handed.

Since the configuration changes both with time and along the cable length, all three vectors are functions of t and p (or s), i.e.:

$$\vec{t}\ (t,p)$$

$$\vec{n}\ (t,p)$$

$$\vec{b}\ (t,p)$$

Strain e. A segment of the cable with unstretched length δs has at a certain time length δp. We define the longitudinal strain e as:

$$e = \lim_{\delta s \to 0} \left(\frac{\delta p - \delta s}{\delta s} \right) = \frac{dp}{ds} - 1 \qquad (1.1)$$

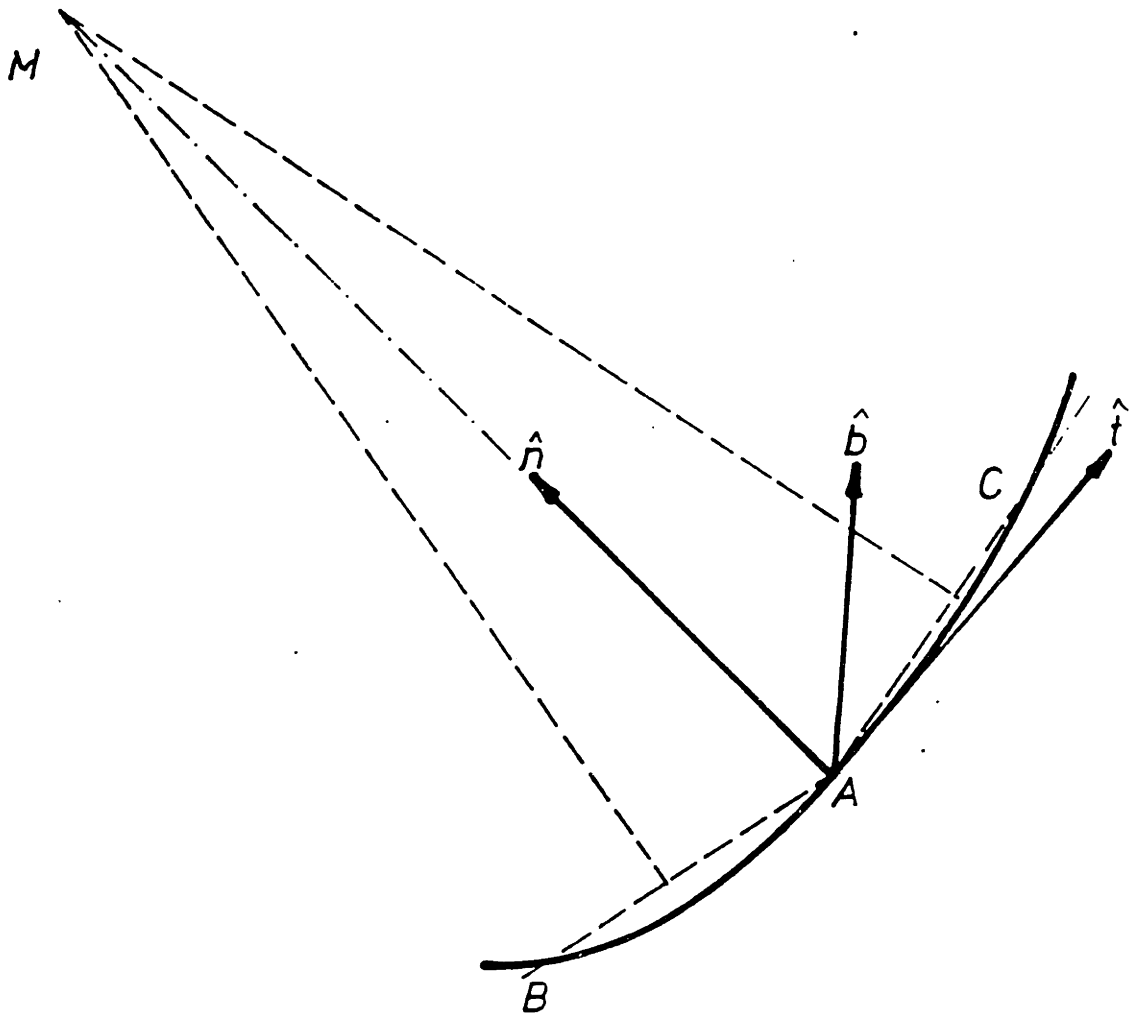

Figure 1-1: Definition of the Natural Coordinate System

As a result of stretching, the cross sectional area of the cable changes also, something that will be discussed later.

Changes in space: The position of $\vec{t}$ varies along p according to the Frenet relations, [Hildebrand 49]:

$$\frac{\partial \vec{t}}{\partial p} = \frac{1}{\rho} \vec{n}$$

$$\frac{\partial \vec{b}}{\partial p} = -\frac{1}{\tau} \vec{n} \tag{1.2}$$

$$\frac{\partial \vec{n}}{\partial p} = \frac{1}{\tau} \vec{b} - \frac{1}{\rho} \vec{t}$$

where ρ is the radius of curvature and τ the radius of torsion. The notation

$$\frac{\partial \vec{t}}{\partial p}$$

indicates the vector which is obtained by subtracting the unit vector $\vec{t}$ (t,p) from the unit vector $\vec{t}$ (t,p+dp), divided by dp, as dp $\rightarrow$ 0.

We rewrite the above relations in terms of the unstretched coordinate s, using the relation dp = (1+e)ds:

$$\frac{\partial \vec{t}}{\partial s} = \frac{1+e}{\rho} \vec{n}$$

$$\frac{\partial \vec{b}}{\partial s} = -\frac{1+e}{\tau} \vec{n} \tag{1.3}$$

$$\frac{\partial \vec{n}}{\partial s} = \frac{1+e}{\tau} \vec{b} - \frac{1+e}{\rho} \vec{t}$$

We redefine ρ_s as $\rho/(1+e)$, and τ_s as $\tau/(1+e)$. These are the curvature and the torsion in the unstretched coordinate s. The subscript s will be omitted in the sequel, while ρ and τ wil denote the unstretched quantities.

Next we define the Darboux vector $\vec{\Omega}$:

$$\vec{\Omega} = \frac{1}{\tau}\vec{t} + \frac{1}{\rho}\vec{b} = (\Omega_1, \Omega_2, \Omega_3) \tag{1.4}$$

$$\Omega_1 = \frac{1}{\tau}$$

$$\Omega_2 = 0$$

$$\Omega_3 = \frac{1}{\rho}$$

which is a mathematical fabrication to facilitate operations involving spatial derivatives in the $(\vec{t}, \vec{n}, \vec{b})$ system. Let $\vec{F}$ (t,s) denote a vector which varies along the length of the cable and let its coordinates be F_1, F_2, F_3, i.e.

$$\vec{F} = F_1\vec{t} + F_2\vec{n} + F_3\vec{b} \tag{1.5}$$

Then the derivative of $\vec{F}$ in the $(\vec{t}, \vec{n}, \vec{b})$ system denoted as

$$\left[\frac{D\vec{F}}{Ds}\right]_{(\vec{t}, \vec{n}, \vec{b})}$$

becomes quite complex because in addition to the change of F_1, F_2, F_3 we must account for the rotation of the system $(\vec{t}, \vec{n}, \vec{b})$ along the cable length. To simplify the notation, we denote:

$$\left[\frac{D\vec{F}}{Ds}\right]_{(\vec{t}, \vec{n}, \vec{b})} = \frac{D\vec{F}}{Ds} \tag{1.6}$$

We will then prove that

$$\frac{D\vec{F}}{Ds} = \frac{\partial \vec{F}}{\partial s} + \vec{\Omega} \times \vec{F} \tag{1.7}$$

where

$$\frac{\partial \vec{F}}{\partial s} = \left[\frac{\partial F_1}{\partial s}, \frac{\partial F_2}{\partial s}, \frac{\partial F_3}{\partial s} \right]$$

Proof:

$$\frac{D\vec{F}}{Ds} = \frac{\partial \vec{F}}{\partial s} + F_1 \frac{\partial \vec{t}}{\partial s} + F_2 \frac{\partial \vec{n}}{\partial s} + F_3 \frac{\partial \vec{b}}{\partial s}$$

Using the Frenet relations (1.2) we find that

$$\frac{D\vec{F}}{Ds} = \frac{\partial \vec{F}}{\partial s} - \vec{t} \frac{F_2}{\rho} - \vec{n} \left[\frac{1}{\tau} F_3 - \frac{1}{\rho} F_1 \right] + \vec{b} \frac{F_2}{\tau}$$

$$= \frac{\partial \vec{F}}{\partial s} + \vec{\Omega} \times \vec{F}$$

Changes in time. For the same reason that changes in space become complicated in the $(\vec{t}, \vec{n}, \vec{b})$ system, changes in time must also be reformulated. We simply denote:

$$\left[\frac{D\vec{F}}{Dt} \right]_{(\vec{t}, \vec{n}, \vec{b})} = \frac{D\vec{F}}{Dt}$$

The equivalent of the Darboux vector is now the rotation vector of the classical dynamics:

$$\vec{\omega} = \omega_1 \vec{t} + \omega_2 \vec{n} + \omega_3 \vec{b}$$

and we obtain from dynamics that [Crandall 56]:

$$\frac{D\vec{F}}{Dt} = \frac{\partial \vec{F}}{\partial t} + \vec{\omega} \times \vec{F} \tag{1.8}$$

where

$$\frac{\partial \vec{F}}{\partial t} = \left[\frac{\partial F_1}{\partial t}, \frac{\partial F_2}{\partial t}, \frac{\partial F_3}{\partial t} \right]$$

1.3 Cable Dynamics

We define a velocity of a point on a the cable as:

$$\vec{v} = v_1\vec{t} + v_2\vec{n} + v_3\vec{b} \tag{1.9}$$

Newton's law can be written for an element with unstretched length ds and stretched length dp as:

$$m_o \frac{D\vec{v}}{Dt} ds = \sum_{i=0}^{n} \vec{F}_i dp \tag{1.10}$$

where m_o is the mass per unit length in the instretched coordinate and $\vec{F}$ the force per unit length on the cable.

$$m_o \frac{D\vec{v}}{Dt} = \sum_{i=0}^{n} \vec{F}_i(1+e) \tag{1.11}$$

The equation is rewritten using (1.8):

$$m_o \left[\frac{\partial \vec{v}}{\partial t} + \vec{\omega} \times \vec{v} \right] = \sum_{i=0}^{n} \vec{F}_i(1+e) \tag{1.12}$$

explicitly this is written as;

$$m_o \left[\frac{\partial v_1}{\partial t} - v_2\omega_3 + v_3\omega_2\right] = \sum_{i=0}^{n} F_{ti}(1+e)$$

$$m_o \left[\frac{\partial v_2}{\partial t} - v_3\omega_1 + v_1\omega_3\right] = \sum_{i=0}^{n} F_{ni}(1+e)$$

$$m_o \left[\frac{\partial v_3}{\partial t} - v_1\omega_2 + v_2\omega_1\right] = \sum_{i=0}^{n} F_{bi}(1+e)$$

Equation (1.12) is the equation of motion for a cable expressed in the natural coordinate system.

1.4 Compatibility Relations

Compatibility relations can be formulated directly in terms of displacements, or they can be formulated in terms of velocities. The two formulations are completely equivalent, and both can be used to solve the problem.

We will derive the compatibility relations using displacements. An alternative derivation to find the compatibility relations in terms of velocities can be found in appendix A.

We define $\vec{r}$ as the vector from the origin of a fixed coordinate system to a point on the cable. A reference state is defined as the position of the cable at some arbitrary, fixed time t_o. The vector to the same material point at that time is denoted by $\vec{r}_o$. (see figure 1-2)

Expressing the spatial changes using the Darboux vector of the reference state, we find:

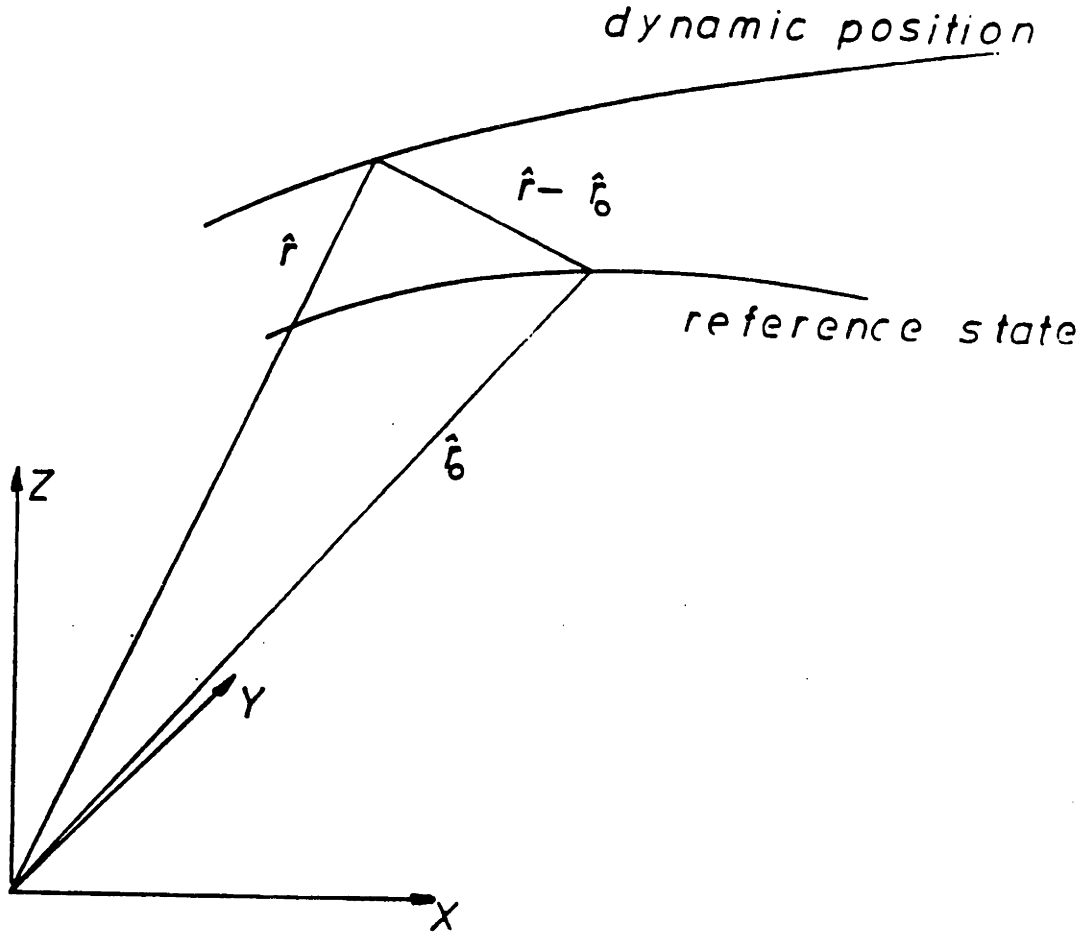

Figure 1-2: Derivation of the Compatibility Relations

$$\frac{D(\vec{r} - \vec{r}_o)}{Ds} = \frac{\partial(\vec{r} - \vec{r}_o)}{\partial s}_{(\vec{t}_o,\vec{n}_o,\vec{b}_o)} + \vec{\Omega}_o \times (\vec{r} - \vec{r}_o)$$

$$\frac{D\vec{r}}{Ds} - \frac{D\vec{r}_o}{Ds} = \frac{\partial(\vec{r} - \vec{r}_o)}{\partial s}_{(\vec{t}_o,\vec{n}_o,\vec{b}_o)} + \vec{\Omega}_o \times (r - r_o) \qquad (1.13)$$

According to the definition of the tangential vector [Hildebrand·49]:

$$\vec{t}(t,p) = \frac{D\vec{r}}{Dp}(t,p)$$

$$= \frac{1}{(1+e)} \frac{D\vec{r}}{Ds} \qquad (1.14)$$

Therefore, we obtain:

$$(1+e)\vec{t} - (1+e_o)\vec{t}_o = \frac{\partial(\vec{r} - \vec{r}_o)}{\partial s}_{(\vec{t}_o,\vec{n}_o,\vec{b}_o)} + \vec{\Omega}_o \times (\vec{r} - \vec{r}_o) \qquad (1.15)$$

(1.15) is the compatibility relations in terms of displacements. To obtain the compatibility relations in terms of velocities, (1.15) is rewritten as:

$$(1+e)\vec{t} - (1+e_o)\vec{t}_o = \frac{D(\vec{r} - \vec{r}_o)}{Ds} \qquad (1.16)$$

Taking the time derivative :

$$\frac{D}{Dt}\left[(1+e)\vec{t}\right] = \frac{D\vec{v}}{Ds}$$

$$\frac{D\vec{v}}{Ds} = \frac{\partial e}{\partial t}\vec{t} + (1+e)(\vec{\omega} \times \vec{t}) \qquad (1.17)$$

These are the compatibility relations in terms of velocities. In this case, no reference system is involved. Explicity this can be written as:

$$\frac{\partial v_1}{\partial s} - v_2\Omega_3 = \frac{\partial e}{\partial t}$$

$$\frac{\partial v_2}{\partial s} + v_1\Omega_3 - v_3\Omega_1 = (1+e)\omega_3 \qquad (1.18)$$

$$\frac{\partial v_3}{\partial s} + v_2\Omega_1 = -(1+e)\omega_2$$

1.5 Relation between the Rotation and the Darboux Vectors

The rotation and the Darboux vectors are related. This can be shown as follows. Equality of the mixed derivatives can be expressed as:

$$\frac{D}{Dt}\left[\frac{D\vec{v}}{Ds}\right] = \frac{D}{Ds}\left[\frac{D\vec{v}}{Dt}\right] \qquad (1.19)$$

When expressing (1.19) in terms of the Darboux vector and the rotation vectors, using the formulas for triple vector products, the following equality is obained:

$$\frac{\partial\vec{\Omega}}{\partial t} = \frac{\partial\vec{\omega}}{\partial s} + \vec{\Omega}\times\vec{\omega} \qquad (1.20)$$

or explicity

$$\frac{\partial\Omega_1}{\partial t} = \frac{\partial\omega_1}{\partial s} - \Omega_3\omega_2$$

$$0 = \frac{\partial\omega_2}{\partial s} - \Omega_1\omega_3 + \Omega_3\omega_1$$

$$\frac{\partial\Omega_3}{\partial t} = \frac{\partial\omega_3}{\partial s} + \Omega_1\omega_2$$

1.6 Forces Acting on the Cable

The forces acting on the cable are (a) the tension, (b) its weight, (c) external forces. The external forces include fluid related forces such as hydrostatic forces, drag forces and inertia forces.

1.6.1 Weight and Buoyancy forces

As shown in figure 1-3 the segment is in contact with the fluid only at its sides, so that the hydrostatic force is always perpendicular to the cable configuration (i.e., in the $\vec{t}$, $\vec{n}$ plane). It is very convenient to add and subtract the "missing" hydrostatic forces from a cable element (as shown in figure 1-3). Then, by lumping together all the hydrostatic forces pointing towards the interior of the cable element, we obtain Archimede's force in the vertical direction.

$$B = \rho_w \cdot A \cdot dp$$

where A is the (stretched) cable sectional area, while we lump together the tension T (pointing always in the tangential direction towards the exterior of the cable element) and the hydrostatic force acting in the same direction, to create the effective tension T_e.

$$T_e = T + \rho \cdot A$$

The introduction of the effective tension causes the equations in water to have the same form as the equations in air, except that the weight must be replaced by the net weight and the tension by the effective tension.

If m_o denotes the unstretched mass of the cable per unit length, and m the corresponding stretched quantity, then conservation of mass implies:

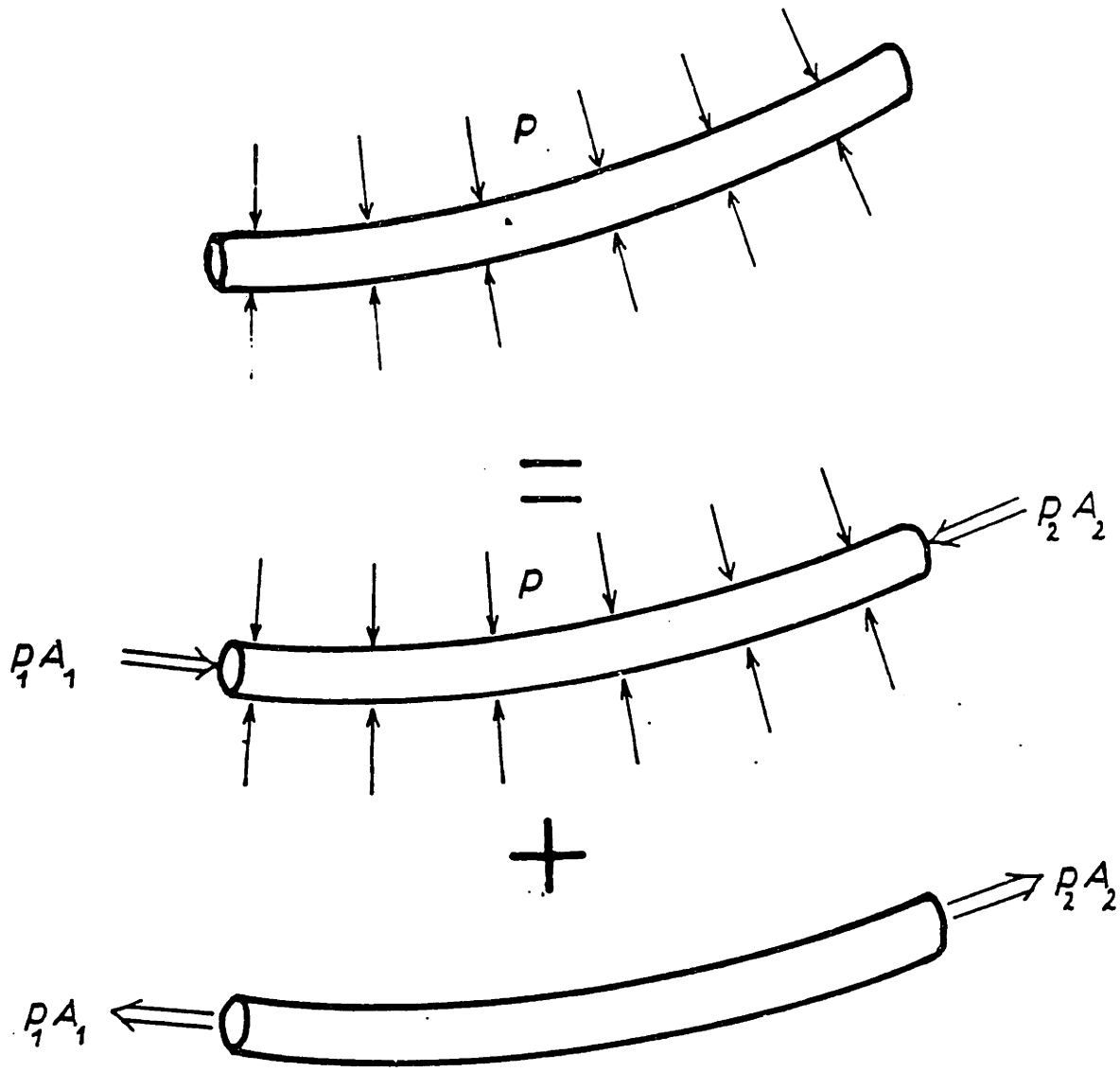

Figure 1-3: Effective Tension

$$m_o \cdot ds = m \cdot dp$$

Since we managed to artificially create a buoyancy force by introducing the effective tension, we can now use the net weight of the cable per unit (stretched) length in water,

$$m \cdot g - \rho_w \cdot g \cdot A$$

We assume for simplicity, following Breslin [Breslin 74] that the volume per unit length of the cable remains unchanged (which implies that Poisson's ratio ν is equal to 1/2) to obtain the net weight per unstretched unit length in water w_o as

$$w_o = g \cdot (m - \rho_w \cdot A_o)$$

where A_o is the unstretched cable sectional area. The corresponding quantity per stretched unit length, w_a, is related to w_o by the relation (based on $\nu = 1/2$):

$$w_o \cdot ds = w_a \cdot dp$$

Therefore

$$\vec{F}_W \cdot dp = - w_o \cdot \vec{k} \cdot ds$$

where $\vec{k}$ is the unit vector in positive direction in a fixed reference system.

1.6.2 Fluid Hydrodynamic Forces

In addition to the hydrostatic force, the cable is subject to a fluid force, which includes a fluid inertia component (related to the added mass m_a) and a viscosity related component (drag force). If a Morison type of loading is used, then the fluid forces are decomposed simply in an added mass force and

a velocity drag force.

The subject of the added mass for cables has attracted some attention in the literature, especially when a current is present. Lighthill [Lighthill 60] showed that for the transverse oscillations of a horizontal slender body whose longitudinal axis is parallel to the current, the added mass force can be approximated as:

$$F_A = - \frac{D}{Dt} \left[m_a \frac{DW}{Dt} \right]$$

where W is the vertical displacement, m_a the added mass per unit length of an infinite cylinder with the same cross section as the local section of the body, and D/DT denotes the substantial derivative, i.e. if U is the current speed:

$$F_A = - \left(\frac{\partial}{\partial t} - U \cdot \frac{\partial}{\partial x} \right) \left\{ m_a(x) \cdot \left(\frac{\partial}{\partial t} - U \cdot \frac{\partial}{\partial x} \right) \cdot W(x,t) \right\} \qquad (1.21)$$

The direction of F_A is vertical. Lighthill showed that this approximation is good, provided the wave length to diameter ratio is larger than 5, and the amplitude of oscillation is small. An extension to a curved inclined configuration must account for possible interactions among the various cable sections and, primarily, for separation effects. Breslin [Breslin 74] used potential theory to derive an expression for the added mass force for a cable, but his final expression, obtained by a strip theory approach is in error and does not reduce to Lighthill's expression. What is actually missing is a double material derivative as shown in (1.21). Breslin's expression contains a material and a regular derivative. In Lenskii [Lenskii 78] an expression to include stretching effects was derived.

It is the author's opinion that separation effects are predominant. As

shown in Allen and Perkins [Allen 51] any inclination above 3^o - 5^o causes expression (1.21) to fail. It is well known also that vortex shedding has a profound effect on added mass, so that any corrections for current or stretching effects within the frame of the investigators above may not be necessary. Until conclusive experiments are conducted therefore, and with the exception of cables towed along their axis, it is suggested in the present study to use an added mass force per unit length in the direction normal to the cable.

$$\vec{F}_A \, dp = - \, m_a \frac{\partial \vec{v}_n}{\partial t} \cdot ds \qquad (1.22)$$

where m_a the two-dimensional mass per unit length of an infinite cylinder with the same cross section as the cable, and under identical flow conditions, and $\vec{v}_n$ the normal relative velocity between the cylinder and the fluid particles. The value of m_a of course is difficult to find and only partial information is available as in Ramberg and Griffin [Ramberg 77].

To obtain the drag force, we use the separation principle. The drag force on an inclined cylinder is separated into a normal drag component, proportional to the square of the normal relative velocity and a tangential frictional drag component, proportional to the square of the tangential relative velocity. This force can be easily decomposed into a normal, tangential and binormal drag components [Breslin 74].

$$\vec{F}_t dp = -\frac{1}{2}\rho_w C_{Dt}(Re) D_o v_{rt} |v_{rt}| \vec{t}(1+e/2)\, ds$$

$$\vec{F}_n dp = -\frac{1}{2}\rho_w C_{Dn}(Re) D_o v_{rn} \left[v_{rn}^2 + v_{rb}^2\right]^{\frac{1}{2}} \vec{n}(1+e/2)ds \qquad (1.23)$$

$$\vec{F}_b dp = -\frac{1}{2}\rho_w C_{Db}(Re) D_o v_{rb} \left[v_{rb}^2 + v_{rn}^2\right]^{\frac{1}{2}} \vec{b}(1+e/2)ds$$

where: D_o : the diameter of the cable
v_{rt}, v_{rn}, v_{rb} : the component of the relative velocity

Unsteady fluid forces, such as due to waves, vortex shedding and galloping are not considered in the present work.

1.6.3 Tension Force

The force on an element with unstretched length can be written as:

$$\frac{d}{ds}(T_e \vec{t})\, ds = \left[\frac{\partial T_e}{\partial s}\vec{t} + T_e \frac{d\vec{t}}{ds}\right]ds$$

$$= \left[\frac{\partial T_e}{\partial s}\vec{t} + \frac{T_e}{\rho}\vec{n}\right]ds \qquad (1.24)$$

1.7 Equation of Motion

Using (1.22), (1.23) and (1.24), the equation of motion (1.10) can be rewritten as:

$$m_o \left[\frac{\partial \vec{v}}{\partial t} + \vec{\omega}\times\vec{v}\right] = \frac{\partial T_e}{\partial s}\vec{t} + \frac{T_e}{\rho}\vec{n}$$

$$- w_o\vec{k} - \left(m_{an}\frac{\partial v_n}{\partial t}\vec{n} + m_{ab}\frac{\partial v_b}{\partial t}\vec{b}\right)$$

$$+ \left(F_t\vec{t} + F_n\vec{n} + F_b\vec{b}\right)\frac{\partial p}{\partial s} \qquad (1.25)$$

The above equation is the complete equation of motion expressed in its natural coordinate system.

1.8 Governing Equations

The complete set of governing equations is obtained by combining (1.17), (1.20) and (1.25).

$$m_o \left[\frac{\partial \vec{v}}{\partial t} + \vec{\omega}\times\vec{v}\right] = \frac{\partial T_e}{\partial s}\vec{t} + T_e\Omega_3\vec{n}$$

$$- w_o\vec{k} - m_{an}\frac{\partial v_n}{\partial t}\vec{n} - m_{ab}\frac{\partial v_b}{\partial t}\vec{b}$$

$$+ \left(F_t\vec{t} + F_n\vec{n} + F_b\vec{b}\right)(1+e)$$

$$\frac{\partial \vec{v}}{\partial s} + \vec{\Omega}\times\vec{v} = \frac{\partial e}{\partial t}\vec{t} + (1+e)\vec{\omega}\times\vec{t} \qquad (1.26)$$

$$\frac{\partial \vec{\Omega}}{\partial t} = \frac{\partial \vec{\omega}}{\partial s} + \vec{\Omega}\times\vec{\omega}$$

This has to be supplemented with a tension-strain relation.

$$T_e = f(e\ ,\ \frac{\partial e}{\partial t}\ ,\ s) \tag{1.27}$$

The above is a set of 10 equations with 10 variables: v_1, v_2, v_3, ω_1, ω_2, ω_3, Ω_1, Ω_3, T_e, e . Given appropriate boundary conditions, a solution can be obtained. In the sequel, we will refer to m_o (the mass per unit unstretched length) as m, dropping the subscript o for convenience.

1.9 Euler Angles

The governing equations are best expressed in terms of Euler angles. Let ϕ, θ, ψ be the Euler angles defining the position of the $\vec{t}$, $\vec{n}$, $\vec{b}$ system relative to the (x,y,z) system. (See figure 1-4)

First we perform a rotation around the y axis by θ, then a rotation around the z_1 axis by ϕ. The x_2 axis is now the new tangential direction and the (y_2,x_2) plane is a vertical plane. Finally we perform a rotation ψ around the x_2 axis, so that finally x_3 corresponds to $\vec{t}$, y_3 corresponds to $\vec{n}$ and z_3 corresponds to $\vec{b}$.

It is possible to solve the equations without performing the rotation ψ. The (y_2,x_2) plane is then vertical, while this eliminates one variable ψ out of the equations. The expressions which were derived for the Darboux vector and also for the force component of the tension are not valid, however, and must be reformulated. For more details, see [Cannon 72a], [Cannon 72b] and [Firebaugh 72].

To investigate the properties of three dimensional dynamics, it is preferable to use the natural coordinates. The transformation between the two coordinate systems is given by:

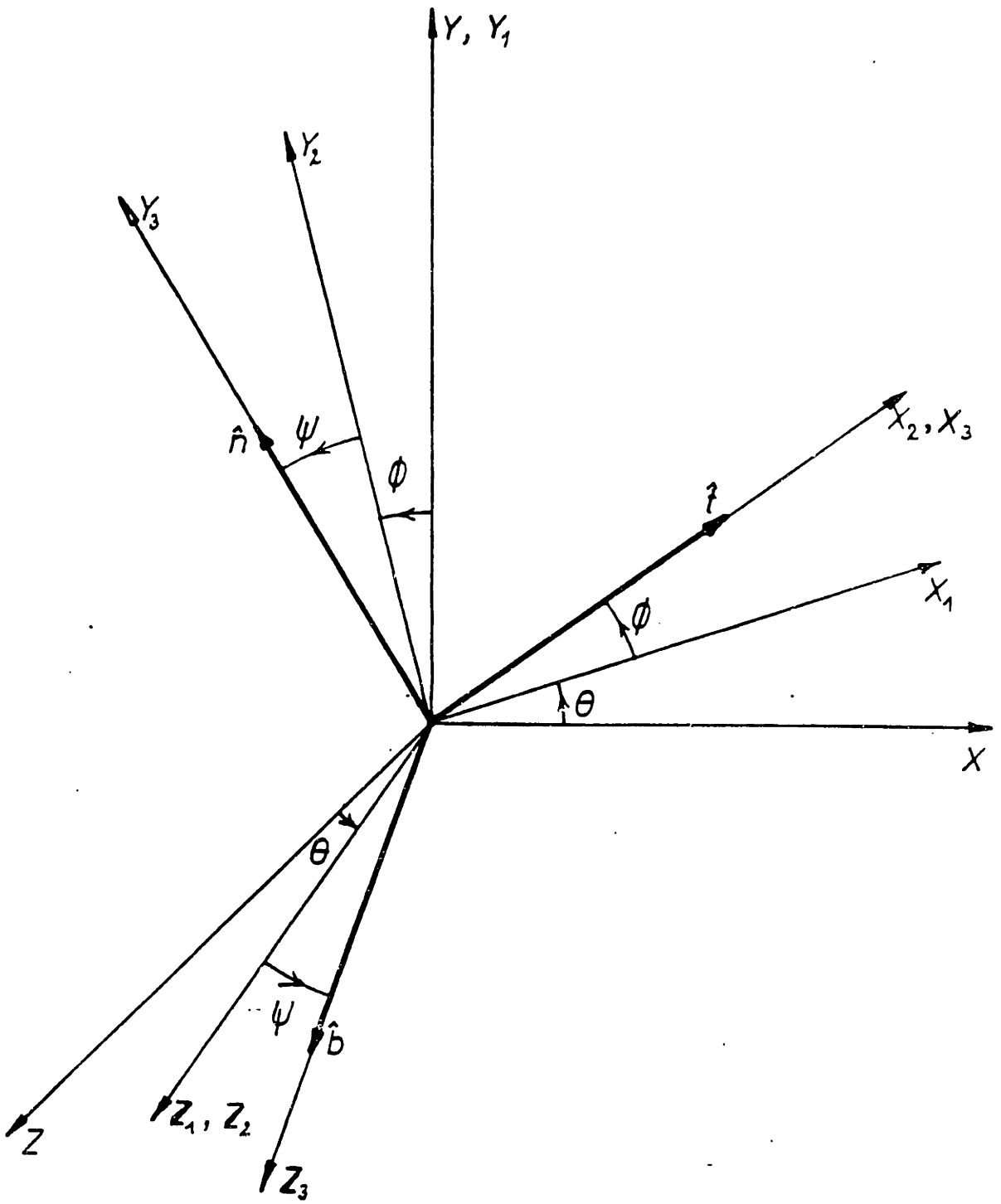

Figure 1-4: Definition of Euler Angles

$$x = \cos\theta \cdot \cos\phi\ x_o + \sin\phi\ y_o - \sin\theta \cdot \cos\phi\ z_o$$

$$y = (\sin\psi \cdot \sin\theta - \cos\psi \cdot \sin\phi \cdot \cos\theta)\ x_o + \cos\psi \cdot \cos\phi\ y_o + (\sin\psi \cdot \cos\theta + \cos\psi \cdot \sin\phi \cdot \sin\theta)\ z_o \qquad (1.28)$$

$$z = (\cos\psi \cdot \sin\theta + \sin\psi \cdot \sin\phi \cdot \cos\theta)\ x_o - \sin\psi \cdot \cos\phi\ y_o + (\cos\psi \cdot \cos\theta - \sin\psi \cdot \sin\phi \cdot \sin\theta)\ z_o$$

where x_o, y_o, z_o are the coordinates in the fixed coordinate system and x,y,z are the coordinates in the natural coordinate system.

We can express the vertical unit vector in terms of the natural vector, using the transpose of (1.28)

$$\vec{k} = \sin\phi\ \vec{t} + \cos\psi \cdot \cos\phi\ \vec{n} - \cos\phi \cdot \sin\psi\ \vec{b} \qquad (1.29)$$

The equations of motion are obtained as:

$$m\left[\frac{\partial v_1}{\partial t} + \omega_2\ v_3 - \omega_3\ v_2\right] = \frac{\partial T_e}{\partial s} + F_t(1+e) - w_o \cdot \sin\phi$$

$$(m+m_{an})\frac{\partial v_2}{\partial t} + m(\omega_3 v_1 - \omega_1 v_3) = \Omega_3\ T_e + F_n(1+e) - w_o\ \cos\phi\ \cos\psi \qquad (1.30)$$

$$(m+m_{ab})\frac{\partial v_3}{\partial t} + m(\omega_1 v_2 - \omega_2 v_1) = F_b(1+e) + w_o\ \cos\phi \cdot \sin\psi$$

The rotation vector expressed in Euler angles gives:

$$\vec{\omega}\ dt = (\sin\phi\ \delta\theta + \delta\psi)\ \vec{t} + (\cos\phi \cdot \cos\psi\ \delta\theta + \sin\psi\ \delta\phi)\ \vec{n} + (-\cos\phi \cdot \sin\psi\ \delta\theta + \cos\psi\ \delta\phi)\ \vec{b} \qquad (1.31)$$

In component form we obtain:

$$\omega_1 = \sin\phi \cdot \frac{\partial\theta}{\partial t} + \frac{\partial\psi}{\partial t}$$

$$\omega_2 = \cos\psi \cdot \cos\phi \cdot \frac{\partial\theta}{\partial t} + \sin\psi \cdot \frac{\partial\phi}{\partial t} \tag{1.32}$$

$$\omega_3 = -\sin\psi \cdot \cos\phi \cdot \frac{\partial\theta}{\partial t} + \cos\psi \cdot \frac{\partial\phi}{\partial t}$$

The Darboux vector expressed in terms of Euler angles gives, using Frenet's formulas:

$$\frac{1}{\rho} = \frac{\partial\phi}{\partial s} \cdot \frac{1}{\cos\psi}$$

$$\frac{1}{\tau} = \frac{\partial\psi}{\partial s} - \tan\psi \cdot \tan\phi \cdot \frac{\partial\phi}{\partial s} \tag{1.33}$$

$$0 = \frac{\partial\theta}{\partial s} + \frac{\partial\phi}{\partial s} \cdot \tan\psi \cdot \frac{1}{\cos\phi}$$

1.10 Governing Equations using the Euler Angles

If (1.32) and (1.33) are substituted in the equations of motion and the compatibility relations, the governing equations in terms of Euler angles are obtained.

$$m\left[\frac{\partial v_1}{\partial t} + \left(\cos\phi \cdot \cos\psi \cdot \frac{\partial\theta}{\partial t} + \sin\psi \cdot \frac{\partial\phi}{\partial t}\right) v_3 \right.$$

$$\left. - \left(-\cos\phi \cdot \sin\psi \cdot \frac{\partial\theta}{\partial t} + \cos\psi \cdot \frac{\partial\phi}{\partial t}\right) v_2 \right]$$

$$= \frac{\partial T_e}{\partial s} + F_t(1+e) - w_o \sin\phi$$

$$(m + m_{an})\frac{\partial v_2}{\partial t} - m(\sin\phi \cdot \frac{\partial \theta}{\partial t} + \frac{\partial \psi}{\partial t})\, v_3$$

$$+ m(-\cos\phi \cdot \sin\psi \cdot \frac{\partial \theta}{\partial t} + \cos\psi \cdot \frac{\partial \phi}{\partial t})\, v_1$$

$$= \frac{\partial \phi}{\partial s} \cdot \frac{1}{\cos\psi} T_e + F_n(1+e) - w_o \cos\phi \cdot \cos\psi$$

$$(m + m_{ab})\frac{\partial v_3}{\partial t} + m(\sin\phi \cdot \frac{\partial \theta}{\partial t} + \frac{\partial \psi}{\partial t})\, v_2$$

$$- m(\cos\phi \cdot \cos\psi \cdot \frac{\partial \theta}{\partial t} + \sin\psi \cdot \frac{\partial \phi}{\partial t})\, v_1$$

$$= F_b(1+e) + w_o \cos\phi \cdot \sin\psi \qquad (1.34)$$

$$\frac{\partial v_1}{\partial s} - \frac{v_2}{\cos\psi}\frac{\partial \phi}{\partial s} = \frac{\partial e}{\partial t}$$

$$\frac{\partial v_2}{\partial s} - \left[\frac{\partial \psi}{\partial s} - \tan\psi \cdot \tan\phi \cdot \frac{\partial \phi}{\partial s}\right] v_3 + \frac{v_1}{\cos\psi}\frac{\partial \phi}{\partial s}$$

$$= (1+e)\left[-\cos\phi \cdot \sin\psi \cdot \frac{\partial \theta}{\partial t} + \cos\psi \cdot \frac{\partial \phi}{\partial t}\right]$$

$$\frac{\partial v_3}{\partial s} + \left[\frac{\partial \psi}{\partial s} - \tan\psi \cdot \tan\phi \cdot \frac{\partial \phi}{\partial s}\right] v_2$$

$$= -(1+e)\left[\cos\phi \cdot \cos\psi \cdot \frac{\partial \theta}{\partial t} + \sin\psi \cdot \frac{\partial \phi}{\partial t}\right]$$

$$T_e = f(e)$$

These constitute a set of seven equations with seven unknows. (1.34) are the non-linear governing equations in terms of Euler angles.

1.11 Two Dimensional Non-Linear Governing Equations

The governing equations (1.26) are simplified significantly when the motions are planar. (see figure 1-5)

$$\Omega_1 = \Omega_2 = 0$$

$$\omega_1 = \omega_2 = 0$$

$$v_3 = 0$$

Therefore the equations can be written explicitly as:

$$m\left[\frac{\partial v_1}{\partial t} - v_2\omega_3\right] = \frac{\partial T_e}{\partial s} - w_o\sin\phi + F_{dt}$$

$$m\left[\frac{\partial v_2}{\partial t} + v_1\omega_3\right] = T_e\frac{\partial \phi}{\partial s} - w_o\cos\phi + F_{dn} - m_a\frac{\partial v_2}{\partial t}$$

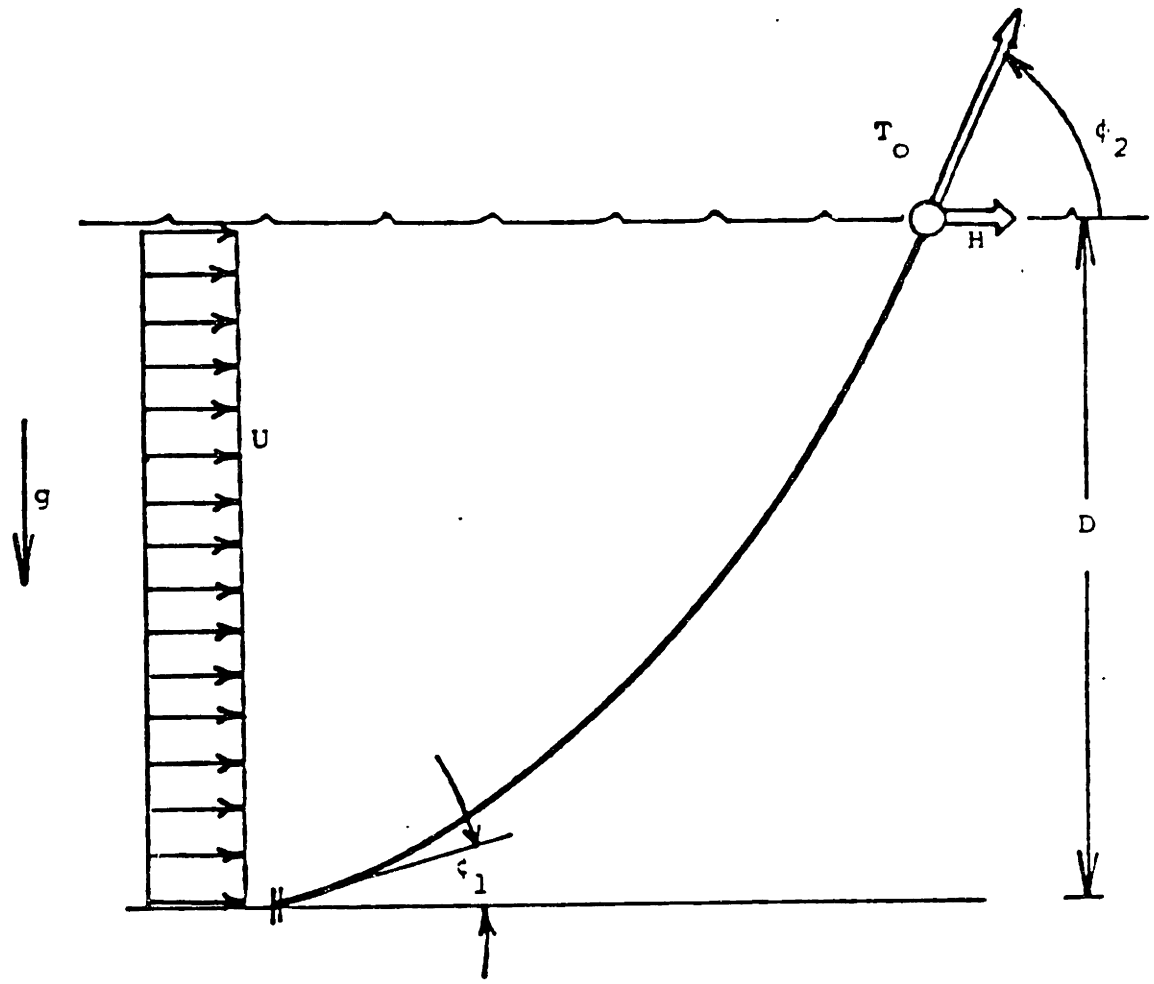

Figure 1-5: Two dimensional Cable Dynamics

$$\frac{\partial v_1}{\partial s} - \frac{v_2}{\rho} = \frac{\partial e}{\partial t} \qquad (1.35)$$

$$\frac{\partial v_2}{\partial s} + \frac{v_1}{\rho} = (1+e)\omega_3$$

$$\frac{\partial 1/\rho}{\partial t} = \frac{\partial \omega_3}{\partial s}$$

where: $F_{dt} = \frac{1}{2}\rho_w C_{Dt} D_o (U\cos\phi - v_{rt}) |U\cos\phi - v_{rt}| (1+e/2)$

$$F_{dn} = -\frac{1}{2}\rho_w C_{Dn} D_o (U\sin\phi + v_{rn}) |U\sin\phi + v_{rn}| (1+e/2)$$

U = current

In the two dimensional case we have:

$$\frac{1}{\rho} = \phi_s$$

$$\omega_3 = \phi_t$$

Therefore we obtain the final form of the non-linear, two dimensional equations expressed in natural coordinates:

$$m\left[\frac{\partial v_1}{\partial t} - v_2\phi_t\right] = \frac{\partial T_e}{\partial s} - w_o\sin\phi + F_{dt}$$

$$m\left[\frac{\partial v_2}{\partial t} + v_1\phi_t\right] = T_e\frac{\partial \phi}{\partial s} - w_o\cos\phi + F_{dn} - m_a\frac{\partial v_2}{\partial t}$$

$$\frac{\partial v_1}{\partial s} - \phi_s \, v_2 = \frac{\partial e}{\partial t} \tag{1.36}$$

$$\frac{\partial v_2}{\partial s} + \phi_s \, v_1 = (1+e)\phi_t$$

$$T_e = f(e \, , \frac{\partial e}{\partial t} \, , \, s)$$

(5 equations with 5 unknowns)

1.12 Investigation of the Characteristics of the Governing Equations

The non-linear cable equations can be classified mathematically as a quasi-linear first order system, when the constitutive relation is of the form:

$$T_e = f(e)$$

In the case of a Kelvin visco-elastic damping model, the system is not quasi-linear and the investigation of the properties of the governing equations becomes very difficult. When restricted to the constitutive relation above, the system can be written as[1]:

$$\frac{\partial v_i}{\partial t} + a_{ij} \frac{\partial v_j}{\partial x} + b_i = 0 \tag{1.37}$$

To investigate whether characteristic lines $x = \xi(t)$ exist, or equivalently whether the system can be written in terms of total derivatives only, linear

---

[1]The tensor summation convention is used.

combinations of the set of equations (1.37) are formed [Whitham 74].

$$l_i \frac{\partial v_i}{\partial t} + l_i\, a_{ij} \frac{\partial v_j}{\partial x} + b_i\, l_i = 0 \tag{1.38}$$

We want to rewrite these equations using total derivatives along the characteristic curves.

$$l_i \frac{dv_i}{dt} + b_i\, l_i = 0 \qquad \text{on} \quad \frac{d\xi}{dt} = c \tag{1.39}$$

This is only possible when:

$$l_i\, a_{ij} = l_j\, c$$

This is the condition to determine a characteristic line. To be able to determine completely the system, we must have n different characteristics, so that the condition:

$$|a_{ij} - c| = 0$$

must provide n real eigenvalues.

We restrict our analysis to the two dimensional case. See [Critescu 67] for a derivation in three dimensions and in a Cartesian coordinate system. The quasi-linear form of the non-linear, two dimensional equations is given in the next page.

After some manipulation, the characteristics can be found as:

$$c_{el} = \pm \left[\frac{1}{m} \cdot \frac{\partial f}{\partial e} \right]^{\frac{1}{2}}$$

$$c_{tr} = \pm \left[\frac{T}{M(1+e)} \right]^{\frac{1}{2}} \tag{1.40}$$

Four real and distinct eigenfrequencies are obtained, so the system is hyperbolic. Critescu obtained the same result for three dimensional shapes.

$$\begin{bmatrix} \frac{\partial v_t}{\partial t} \\ \frac{\partial v_n}{\partial t} \\ \frac{\partial \phi}{\partial t} \\ \frac{\partial e}{\partial t} \end{bmatrix} = \begin{bmatrix} 0 & \frac{v_n}{1+e} & \frac{v_n v_t}{1+e} & \frac{\partial f}{\partial e}\frac{1}{m} & \frac{\partial v_t}{\partial s} \\ 0 & -\frac{v_t}{1+e} & \frac{T}{M} - \frac{v_t^2}{1+e} & 0 & \frac{\partial v_n}{\partial s} \\ 0 & \frac{1}{1+e} & \frac{v_t}{1+e} & 0 & \frac{\partial \phi}{\partial s} \\ 1 & 0 & -v_n & 0 & \frac{\partial e}{\partial s} \end{bmatrix} + B$$

where:

$$B = \begin{bmatrix} -\frac{w_o}{m}\sin\phi + \frac{F_{dt}}{m}(1+e/2) + \frac{1}{m}\frac{\partial f}{\partial s} \\ -\frac{w_o}{M}\cos\phi + \frac{F_{dn}(1+e/2)}{M} \\ 0 \\ 0 \end{bmatrix}$$

$(M = m + m_a)$

Table 1-I: Quasi-linear Form of the Two Dimensional Equations of Motion

The resulting waves can be classified as elastic waves and transverse waves. If the system is considered inextensible, the elastic wave speed goes to infinity and the system can be classified as hyperbolic-parabolic. For a linear-tension strain relation the elastic wavespeed can be rewritten as:

$$c_{el} = \left[\frac{E}{\rho} \right]^{\frac{1}{2}}$$

1.13 References

[Allen 51] Allen, H. J. and Perkins, E. W.
A Study of the Effects of Viscosity on Flow over Slender Bodies of Revolution.
Technical Report 1048, NACA, 1951.

[Barr 74] Barr, R.A.
The Non-Linear Dynamics of Cable Systems.
Technical Report UM-1MR 74-1, Sea Grant, University of California, 1974.

[Breslin 74] Breslin, J. P.
Dynamic Forces Exerted by Oscillating Cables.
Journal of Hydronautics 8(1):18-31, January, 1974.

[Cannon 72a] Cannon, T. C. and Genin, J.
Three Dimensional Dynamical Behaviour of a Flexible Towed Cable.
Aeronautical Quarterly 25:201-210, August, 1972.

[Cannon 72b] Cannon, T. C.
Dynamical Behaviour of a Materially Damped Flexible Towed Cable.
Aeronautical Quarterly 23:109-120, May, 1972.

[Crandall 56] Crandall, S.H.
Engineering Analysis.
McGraw-Hill, New York, 1956.

[Critescu 67] Critescu, N.
Dynamic Plasticity.
North Holland Publishing Company, Amsterdam, Holland, 1967, chapter Extensible Strings.

[Firebaugh 72] Firebaugh, M. S.
An Analysis of the Dynamics of Towing Cables.
PhD thesis, M.I.T., Department of Ocean Engineering, 1972.

[Goodman 76] Goodman, T. R. and Breslin, J. P.
Statics and Dynamics of Anchoring Cables in Waves.
Journal of Hydronautics 10(4):113-120, October, 1976.

[Hildebrand 49] Hildebrand, F.B.
Advanced Calculus for Applications.
Prentice Hall, Englewood Cliffs N.J., 1949.

[Lenskii 78] Lenskii, E. V.
Motion of Flexible Strings in an Ideal Liquid.
Vestnik Moskovskogo Universiteta Mekhanika 33(1):116-127, 1978.
In Russian, translation Allerton Press 1978.

[Lighthill 60] Lighthill, M. J.
Note on the Swimming of Slender Fish.
Journal of Fluid Mechanics 9:305-317, 1960.

[Ramberg 77] Ramberg, S. E. and Griffin, O. M.
Free Vibrations of Taut and Slack Marine Cables.
Journal of the Structural Division, ASCE 103(ST11):2079-2092, November, 1977.

[Whitham 74] Whitham, G.B.
Linear and Non-Linear Waves.
John Wiley & Sons, New York, 1974, chapter Hyperbolic Systems.

Chapter 2

STATICS AND LINEARISED CABLE DYNAMICS

2.1 Introduction

Static solutions can be obtained from the governing equations derived in chapter 1 by retaining only the time independent terms. For a cable hanging solely under its own weight, the results are the well known catenary equations [Irvine 81]. An important simplification of the dynamic problem is obtained when the solution is assumed to consist of a static part and small oscillations around this mean position. The governing equations can then be separated in non-linear static and linearised dynamic equations.

The static problem, including hydrodynamic loading, has been investigated extensively. For a review see [Casarella 70]. The linearised cable dynamic equations have been derived by Goodman and Breslin [Breslin 74] for two dimensions. Linearised dynamic equations for the case of a towed configuration can be found in [Firebaugh 72].

2.2 Static Equations in Three Dimensions

By setting all dynamic quantities equal to zero in (1.30) and (1.33) we obtain the following set of static equations, with a subscript o to denote static quantities:

$$\frac{\partial T_{eo}}{\partial s} + F_{to} - w_o \cdot \sin\phi_o = 0$$

$$\Omega_{30} \cdot T_{eo} + F_{no} - w_o \cdot \cos\phi_o \cdot \cos\psi_o = 0$$

$$F_{bo} + w_o \cdot \cos\phi_o \cdot \sin\psi_o = 0$$

$$\Omega_{30} = \frac{1}{\cos\psi_o} \cdot \frac{\partial \phi_o}{\partial s} \tag{2.1}$$

$$\Omega_{10} = \frac{\partial \psi_o}{\partial s} - \tan\psi_o \cdot \tan\phi_o \cdot \frac{\partial \phi_o}{\partial s}$$

$$\frac{\partial \theta_o}{\partial s} + \frac{\partial \phi_o}{\partial s} \cdot \tan\psi_o \cdot \frac{1}{\cos\phi_o} = 0$$

where F_{to} , F_{no} , F_{bo} are the components in the $(\vec{t}_o , \vec{n}_o , \vec{b}_o)$ system of the hydrodynamic drag forces. The external forces can be expressed in terms of the Euler angles as:

$$F_{to} = -\frac{1}{2} \rho_w C_{dt} D_o v_{tr} | v_{tr} | (1+e_o/2)$$

$$F_{no} = -\frac{1}{2} \rho_w C_{dn} D_o (v_{nr}^2 + v_{br}^2)^{\frac{1}{2}} v_{nr}(1+e_o/2)$$

$$F_{bo} = -\frac{1}{2} \rho_w C_{db} D_o (v_{nr}^2 + v_{br}^2)^{\frac{1}{2}} v_{br}(1+e_o/2)$$

where v_{tr} , v_{nr} , v_{br} are, in this case, the components in the ($\vec{t}_o$, $\vec{n}_o$, $\vec{b}_o$) system of the current velocity, which can be expressed as:

$$v_{tr} = - U \cdot \cos(\theta_o - \alpha) \cdot \cos\phi_o$$

$$v_{nr} = - U \left[\sin(\theta_o - \alpha) \cdot \sin\psi - \cos(\theta_o - \alpha) \cdot \sin\phi_o \cdot \cos\psi_o \right]$$

$$v_{nb} = - U \left[\sin(\theta_o - \alpha) \cdot \cos\psi + \cos(\theta_o - \alpha) \cdot \sin\phi_o \cdot \sin\psi_o \right]$$

where α is the angle between the current velocity U and the (x,y) plane (see figure 2-1).

The above equations can be simplified as:

$$\frac{\partial T_{eo}}{\partial s} + F_{to} - w_o \cdot \sin\phi_o = 0$$

$$\frac{T_{eo}}{\cos\psi_o} \cdot \frac{\partial \phi_o}{\partial s} + F_{no} - w_o \cdot \cos\psi_o \cdot \cos\phi_o = 0$$

$$F_{bo} + w_o \cdot \sin\psi_o \cdot \cos\phi_o = 0 \qquad (2.2)$$

$$\frac{T_{eo} \cos\phi_o}{\sin\psi_o} \cdot \frac{\partial \theta_o}{\partial s} - F_{no} + w_o \cdot \cos\psi_o \cdot \cos\phi_o = 0$$

The following three geometric relations must be added:

$$\frac{\partial x}{\partial s_o} = (1+e_o) \cos\theta_o \cdot \cos\phi_o$$

$$\frac{\partial y}{\partial s_o} = (1+e_o) \cos\theta_o \cdot \sin\phi_o \qquad (2.3)$$

$$\frac{\partial z}{\partial s_o} = - (1+e_o) \sin\theta_o \cdot \cos\phi_o$$

together with a tension-strain relation:

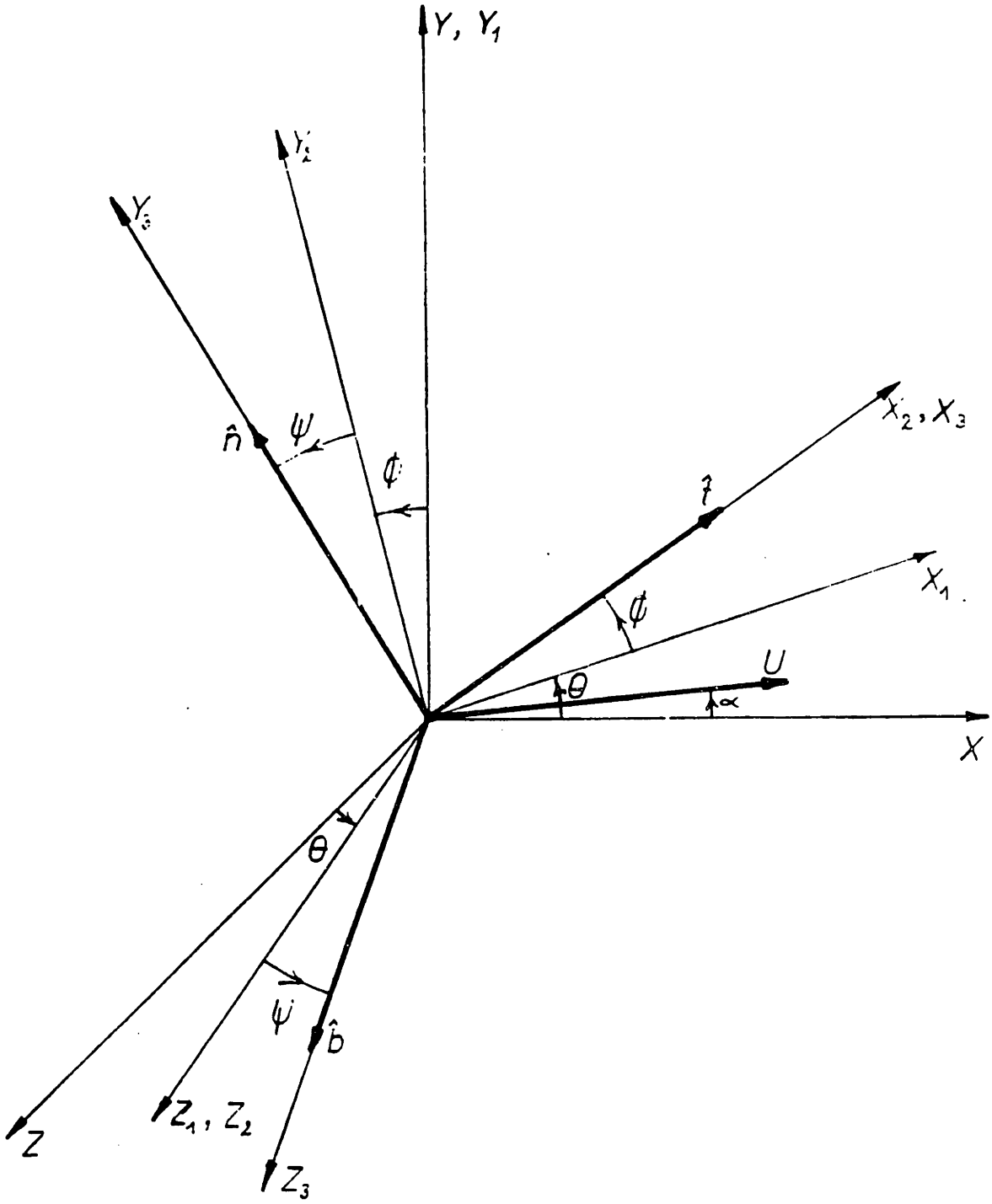

Figure 2-1: Definition of the Current in Euler Angles

$$T_{eo} = E \cdot A \cdot e_o$$

Equations (2.2) and (2.3) constitute the complete set of governing equations for static analysis. The non-linear ordinary differential equations must be supplemented with appropriate initial conditions for numerical integration. In most mooring applications a horizontal force or tension is applied at the top, in a prescribed direction. The prescribed water depth D_w is an integral constraint:

$$D_w = \int_o^l (1+e_o)\cos\theta_o \cdot \sin\phi_o \, ds \tag{2.4}$$

An iterative, shooting method, using the angle ϕ_o, can be used to satisfy this constraint.

In two dimensions the static equations can be written, with $\psi_o = 0$ and $\theta_o = 0$, as[2]:

$$\begin{aligned} \frac{\partial T_{eo}}{\partial s} &= w_o \sin\phi_o - F_{to} \\ T_{eo} \frac{\partial \phi_o}{\partial s} &= w_o \cos\phi_o - F_{no} \end{aligned} \tag{2.5}$$

with: $F_{to} = + 0.5\rho_w C_{Dt} D_o U \cos\phi_o \mid U\cos\phi_o \mid (1+e_o/2)$

$$F_{no} = - 0.5\rho_w C_{Dn} D_o U \sin\phi_o \mid U\sin\phi_o \mid (1+e_o/2)$$

The static equations (2.5) are accompanied by the following two geometric relations:

---

[2]The subscript $_o$ indicates static variables.

$$\frac{\partial x}{\partial s} = (1+e_o)\cos\phi_o$$

$$\frac{\partial y}{\partial s} = (1+e_o)\sin\phi_o \qquad (2.6)$$

and a tension-strain relation as in the three-dimensional case.

2.3 Linear Dynamic Equations

Next we derive the equations governing the dynamics of small deviations from the static configuration, i.e. we set:

$$T_e = T_o + T_1$$

$$\phi = \phi_o + \phi_1$$

$$\theta = \theta_o + \theta_1$$

$$\psi = \psi_o + \psi_1$$

$$\Omega_1 = \Omega_{10} + \Omega_{11}$$

$$\Omega_3 = \Omega_{30} + \Omega_{33}$$

The dynamic part[3], T_1 etc., is small compared with the static part, T_o etc. Similarly, the velocities (v_1, v_2, v_3) and rotations (ω_1, ω_2, ω_3) are assumed to be small when properly non-dimensionalized. Then we proceed to subtract the static equations from the dynamic equations and to simplify the remaining terms by retaining only first order combinations in the dynamic quantities. We obtain, after a lengthy linearisation process, the equations:

---

[3]The subscript for the effective tension will be dropped, for convenience, in the sequel.

$$m \cdot \frac{\partial v_1}{\partial t} = \frac{\partial T_1}{\partial s} + F_{t1} - w_o \cdot \cos\phi_o \cdot \phi_1$$

$$M_2 \cdot \frac{\partial v_2}{\partial t} = \Omega_{30} \cdot T_1 + \Omega_{31} \cdot T_o + F_{n1}$$

$$+ w_o \cdot (\cos\phi_o \cdot \sin\psi_o \cdot \psi_1 + \sin\phi_o \cdot \cos\psi_o \cdot \phi_1) \qquad (2.7)$$

$$M_3 \cdot \frac{\partial v_3}{\partial t} = F_{b1} + w_o \cdot (\cos\phi_o \cdot \cos\psi_o \cdot \psi_1 - \sin\phi_o \cdot \sin\psi_o \cdot \phi_1)$$

where $M_2 = m+m_{an}$, $M_3 = m+m_{ab}$ and F_{t1} , F_{n1} , F_{b1} denote the linearisation of the hydrodynamic drag forces F_t , F_n , F_b respectively. Similarly, we proceed to linearise the compatibility relations.

$$\frac{\partial v_1}{\partial s} - v_2 \cdot \Omega_{30} = \frac{\partial e_1}{\partial t} = \frac{1}{EA} \cdot \frac{\partial T_1}{\partial t}$$

$$\frac{\partial v_2}{\partial s} + v_1 \cdot \Omega_{30} - v_3 \cdot \Omega_{10} = \omega_3 (1+e_o) \qquad (2.8)$$

$$\frac{\partial v_3}{\partial s} + v_2 \cdot \Omega_{10} = - \omega_2 (1+e_o)$$

The linearisation of the relation between the rotation and the Darboux vectors gives:

$$\frac{\partial \Omega_{11}}{\partial t} = \frac{\partial \omega_1}{\partial s} - \omega_2 \cdot \Omega_{30}$$

$$0 = \frac{\partial \omega_2}{\partial s} + \omega_1 \cdot \Omega_{30} - \omega_3 \cdot \Omega_{10} \qquad (2.9)$$

$$\frac{\partial \Omega_{33}}{\partial t} = \frac{\partial \omega_3}{\partial s} + \omega_2 \cdot \Omega_{10}$$

The Darboux vector expressed in Euler angles gives:

$$\Omega_{31} \cdot \cos\psi_o - \Omega_{30} \cdot \sin\psi_o \cdot \psi_1 = \frac{\partial \phi_1}{\partial s}$$

$$\Omega_{11} = -\frac{\partial \psi_1}{\partial s} - \left(\frac{\tan\phi_o}{\cos^2 \psi_o} \cdot \psi_1 + \frac{\tan\psi_o}{\cos^2 \phi_o} \cdot \phi_1 \right) \frac{\partial \phi_o}{\partial s}$$

$$- \tan\psi_o \cdot \tan\phi_o \frac{\partial \phi_1}{\partial s} \qquad (2.10)$$

$$0 = \frac{\partial \theta_1}{\partial s} + \frac{\partial \phi_1}{\partial s} \cdot \tan\psi_o \cdot \frac{1}{\cos\phi_o} + \frac{\partial \phi_o}{\partial s} \cdot \frac{1}{\cos^2 \psi_0} \cdot \psi_1 \cdot \frac{1}{\cos\phi_o}$$

$$+ \frac{\partial \phi_o}{\partial s} \tan\psi_o \cdot \frac{\tan\phi_o}{\cos\phi_o} \cdot \phi_1$$

The rotation vector, expressed in Euler angles, gives:

$$\omega_1 = \sin\phi_o \cdot \frac{\partial \theta_1}{\partial t} + \frac{\partial \psi_1}{\partial t}$$

$$\omega_2 = \cos\psi_o \cdot \cos\phi_o \cdot \frac{\partial \theta_1}{\partial t} + \sin\psi_o \cdot \frac{\partial \phi_1}{\partial t} \qquad (2.11)$$

$$\omega_3 = - \sin\psi_o \cdot \cos\phi_o \cdot \frac{\partial \theta_1}{\partial t} + \cos\psi_o \cdot \frac{\partial \phi_1}{\partial t}$$

Next we introduce small dynamic displacements (p,q,r) along the static ($\vec{t}_o$, $\vec{n}_o$, $\vec{b}_o$) directions respectively. To first order the velocities are given as:

$$v_1 = \frac{\partial p}{\partial t} + (\text{H.O.T.})$$

$$v_2 = \frac{\partial q}{\partial t} + (\text{H.O.T.}) \qquad (2.12)$$

$$v_3 = \frac{\partial r}{\partial t} + (\text{H.O.T.})$$

We should point out here that relations (2.12) will be modified substantially in the non-linear case, because p, q, r are defined in the direction of the static vectors $\vec{t}_o$, $\vec{n}_o$, $\vec{b}_o$ while the velocities are defined along the dynamic vectors $\vec{t}$, $\vec{n}$, $\vec{b}$.

Next, we observe that all dynamic equations, except for (2.7), can be reduced by one time derivative if we use equations (2.11) to eliminate (ω_1 , ω_2 , ω_3). Thus we obtain for the equations of motion:

$$m \cdot \frac{\partial^2 p}{\partial t^2} = \frac{\partial T_1}{\partial s} + F_{t1} - w_o \cdot \cos\phi_o \cdot \phi_1$$

$$M_2 \cdot \frac{\partial^2 q}{\partial t^2} = \Omega_{30} \cdot T_1 + \Omega_{31} \cdot T_o + F_{n1}$$
$$+ w_o (\cos\phi_o \cdot \sin\psi_o \cdot \psi_1 + \sin\phi_o \cdot \cos\psi_o \cdot \phi_1) \qquad (2.13)$$

$$M_3 \cdot \frac{\partial^2 r}{\partial t^2} = F_{b1} + w_o (\cos\phi_o \cdot \cos\psi_o \cdot \psi_1 - \sin\phi_o \cdot \sin\psi_o \cdot \phi_1)$$

The compatibility relations become:

$$\frac{\partial p}{\partial s} - q \cdot \Omega_{30} = \frac{T_1}{E \cdot A}$$

$$\frac{\partial q}{\partial s} + p \cdot \Omega_{30} - r \cdot \Omega_{10} = (- \sin\psi_o \cdot \cos\phi_o \cdot \theta_1 + \cos\psi_o \cdot \phi_1)(1+e_o) \quad (2.14)$$

$$\frac{\partial r}{\partial s} + q \cdot \Omega_{10} = - (\cos\psi_o \cdot \cos\phi_o \cdot \theta_1 + \sin\psi_o \cdot \phi_1)(1+e_o)$$

where the linearised component of the Darboux vector satisfies relation (2.10).

We have as dynamic variables the quantities p, q, r, ϕ_1, θ_1, ψ_1, Ω_{11}, Ω_{31} and T_1, which must satisfy a set of nine differential equations (2.10), (2.13) and (2.14). The above equations are the complete, linear, three-dimensional equations of motion of a cable about an arbitrary, three-dimensional, static configuration.

2.4 Three-dimensional Linear Dynamics of a Cable with Two-Dimensional Static Configuration

In the particular case of a cable with a two-dimensional static configuration, the governing equations can be set in a simple form, which can provide a number of important solutions.

When the static configuration is planar then:

$$\psi_o = 0$$

$$\theta_o = \text{const } (= 0 \text{ for convenience})$$

$$\Omega_{10} = 0$$

and equations (2.13) through (2.14) can be simplified as follows:

$$m \cdot \frac{\partial^2 p}{\partial t^2} = \frac{\partial T_1}{\partial s} + F_{t1} - w_o \cdot \cos\phi_o \cdot \phi_1$$

$$M_2 \cdot \frac{\partial^2 q}{\partial t^2} = \frac{d\phi_o}{ds} \cdot T_1 + \frac{\partial \phi_1}{\partial t} \cdot T_o + F_{n1} + w_o \cdot \sin\phi_o \cdot \phi_1 \qquad (2.15)$$

$$M_3 \cdot \frac{\partial^2 r}{\partial t^2} = F_{b1} + w_o \cdot \cos\phi_o \cdot \psi_1$$

where we used that in this case

$$\Omega_{30} = \frac{d\phi_o}{ds}$$

$$\Omega_{31} = \frac{\partial \phi_1}{\partial s}$$

with the compatibility relations:

$$\frac{\partial p}{\partial s} - q \frac{\partial \phi_o}{\partial s} = \frac{T_1}{E \cdot A}$$

$$\frac{\partial q}{\partial s} + p \frac{\partial \phi_o}{\partial s} = \phi_1 (1+e_o) \qquad (2.16)$$

$$\frac{\partial r}{\partial s} = - \cos\phi_o \cdot \theta_1 (1+e_o)$$

The equations for the in-plane dynamics (p,q), therefore, including the compatibility relations, are completely decoupled from the equation for the out-of-plane motion r, for the case of a static two-dimensional configuration:

$$m \cdot \frac{\partial^2 p}{\partial t^2} = \frac{\partial T_1}{\partial s} - w_o \cdot \cos\phi_o \cdot \phi_1 + F_{t1}$$

$$M_2 \cdot \frac{\partial^2 q}{\partial t^2} = \frac{d\phi_o}{ds} \cdot T_1 + \frac{\partial \phi_1}{\partial s} \cdot T_o + w_o \cdot \sin\phi_o \cdot \phi_1 + F_{n1}$$

$$\frac{\partial p}{\partial s} - q \cdot \frac{d\phi_o}{ds} = \frac{T_1}{E \cdot A} \qquad (2.17)$$

$$\frac{\partial q}{\partial s} + p \cdot \frac{d\phi_o}{ds} = \phi_1 (1+e_o)$$

The solution method for the above equations will be the focus of chapter 3.

2.5 Out-of-Plane Dynamics

From equation (2.10) by setting $\psi_o = 0$, we obtain:

$$\psi_1 = - \left[\frac{\partial \phi_o}{\partial s} \right]^{-1} \cos\phi_o \cdot \frac{\partial \theta_1}{\partial s}$$

Using the third compatiblity relation of (2.16), this can be written as:

$$\psi_1 = \left[\frac{\partial \phi_o}{\partial s} \right]^{-1} \cdot \frac{\partial}{\partial s} \left[\frac{1}{1+e_o} \cdot \frac{\partial r}{\partial s} \right] + \frac{\tan\phi_o}{1+e_o} \cdot \frac{\partial r}{\partial s}$$

The equation of motion in the out-of-plane direction becomes:

$$M_3 \cdot \frac{\partial^2 r}{\partial t^2} = F_{b1} + \frac{w_o \cdot \cos\phi_o}{[d\phi_o/ds]} \cdot \frac{\partial}{\partial s} \left[\frac{1}{1+e_o} \cdot \frac{\partial r}{\partial s} \right] + w_o \cdot \frac{\sin\phi_o}{1+e_o} \cdot \frac{\partial r}{\partial s} \qquad (2.18)$$

which is a string equation with variable tension. The out-of-plane dynamics are completely uncoupled within linear theory, therefore, and their governing equation can be brought to the simple form of (2.18).

2.6 Linearisation of External Forces

The linearisation of the external forces is a difficult problem. Not only are the hydrodynamic forces difficult to linearise due to their quadratic form, but they depend also on the local inclination angle. Therefore, their linearisation will provide additional angle dependent terms, which should be included in the equations. In the author's opinion direct expression along the natural coordinates of the static solution is more useful in that case.

2.7 References

[Breslin 74] Breslin, J. P.
Dynamic Forces Exerted by Oscillating Cables.
Journal of Hydronautics 8(1):18-31, January, 1974.

[Casarella 70] Casarella, M. J. and Parsons, M.
A Survey of Investigations and Motions of Cable Systems under Hydrodynamic Loading.
Marine Technology Society Journal 4(4), July-August, 1970.

[Firebaugh 72] Firebaugh, M. S.
An Analysis of the Dynamics of Towing Cables.
PhD thesis, M.I.T., Department of Ocean Engineering, 1972.

[Irvine 81] Irvine, H. M.
Cable Structures.
MIT Press, Cambridge, MA and London, England, 1981.

Chapter 3

SOLUTIONS FOR LINEAR DYNAMICS

3.1 Introduction

In this chapter, we will describe in detail the solution for the linearised equations of a uniform, single span cable, with a two dimensional static configuration. To highlight the interesting dynamic properties of cables, we will restrict ourselves to the case where the gravity force is dominant over the static current force, although the methodology can be extended to include a current. This assumption will also permit direct comparison with previous work on linearised cable dynamics.

The emphasis was put on analytical solutions and the physical explanation of the dynamic characteristics. This will hopely lead to a better understanding and improved designs of cable systems which are subject to dynamic loads.

Our primary interest will be in the calculation of the eigenmodes and eigenvalues, which can be used, within the frame of linear systems analysis, to solve any loading problem of the cable.

3.2 Governing Equations

The governing equations were derived in chapter 2. The in-plane and out-of-plane dynamics are uncoupled and can be written, under the assumptions described above, as:

In-plane motion:

$$m \frac{\partial^2 p}{\partial t^2} = \frac{\partial T_1}{\partial s} - w_o \cos\phi_o \, \phi_1$$

$$M \frac{\partial^2 q}{\partial t^2} = \frac{\partial \phi_o}{\partial s} T_1 + \frac{\partial \phi_1}{\partial s} T_o + w_o \sin\phi_o \, \phi_1 \qquad (3.1)$$

$$\frac{\partial p}{\partial s} - q \frac{\partial \phi_o}{\partial s} = e_1$$

$$\frac{\partial q}{\partial s} + p \frac{\partial \phi_o}{\partial s} = \phi_1 (1+e_o)$$

Out-of-plane motion:

$$M \frac{\partial^2 r}{\partial t^2} = \frac{\partial}{\partial s} \left[\left(\frac{\partial \phi_o}{\partial s} \right)^{-1} w_o \frac{\cos\phi_o}{1+e_o} \frac{\partial r}{\partial s} \right] \qquad (3.2)$$

The out-of-plane equation is a simple taut string equation with variable tension along the length.

3.3 Strings

The taut wire is the first cable to attract attention, because it was used for musical instruments. Pythagoras in the 6th century BC and Aristotle in the 3rd century BC knew quantatively the relation between frequency, tension and length of a taut chord. Galileo (1564 - 1642) in 1638, and the monk M. Mersenne (1588 - 1648) in 1636, published qualitative relations based on experimental measurements. R. Hooke (1635 - 1703) and J. Sauveur (1653 - 1716) published also experimental measurements of taut wire frequencies and

obeservations of modes for the various harmonics.

B. Taylor (1685 - 1731) in 1713 published the first dynamic solution of the transverse cable dynamics by assuming a response shape. Daniel Bernoulli (1700 - 1782) published in 1738 theorems of oscillations of hanging chains and in 1755 his superposition principle of several harmonics for the taut wire, which was opposed, surprisingly, both by D'Alembert and Euler and remained controversial until 1822, when Fourier illustrated such superpositions. D'Alembert (1736 - 1813) was the first to derive the partial differential equation governing the small amplitude transverse motion of a taut wire and J.L. Lagrange (1736 -1813) solved fully the problem by considering the string as consisting of many (n) interconnected mass particles and then taking the limit as $n \rightarrow \infty$.

Euler (1707 - 1783) derived the equation of a hanging chain and then obtained a series solution and an estimate of the 3 first natural frequencies. S.D. Poisson (1781 - 1840) derived the equation of a cable element subject to an external force in 1820, and used it to derive a final solution to the problems of the hanging chain and of the taut wire.

In the case of a taut wire with zero gravity force, the static angle ϕ_o and the curvature $d\phi_o/ds$ are zero, so we obtain (see figure 3-1):

$$m \frac{\partial^2 p}{\partial t^2} = \frac{\partial T_1}{\partial s}$$

$$M \frac{\partial^2 q}{\partial t^2} = T_o \frac{\partial \phi_1}{\partial s}$$

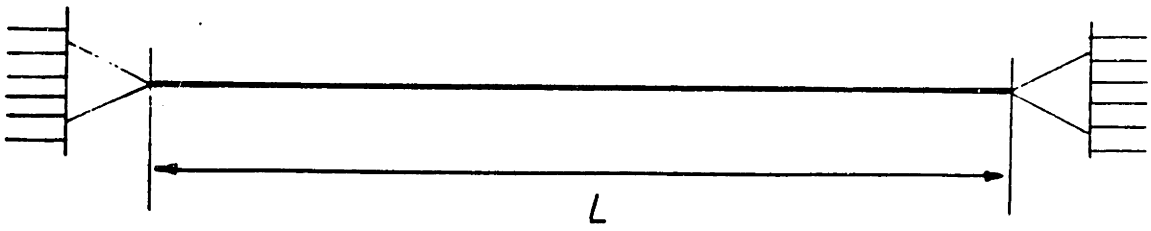

Figure 3-1: Taut String

(3.3)

$$\frac{\partial p}{\partial s} = e_1$$

$$\frac{\partial q}{\partial s} = \phi_1 \, (1+e_o \,)$$

with $T_1 = E \cdot A_o \cdot e_1$

Assuming a taut wire in air, we obtain:

$$\rho A_o \frac{\partial^2 q}{\partial t^2} = \frac{T_o}{1+e_o} \cdot \frac{\partial^2 q}{\partial s^2}$$

(3.4)

$$\rho \frac{\partial^2 p}{\partial t^2} = E \frac{\partial^2 p}{\partial s^2}$$

Equations (3.4) are the equations for the transverse and for the longitudinal (elastic) dynamics. The two equations are uncoupled and the first equation gives the impression that elasticity plays no role in the transverse

dynamics. This is of course erroneous, because an inelastic wire simply can not vibrate (it is geometrically impossible to create waves on an inelastic straight line, because it can not accept even the infinitesimal stretch, which is required to adjust the increased length of a non-straight configuration). So elasticity is not important quantitatively, but very important qualitatively, and any solution that assumes the elastic stiffness as infinite is bound to fail to reproduce the taut wire results.

The natural frequencies for a taut wire of length L are obtained by taking the Fourier transform of (3.4).[4]

$$
\begin{aligned}
-\rho A_o\, \omega^2\, q &= \frac{T_o}{1+e_o}\,\frac{d^2q}{ds^2} \\
-\rho\, \omega^2\, p &= E\,\frac{d^2p}{ds^2}
\end{aligned}
\qquad (3.5)
$$

with: $q(0) = q(L) = 0$

$p(0) = p(L) = 0$

and since the general solution is:

$$q(s) = c_1 \sin(k_1 s) + c_2 \cos(k_1 s)$$

$$p(s) = c_3 \sin(k_2 s) + c_4 \cos(k_2 s)$$

---

[4]When an equation is written in the sequel in the frequency domain, the dynamic variables represent the complex amplitude of the dynamic quantities.

with: $k_1 = \dfrac{\omega}{\left[T/\rho A_o(1+e_o)\right]^{1/2}}$

$$k_2 = \frac{\omega}{\left[E/\rho\right]^{1/2}}$$

we obtain:

$$\omega_n = \frac{n\pi}{L}\left[\frac{T}{\rho A^o(1+e_o)}\right]^{1/2} \qquad \text{transverse, } n=1,2,3...$$

$$\omega_m = \frac{m\pi}{L}\left[\frac{E}{\rho}\right]^{1/2} \qquad \text{elastic, } m=1,2,3...$$

3.4 Hanging Chains

The freely hanging cable in air (see figure 3-2) has also been studied extensively, first by, Poisson who derived the governing equations. Within the present framework, we have $\phi_o = \pi/2$, $\dfrac{d\phi_o}{ds} = 0$, $T_o = w_o s$:

$$m\frac{\partial^2 q}{\partial t^2} = \frac{\partial}{\partial s}\left[\frac{w_o\, s}{1+e_o}\frac{\partial q}{\partial s}\right]$$

$$\rho\frac{\partial^2 p}{\partial t^2} = E\frac{\partial^2 p}{\partial s^2} \qquad (3.6)$$

The same elastic solution is found, therefore, in the tangential direction. In the normal direction, after making the assumption that the cable extension caused by its own weight is negligible, we obtain in air the equation:

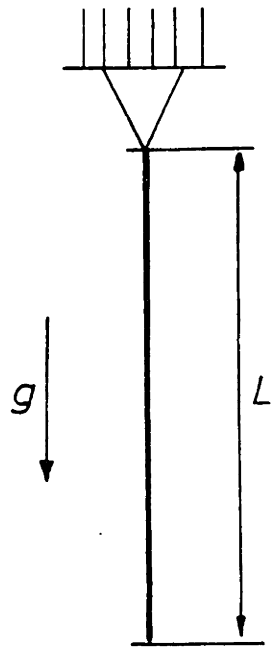

Figure 3-2: Hanging Chain

$$- \omega^2 \, q = \frac{d}{ds} \left[gs \, \frac{dq}{ds} \right] \tag{3.7}$$

and the solution is:

$$q(s) = c_1 \, J_o \left(2\omega \left[\frac{s}{g} \right]^{1/2} \right) + c_2 \, y_o \left(2\omega \left[\frac{s}{g} \right]^{1/2} \right) \tag{3.8}$$

where J_o is the Bessel function of the first kind and order zero, and y_o the Bessel function of the second kind and order zero. In order for the solution to remain finite at $s = 0$, the second term must vanish since y_o is infinite at $s = 0$, so the natural frequencies are obtained simply as roots of

$$J_o \left(2\omega \left[\frac{L}{g} \right]^{1/2} \right) = 0 \qquad (3.9)$$

The first five roots can be found as [Hildebrand 49]

n	1	2	3	4	5
$\omega\left[L/g\right]^{1/2}$	1.204	2.760	4.327	5.896	7.465

In the case of a vertical chain with non zero lower end tension, the equation for the transverse dynamics becomes, after neglecting the effect of the static strain:

$$m \frac{\partial^2 q}{\partial t^2} = \frac{\partial}{\partial s} \left[(T_o + w_o s) \frac{\partial q}{\partial s} \right] \qquad (3.10)$$

The static tension is lineary varying from the bottom to the top. To find the eigenfrequencies, we have to solve the following eigenvalue problem:

$$- \omega^2 q = \frac{d}{ds} \left[\left(\frac{T_o}{m} + gs\right) \frac{dq}{ds} \right] \qquad (3.11)$$

with boundary condition $q(0) = q(L) = 0$

The solution of known problem is also expressible in terms of zeroth order Bessel functions:

If we denote: $\gamma = \dfrac{2(m)^{1/2}}{w_o}$

then: $q(s) = c_1 J_o \left[\gamma\omega (w_o s + T_o)^{1/2} \right]$

$$+ c_2 y_o \left[\gamma\omega (w_o s + T_o)^{1/2} \right] \qquad (3.12)$$

3.5 WKB Solution for Strings with Variable Tension

The transverse equation for strings with variable tension is given by:

$$M(s)\,\frac{\partial^2 q}{\partial t^2} = \frac{\partial}{\partial s}\left[\, T(s)\,\frac{\partial q}{\partial s}\,\right] \tag{3.13}$$

Taking the Fourier Transform and non-dimensionalising the length variable $\sigma = s/L$, we obtain:

$$\frac{d}{d\sigma}\left[\, T(\sigma)\,\frac{dq}{d\sigma}\,\right] + L^2\, M(\sigma)\,\omega^2\, q = 0 \tag{3.14}$$

This equation is suitable to be solved using asymptotic analysis, if we assume that:

- $T(\sigma)$ and $M(\sigma)$ are slowly varying (compared with the dynamic solution) functions of σ

- or the non-dimensional frequency $\bar{\omega}^2$ is large. $\bar{\omega}^2 = M\omega^2\, L^2/T$

It is important to note that if one or both of the above conditions are met, the asymptotic analysis will be valid. We perform a transformation of variables suggested by Nayfeh [Nayfeh 73]

$$\xi = \left[\, T \,\right]^{1/2} q$$

After substitution and expansion of the derivatives, we obtain:

$$\ddot{\xi} + \left[\, -\frac{1}{2}\,\frac{\ddot{T}}{T} + \frac{1}{4}\,\frac{\dot{T}^2}{T^2} + \frac{\omega^2\, L^2\, M}{T} \,\right] \xi = 0 \tag{3.15}$$

If the conditions formulated above are met, we can try to find a WKB[5]

---

[5]Expansion named after Wentzel, Kramers and Brillouin

expansion of the form:

$$\xi = e^{\omega g_o} + g_1 + g_2/\omega + g_3/\omega^2 \tag{3.16}$$

where the coefficients are determined from substitution in (3.15). The leading order approximation is:

$$\xi = \frac{1}{(M/T)^{1/4}} \exp\{ \pm i\omega L \int_0^{\sigma} (M/T)^{1/2} \, d\sigma \} \tag{3.17}$$

So the following solution for the transverse displacement is obtained:

$$q = \frac{1}{(MT)^{1/4}} \exp\{ \pm i\omega L \int_0^{\sigma} (M/T)^{1/2} \, d\sigma \} \tag{3.18}$$

(for a higher order approximation, see appendix B.)

Example: WKB solution for a string with linearly varying tension. The solution is given as:

$$q = \frac{1}{\left[M(w_o L\sigma + T_o)\right]^{1/4}} \exp\left(\pm i \, 2\omega (M^{1/2}/w_o)\left[(w_o L\sigma + T_o)^{1/2} - T_o^{1/2}\right] \right) \tag{3.19}$$

where σ is the non-dimensional length.

This example is used in chapter 4, to find the accuracy of the WKB method versus the exact solution. The above solution is increasingly more accurate as the tension variation per wavelength becomes smaller.

The solution breaks down when the lower end tension becomes zero as can be seen in (3.19). The governing equation has a singular turning point. The solution was first formulated by Langer and can be found in [Nayfeh 73] as follows:

We assume an expansion for the tension as:

$$T = a\sigma + b\sigma^2$$

The solution can be written as:

$$q(s) = \frac{(W)^{1/2}}{(TM)^{1/4}} C_o (\omega L W) \tag{3.20}$$

$$\text{where: } W = \int_0^{\sigma} \frac{d\sigma}{(T/M)^{1/2}}$$

C_o are the cylinder functions of zeroth order (J_o , Y_o). In the case of a freely hanging chain, the solution (3.20) is identical with the exact solution. The WKB solution can be found from (3.20) or from the exact solution (3.8) using the large argument asymptotic approximation for the Bessel functions.

It is interesting to note that for constant tension, the WKB solution is the exact solution, and for linear varying tension, the singular turning point analysis gives the exact solution. In most cable analyses the tension variation between top and bottom is not very large, so that a regular WKB solution seems more than adequate to solve equations of the type (3.13)

Although the WKB method is not valid for a first order pole of the equation (3.15), the WKB method remains valid fore a second order pole of (3.15). This means that for static tension of quadratic dependence in the space coordinate, the WKB solution remains valid, even close to the singularity. This relatively unknown feature of the WKB solution is particular important in very slack cables, where the tension at the point of lowest tension varies quadratically.

This can be proved as follows: we consider a quadratic tension variation $T = b\sigma^2$. The first order WKB solution is obtained from:

$$\ddot{\xi} + \frac{\omega^2 L^2 M}{b\sigma^2} \cdot \xi = 0 \tag{3.21}$$

The solution is:

$$\xi = \frac{1}{(M/T)^{1/4}} \exp \{ \pm i\omega L \int_0^{\sigma} [(M/T)^{1/2}] ds \} \tag{3.22}$$

Expansion of (3.22) for small values of σ, assuming $\omega L(M/b)^{1/2}$ large, gives:

$$\xi \sim \sigma \exp \{1/2 \pm i\omega L (M/b)^{1/2}\} \tag{3.23}$$

If we perform local analysis of (3.21) directly by assuming a solution x^{ν} near $\sigma = 0$, we obtain again as solution:

$$\xi \sim \sigma \exp \{1/2 \pm i\omega L (M/b)^{1/2}\} \tag{3.24}$$

i.e., the WKB method has the correct asymptotic behavior for small σ.

3.6 Inextensible Cables

Next we consider the dynamic behavior of a uniform inextensible chain in the plane of its equilibrium configuration. The oscillations are assumed to be small, so that the linearised equations can be used. The governing equations (3.1) can now be written as:

$$m \frac{\partial^2 p}{\partial t^2} = \frac{\partial T_1}{\partial s} - w_o \cos\phi_o \, \phi_1$$

$$M \frac{\partial^2 q}{\partial t^2} = \frac{\partial \phi_o}{\partial s} T_1 + \frac{\partial \phi_1}{\partial s} T_o + w_o \sin\phi_o \, \phi_1$$

(3.25)

$$\frac{\partial p}{\partial s} - q \frac{\partial \phi_o}{\partial s} = 0$$

$$\frac{\partial q}{\partial s} + p \frac{\partial \phi_o}{\partial s} = \phi_1$$

where m and M are assumed to be constant.

The previous equations were obtained from (3.1) using the assumption that the strain is zero. Note, however, that the dynamic tension is not equal to zero, i.e. a motion of the cable can still generate tension, although it does not generate strain. We write the displacements p and q in non-dimensional form as ξ , η . The variable σ now denotes the non-dimensional length. Taking the Fourier transform of (3.25):

$$- mL^2 \omega^2 \xi = \frac{dT_1}{d\sigma} - w_o L \cos\phi_o \phi_1$$

$$- ML^2 \omega^2 \eta = T_1 \frac{d\phi_o}{d\sigma} + T_o \frac{d\phi_1}{d\sigma} + w_o L \sin\phi_o \phi_1$$

(3.26)

$$\frac{d\xi}{d\sigma} - \eta \frac{d\phi_o}{d\sigma} = 0$$

$$\frac{d\eta}{d\sigma} + \xi \frac{d\phi_o}{d\sigma} = \phi_1$$

The study of the eigenfrequencies and modes of an inextensible chain hanging between two points at the same level was initiated by Rohrs in 1851 [Rohrs 51]. Routh studied the exact solution for a chain hanging in the

form of a cycloid [Routh 55]. He obtained his cycloidal shape by taking a cable with non-uniform mass. For this case, the dynamic equations can be solved exactly. For the small sag case his results are reduced to the results of Rohrs who used a priori the small sag assumption for his analysis.

Pugsley [Pugsley 49] derived semi-empirical formulas to predict the eigenfrequencies for a uniform chain. An approximate solution for the linearised chain problem was derived by Saxon and Cahn [Saxon 53]. Their results, based on a second order perturbation method, predict accurately the eigenfrequencies and eigenmodes for relatively flat chains, or for higher order modes. Goodey [Goodey 61] arrived at similar results starting from the intrinsic form of the chain problem.

This analysis will follow closely the one used by Saxon and Cahn. A more careful perturbation analysis of the problem reveals however that a revised first order perturbation scheme is able to predict the eigenfrequencies and eigenmodes far beyond the validity of the second order solution derived by Saxon and Cahn.

The effect of added mass is directly included in the derivation. The derived solutions can be used equally well to predict eigenmodes and eigenfrequencies of inclined inextensible chains, or to calculate the response to an imposed excitation at one end.

3.6.1 Statics

Some basic equations from the static analysis are needed in our derivation For a catenary differential element equilibrium of the forces gives: (The following relations are valid for extensible cables as well, if the weight is

the only external force.)

$$T_o \frac{d\phi_o}{d\sigma} = w_o L \cos\phi_o$$

$$\frac{dT_o}{d\sigma} = w_o L \sin\phi_o \qquad (3.27)$$

Then the following basic static relations are obtained from (3.27):

$$T_o = \frac{H}{\cos\phi_o}$$

$$\frac{d\phi_o}{d\sigma} = \alpha \cos^2\phi_o \qquad (3.28)$$

H is the horizontal tension in the chain and α ($=w_o L/H$) is the ratio of the total weight of the catenary in the appropriate fluid and the horizontal tension.

The ratio α and the value of the static angle at some specific point along the cable define completely the static shape of the chain hanging under its own weight. As it will be seen in the sequel, they define also, together with the added mass, the dynamic behavior. The following useful relation exists between the top angle ϕ_t, the bottom angle ϕ_b and α:

$$\tan\phi_t = \tan\phi_b + \alpha$$

For a chain which is tangential to the bottom:

$$\tan\phi_t = \alpha$$

while for the case of a horizontal chain:

$$\phi_t = - \phi_b$$

so:

$$2 \tan\phi_b = \alpha.$$

3.6.2 Horizontal, Small Sag, Inextensible Cable

Rohrs derived the dynamic solution for a shallow sag, inextensible cable, which we will re-derive here to illustrate the various concepts involved.

The case of an inextensible cable, hanging between two points of equal height is considered. A Lagrangian coordinate σ, with the origin at the center of the cable is introduced. (See figure 3-3). When the cable is assumed to be shallow (sag over span less than 1/8) the following approximations are valid.

$$T_o = \frac{H}{\cos\phi_o} \cong H$$

$$\frac{d\phi_o}{d\sigma} = \alpha \cos^2\phi_o \cong \alpha$$

$$\phi_o = \alpha \sigma \tag{3.29}$$

$$\frac{b}{L} = \frac{\alpha}{8}$$

$$l = L\left[1 - \frac{1}{24}(\alpha^2)\right]$$

where: b = sag
l = span
$\alpha = w_o L/H$
H = horizontal tension
L = length of the cable

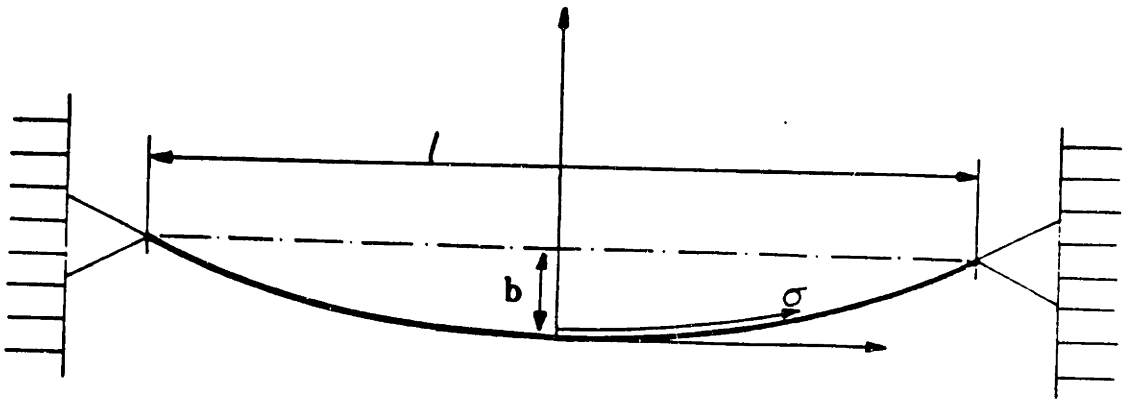

Figure 3-3: Shallow Sag, Horizontal Cable

l: Span of the cable
L: Length of the cable
H: Horizontal tension
b: sag

From the above equations, we note that for shallow sag cables:

$$\alpha = \frac{w_o L}{H} << 1$$

Rohrs derived solutions for the eigenfrequencies and mode shapes. Starting with the general inextensible governing equations:

$$- mL^2 \omega^2 \xi = \frac{dT_1}{d\sigma} - w_o L \cos\phi_o \phi_1$$

$$- ML^2 \omega^2 \eta = T_1 \frac{d\phi_o}{d\sigma} + T_o \frac{d\phi_1}{d\sigma} + w_o L \sin\phi_o \phi_1 \qquad (3.30)$$

$$\frac{d\xi}{d\sigma} - \eta \frac{d\phi_o}{d\sigma} = 0$$

$$\frac{d\eta}{d\sigma} + \xi \frac{d\phi_o}{d\sigma} = \phi_1$$

Note that the non-dimensional natural frequencies will be of the same order of magnitude as those of a taut string with equivalent mass and average tension. This means that:

$$\omega_n^2 \frac{ML^2}{H} = O(n^2 \pi^2) \qquad n=1,2,3...$$

is a number much larger than 1 even for the first eigenfrequencies. Therefore we can conclude that:

$$\omega_n^2 \frac{ML^2}{H} >> \frac{w_o L}{H} \qquad (3.31)$$

From the third relation of (3.30), we note that:

$$\frac{d\xi}{d\sigma} = \eta \frac{d\phi_o}{d\sigma} \qquad (3.32)$$

so that the rate of change for ξ is small, of order α. Our main interest is in motions for which the boundary conditions are fixed (or at least at one end is fixed). If we assume that η is of the same order as ϵ, then we can conclude that:

$$\xi = O(\epsilon^2)$$

Using the last relation of (3.25), the order of ϕ_1 can be determined as:

$$\phi_1 = O(\epsilon)$$

We obtain from the equation for tangential dynamics, using (3.29):

$$T_1 = T_{io} + \int_0^\sigma (-\, m\omega^2 L^2 \xi + w_o L \phi_1)\, ds \tag{3.33}$$

where T_{1o} is an integration constant.

This can be substituted in the relation for the normal dynamics, using (3.29):

$$M\omega^2 L^2 \eta = \alpha \left[T_{1o} + \int_0^\sigma (-m\omega^2 L^2 \xi + w_o L \phi_1)\, ds \right]$$

$$+ H \frac{d\phi_1}{d\sigma} + w_o L \alpha \sigma \phi_1 \tag{3.34}$$

To leading order:

$$-\, M\omega^2 L^2 \eta = \alpha T_{1o} + H \frac{d^2\eta}{ds^2} + O(\epsilon^2) \tag{3.35}$$

which gives as solution:

$$\eta(\sigma) = c_1 \sin(kL\sigma) + c_2 \cos(kL\sigma) - \frac{\alpha T_{1o}}{M\omega^2 L^2} \tag{3.36}$$

with: $k = \omega \left[\frac{M}{H} \right]^{1/2}$

To find the eigenfrequencies, we impose fixed boundary conditions:

$$\eta(-\frac{1}{2}) = \eta(\frac{1}{2}) = 0$$

Anti-symmetric modes of (3.36) are only possible if:

$$c_2 = 0$$

$$T_{1o} = 0$$

$$\frac{kL}{2} = n\pi \tag{3.37}$$

These are the odd modes with respect to the middle point of the cable and are completely equivalent to the corresponding string modes. Note also that no additional tension is generated.

The even, or symmetric modes (in the transverse natural displacement) are obtained as:

$$\eta(\sigma) = \frac{\alpha T_{1o}}{M\omega^2 L^2} \cdot \left[\frac{\cos kL\sigma}{\cos kL/2} - 1 \right] \tag{3.38}$$

Apparently no eigenfrequencies requirement can be derived from (3.38). However, we have also to consider the boundary conditions in the tangential direction. Expressing the tangential motion as a function of the transverse solution, gives:

$$\xi(\sigma) = \frac{\alpha^2 T_{1o}}{M\omega^2 L^2} \cdot \left[\frac{1}{kL} \cdot \frac{\sin kL\sigma}{\cos kL/2} - \sigma \right] + C \tag{3.39}$$

The boundary conditions in this case are

$$\xi(1/2) = \xi(-1/2) = 0$$

They can only be satisfied if the integral C = 0 and:

$$\tan(kL/2) = kL/2$$

It is interesting to note that in this case a dynamic tension is generated in the cable. The first symmetric eigenfrequency is located at 2.86 π, compared to π for a string. This is due to the fact that the first symmetric mode of a string is possible only if stretching is allowed, so for an inelastic chain the geometric compatibility relations are modifying significantly the modal shapes.

Table 3-I gives the eigenfrequencies for a string and an inextensible cable. Figure 3-4 shows a comparison between their mode shapes. Hopefully this example illustrates the fundamental difference between cables and strings. We will now discuss the general asymptotic solution for inextensible cables, without making the simplifying small sag assumption.

3.6.3 Derivation of the Governing Equation in the form of a Fourth Order Differential Equation

The linearised equations of motion of an inextensible chain can be written as:

$$\begin{aligned} -m\,\omega^2\,\xi\,L^2 &= \frac{dT_1}{d\sigma} - w_o\,L\cos\phi_o\,\phi_1 \\ -M\,\omega^2\,\eta\,L^2 &= T_1\frac{d\phi_o}{d\sigma} + T_o\frac{d\phi_1}{d\sigma} + w_o\,L\sin\phi_o\,\phi_1 \end{aligned} \tag{3.40}$$

By defining a new dynamic angle $\phi_1^* = \phi_1/\alpha$ and a new non-dimensional

Anti-symmetric Modes

	n	1	2	3	4
Chain	$\bar{\omega}_n$	2π	4π	6π	8π
String					

Symmetric Modes

	n	1	2	3	4
Chain	$\bar{\omega}_n$	2.86π	4.92π	6.94π	8.95π
String		π	3π	5π	7π

where: $\bar{\omega}_n = \omega_n \, L \left[\frac{M}{H} \right]^{1/2}$

Table 3-I: Comparison between the Natural Frequencies of a String and of an Inextensible Small Sag Cable

String

Inextensible Cable

Symmetric

does not exist

$\bar{\omega} = \pi$

Anti-Symmetric

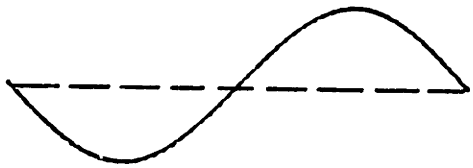

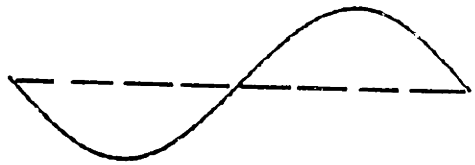

$\bar{\omega} = 2\pi$

$\bar{\omega} = 2\pi$

Symmetric

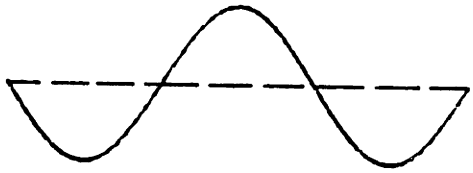

$\bar{\omega} = 3\pi$

$\bar{\omega} = 2.86\pi$

Figure 3-4: Comparison Mode Shapes of a String and of an Inextensible, Small Sag Cable

dynamic tension $T_1^* = T_1/w_oL$, and by using the static relations (3.28), and the relation $d\phi_o/ds = \alpha\cos^2\phi_o$ to change the independent variable from σ to ϕ_o, the linearised equations can be written as:

$$
\begin{aligned}
-\frac{m\omega^2 H}{w_o^2}\,\xi &= \cos^2\frac{dT_1^*}{d\phi_o} - \cos\phi_o\,\phi_1^* \\
-\frac{M\omega^2 H}{w_o^2}\,\eta &= \cos^2\phi_o\,T_1^* + \cos\phi_o\,\frac{d\phi_1^*}{d\phi_o} + \sin\phi_o\,\phi_1^*
\end{aligned}
\tag{3.41}
$$

We introduce two new parameters: h (=m/M), which is the ratio of the mass over the mass plus added mass, and λ^2 ($=M\omega^2 H/w_o^2$), which is the non-dimensional frequency parameter.

After dropping the superscripts, the equations of motion can be written as:

$$
\begin{aligned}
-h\,\lambda^2\,\xi &= \cos^2\phi_o\,\frac{dT_1}{d\phi_o} - \cos\phi_o\,\phi_1 \\
-\lambda^2\,\eta &= \cos^2\phi_o\,T_1 + \cos\phi_o\,\frac{d\phi_1}{d\phi_o} + \sin\phi_o\,\phi_1
\end{aligned}
\tag{3.42}
$$

The non-dimensional frequency parameter λ is fundamental for the perturbation analysis. It can be written as:

$$
\lambda = \frac{\omega\, c_H}{h\, g\, (1-\rho\text{fluid}/\rho\text{mat})} \tag{3.43}
$$

The parameter λ is large for high frequencies and for large horizontal wave speeds (c_H).

The compatibility relations are given by:

$$
\begin{aligned}
\frac{d\xi}{d\sigma} - \eta\,\frac{d\phi_o}{d\sigma} &= 0 \\
\frac{d\eta}{d\sigma} + \xi\,\frac{d\phi_o}{d\sigma} &= \phi_1^*\,\alpha
\end{aligned}
\tag{3.44}
$$

These equations can be rewritten (dropping the superscript) as:

$$\frac{d\xi}{d\phi_o} = \eta$$
$$\frac{d\eta}{d\phi_o} + \xi = \frac{\phi_1}{\cos^2\phi_o} \tag{3.45}$$

Equations (3.42) and (3.45) are the constitutive equations for the dynamics of an inextensible chain. A change of independent variable has been performed. The static angle ϕ_o is now the independent variable instead of the length scale. This results in a simplification of the equations, so that η , ϕ_1 , T_1 can be eliminated and a fourth order differential equation in ξ is obtained:

$$\cos\phi_o\ \xi^{IV} - 2\ \sin\phi_o\ \xi^{III} + \left[\ \cos\phi_o + \frac{\lambda^2}{\cos^2\phi_o}\ \right] \xi^{II}$$
$$- 2\left[\ \sin\phi_o - \frac{\sin\phi_o \lambda^2}{\cos^3\phi_o}\ \right] \xi^{I} - \frac{h\ \lambda^2}{\cos^2\phi_o}\ \xi = 0 \tag{3.46}$$

The superscripts denote differentiation with respect to ϕ_o. If $h = 1$, the original equation derived by Saxon and Cahn is recovered [Saxon 53].

The prescribed boundary conditions for mooring line applications are normally:

$$\xi(\phi_1) = 0 \qquad \xi(\phi_2) = \text{given}$$
$$\eta(\phi_1) = \xi_{\phi_o}(\phi_1) = 0 \qquad \eta(\phi_2) = \xi_{\phi_o}(\phi_2) = \text{given}$$

Other boundary conditions can also be imposed. The eigenmodes and eigenfrequencies are found by imposing homogeous boundary conditions at both ends and searching for non-zero solutions.

3.6.4 Self-Adjoint Form

The constitutive equation is in self-adjoint form and the fourth order differential equation can be written as:

$$\left[\cos\phi_o \ \xi^{II} \right]^{II} + \left[\left(2\cos\phi_o + \frac{\lambda^2}{\cos^2\phi_o} \right)\xi^{I} \right]^{I} - \frac{h\lambda^2}{\cos^2\phi_o}\,\xi = 0 \qquad (3.47)$$

The above equation reduces to (3.46) by expanding the derivatives. Surprisingly, this fact seems to have escaped the attention of previous researchers.

The above equation describes completely the linear dynamic behavior of an inextensible cable under its own weight. The four governing equations can be reduced to a single fourth order differential equation, only for inextensible cables. The independent variable in the above equation is the static angle ϕ_o.

3.6.5 Orthogonality Condition

Using the self-adjoint form of the inextensible cable equation, the following very important property for the eigenmodes can be proven (see appendix C).

$$\int_{\phi_{bot}}^{\phi_{top}} \left[\frac{\xi_i^I \ \xi_j^I}{\cos^2\phi_o} + \frac{h\ \xi_i\ \xi_j}{\cos^2\phi_o} \right] d\phi_o = 0 \qquad \text{for } i \neq j \qquad (3.48)$$

where ξ_i , ξ_j are the eigenmodes in the tangential direction with fixed boundaries. We can rewrite the compatibility condition, using the Lagrangian coordinate as the independent variable as, in the form:

$$\int_0^1 (M\ \eta_i\ \eta_j + m\ \xi_i\ \xi_j\ )\ d\sigma = 0 \qquad \text{for } i \neq j \qquad (3.49)$$

where:

η_i , η_j the components of the eigenmodes in the transverse direction

ξ_i , ξ_j the components of the eigenmodes in the tangential direction

3.6.6 Derivation of Asymptotic Solutions

The solutions are achieved by postulating two different types of motion when λ is large. One is wave-like and fast varying compared to the coefficients of the equation. Physically it represents transverse waves in the chain. The other type of solution is slowly varying in space and represents instant adjustement of the chain to a disturbance, so as to preserve constant length (inextensible chain).

3.6.6.1 The Fast Solution

A solution in WKB form is proposed:

$$\xi = \exp \{ \lambda \int f_1 + \int g_1 + \frac{1}{\lambda} \int h_1 + \frac{1}{\lambda^2} \int i_1 + ... \} \tag{3.50}$$

The novelty of the approach consists of substituting (3.50) directly in (3.46) without making any simplifying assumption a priori.

The results were obtained by using MACSYMA[6]:

---

[6]MACSYMA is a computer program used for performing symbolic and numerical mathematical manipulations. It is developed by the Mathlab Group of the M.I.T. Laboratory of Computer Science

$$O(\lambda^4) \qquad f_1(\phi_o) = \pm \frac{i}{\cos^{3/2}\phi_o}$$

$$f_1^2(\phi_o) = 0 \tag{3.51}$$

The second solution indicates that two slow solutions must exist and will be analysed separately.

$$O(\lambda^3) \qquad g_1(\phi_o) = -\frac{7}{4}\frac{\sin\phi_o}{\cos\phi_o} \tag{3.52}$$

$$O(\lambda^2) \qquad h_1(\phi_o) = \mp i \cos^{3/2}\phi_o \left[\frac{28 - 16h}{32} - \frac{29}{32}\tan^2\phi_o \right] \tag{3.53}$$

Results for $O(\lambda)$ and $O(1)$ were also calculated but for reasons to be given later, the usefulness of these results seems limited.

The fast solution can be written as:

$$\xi_f = \cos^{7/4}\phi_o \begin{matrix}\cos \\ \sin\end{matrix} (\lambda f + h/\lambda) \tag{3.54}$$

where: $f = \int_{\phi_b}^{\phi_o} \frac{1}{\cos^{3/2}\phi_o}\, d\phi_o$

$$h = -\int_{\phi_b}^{\phi_o} \cos^{3/2}\phi_o \left[\frac{28 - 16h}{32} - \frac{29}{32}\tan^2\phi_o \right] d\phi_o$$

For the boundary value problem considered, the solution for the normal displacement is also required. It is given by:

$$\eta_f = -7/4 \cos^{3/4}\phi_o \sin\phi_o \begin{matrix}\cos \\ \sin\end{matrix} (\lambda f + h/\lambda)$$
$$\mp \cos^{7/4}\phi_o (\lambda \dot{f} + \dot{h}/\lambda) \begin{matrix}\sin \\ \cos\end{matrix} (\lambda f + h/\lambda) \tag{3.55}$$

The solution (3.54) and (3.55) is, to leading order, equivalent with the Saxon and Cahn solution. However the second order terms are different from

the ones found by Saxon and Cahn.

Even more important, to obtain the normal displacement correct to O(1), a term obtained directly from the leading order solution in (3.54), appears in (3.55). This term is not appearing in the Saxon and Cahn solution. The correct solution to O(1) is therefore given by:

$$\xi_f = \cos^{7/4}\phi_o \begin{matrix}\cos\\ \sin\end{matrix} (\lambda f) \tag{3.56}$$

$$\eta_f = -\ 7/4\ \cos^{3/4}\phi_o\ \sin\phi_o \begin{matrix}\cos\\ \sin\end{matrix} (\lambda f) \mp \cos^{7/4}\phi_o\ \lambda \dot{f} \begin{matrix}\sin\\ \cos\end{matrix} (\lambda f) \tag{3.57}$$

3.6.6.2 The Slow Solution

The slow solution is found from (3.46) by assuming λ large, when the equation becomes:

$$\frac{\lambda^2}{\cos^2\phi_o}\,\xi^{II} + 2\,\frac{\sin\phi_o}{\cos^3\phi_o}\,\lambda^2\,\xi^{I} - \frac{h\,\lambda^2}{\cos^2\phi_o}\,\xi = O(1) \tag{3.58}$$

Simplification gives:

$$\xi^{II} + 2\tan\phi_o\ \xi^{I} - h\xi = O(1/\lambda^2) \tag{3.59}$$

This equation is independent of the frequency. The solutions are [Triantafyllou 82a]:

$$\xi_{s1} = (1-h^2) + h^2\sin\phi_o + \frac{h}{2}(h-1)\cos^2\phi_o + O(h^3) \tag{3.60}$$

$$\xi_{s2} = (1-h)\cos^3\phi_o + 3(3+h)\left[(\phi_o - \frac{\pi}{2})\sin\phi_o + \cos\phi_o\right] + O(h^3) \tag{3.61}$$

$$\eta_{s1} = \left[h^2 - h(h-1)\sin\phi_o\right]\cos\phi_o + O(h^3) \tag{3.62}$$

$$\eta_{s2} = -\ 3\cos\phi_o\left[(1-h)\cos\phi_o\sin\phi_o - (3+h)(\phi_o - \frac{\pi}{2})\right] + O(h^3) \tag{3.63}$$

3.6.6.3 Total Solution

The total solution to (3.46) is given by linear combination of (3.56) (3.57) and (3.60) - (3.63).

$$\xi = A\xi_{f1} + B\xi_{f2} + C\xi_{s1} + D\xi_{s2}$$

$$\eta = A\eta_{f1} + B\eta_{f2} + C\eta_{s1} + D\eta_{s2} \tag{3.64}$$

The eigenvalues can be found, by finding the values of λ for which:

$$\text{Det} \begin{bmatrix} \eta_{f1}(\phi_1) & \eta_{f2}(\phi_1) & \eta_{s1}(\phi_1) & \eta_{s2}(\phi_1) \\ \xi_{f1}(\phi_1) & \xi_{f2}(\phi_1) & \xi_{s1}(\phi_1) & \xi_{s2}(\phi_1) \\ \eta_{f1}(\phi_2) & \eta_{f2}(\phi_2) & \eta_{s1}(\phi_2) & \eta_{s2}(\phi_2) \\ \xi_{f1}(\phi_2) & \xi_{f2}(\phi_2) & \xi_{s1}(\phi_2) & \xi_{s2}(\phi_2) \end{bmatrix} = 0 \tag{3.65}$$

3.7 Verification of the Solution

We will verify the results by calculating the eigenfrequencies of an inextensible chain hanging between two points at the same level. Many experimental and calculated results have been published. [Pugsley 49], [Saxon 53], [Goodey 61]

3.7.1 Eigenfrequencies

The solution is considerably simplified by noting that one slow and one fast solution are symmetric and the other anti-symmetric. The eigenfrequency equation (3.65) can be separated, therefore, in one for even modes and one for odd modes.

3.7.1.1 Odd Normal Modes

The requirement becomes[7]:

$$\frac{\eta_{f1}(\phi_o)}{\xi_{f1}(\phi_o)} = \frac{\eta_{s1}(\phi_o)}{\xi_{s1}(\phi_o)}$$

$$\tan(\lambda f+h/\lambda) = - \frac{1}{\lambda[1 + h/(\lambda^2 f)]} \left[\frac{\phi_o \cos^{5/2}\phi_o}{\cos\phi_o + \phi_o \sin\phi_o} + 7/4 \sin\phi_o \cos^{1/2}\phi_o\right] \quad (3.66)$$

3.7.1.2 Even Normal Modes

The requirement becomes

$$\frac{\eta_{f2}(\phi_o)}{\xi_{f2}(\phi_o)} = \frac{\eta_{s2}(\phi_o)}{\xi_{s2}(\phi_o)}$$

$$\cot(\lambda f+h/\lambda) = \frac{1}{\lambda[1+h/(\lambda^2 f)]} \left[\frac{\cos^{5/2}\phi_o}{\sin\phi_o} + 7/4 \sin\phi_o \cos^{1/2}\phi_o\right] \quad (3.67)$$

3.7.2 Consistency with Previous Results

For large λ, the eigenfrequencies calculated by (3.66) and (3.67) give the same results as derived by Saxon and Cahn [Saxon 53] and Goodey [Goodey 61].

3.7.2.1 Odd Normal Modes

Equation (3.66) can be rewritten for high order modes as:

---

[7] To make use of the symmetry, the origin is selected in the middle of the cable. The lower limit of the integrals in f and h is therefore 0. The angle ϕ_o is the static angle at the end point.

$$\lambda = \frac{n\pi}{f}\left[\,1 - \frac{f(h + k_1)}{n^2\,\pi^2}\,\right] + O\left[\,\left(\frac{1}{n^4}\right)\,\right] \tag{3.68}$$

where: $$(h + k_1) = -\frac{1}{32}\int_0^{\phi_o}(12 - 29\tan^2\phi_o)\cos^{3/2}\phi_o d\phi_o + \frac{\phi_o\cos^{5/2}\phi_o}{\phi_o\sin\phi_o + \cos\phi_o} + \frac{7}{4}\sin\phi_o\cos^{1/2}\phi_o$$

which is identical to the formula derived by Saxon and Cahn, and by Goodey.

3.7.2.2 Even Normal Modes

Equation (3.67) can be rewritten for high order modes as:

$$\lambda = \frac{(n + 0.5)\pi}{f}\left[\,1 - \frac{f(h + k_2)}{(n + 0.5)^2\pi^2} + O\left(\frac{1}{n^4}\right)\,\right] \tag{3.69}$$

where: $$(h + k_2) = -\frac{1}{32}\int_0^{\phi_o}(12 - 29\tan^2\phi_o)\cos^{3/2}\phi_o d\phi_o + \frac{\cos^{5/2}\phi_o}{\sin\phi_o} + \frac{7}{4}\sin\phi_o\cos^{1/2}\phi_o$$

which is also identical to the result of Saxon and Cahn, and Goodey.

3.7.3 Comparison of the Perturbation Results with the Numerical Solutions

We will now compare numerically the results obtained by the new perturbation theory, with those of Saxon and Cahn and those of the finite difference scheme. The figures on which the results are plotted have the same format as the one used by Goodey (see figure 3-5). The horizontal axis is the static angle at the top. The frequency is non-dimensionalised with respect to the natural frequency of a pendulum with length equal to the chain span:

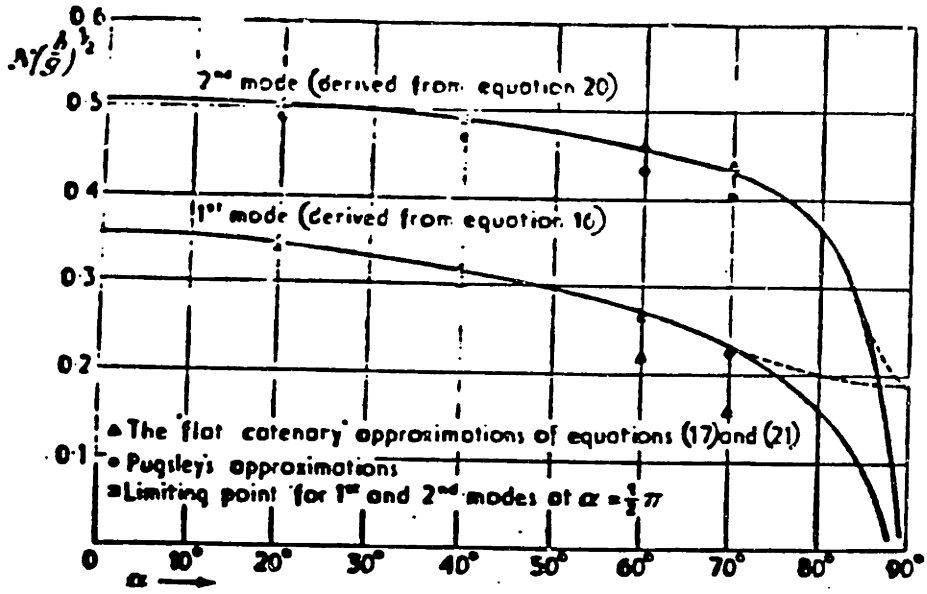

Figure 3-5: Eigenfrequencies of a Catenary [Goodey 61]

$$f\left[\frac{b}{g}\right]^{1/2} \tag{3.70}$$

where: f = frequency
b = sag at midspan

The relation between the non-dimensional parameter λ and the new non-dimensional frequency parameter is obtained directly from statics:

$$f\left[\frac{b}{g}\right]^{1/2} = 0.5\left[\frac{1 - \cos\phi_{top}}{\cos\phi_{top}}\right]^{1/2}\frac{\lambda}{\pi} \tag{3.71}$$

The results are shown in the figures 3-6 and 3-7 and are significant, because:

- They clearly demonstrate the improved accuracy of the new first order theory compared to the first order theory derived by Saxon and Cahn.

- The new second order theory and that of Saxon and Cahn seem to agree very well up to a certain point, when λ becomes small and they break down.

- It is quite interesting that the new first order theory gives good results even for λ small, which is outside of the validity range of the assumptions used. No breakdown of the solution is observed.

- There are some erroneous roots of very low frequency appearing in the first order Saxon and Cahn solution and to a lesser extent in the second order perturbation solution. (Not shown on figure.) The new first order solution does not have this problem.

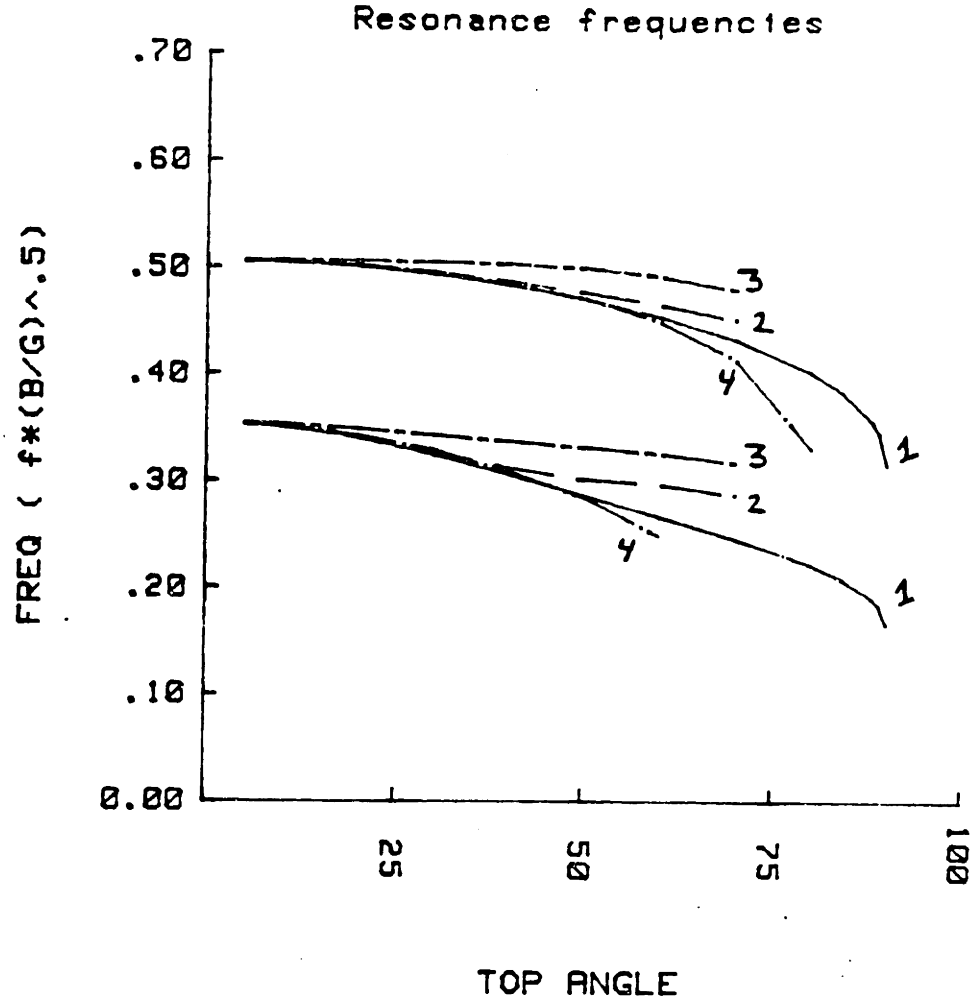

Figure 3-6: Comparison between Perturbation and Saxon and Cahn

1. New perturbation theory (first order)

2. New perturbation theory (second order)

3. Saxon and Cahn (first order)

4. Saxon and Cahn (second order)

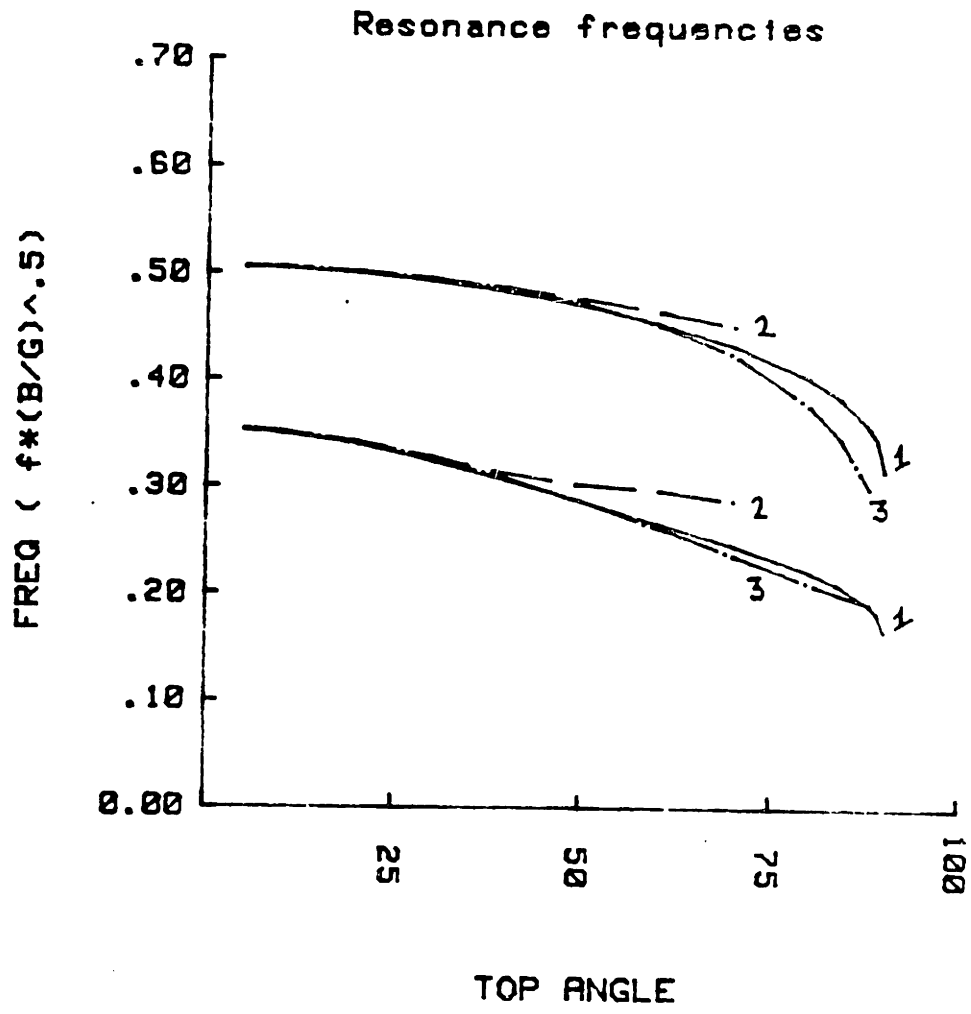

Figure 3-7: Comparison between the Perturbation Solution and the Finite Difference Solution

1. New perturbation theory (first order)

2. New perturbation theory (second order)

3. Numerical solution (explicit centered differences, 100 gridpoints, see section 3.9)

- The first order solution provides valid results even for top angles very close to the limiting value of 90^o.

3.7.4 Nearly Vertically Hanging Cables

The limit, as the top angle approaches 90^o, exists for the first order perturbation theory.

For odd modes:

$$\tan(4\pi\bar{f}) = -\frac{1}{2\pi\bar{f}}\frac{7}{4} \rightarrow \tan(2\omega) = -\frac{1}{\omega}\frac{7}{4} \tag{3.72}$$

For even modes:

$$\cotan(4\pi\bar{f}) = \frac{1}{2\pi\bar{f}}\frac{7}{4} \rightarrow \cotan(2\omega) = \frac{1}{\omega}\frac{7}{4} \tag{3.73}$$

$$\text{with: } \bar{f} = f\left[\frac{b}{g}\right]^{1/2} \rightarrow \omega = 2\pi f\left[\frac{b}{g}\right]^{1/2}$$

The roots for ω can be found in table 3-II. The odd modes approach the correct values for higher frequencies. The approximation seems to be slightly better than the WKB approximation of the same problem (see table 3-II).

The explanation of this fact can be found in the way the tension is approaching zero at the bottom of a hanging chain. It varies parabolically near the bottom, compared to a linear variation for a vertically hanging chain. One of the lesser known characteristics of a first order WKB approximation is, as discussed before, that it is a valid approximation for singular perturbation problems with parabolic singularities. This may also explain why the derived solution remains valid in regions where the wave propagation speed is low.

The even modes have no counterpart in vertically hanging cables and

new theory (in the limit)		direct solution simple vertically hanging cable attached at one point	
odd modes	even modes	Bessel solution (exact)	WKB first order
1.057		1.204	$\pi/2$
	1.996	-	-
2.868		2.760	π
	3.706	-	-
4.527		4.327	$3\pi/2$

Table 3-II: Frequencies of a Vertically Hanging Chain

they must be always considered for top angles near, but never exactly equal to 90^{o}. Clearly, at the midpoint region the equations break down when the angle is equal to 90^{o}.

3.8 Extensible Cables

In this section the dynamic characteristics of elastic cables will b investigated using the same type of perturbation analysis as for th inextensible cables. The governing equations (3.1) can be written, using nor dimensional displacements and Lagrangian coordinate, as:

$$- m L^2 \omega^2 \xi = \frac{dT_1}{d\sigma} - w_o L \cos\phi_o \phi_1$$

$$- M L^2 \omega^2 \eta = T_1 \frac{d\phi_o}{d\sigma} + T_o \frac{d\phi_1}{d\sigma} + w_o L \sin\phi_o \phi_1$$

(3.74

$$\frac{d\xi}{d\sigma} - \eta \frac{d\phi_o}{d\sigma} = \frac{T_1}{E \cdot A}$$

$$\frac{d\eta}{d\sigma} + \xi \frac{d\phi_o}{d\sigma} = \phi_1 (1 + e_o)$$

The major change, compared to the inextensible governing equation is i the tangential compatibility relation, where allowance is made for stretching The modification of this geometric condition will have a profound effect on th formation of modes.

The rather peculiar dynamic behavior of extensible cables has onl recently received appropriate attention. Davenport [Davenport 65] is one o the first to discuss dynamic properties of extensible cables for the case of th guys of a mast. Analytical solutions have been formulated for horizontal smal sag cables by Simpson [Simpson 66] and independently, using a differen method, by Irvine and Caughey [Irvine 74]. More recent work, of which thi thesis is a part, was done in the Ocean Engineering Departement at M.I.T

See for instance [Triantafyllou 83] and [Triantafyllou 84].

As in the case of inextensible cables, the analysis of a horizontal, sm sag cable, gives us valuable information about the more general cable behavi The static relations derived in subsection 3.6.1 remain valid for the extensil cable.

3.8.1 Horizontal, Small Sag, Extensible Cable

The solution to this problem can be found in [Irvine 81], but will rederived here, using the analogy with the inextensible case.

The derivation is completely similar with the one in subsection 3.6.2. leading order the transverse dynamics can be written as:

$$- M\ \omega^2\ L^2\ \eta = \alpha\ T_{1o} + \frac{H}{1+e_o}\ \frac{d^2\eta}{d\sigma^2} + O(\epsilon^2\ ) \qquad (3.7$$

To find the integration constant T_{1o}, we can use the tangent compatibility relation in (3.74), which can be integrated between the boundar where $\xi(1/2) = \xi(-1/2) = 0$:

$$\frac{T_{1o}}{E \cdot A} = - \alpha \int_{-1/2}^{1/2} \eta(\sigma)\ d\sigma \qquad (3.7$$

In the above equation the implicit assumption was made that T_{1o} constant, and this is a good assumption when no longitudinal dynamics of t cable are excited. An additional requirement for the validity of the theory therefore, that the frequency is much lower than the first elast eigenfrequency of the cable. This additional requirement was not needed the case of an inextensible cable, because the relation between normal a tangential dispiacements are completely fixed due to the tangenti

compatibility relation.

The governing equation is obtained by substituting (3.76) in (3.75).

$$\frac{H}{1.+\ e_o} \cdot \frac{d^2\eta}{d\sigma^2} + M\ \omega^2\ L^2\ \eta = \alpha^2\ E{\cdot}A \int_{-1/2}^{1/2} \eta(\sigma)\ d\sigma \qquad (3.77)$$

where: $\alpha = \dfrac{w_o L}{H}$

The above equation is completely equivalent with the governing equation derived by Irvine and Caughey [Irvine 74]. The only minor difference can be found in the fact that Irvine introduced the concept of an effective length . It is the author's opinion that this introduction is not usefull and the actual unstretched length of the cable should be used consistently.

The eigenmodes of the above equations can easily be determined [Irvine 81]. The requirement for anti-symmetric eigenmodes is:

$$\sin \frac{kL}{2} = 0 \qquad (3.78)$$

with: $k = \omega \left[\dfrac{M(1+e_o)}{H} \right]^{1/2}$

$$\simeq \omega \left[\frac{M}{H} \right]^{1/2}$$

The requirement for symmetric modes is:

$$\tan\left[\frac{kL}{2}\right] - \left[\frac{kL}{2}\right] + \frac{4}{\lambda^2}\left[\frac{kL}{2}\right]^3 = 0 \qquad (3.79)$$

where: $\lambda^2 = \left[\frac{w_o L}{H}\right]^2 \cdot \frac{E \cdot A_o}{H}$

$$A_o = (1 + e_o)A$$

λ^2 is proportional to the ratio of the elastic stiffness to the catenary stiffness. For an infinite elastic stiffness (an inextensible cable) the previous derived results are found. For a cable with infinite catenary stiffness (a perfectly extensible string) the symmetric string eigenmodes are found.

Equation (3.79) allows us to find the symmetric eigenfrequencies for the whole range of λ. For an extensive discussion of the properties of the eigenmodes and eigenfrequencies with varying λ see [Irvine 81] and [Veletsos 82]. We will limit ourselves to a plot of the eigenfrequencies versus λ. (See figure 3-8.) The points where the symmetric eigenfrequencies are equal to the anti-symmetric eigenfrequencies are called modal cross-over points.

It is also interesting to look at the modal shapes with varying λ. The transverse modal shapes for the first symmetric modes were plotted for various values of λ^2. (See figure 3-9)

The results obtained above are only valid for cables with end points on the same horizontal line and with a shallow sag. The case of an inclined cable, treated by Irvine approximately as an extension of the above theory [Irvine 78] is better treated with the more general analysis of the next section.

The theory presumes also that quasi-static stretch is present. If this is not the case, tangential dynamics will be excited and the above theory will not

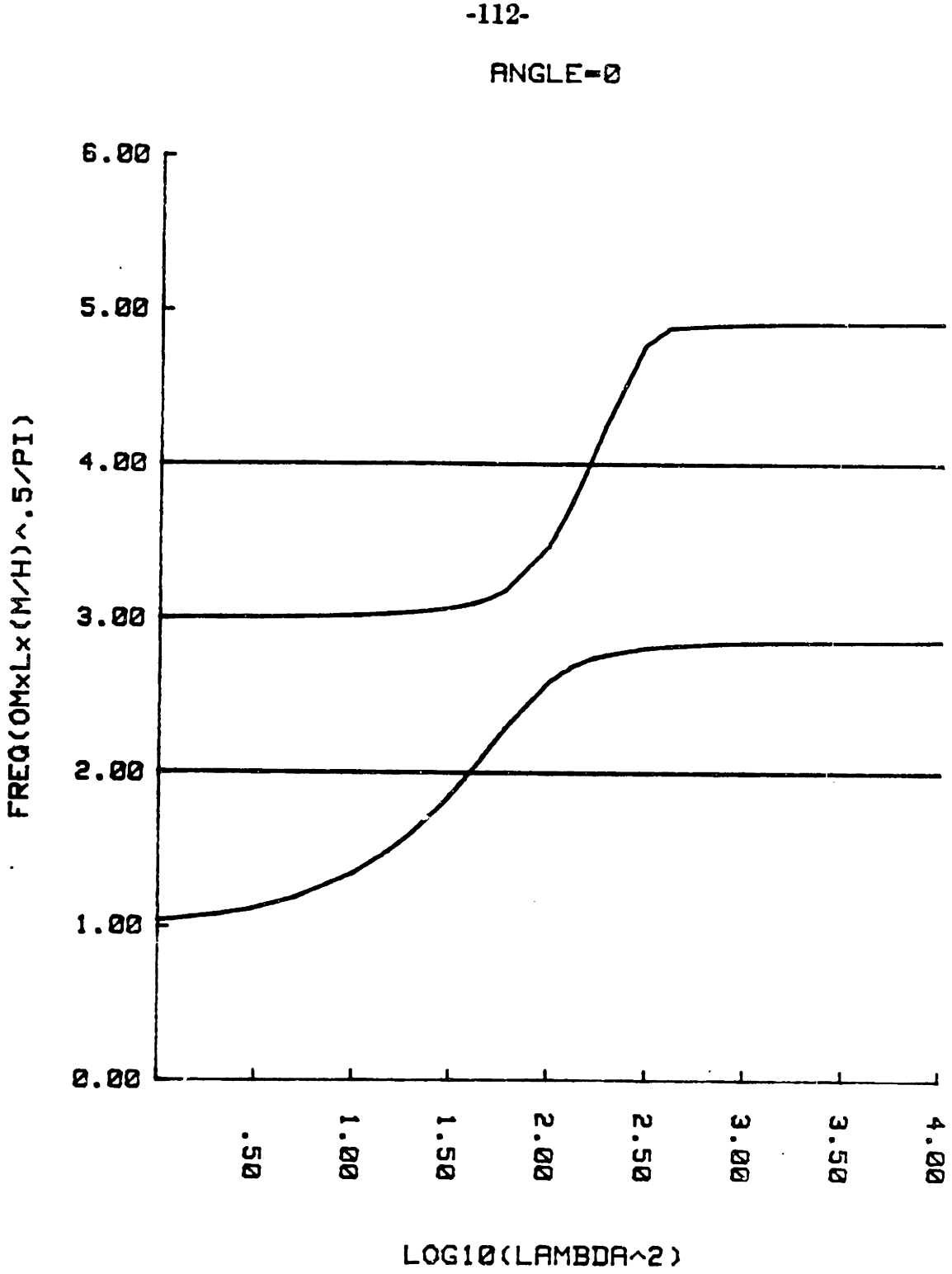

Figure 3-8: Cross-Over Phenomena for Small Sag Cable

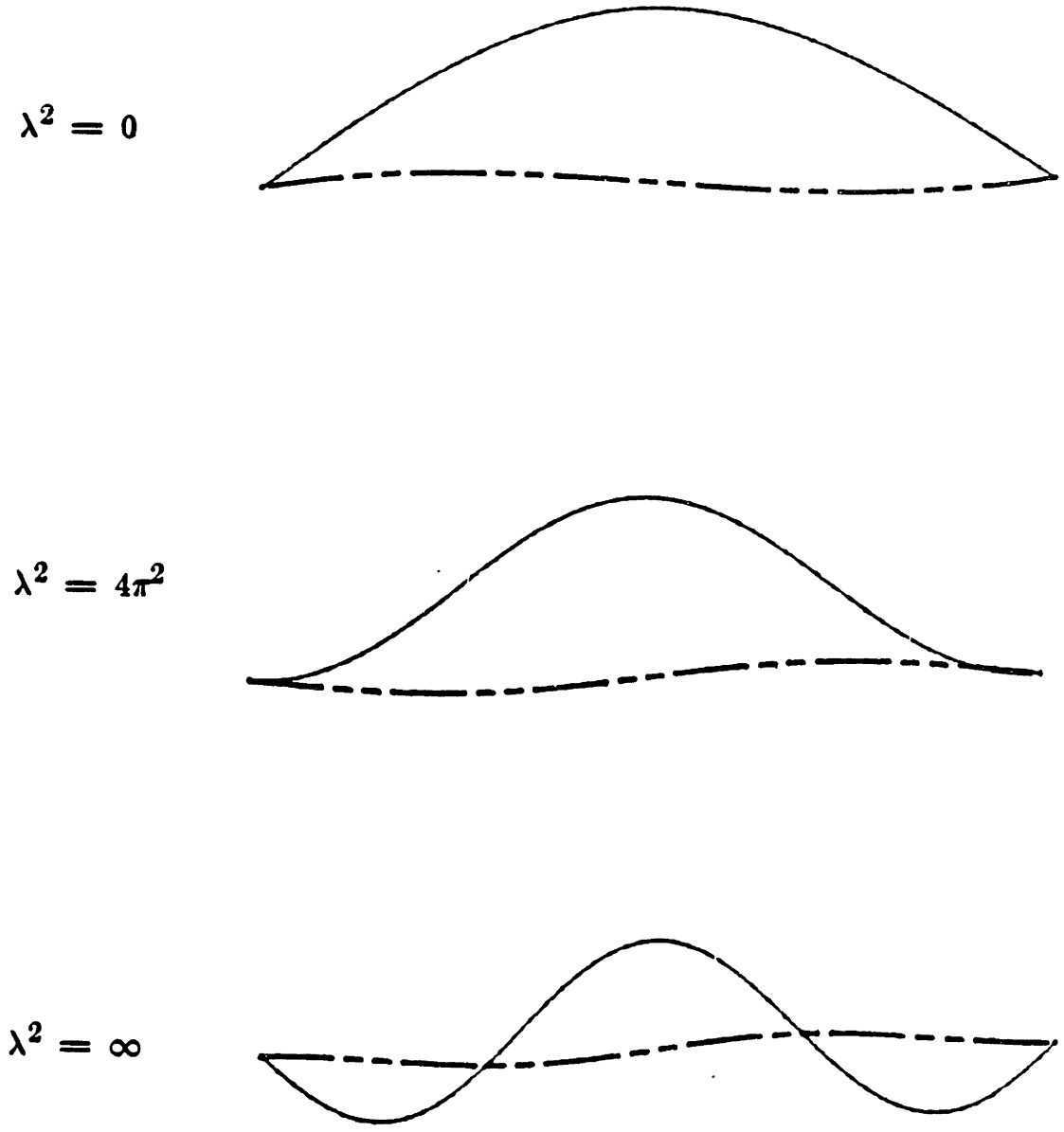

Figure 3-9: Symmetric Mode Shapes for a Small Sag Cable

(Normal displacement: full line)
(10 × tangential displacement: dotted line)

be valid. The elastic wave speed is:

$$c_{el} = \left[\frac{E}{\rho} \right]^{1/2}$$

and the transverse wave speed is:

$$c_{tr} = \left[\frac{M(1+e_o)}{H} \right]^{1/2}$$

therefore:

$$\frac{c_{tr}}{c_{el}} = \left[\frac{h \cdot H}{E \cdot A} \right]^{1/2}$$

The ratio H/EA is in general very small, so that the effects are not important until the 15 - 20 th mode. It is important to note that if we vary λ to smaller values, $w_o L/H$ should be simultaneously reduced to smaller values in order not to violate the quasi-static stretching condition. In other words, for each geometric configuration, there is a minimal value of λ^2 below which the derivations above are not valid.

3.8.2 Orthogonality Condition

In the case of extensible cables, the four differential equations cannot be reduced to one equation as in the case of inextensible cables. This makes the analysis more difficult mathematically. The orthogonality condition for the modes, though, can be proven easily.

We define H(s,r) as the matrix of the influence functions corresponding to the static displacement components in the tangential and normal direction at a point s, due to unit forces in the normal and tangent direction at point r. (H(s,r) is the Green function for the problem.)

Rosenthal proved the following reciprocity relations for cables under static forces [Rosenthal 81], which can be seen as an application of Maxwell's reciprocity principle.

$$[H(s,r)] = [H(r,s)]^T$$

or explicity:

$$H_{11}(s,r) = H_{11}(r,s)$$

$$H_{22}(s,r) = H_{22}(r,s)$$

$$H_{12}(s,r) = H_{21}(r,s)$$

$$H_{21}(s,r) = H_{12}(r,s)$$

Using the above relations, it can be proved that the following orthogonality condition holds: (see Appendix D)

$$\int_0^1 (m\ \xi_i\ \xi_j + M\ \eta_i\ \eta_j)\ d\sigma = 0 \qquad i \neq j \tag{3.80}$$

where: m: mass of the cable, per unit length

M: mass plus added mass of the cable per unit length

ξ_i: tangential components of the i th mode

η_i: normal components of the i th mode

Although the above result is well known for the dynamics of rigid structures, it is believed that it has escaped the attention of previous researchers as applied to cables. In the case of non-extensible cables, the previously derived orthogonality condition is identical with the one derived above.

3.8.3 Derivation of an Approximate Solution

In the case of an inextensible cable, we were able to use a transformation of variables to reduce the governing equations to a single, fourth order differential equation. We could then solve the fourth order differential equation using a perturbation expansion.

For an extensible cable, the equations cannot be reduced to a single, higher order differential equation. We will therefore solve directly the set of differential equations using perturbation techniques. The procedure is more general in the sense that it can be applied to cases where the shape is not dominated by the weight forces [Triantafyllou 83], although the mathematical derivation is less elegant than in the case of an inextensible cable.

The assumptions to obtain the perturbation solution are in both cases completely equivalent and indeed the inextensible results are also obtained as a limiting case of the extensible perturbation theory.

To be able to use the perturbation expansions, two assumptions over the magnitude of the coefficients are necessary.

The first assumption is that the ratio of the wave speed of the elastic waves, versus the speed of the transverse waves is large. This assumption is valid for most cable applications where the material stretching is small. Indeed from chapter 1, we obtained as wave speeds:

$$c_{el} = \left[\frac{E}{\rho} \right]^{1/2} \tag{3.81}$$

$$c_{tr} = \left[\frac{T_o}{M(1+e_o)} \right]^{1/2}$$

therefore:

$$\frac{c_{el}}{c_{tr}} = \left[\frac{E \cdot A}{T_o} \frac{1}{h} \right]^{1/2}$$

where: $h = m/M$

h is a quantity of order 1, therefore the ratio of the wave speed is of the same order as the square root of the inverse of the static strain. Typically the elastic wave speed will be at least 20 times higher than the transverse one. The assumption can therefore be made that the solution consists of a part which is fast oscillating in space (small wave length, transverse waves) and a part which is slowly oscillating in space (large wave length, longitudinal waves).

The second assumption is that the static quantities in the equation are slowly varying in space compared to the transverse oscillation. In other words, the variation of the static tension and curvature is small over a transverse wave length. This assumption can be also stated as a requirement that the variation over the cable length of the static quantities is small and/or that the wave length of the transverse modes is small compared to the cable length. One of these two conditions must be met. Fortunately, it turns out that even for the first modes of oscillation the above conditions are generally satisfied. (See also the discussion on asymptotic strings with variable tension.)

Under the above conditions the four differential equations can be separated asymptotically in two second order differential equations. One will provide the transverse wave type of solution, which will be fast varying in space, while the other differential equation will provide slow solutions in space, which correspond to the elastic waves, or, in the limiting case of inextensible cables, to the instantaneous readjustement of the equilibrium position of the cable.

The equations can be written in non-dimensional form as:

$$
\begin{aligned}
&-\frac{m\,L^2\,\omega^2\,\xi}{T_c} = \frac{dT}{d\sigma} - \frac{w_o L}{T_c}\cos\phi_o\,\phi_1 \\
&-\frac{m\,L^2\,\omega^2\,\eta}{T_c} = T\,\frac{d\phi_o}{d\sigma} - \frac{d\phi_1}{d\sigma}\,\frac{T_o}{T_c} + \frac{w_o L}{T_c}\sin\phi_o\,\phi_1 \\
&\frac{d\xi}{d\sigma} - \eta\,\frac{d\phi_o}{d\sigma} = \frac{T_c}{E\cdot A}\,T \\
&\frac{d\eta}{d\sigma} + \xi\,\frac{d\phi_o}{d\sigma} = \phi_1(1+e_o)
\end{aligned}
\qquad (3.82)
$$

where: T_c: representive static tension along the cable = constant

$T_o(\sigma)$: static tension $dT_o/d\sigma = w_o L\sin\phi_o$

$T(\sigma)$: T_1/T_c non-dimensional dynamic tension

σ: non-dimensional Lagrangian coordinate

ξ: non-dimensional tangential displacement

η: non-dimensional normal displacement

3.8.4 Fast Varying Solution

We will assume that ξ, η are fast varying quantities, compared with the static quantities. We denote by ϵ a quantity which is an order of magnitude smaller than one. In the sequel we rewrite all variables in terms of new quantities wich are of order 1, multiplied by appropriate powers of ϵ to indicate their order of magnitude. (In order not to confuse the reader with different notations, $\bar{\xi}$, $\bar{\eta}$ will still denote tangential and normal displacements, but normalized to be of order 1.) For transverse waves, we know that the tangential displacements are an order of magnitude smaller than the normal displacements and, also that the dynamic tension is a second order effect. This can be expressed as:

$$\xi \rightarrow \epsilon^2 \bar{\xi}\,(\sigma)$$

$$\eta \rightarrow \epsilon \bar{\eta}(\sigma)$$

$$\mathrm{T} \rightarrow \epsilon^2 \bar{\mathrm{T}}(\sigma)$$

$$\phi \rightarrow \epsilon \bar{\phi}(\sigma)$$

These are the basic assumptions we make to obtain a solution of (3.82). Also, we denote as:

$$\bar{\omega}^2 = \frac{\mathrm{M\ L^2\ \omega^2}}{\mathrm{T_r}}$$

$$\frac{\mathrm{w_o L}}{\mathrm{T_c}} = \epsilon\ \bar{\alpha}$$

$$\frac{\mathrm{T_o}}{\mathrm{E \cdot A}} = \epsilon^2\ \bar{\mathrm{e}}\,(\epsilon\sigma) \qquad (3.83)$$

$$\frac{d\phi_o}{d\sigma} = \epsilon\ \bar{\phi}_{o\sigma}(\epsilon\sigma)$$

$$\frac{T_o(\sigma)}{T_c} = \bar{T}_o(\epsilon\sigma)$$

where now all the variables are expressed in terms of quantities of order 1 and powers of ϵ. It can be easily verified by substitution, that the governing equations, to second order, can be written as:

$$\begin{aligned} -\ \bar{\omega}^2\ \bar{\eta} &= \frac{d}{d\sigma}\left[\ \bar{T}_o\ \frac{d\bar{\eta}}{d\sigma}\ \right] + O(\epsilon^2) \\ \frac{d\bar{\xi}}{d\sigma} &= \bar{\phi}_{o\sigma}\bar{\eta} + O(\epsilon^2) \end{aligned} \tag{3.84}$$

The first equation is a simple string equation with variable tension. The unknown variable is fast varying compared to $\bar{T}_o$ and the non-dimensional quantity $\bar{\omega}^2$ is a large quantity when we study the eigenmodes. Therefore, the WKB solution previously discussed in this chapter can be used. However, reasonable care should be used because we want to determine both ξ and η with the same accuracy.

The reader will have noticed that in the case of a non-extensible cable the second order terms were kept in the normal displacement expression. Therefore, we proceed by deriving the equations in terms of $\bar{\xi}$ using the relation:

$$\bar{\eta} = \frac{1}{\bar{\phi}_{o\sigma}}\ \frac{d\bar{\xi}}{d\sigma} \tag{3.85}$$

The equation for the fast solution in the tangential direction can then be written to second order as:

$$- \bar{\omega}^2 \, \bar{\xi} \; = \bar{T}_o \, \frac{d^2\bar{\xi}}{d\sigma^2} - 2\bar{T}_o \, \frac{\bar{\phi}_{o\sigma\sigma}}{\bar{\phi}_{o\sigma}} \, \frac{d\bar{\xi}}{d\sigma} + O(\epsilon^2) \tag{3.86}$$

Verification of (3.86) can easily be obtained by substituting (3.85) in (3.86). The solution to this problem can be obtained using the WKB method for large parameters.

To leading order:

$$\bar{\xi} \; = \bar{\phi}_{o\sigma} \, (\bar{T}_o)^{1/4} \, \exp(\pm \, W) \tag{3.87}$$

$$\text{where:} \quad W \; = i \, \bar{\omega} \int_0^{\sigma} \frac{1}{(\bar{T}_o)^{1/2}} \, d\sigma$$

This can be rewritten, in terms of dimensional quantities, as:

$$\xi \; = \frac{d\phi_o}{d\sigma} (T_o)^{1/4} \, \exp\Big[\pm \, i \, \omega \, L \int_0^{\sigma} \frac{1}{(T_o/M)^{1/2}} \, d\sigma \Big] \tag{3.88}$$

Using the relation (3.84), we obtain the solution in the normal direction as:

$$\eta \; = \frac{1}{(T_o)^{1/4}} \Big[\pm \, i \, \omega - \frac{7 \;\; w_o \, \sin\phi_o}{4 \; (T_o \, M)^{1/2}} \Big] \cdot$$

$$\exp\Big[\pm \, i \, \omega \, L \int_0^{\sigma} \frac{1}{(T_o/M)^{1/2}} \, d\sigma \Big] \tag{3.89}$$

This result is identical with the result for inextensible cables, which was derived by applying the WKB method to the fourth order differential equation, i.e. the extensibility does not affect, to second order, the solution for transverse waves.

When the curvature is zero, the solution is the same as the WKB solution for a string with varying tension. The asymptotic WKB solutions were found to be very accurate even if the assumption of slowly varying static quantities is violated. The dynamic angle can be obtained as:

$$\phi_1 = \frac{\partial \eta}{\partial \sigma} \tag{3.90}$$

The validity of the assumed order of magnitude of the dynamic variables can be checked using the obtained solution.

3.8.5 Slowly Varying Solution

We now assume that ξ, η are slowly varying quantities in space (compared to the fast transverse waves). The normal and tangential motions are now of the same order. The consistent perturbation assumption in this case are:

$$\xi \rightarrow \epsilon \bar{\xi}\,(\epsilon\sigma)$$

$$\eta \rightarrow \epsilon \bar{\eta}(\epsilon\sigma)$$

$$T \rightarrow \bar{T}(\epsilon\sigma)$$

$$\phi \rightarrow \epsilon^2\, \bar{\phi}(\epsilon\sigma)$$

The governing equations to second order can be written in terms of perturbation quantities:

$$- \bar{\omega}^2 \, \bar{\eta} = \bar{T} \, \bar{\phi}_{o\sigma} + O(\epsilon^2)$$

$$- h \, \bar{\omega}^2 \, \bar{\xi} = \frac{d\bar{T}}{d\sigma} + O(\epsilon^2) \tag{3.91}$$

where: $h = m/M$

The set of the above equations can be written as a single differential equation in terms of η, by using the tangential compatibility relation.

The compatibility can be rewritten in terms of perturbation quantities as:

$$\bar{T} \, \bar{e} = \frac{d\bar{\xi}}{d\sigma} - \bar{\phi}_{o\sigma} \, \bar{\eta} \tag{3.92}$$

Using (3.91) and (3.92) the approximate constitutive equation for the slow dynamics is obtained as:

$$\frac{d^2}{d\sigma^2}\left[\frac{\bar{\eta}}{\bar{\phi}_{o\sigma}}\right] - h\bar{\phi}^2_{o\sigma}\left[1 - \frac{\bar{\omega}^2\bar{e}}{\bar{\phi}^2_{o\sigma}}\right]\frac{\bar{\eta}}{\bar{\phi}_{o\sigma}} = 0 + O(\epsilon^2) \tag{3.93}$$

We can rewrite the governing equation as:

$$\frac{d^2}{d\sigma^2}\left[\frac{\eta}{\phi_{o\sigma}}\right] + Q(\sigma)\left[\frac{\eta}{\phi_{o\sigma}}\right] = 0 \tag{3.94}$$

where: $Q(\sigma) = - \frac{m}{M} \phi^2_{o\sigma} \left[1 - \frac{M \, \omega^2 \, L^2}{E \cdot A \, \phi^2_{o\sigma}}\right]$

$$\phi_{o\sigma} = \frac{d\phi_o}{d\sigma}$$

The dynamic tension generated and the tangential displacement can be

found as:

$$T_1 = - M \omega^2 L^2 \frac{\eta}{\phi_{o\sigma}}$$

$$\xi = h \frac{d}{d\sigma} \left[\frac{\eta}{\phi_{o\sigma}} \right] \tag{3.95}$$

If (3.94) can be solved, (3.95) can provide the other dynamic quantities, to obtain the complete slow solution.

The solution of equation (3.94) is unfortunately not possible analytically in the general case. The variation of the solution is of the same order as the variation of $Q(\sigma)$. Therefore a WKB type of solution cannot be used in this case.

The solution of equation (3.94) has been the subject of a major research effort at M.I.T, mainly by professor Triantafyllou. See [Triantafyllou 82b], [Triantafyllou 82c], [Triantafyllou 83] and [Triantafyllou 84].

The governing quantity is:

$$Q(\sigma) = - h \left[\phi_{o\sigma}^2 - \frac{M \omega^2 L^2}{E \cdot A} \right] \tag{3.96}$$

The only coefficient that is varying along the length is the curvature $\phi_{o\sigma}$. The solution of (3.94), therefore, strongly depends on the analytical functional form of the curvature.

The interesting features of the behavior of the slow equations are caused by the opposing effect of elasticity and curvature in (3.96). The sign of Q can be positive, negative or zero. The sign can even change at a point along the cable. This has a significant effect on the solution of the slow equation and

on the overall cable behavior.

We will briefly discuss the different forms the solution can take, depending on the quantity $Q(\sigma)$. As mentioned in the introduction of chapter 3, only the weight dominated case will be considered.

For the weight dominated case, we can express the curvature in terms of the non-dimensional length using the following relation between static quantities:

$$\begin{aligned} \frac{d\phi_o}{d\sigma} &= \alpha \cos^2\phi_o \\ \alpha &= \frac{w_o L}{H} \\ \tan\phi_o &= \tan\phi_b + \frac{w_o L}{H}\sigma \end{aligned} \tag{3.97}$$

then $\phi_{o\sigma}$ can be expressed as:

$$\frac{d\phi_o}{d\sigma} = \alpha \cos^2\left[\operatorname{atan}\{ \tan\phi_b + \frac{w_o L}{H}\sigma \} \right] \tag{3.98}$$

where: ϕ_b is the static angle at the origin,
atan(x) denotes the inverse tangent function of x.

The curvature is a complicated function of σ, so that additional simplifications must be made to solve the governing slow equation analytically.

Large Sag Cable

In the case of a large sag cable, the elasticity effects are normally negligible, compared to the curvature effects. This can be expressed as:

$$\phi_{o\sigma}^2 >> \frac{M\ \omega^2\ L^2}{E \cdot A} \tag{3.99}$$

which implies that the cable behaves essentially as an inextensible cable.

(3.99) can, therefore, be used to determine whether the cable can be treated as inextensible or not. Note that the assumption of inextensibility depends on the frequency and for high frequencies the elasticity effects will be important. If (3.99) is valid, the governing equation (3.94) becomes:

$$\frac{d^2}{d\sigma^2}\left[\frac{\eta}{\phi_{o\sigma}}\right] - h\,\phi_{o\sigma}\,\eta = 0 \tag{3.100}$$

By changing the independent variable from σ to ϕ_o, we can proceed to transform (3.100) into an equation expressed in terms of ϕ_o. We also use the compatibility relation for inextensible cables, written in the form:

$$\eta = \frac{d\xi}{d\phi_o}$$

and the slow equation can now be written in terms of ξ as:

$$\frac{d^2\xi}{d\phi_o^2} - \frac{d\phi_{o\sigma}/d\phi_o}{\phi_{o\sigma}}\frac{d\xi}{d\phi_o} - h\,\xi = 0 \tag{3.101}$$

Using the fact that $\phi_{o\sigma} = \alpha\,\cos^2\phi_o$ for a catenary, the final form for the slow solution for an inextensible cable is:

$$\frac{d^2\xi}{d\phi_o^2} + 2\,\tan\phi_o\,\frac{d\xi}{d\phi_o} - h\,\xi = 0 \tag{3.102}$$

The solution of this equation has already been given in (3.60)-(3.63). The two independent solutions were obtained by series expansions around h = 1, where, fortunately, an approximate analytic solution to (3.102) can be found.

for h = 1

$$\xi_{s1} = \sin\phi_o$$

$$\xi_{s2} = (\phi_o - \pi/2)\sin\phi_o + \cos\phi_o$$

$$\eta_{s1} = \cos\phi_o$$

$$\eta_{s2} = (\phi_o - \pi/2)\cos\phi_o$$

The general solution, as already mentioned in paragraph 3.6.6.2 to $O(1 - h^3)$ is:

$$\xi_{s1} = (1-h^2) + h^2\sin\phi_o + \frac{h}{2}(h-1)\cos^2\phi_o + O(h^3)$$

$$\xi_{s2} = (1-h)\cos^3\phi_o + 3(3+h)\left[(\phi_o - \frac{\pi}{2})\sin\phi_o + \cos\phi_o\right] + O(h^3)$$

$$\eta_{s1} = \left[h^2 - h(h-1)\sin\phi_o\right]\cos\phi_o + O(h^3) \qquad (3.103)$$

$$\eta_{s2} = -3\cos\phi_o\left[(1-h)\cos\phi_o\sin\phi_o - (3+h)(\phi_o - \frac{\pi}{2})\right] + O(h^3)$$

The approach followed here provides, therefore, the same asymptotic solution, as the one for an inextensible cable, which was obtained by expanding a single fourth order governing equation. The agreement can be seen as a confirmation of the validity of the perturbation assumptions.

Small Sag Cable

In the case of a small sag cable, the curvature in the cable will not vary significantly and we can approximate it by a truncated Taylor series in terms of σ_o. To minimize the error in the approximation the expansion is made around a point near the middle of the cable. (See figure 3-10). We define a new origin of the Lagrangian coordinate at the point where the static angle is equal to the inclination angle of the line. The new non-dimensional Lagrangian coordinate is therefore defined as:

$$z = \sigma - \sigma_a$$

where σ_a is the length coordinate of a point where $\phi_o = \phi_a$, and which can be found from the static solution. The curvature can now be expanded around $z = 0$. The coefficients are only functions of the static quantities.

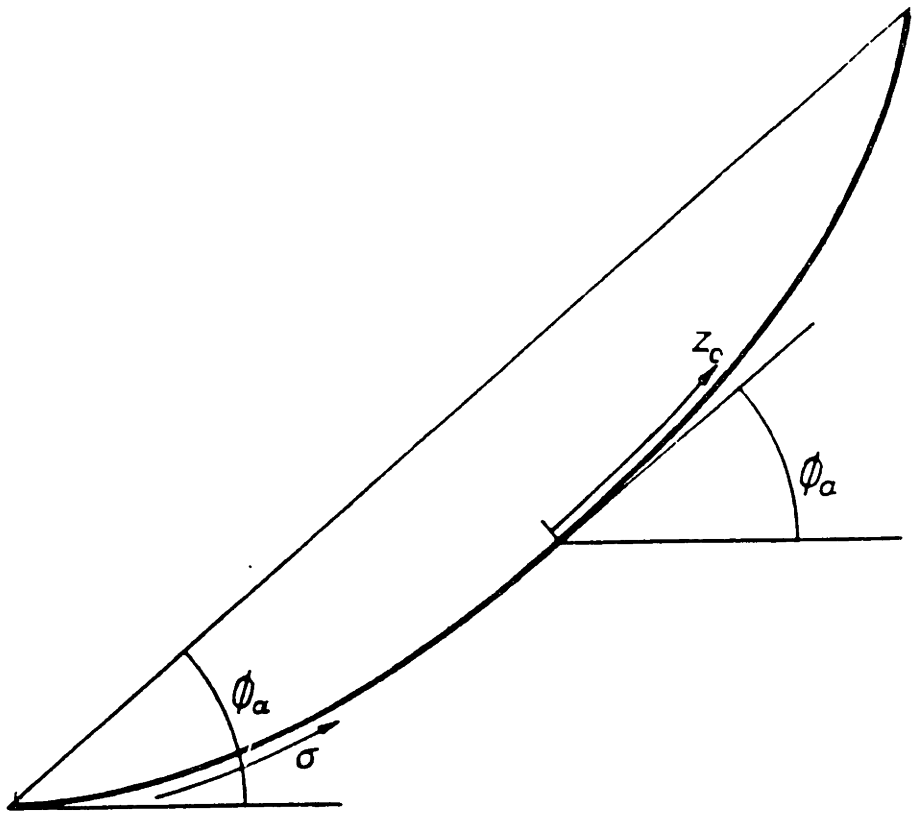

Figure 3-10: Definition of the New Lagrangian Coordinate

$$\phi_{o\sigma} = \phi_{o\sigma,a} \left(1 + a_1 z + a_2 z^2 + \ldots \right) \tag{3.104}$$

By using the static solution, we obtain:

$$a_1 = -\, 2\alpha \cdot \cos\phi_a \cdot \sin\phi_a$$

$$a_2 = \alpha^2 \cos^2\phi_a \cdot (3\sin^2\phi_a - \cos^2\phi_a) \tag{3.105}$$

where: $\alpha = w_o L/H$

The quantity $Q(\sigma)$ can now be expressed in terms of z as:

$$Q(z) = -\, h \left[\phi^2_{o\sigma,a}\{1 + 2a_1 z + (a_1^2 + 2a_2) z^2\} - \frac{M\ \omega^2\ L^2}{E \cdot A} \right] \tag{3.106}$$

or explicitly:

$$Q(z) = -\, h \left[\{\phi^2_{o\sigma,a} - \frac{M\ \omega^2\ L^2}{E \cdot A}\} \right.$$

$$- 4\alpha\ \phi^2_{o\sigma,a} \cos\phi_a \cdot \sin\phi_a\ z$$

$$+ \alpha^2\ \phi^2_{o\sigma,a} (10\cos^2\phi_a \cdot \sin^2\phi_a - 2\cos^4\phi_a) z^2$$

$$\left. + O(\alpha^3 z^3) \right] \tag{3.107}$$

we write this as: $Q(z) = Q_o + Q_1 z + Q_2 z^2$ (3.108)

$$\text{with:} \quad Q_o = -\, h \left[\phi^2_{o\sigma,a} - \frac{M\ \omega^2\ L^2}{E \cdot A} \right]$$

$$Q_1 = 4\alpha h\ \phi^2_{o\sigma,a} \cos\phi_a \cdot \sin\phi_a$$

$$Q_2 = -\alpha^2\ h\ \phi^2_{o\sigma,a} (10\cos^2\phi_a \cdot \sin^2\phi_a - 2\cos^4\phi_a)$$

We are now in a position to obtain approximate solutions for a small sag cable. We will consider three different cases.

1. Q(z) is approximated as a constant.

$$Q(z) = - h \left[\phi^2_{o\sigma,a} - \frac{M\ \omega^2\ L^2}{E \cdot A} \right] = Q_o$$

This is equivalent to assuming a constant curvature along the cable, i.e. the static shape is parabolic. The governing equation (3.100) can be written as:

$$\frac{d^2\eta}{dz^2} - h \left[\phi^2_{o\sigma,a} - \frac{M\ \omega^2\ L^2}{E \cdot A} \right] \eta = 0 \qquad (3.109)$$

$$\frac{d^2\eta}{dz^2} + Q_o\ \eta = 0$$

where: $\phi_{o\sigma} \cong \phi_{o\sigma,a} \cong \alpha \cos^2 \phi_a$

The solution can be written as:

$$\eta(\sigma) = \exp \{ \pm (- Q_o)^{1/2}\ \sigma \}$$

$$\xi(\sigma) = \pm (- Q_o)^{1/2} \exp \{ \pm (- Q_o)^{1/2}\ \sigma \} \qquad (3.110)$$

When the curvature is large compared to the elastic parameters, the solution is exponential, otherwise it provides elastic waves. The behavior of the slow solution can change from sinusoidal to exponential elastic waves, depending on the magnitude of the curvature and the elasticity.

The cross-over phenomena are predicted accurately with the above theory. Cross-over occurs when $Q_o = 0$, i.e.

$$\alpha^2 = \frac{M\ \omega^2\ L^2}{E \cdot A}$$

For horizontal cables, the leading order approximation is correct to order $\alpha^2 z^2$, which explains the good accuracy of the horizontal small sag theory.

The leading order slow solution predicts a change of the type of solution (exponential to sinusoidal) uniformly over the cable.

2. Q(z) is approximated as a linear function.

The solution can now be written in terms of Airy and Bairy functions, (Airy functions of the first and second kind) for the normal displacement, and their derivates for the tangential displacement [Triantafyllou 84]. The parameter Q varies linearly with z only when the cable is inclined.

$$\begin{aligned} Q(z) &= Q_o + Q_1 z \\ &= Q_1 \left[z + \frac{Q_o}{Q_1} \right] \\ &= Q_1 (z - z_o) \end{aligned}$$

with: $z_o = - \dfrac{Q_o}{Q_1}$

The governing equation becomes:

$$\frac{d^2}{dz^2} \cdot \left[\frac{\eta}{\phi_{o\sigma}} \right] + Q_1 (z - z_o) \frac{\eta}{\phi_{o\sigma}} = 0 \qquad (3.111)$$

the solutions in this case are:

$$\eta(z) \begin{cases} = \phi_{o\sigma}(z) A_i \left[-Q_1^{1/3} (z - z_o) \right] \\ = \phi_{o\sigma}(z) B_i \left[-Q_1^{1/3} (z - z_o) \right] \end{cases}$$

(3.112)

$$\xi(z)\begin{cases} = - Q_1^{1/3} \; \dot{A}_i \left[-Q_1^{1/3} (z - z_o) \right] \\ = - Q_1^{1/3} \; \dot{B}_i \left[-Q_1^{1/3} (z - z_o) \right] \end{cases}$$

This solution allows for a change from an exponential to a sinusoidal behavior along the cable length. If the transition point lies within the cable span, the lower part behaves as an inextensible chain and the upper part as a taut wire.

3. Q(z) is approximated as a quadratic function.

The slow solution can be expressed in terms of parabolic cylinder functions for the normal displacement, and their derivatives for the tangential displacement.

The governing equation is:

$$\frac{d^2}{dz^2} \left[\frac{\eta}{\phi_{o\sigma}} \right] + \frac{\eta}{\phi_{o\sigma}} (Q_o + Q_1 z + Q_2 z^2) = 0 \qquad (3.113)$$

This can be rewritten as:

$$\frac{d^2}{dv^2} \left[\frac{\eta}{\phi_{o\sigma}} \right] \mp (1/4 \; v^2 \pm a) \frac{\eta}{\phi_{o\sigma}} = 0 \qquad (3.114)$$

where: $v = \dfrac{z - b_o}{b_1}$

$$b_1 = \frac{1}{(4 \mid Q_2 \mid)^{1/4}}$$

$$b_o = - \frac{Q_1}{2Q_2}$$

$$a = - \frac{1}{(4 \mid Q_2 \mid)^{1/2}} \cdot \left[Q_o - \frac{Q_1^2}{4Q_2} \right]$$

The changes in sign are due to the use of an absolute value in the expression for b_1. The solution in this case is:

$$\eta(z) \begin{cases} = \phi_{o\sigma} W_1(v,a) \\ = \phi_{o\sigma} W_2(v,a) \end{cases}$$

$$\xi(z) \begin{cases} = \frac{1}{b_1} \frac{dW_1}{dv} (v,a) \\ = \frac{1}{b_1} \frac{dW_2}{dv} (v,a) \end{cases} \qquad (3.115)$$

where W_1 , W_2 are the parabolic cylinder functions of the first kind for $Q_2 < 0$ and W_1 , W_2 are the parabolic cylinder functions of the second kind for $Q_2 > 0$.

3.8.6 Total solution

Two fast varying solutions were derived in subsection 3.8.4, and two slow solutions were derived in subsection 3.8.5. The total solution is obtained by a linear combination of the four solutions that satisfies the boundary conditions.

The eigenfrequencies can be obtained by searching for the non-trivial solutions of the homogeneous problem.

3.8.7 Discussion and Validation

When we let the elastic stiffness go to infinity, the solutions obtained for extensible cables (both slow and fast) are identical to the results obtained from the perturbation expansion of the fourth order differential equation obtained for inelastic cables.

In the case of a shallow sag horizontal cable, by making the assumption used in subsection 3.8.1 of constant tension and quasi-static stretching, and by using the leading order approximation of the slow solution, the shallow sag horizontal cable results are obtained [Irvine 74] [Triantafyllou 83]. The theory is more general, however, because it also predicts the eigenfrequencies of the elastic modes and the quasi-static stretching assumption need not be made. For deep sag, horizontal cables the derived perturbation theory predicts correctly the change of eigenfrequencies with increasing sag (see the next chapter). The predictions are valid for extensible, as well as for inextensible cables. The theory is therefore more general than [Irvine 74] or [Saxon 53].

The shallow sag elastic cable theory has been applied by Irvine to inclined cables [Irvine 78]. The small sag approximation can be used approximately to predict the symmetric modes as follows:

$$\tan\left[\frac{k_* L}{2}\right] - \left[\frac{k_* L}{2}\right] + \frac{4}{\lambda_*^2}\left[\frac{k_* L}{2}\right]^3 = 0 \qquad (3.116)$$

with: $k_* = \omega \left[\frac{M}{H_*}\right]^{1/2}$

$$\lambda_*^2 = \left[\frac{w_o L}{H_*}\right]^2 \frac{E \cdot A_o}{H_*} \cdot \cos^2\phi_a$$

$$H_* = \frac{H}{\cos\phi_a}$$

ϕ_a = inclination angle between the cable chord and the horizontal

Again, cross-over of the modes is predicted, as shown in figure 3-8, where ω has been replaced with ω_* and λ^2 with λ_*^2. For inclined cables, however, the perturbation solution derived in previous sections should be used to reflect the basic assymmetry introduced in the problem. The perturbation solutions predict hybrid mode formation and no cross-over phenomena. In figure 3-11 the eigenfrequencies are plotted versus λ_*^2. The inclination angle is 30^o and $w_o L/H_* = 0.5$. The eigenfrequencies are not crossing. The curve of the first mode is, at high values of λ_*^2, the continuation of the curve of the second mode, at low values of λ_*^2, and the second mode is, at high values of λ_*^2, the continuation of the curve of the first mode, at low values of λ_*^2. Figure 3-8 can be seen as the limit case of figure 3-11, for inclination angle 0^o and/or $w_o L/H_* = 0$, and can still be used to predict the eigenfrequencies accurately for moderately small values of $w_o L/H_*$ and ϕ_a, except in the transition region. The size of the transition region increases with increasing values of $w_o L/H_*$ and ϕ_a. It is interesting to note that for low values of λ_*^2 no curves were

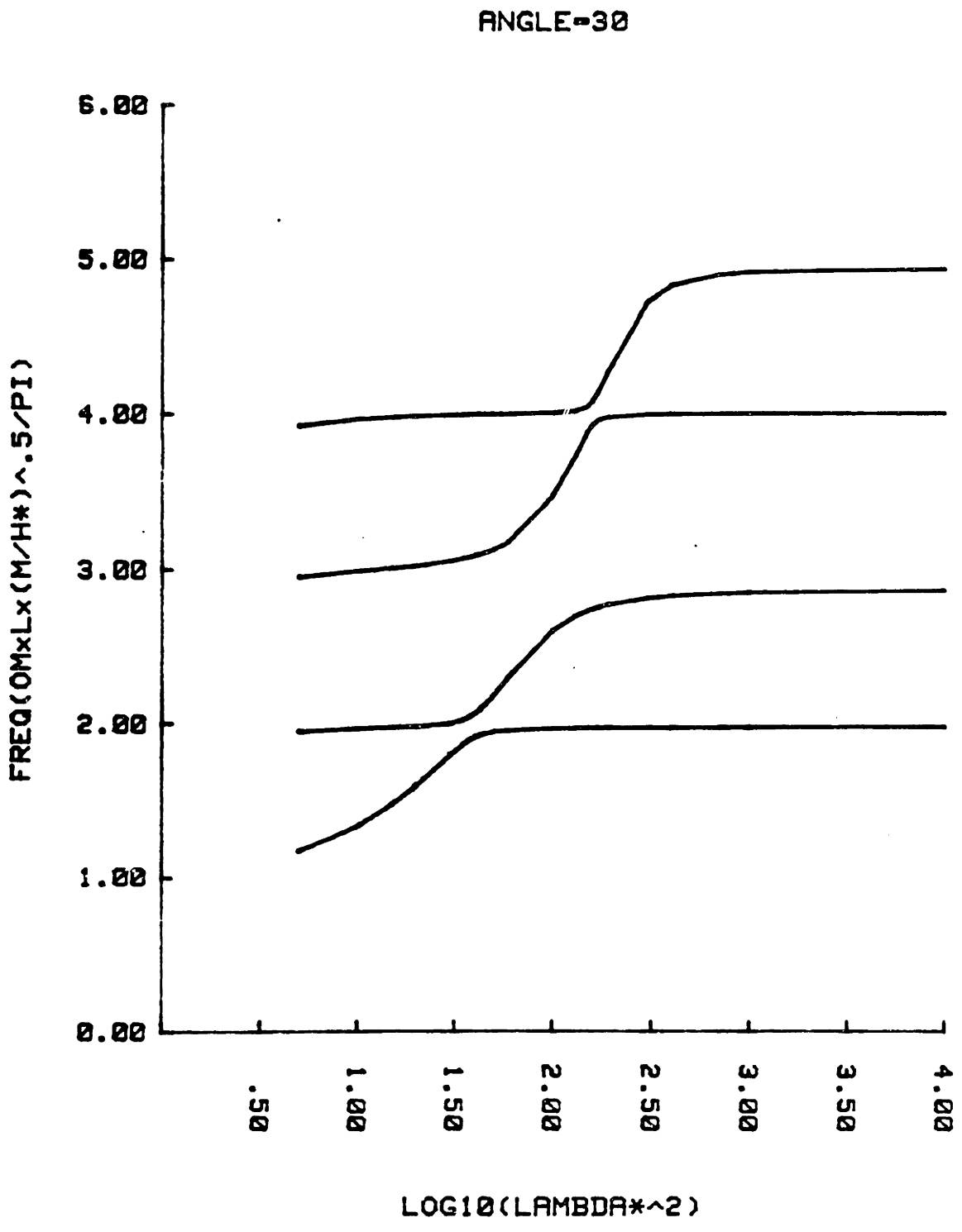

Figure 3-11: Eigenfrequencies of an Inclined Cable

($\phi_a = 30^o$, $w_o L/H_* = 0.5$)

plotted. At such a low value of λ_*^2, the elastic strain in the cable becomes large, and cannot exist in real cables. Cut-off was selected at the point where the elastic wave speed is 10 times the transverse wave speed. This is approximately the minimal value for steel cables and chains used in mooring applications.

In figure 3-12 the shape of the first two modes for various values of λ_*^2 have been plotted. The symmetric[8] and anti-symmetric modes are changing over to hybrid modes in the transition region, and for high values of λ_*^2 to the anti-symmetric and symmetric mode of an inelastic chain. See also [Triantafyllou 84].

The application of numerical techniques to study the same phenomena confirms the existence of hybrid modes and the non-crossing of the modes (see chapter 4). Yamaguchi [Yamaguchi 79] used Galerkin's method to solve for the eigenmodes. A cartesian description of the problem is used and the expansions are made using sinusoidal functions in space. The hybrid modes and the non-crossing of the modes are also obtained.

3.9 Numerical Solution of the Linearised Problem

The governing equations (3.1), which were solved using asymptotic methods, can also be solved using numerical methods. The governing equations written in the Fourier domain are:

---

[8]The reference to symmetric and anti-symmetric modes is of course approximate. The inclination of the cable destroys the fundamental symmetry of the problem.

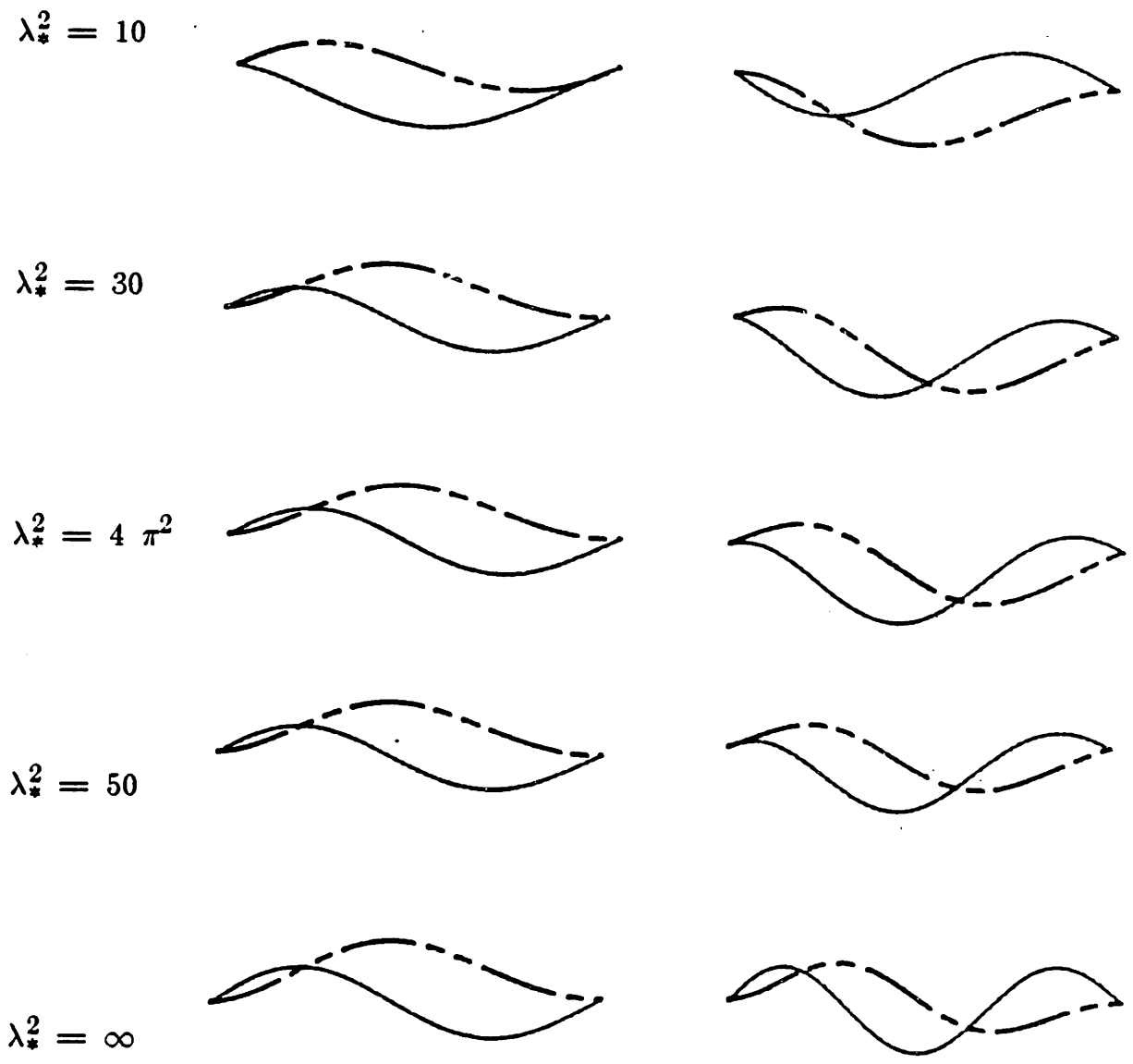

Figure 3-12: Formation of Hybrid Modes

($\phi_a = 30$, $w_o L/H_* = 0.5$)
(Normal displacement: solid line)
(10 $\times$ tangential displacement: dotted line)

$$- m \omega^2 p = \frac{dT_1}{ds} - w_o \cos\phi_o \phi_1$$

$$- M \omega^2 q = T_o \frac{d\phi_1}{ds} + T_1 \frac{d\phi_o}{ds} + w_o \sin\phi_o \phi_1 \qquad (3.117)$$

$$\frac{dp}{ds} - q \frac{d\phi_o}{ds} = e_1$$

$$\frac{dq}{ds} + p \frac{d\phi_o}{ds} = (1 + e_o)\phi_1$$

The problem is reduced to a set of four ordinary differential equations with two boundary conditions at each end.

Different methods can be used to solve the problem numerically. Using the linearity of the equations, shooting techniques can be used to reduce it to an initial value problem, which can be solved by classical integration techniques.

Another possible method is the use of implicit differences, to reduce the problem to a set of linear algebraic equations. Unfortunately, when a realistic grid length is used, the number of equations becomes very large.

An explicit centered difference scheme was selected to solve this problem. The centered difference scheme allows a transfer matrix formulation of the problem. The boundary conditions can easily be handled in this formulation [Keller 69].

The linearized dynamic equations are rewritten in matrix form.

$$\begin{bmatrix} \frac{dT_1}{ds} \\ \frac{d\phi_1}{ds} \\ \frac{dp}{ds} \\ \frac{dq}{ds} \end{bmatrix} = \begin{bmatrix} 0 & w_o\cos\phi_o & -m\omega^2 & 0 \\ -\frac{d\phi_o}{T_o ds} & -\frac{w_o\sin\phi_o}{T_o} & 0 & \frac{1}{T_o}(-M\omega^2) \\ \frac{1}{EA} & 0 & 0 & \frac{d\phi_o}{ds} \\ 0 & 1+e_o & \frac{d\phi_o}{ds} & 0 \end{bmatrix} \begin{bmatrix} T_1 \\ \phi_1 \\ p \\ q \end{bmatrix}$$

We rewrite this as:

$$\frac{dy}{ds} = A(s)\ y(s) \tag{3.118}$$

$$\text{with:}\quad y^T(s) = (T_1\ \phi_1\ p\ q\ )$$

Using centered differences, the following difference scheme is obtained:

$$y_{i+1} = \left[I - \frac{\Delta s_{i,\,i+1}}{2} A(s_{i+1})\right]^{-1} \left[I + \frac{\Delta s_{i,\,i+1}}{2} A(s_i)\right] y_i$$

$$= B_i\ y_i \tag{3.119}$$

Due to the fact that the static variables are slowly changing with respect to the spatial coordinate, the difference scheme will give acceptable results, except when the wave length becomes of the same order as the grid length. The overall error is $O(\Delta s^2)$. To find the expression relating the two ends, we can write:

$$y_n = \left(\prod_{i=1}^{n-1} B_i \right) y_1 \tag{3.120}$$

We write:

$$\prod_{i=1}^{n-1} B_i = \begin{bmatrix} \alpha_{11} & \alpha_{12} \\ \alpha_{21} & \alpha_{22} \end{bmatrix} \tag{3.121}$$

If motions are imposed at the upper end of the cable, the following relation is obtained:

$$\begin{bmatrix} T_{top} \\ \phi_{top} \\ p_{top} \\ q_{top} \end{bmatrix} = \begin{bmatrix} \alpha_{11} & \alpha_{12} \\ \alpha_{21} & \alpha_{22} \\ & \end{bmatrix} \begin{bmatrix} T_{bot} \\ \phi_{bot} \\ 0 \\ 0 \end{bmatrix}$$

Therefore:

$$\begin{bmatrix} p_{top} \\ q_{top} \end{bmatrix} = \alpha_{21}\, \alpha_{11}^{-1} \begin{bmatrix} T_{top} \\ \phi_{top} \end{bmatrix} \tag{3.122}$$

This provides a direct relation between the imposed motions at the top and the unknown dynamic angle and tension at the top. The matrices α_{11} and α_{21} are obtained from the matrix multiplication $\prod_{i=1}^{n-1} B_i$. These matrices can be calculated explicitly and they are functions of the static quantities, the frequency and the grid length.

The difference scheme can also be used to calculate the dynamic variables along the cable. When the displacements and the dynamic tension and angle at the top are known, the problem is an initial value problem which can be integrated directly.

The eigenfrequencies for the cable can be found by imposing zero motion

boundary conditions at the top, and by searching for the frequencies which give the governing equations a non-trivial solution. This can be written according to (3.122) as:

$$\text{Det } [\ \alpha_{21}\ (\omega)] = 0 \tag{3.123}$$

A search of the roots of (3.123) is done by a root-finding method which locates the eigenfrequencies within a desired accuracy.

3.10 References

[Davenport 65] Davenport, A. G. and Steels, G. N.
Dynamic Behavior of Massive Guy Cables.
Journal of the Structural Division, ASCE 91(ST2):43-70, April, 1965.

[Goodey 61] Goodey, W. J
On the Natural Modes and Frequencies of a Suspended Chain.
Quarterly Journal of Mechanics and Applied Mathematics 14(1):118-127, 1961.

[Hildebrand 49] Hildebrand, F.B.
Advanced Calculus for Applications.
Prentice Hall, Englewood Cliffs N.J., 1949.

[Irvine 74] Irvine, H. M. and Caughey, T. K.
The Linear Theory of Free Vibrations of a Suspended Cable.
Proceedings of the Royal Society Series A 341:299-315, 1974.

[Irvine 78] Irvine, H. M.
Free Vibrations of Inclined Cables.
Journal of the Structural Division, ASCE 104(ST2):343-347, February, 1978.

[Irvine 81] Irvine, H. M.
Cable Structures.
MIT Press, Cambridge, MA and London, England, 1981.

[Keller 69] Keller, H. B.
Accurate Difference Methods for Linear Ordinary Differential Systems Subject to Linear Constraints.
S.I.A.M. Journal of Numerical Analysis 6(1), March, 1969.

[Nayfeh 73] Nayfeh, A.M.
Perturbation Methods.
John Wiley & Sons, New York, 1973.

[Pugsley 49] Pugsley, A. G.
On the Natural Frequencies of Suspension Chains.
Quarterly Journal of Mechanics and Applied Mathematics 2(4):412-418, 1949.

[Rohrs 51] Rohrs, J. H.
On the Oscillation of a Suspension Chain.
Transactions of the Cambridge Philosophical Society 9:397-398, 1851.

[Rosenthal 81] Rosenthal, F.
Vibrations of Slack Cables with Discrete Masses.
Journal of Sound and Vibration 78:573-583, 1981.

[Routh 55] Routh, E. J.
Dynamics of a System of Rigid Bodies.
Dover, New York, New York, 1955.

[Saxon 53] Saxon, D. S. and Cahn, A. S. .
Modes of Vibration of Suspension Chain.
Quarterly Journal of Mechanics and Applied Mathematics 6:273-285, 1953.

[Simpson 66] Simpson, A.
Determination of the In-Plane Natural Frequencies of Multispan Transmission Lines by a Transfer Matrix Method.
Proceedings IEE 113(5), May, 1966.

[Triantafyllou 82a]
Triantafyllou, M. S.
Preliminary Design of Mooring Systems.
Journal of Ship Research 26(1):25-35, March, 1982.

[Triantafyllou 82b]
Triantafyllou, M. S. and Bliek, A.
Dynamic Analysis of Mooring Lines Using Perturbation Techniques.
In *Proceedings OCEANS '82*, pages 496-501. Washington, D.C., September, 1982.

[Triantafyllou 82c]
Triantafyllou, M. S., Kardomateas, G. and Bliek, A.
The Statics and Dynamics of the Mooring Lines of a Guyed Tower for Design Applications.
In C. Chryssostomidis and J. J. Connor (editors), *Proceedings of BOSS '82.* Hemisphere Publishing Company, Washington, August, 1982.

[Triantafyllou 83]
Triantafyllou, M. S. and Bliek, A.
The Dynamics of Inclined Taut and Slack Marine Cables.
Proceedings Offshore Technology Conference (OTC 4498):469-476, 1983.

[Triantafyllou 84]
Triantafyllou, M. S.
The Dynamics of Taut Inclined Cables.
Quarterly Journal of Mechanics and Applied Mathematics , 1984.
To Appear.

[Veletsos 82] Veletsos, A. S. and Darbre, G. R.
Free Vibrations of Parabolic Cables.
Technical Report 23, Rice University, Department of Civil Engineering, March, 1982.

[Yamaguchi 79] Yamaguchi, H. and Ito, H.
Linear Theory of Free Vibrations of an Inclined Cable in Three Dimensions.
Proceedings Japanese Society of Civil Engineers (286):29-36, June, 1979.
In Japanese, Summary in English, Transactions Japanese Society of Civil Engineers 1979.

Chapter 4

NUMERICAL APPLICATIONS OF THE LINEAR DYNAMICS

4.1 Introduction

In this chapter, three possible applications of the asymptotic solutions for linear cable dynamics are discussed, with the intention to illustrate the presented theory.

4.2 WKB Approximation of the Dynamics of Strings with Varying Tension

The accuracy of the WKB solution for strings with varying tension was tested for a linear tension variation. The legs of a tension leg platform were modeled as a string fixed at both ends. We consider two cases.

	Case A	Case B
Length (m)	549	549
Area (m^2)	0.00215	0.00215
Density (kg/m^3)	7870	7870
Lower tension (N)	$371\ 10^6$	$5\ 10^3$
Weight (N/m)	1449	1449
Mass (kg/m)	1907	1907

In the mass term the transverse added mass was included. The ratio of the top tension to the bottom tension was:

T_t/T_b	1.21	160

The second case was only selected to show the behavior of the WKB method near the turning point.

Comparison of the eigenfrequencies

	Case A		Case B	
Eigenmode	Bessel	WKB	Bessel	WKB
1	0.83733	0.83744	0.18796	0.19963
2	1.67482	1.67488	0.39076	0.39925
3	2.51228	2.51231	0.59224	0.59888

The WKB method provides accurate results, even very close to the turning point of the solution. The approximation is increasingly better for higher frequencies, because the variation of the static quantities over a wave length is smaller. In addition to the eigenfrequencies, the eigenmodes are also well approximated. The "worst" case result is given in figure 4-1, which shows the approximation for the first mode of case B. Agreement in this case is still surprisingly good.

The extension of the above ideas to include bending rigidity (necessary for accurate analysis) has been carried out by [Kim 83], where similarly good agreement was found. First order WKB solutions can give very accurate results with a minimum of computational requirements.

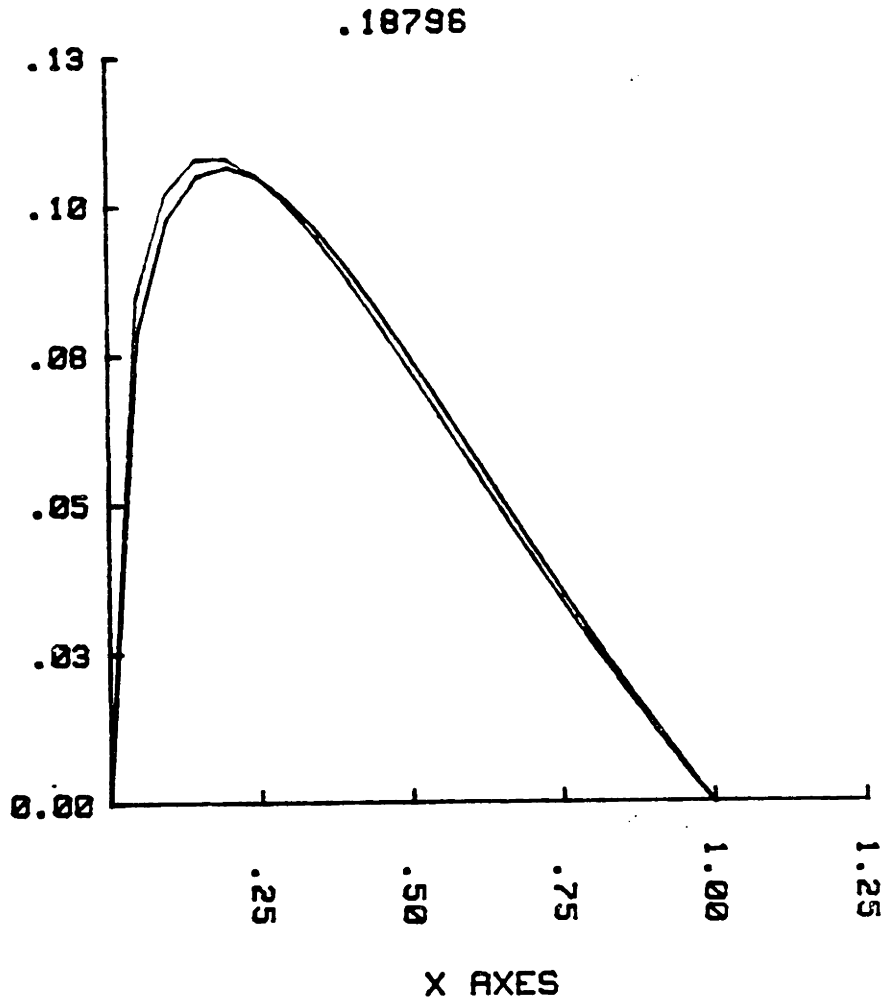

Figure 4-1: Comparison between the Mode Shapes of the WKB Solution and the Bessel Solution

4.3 Parametric Study of the Eigenfrequencies of a Two-Dimensional Cable

The eigenfrequencies of a two-dimensional cable hanging under its own weight have been studied extensively numerically, as well as experimentally.

Pugsley [Pugsley 49], Saxon and Cahn [Saxon 53] and Goodey [Goodey 61] studied the behavior of inextensible cables. Pugsley, and Saxon and Cahn performed also a limited number of experiments.

Irvine and Caughey [Irvine 74] predicted succesfully using approximate analytic techniques the cross-over phenomena for a small sag, horizontal cable. Among the most recent numerical contributions on eigenfrequencies of extensible cables are: West et al. [West 75], Gambhir and Batchelor [Gambhir 77] and Henghold et al. [Henghold 77]. Ramberg and Bartholomew [Ramberg 82] did some experiments on the vibration of inclined slack cables. Although all of the above authors were able to confirm the existence of cross-over phenomena for extensible cables in the horizontal case, the phenomena of hybrid modes were not detected. This is mainly due, in the author's opinion, to the very small transition region in the cases considered by the above researchers. Yamaguchi [Yamaguchi 79] used a Galerkin's expansion with sinusoidal terms to calculate the eigenfrequencies. He obtained hybrid modes and the non-crossing of the modes.

In the course of this thesis, a number of perturbation and numerical calculations of eigenfrequencies were carried out. We will briefly discuss some of the results, but the complete set of results is very extensive and will be published as a seperate report [Bliek 84].

4.3.1 Non-Dimensional Parameters

The governing equations in non-dimensional form depend only on 4 non-dimensional parameters when a uniform cable hanging under its own weight is considered. They can be written as:

1. The angle of inclination (ϕ_a) of the line connecting the two end points with a horizontal.

2. The ratio of the total weight of the cable and the tension projected on the chord ($\alpha = w_o L/H \cos\phi_a = w_o L/H_*$).

3. The projected elastic strain: the ratio of the projected tension and the uniform stiffness of the cable ($\beta = H_*/E{\cdot}A$).

4. The ratio of the mass and the mass plus the added mass.

The non-dimensional frequency was selected as follows:

$$\bar{\omega} = \frac{\omega L (M/H_*)^{1/2}}{\pi} \tag{4.1}$$

where: ω is the frequency

L is the length of the cable

H_* is $H/\cos\phi_a$

M is the mass plus the added mass

H is the horizontal tension

In the case of string: $\bar{\omega} = n$ $\quad n = 1, 2, 3 \ldots$

The above non-dimensionalisation of the frequency has the advantage that it virtually eliminates the dependency of the eigenfrequencies on h. The influence of the variation of h on $\bar{\omega}$ is small and will not be discussed here. In the sequel, cables in air will be analysed (h = 1). The results, though, should be a good approximation for the eigenfrequencies in water when (4.1) is used.

4.3.2 Inextensible Cables

The non-dimensional parameters are in this case:

1. ϕ_a, the inclination angle

2. $\alpha = \frac{w_o L}{H_*}$, the non-dimensional weight parameter

Three representative inclination angles were selected: 0^o , 30^o , 60^o. The non-dimensional weight parameter was varied between 0 and 5. The cables for high values of α are extremely slack (for a horizontal cable, $\alpha = 5$ corresponds to a top angle of 68^o).

The results can be found in figure 4-2 – 4-4. The solid lines are the results obtained with the inextensible perturbation theory. The + marks denote the results obtained with the numerical central difference scheme (100 points). The numerical solution can be considered as an "exact" solution, considering the resolution of the graph. For small α, the shallow sag inextensible eigenfrequencies are recovered. The curves are tangential to a horizontal line for the small sag inextensible eigenfrequencies. The small sag results can, therefore, be extrapolated to moderately large values of α.

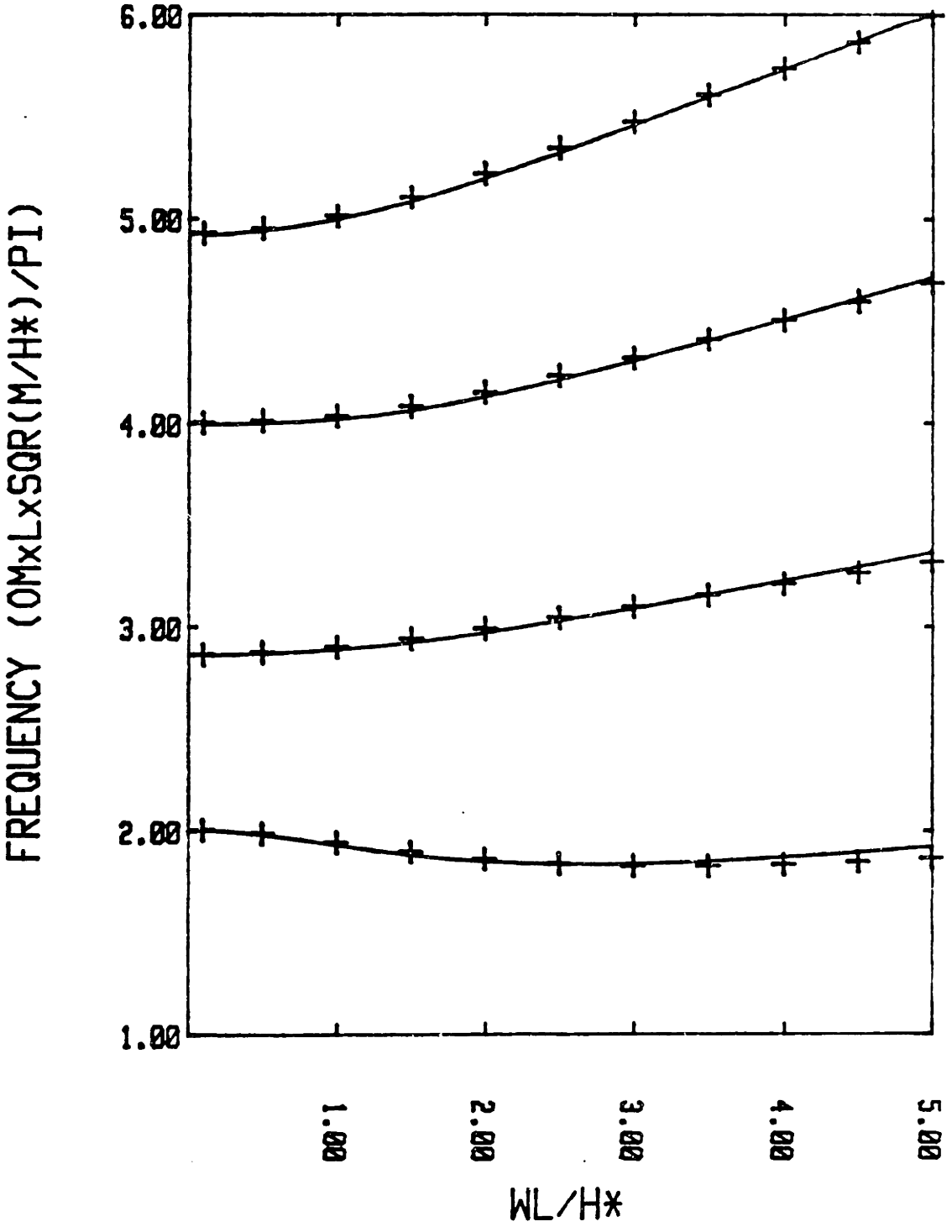

Figure 4-2: Eigenfrequencies for an Inextensible Cable, $\phi_a = 0^o$

(Solid line: inextensible perturbation theory)
(+ marks: numerical central difference scheme with 100 points)

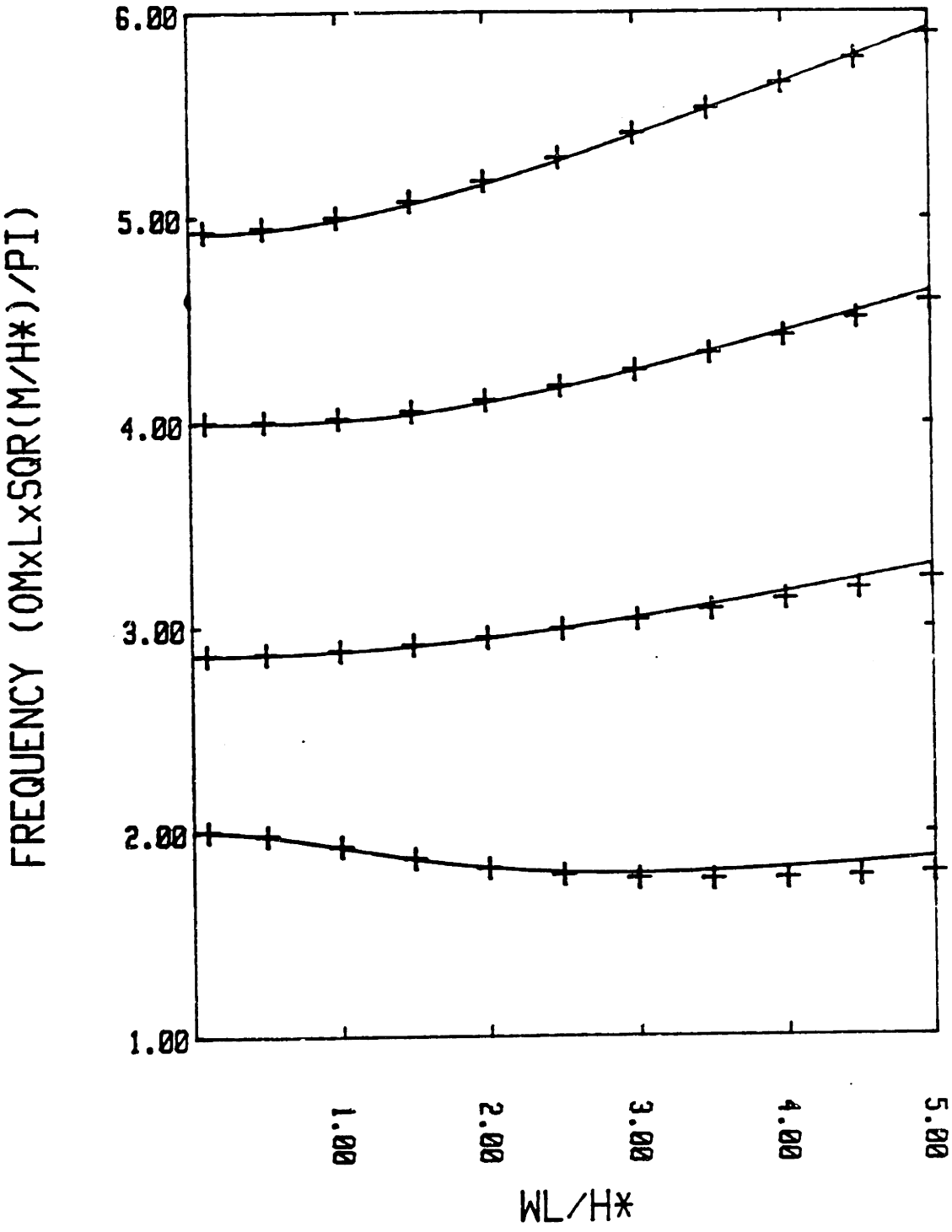

Figure 4-3: Eigenfrequencies for an Inextensible Cable, $\phi_a = 30^o$

(Solid line: inextensible perturbation theory)
(+ marks: numerical central difference scheme with 100 points)

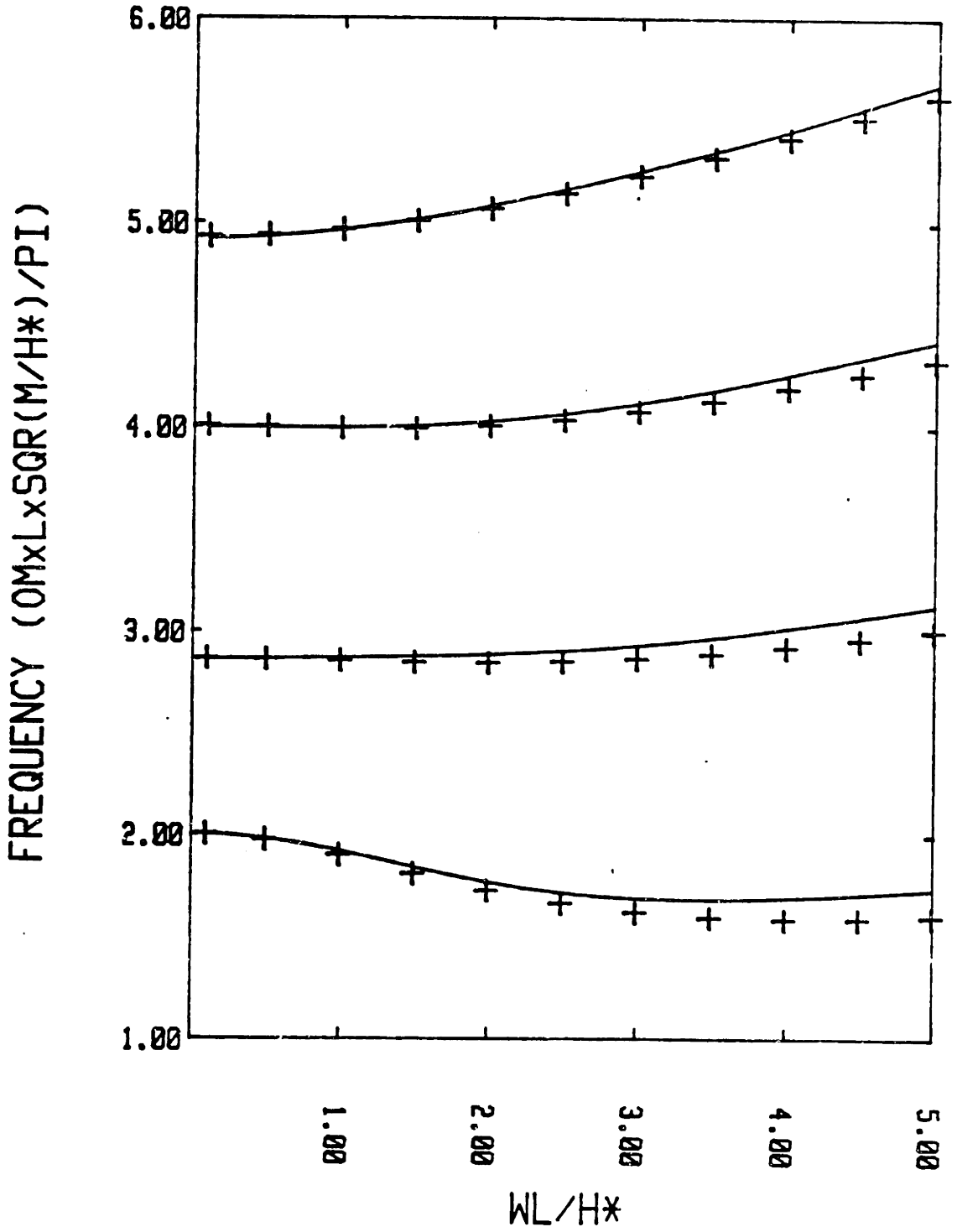

Figure 4-4: Eigenfrequencies for an Inextensible Cable, $\phi_a = 60^o$

(Solid line: inextensible perturbation theory)
(+ marks: numerical central difference scheme with 100 points)

The perturbation theory predicts fairly accurately the eigenfrequencies for the whole range of α and ϕ_a. Only for very high values of α and/or high inclination angles the predictions are deteriorating. Due to the nature of the perturbation expansions the prediction will be more accurate for the higher modes. This can be clearly seen on figure 4-4.

4.3.3 Extensible Cables

The eigenfrequencies of extensible cables (with h = 1) depends on 3 non-dimensional parameters:

1. ϕ_a, the inclination angle

2. α, the non-dimensional weight parameter ($w_o L/H_*$)

3. β, the projected elastic strain ($H_*/E{\cdot}A$)

There are several possibilities to represent the variation of the eigenfrequencies in terms of these three parameters. We will briefly discuss two of them.

First, the projected elastic strain was selected as a fixed parameter. This corresponds to choosing the ratio of the elastic and the transverse wave speed. This is a fairly good choice, because the elastic strain is restricted in design applications to be within a certain range. Yamaguchi [Yamaguchi 79] used this approach in his paper, while the non-dimensional weight parameter was selected as the independent variable. This allows direct comparison with the inextensible cables (A good alternative to this could be λ_*^2.)

The following relation between the ratio of the wave speed and the projected elastic strain exists:

$$\frac{c_{el}^2}{c_{tr}^2} = \frac{E \cdot A}{H_*} = \frac{1}{\beta} \qquad (h = 1) \tag{4.2}$$

For steel cables, a value of 400 was selected for $1/\beta$ (wave speed ratio of 20). This can be considered to be close to the lowest acceptable value.

The results can be found in figures 4-5 through 4-8. The solid lines are the results obtained using the perturbation theory and assuming an extensible cable. For the slow solution, the first order approximation ($Q(\sigma) = Q_o$) was used, which provides exponential or sinusoidal slow solutions. The + marks denote the results obtained using a numerical central difference scheme (100 points). The cross-over is predicted accurately for an inclination angle of 0^o. For inclined cables the transition region is also well predicted by the perturbation theory. To prove clearly that no cross-over exists, an enlargement of the transition zone for an inclination angle of 30^o was made in figure 4-7. Again, the solution breaks down for large values of α and large inclination angles, as seen in figure 4-8. When the parabolic cylinder functions are used instead of the exponentials in the slow solution, a much better approximation for large α and large ϕ_a is obtained. This has a drawback in that the perturbation approximation becomes, of course, numerically more complicated. Overall, the simple exponential slow solution predicts the eigenfrequencies fairly accurately. The case selected here ($\beta = 1/400$) implies high straining of the cable and, therefore, for most applications the transition will occur for smaller values of α_*, for which the perturbation solution will be increasingly more accurate. For very low values of α_* the solution tends to the eigenfrequencies of the taut string, while for high values of α_* the

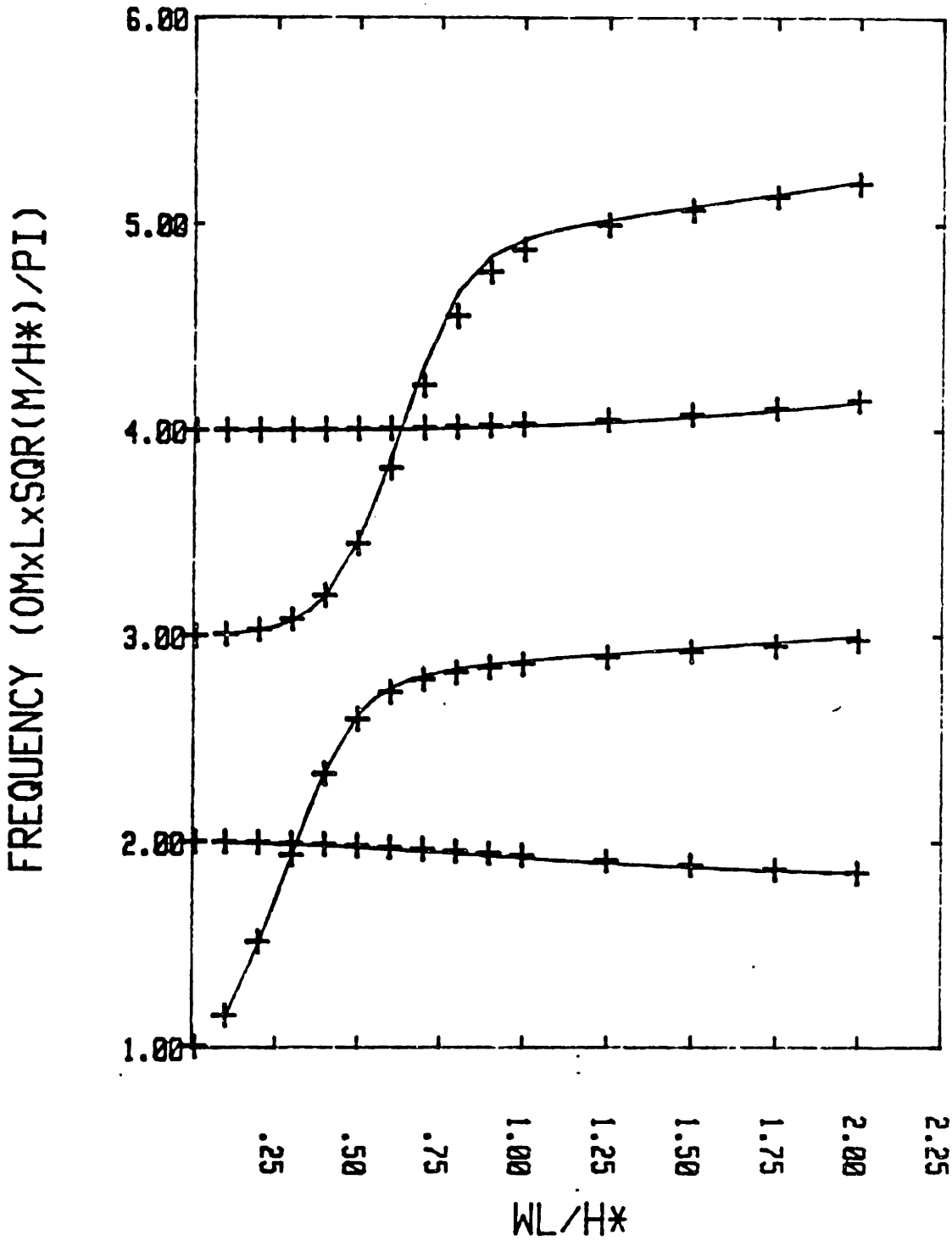

Figure 4-5: Eigenfrequencies for an Extensible Cable, $\phi_a = 0^o$, $\beta = 1/400$

(Solid line: extensible perturbation theory)
(+ marks: numerical central difference scheme)

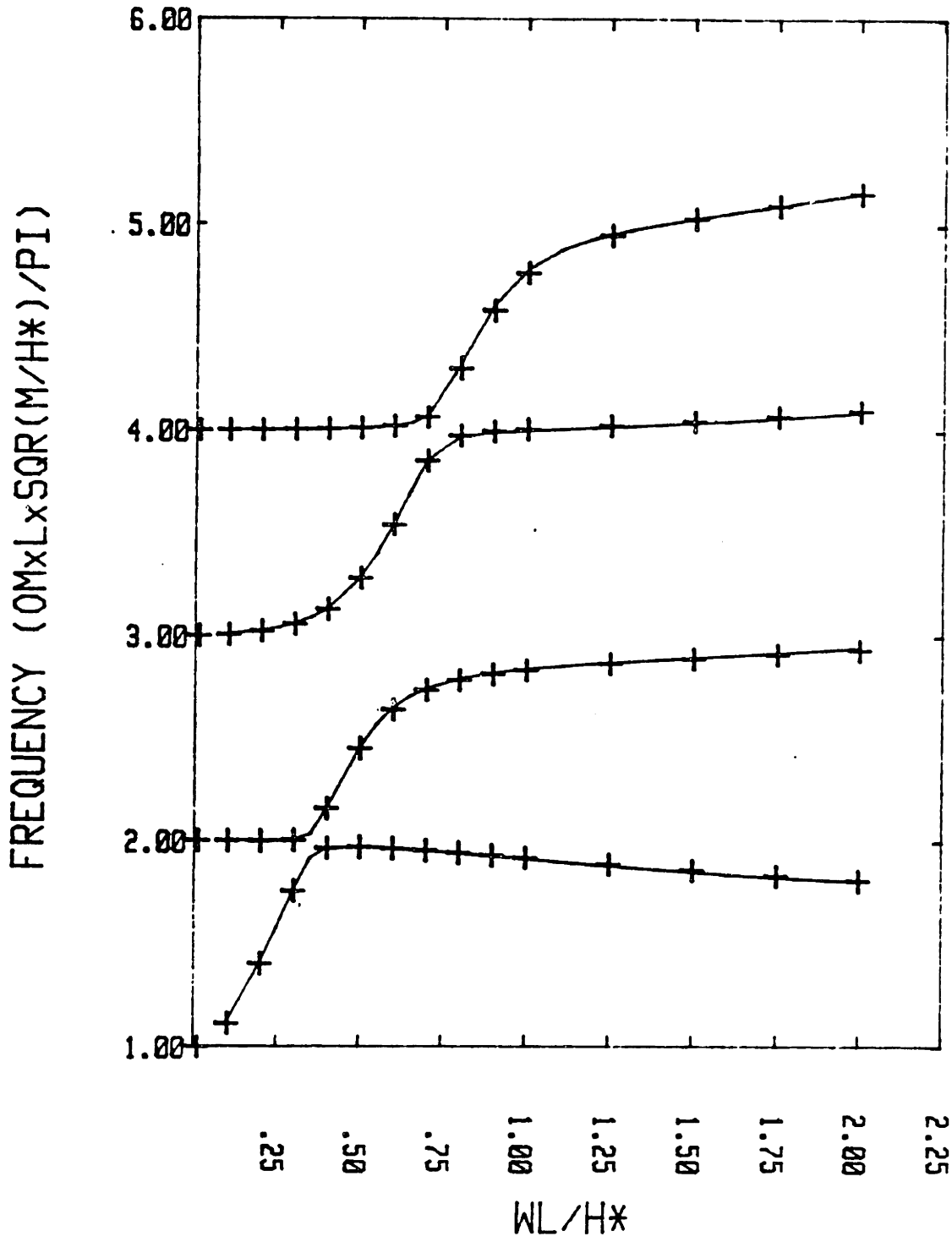

Figure 4-6: Eigenfrequencies for an Extensible Cable, $\phi_a = 30^\circ$, $\beta = 1/400$

(Solid line: extensible perturbation theory)
(+ marks: numerical central difference scheme)

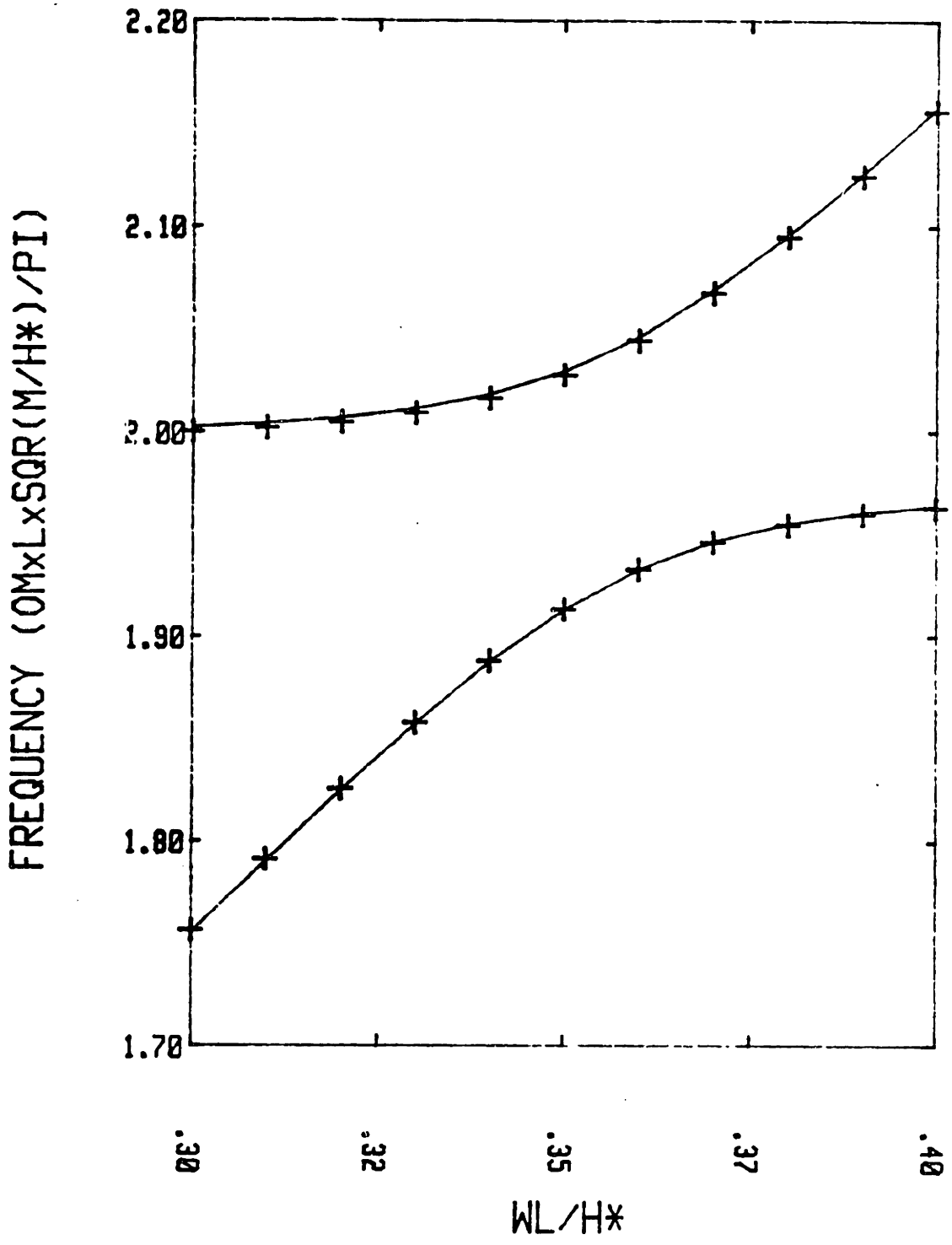

Figure 4-7: Transition zone:
Eigenfrequencies for an Extensible Cable,
$\phi_a = 30^o$, $\beta = 1/400$

(Solid line: extensible perturbation theory)
(+ marks: numerical central difference scheme)

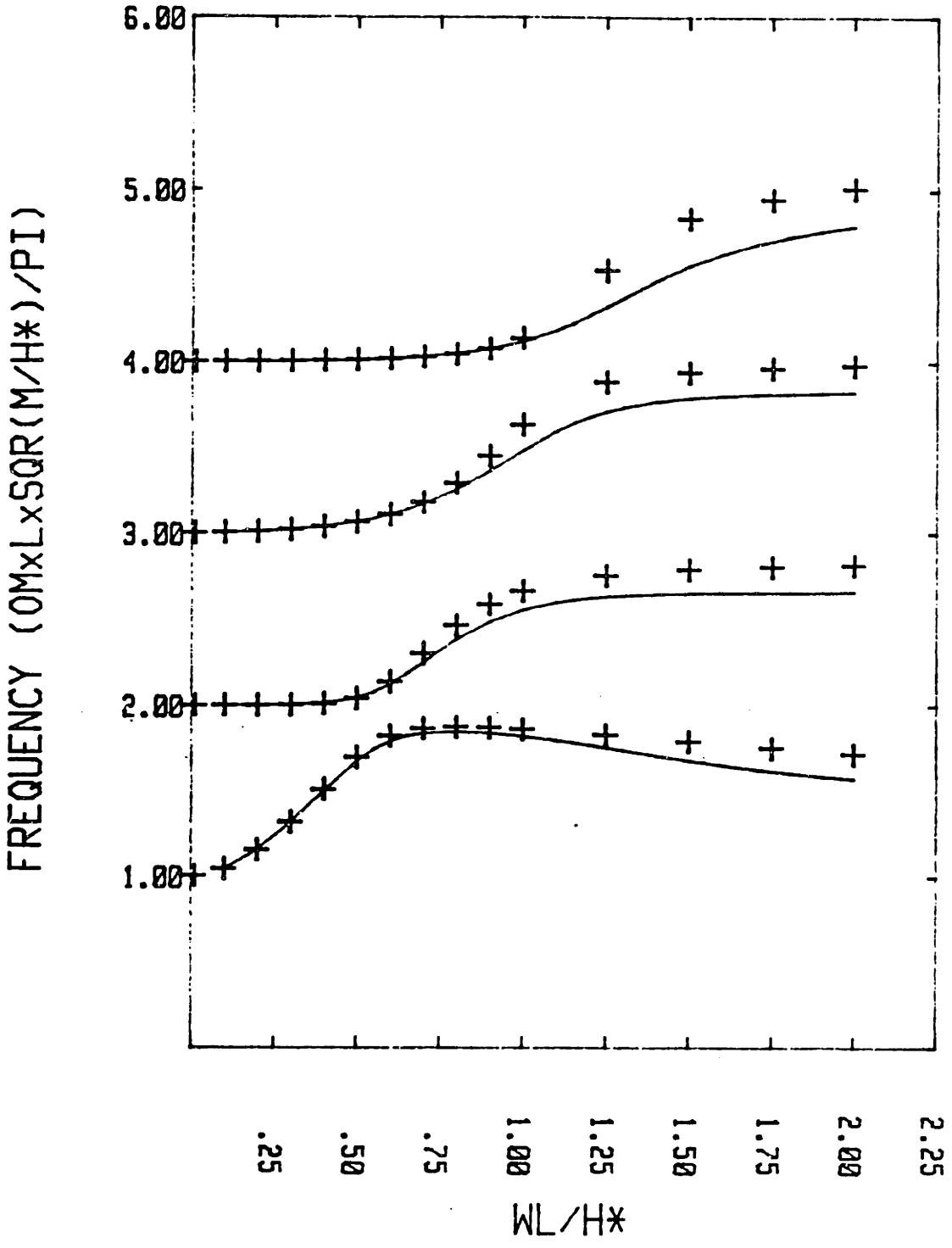

Figure 4-8: Eigenfrequencies for an Extensible Cable, $\phi_a = 60^\circ$, $\beta = 1/400$

(Solid line: extensible perturbation theory)
(+ marks: numerical central difference scheme)

eigenfrequencies of the inextensible cable are obtained.

The previous graphs have the drawback that the transition zone is strongly dependent on β. This can be reduced by plotting the eigenfrequencies versus λ_*^2. For small sag cables, as demonstrated in chapter 3, the eigenfrequencies depend only on λ_*^2. For large sag cables this is not valid, but the representation in terms of λ_*^2 is still useful. λ_*^2 can be expressed as:

$$\lambda_*^2 = \left[\frac{w_o L}{H_*} \right]^2 \cdot \left[\frac{E \cdot A}{H_*} \right] \cdot \cos^2(\phi_a) \qquad (4.3)$$

$$= \frac{\alpha_*^2}{\beta}$$

In figure 4-9 and 4-10 the eigenfrequencies are plotted versus λ_*^2. The parameter α_* is kept fixed and is allowed to take three values (0 , 0.5 , 1). Figure 4-10 is an enlargement of the transition zone of the first and second modes. The eigenfrequency curves were cut off at $\beta = 1/100$. The cut-off value of λ_*^2 is higher for higher values of α_*^2, for which the transition zone becomes clearly more pronounced. With the exception of the transition zone, the shallow sag extensible theory gives a good approximation for values of $\alpha_* < 0.5$. Figure 4-11 provides the shallow sag eigenfrequencies and can be considered a fairly good approximation for $\alpha_* < 0.5$, outside the transition zone. For horizontal cables, the modes are crossing over and figure 4-11 will be approximately valid even for higher values of α_*.

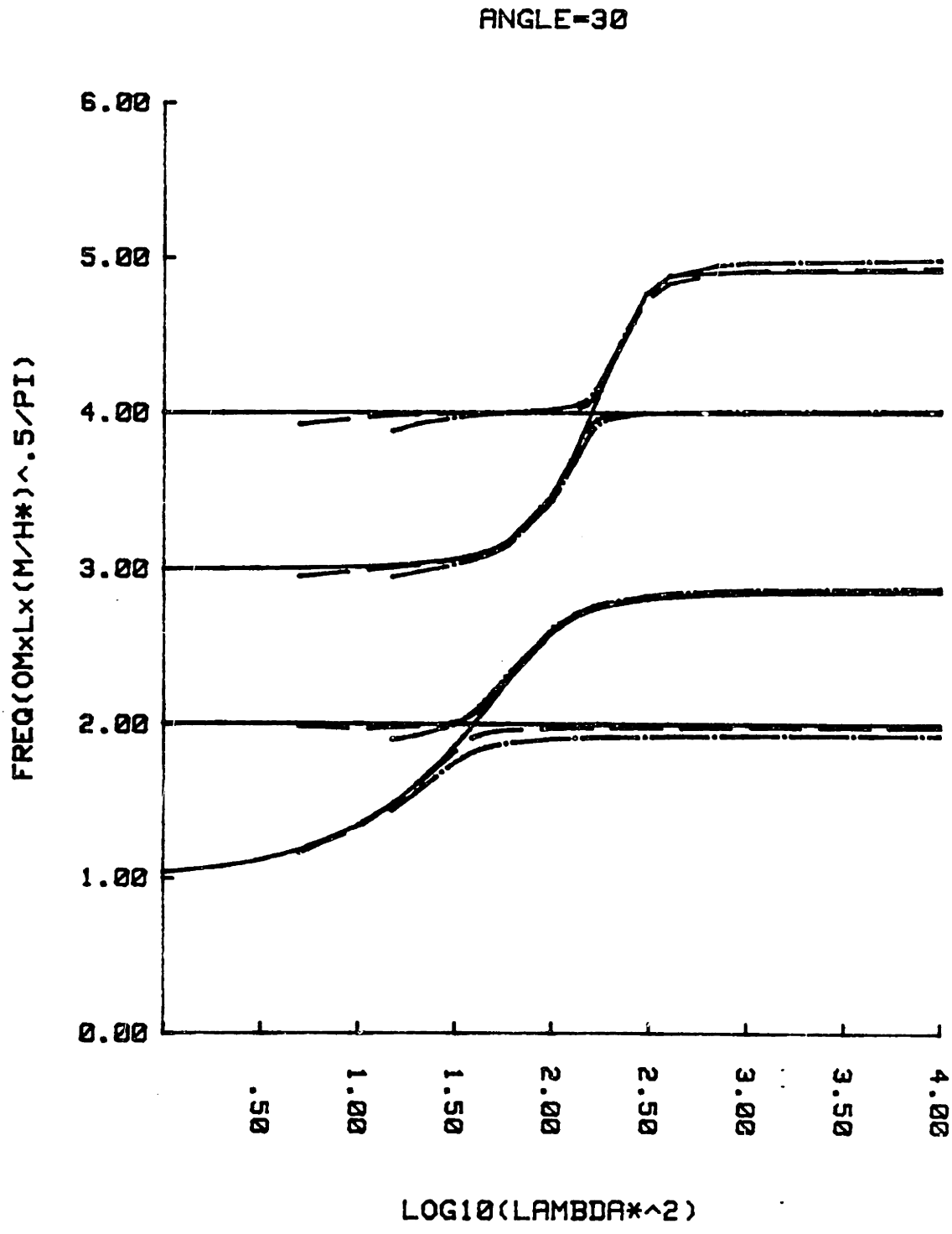

Figure 4-9: Eigenfrequencies of Extensible Cables vs. λ_*^2 ($\phi_a = 30$)

(solid line: $\alpha_* = 0$; dash line: $\alpha_* = 0.5$;
dot-dash line: $\alpha_* = 1$)

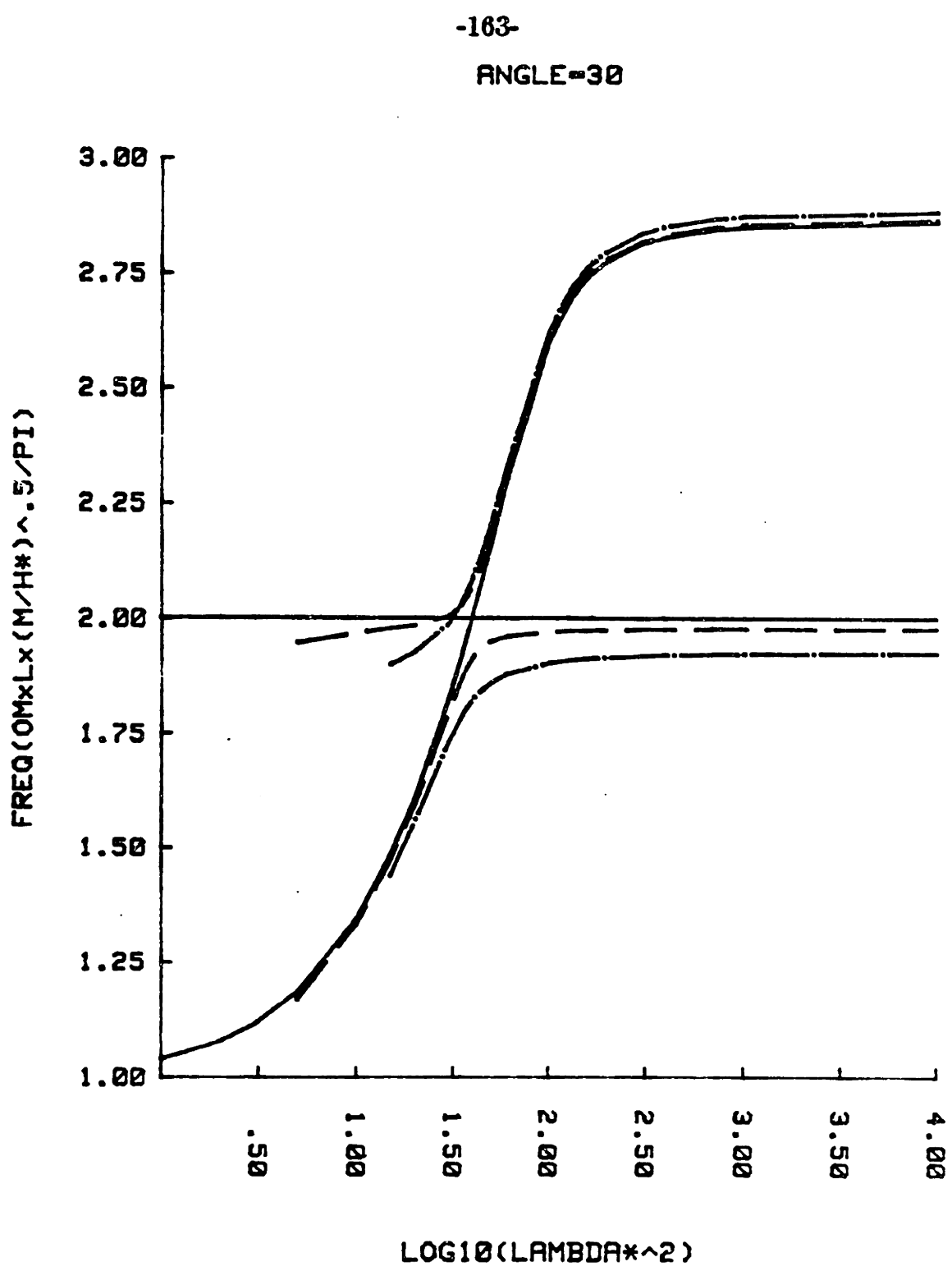

Figure 4-10: Enlargement of the Plot of the First Two Eigenfrequencies of Extensible Cables vs. λ_*^2 ($\phi_a = 30$)

(solid line: $\alpha_* = 0$; dash line: $\alpha_* = 0.5$;
dot-dash line: $\alpha_* = 1$)

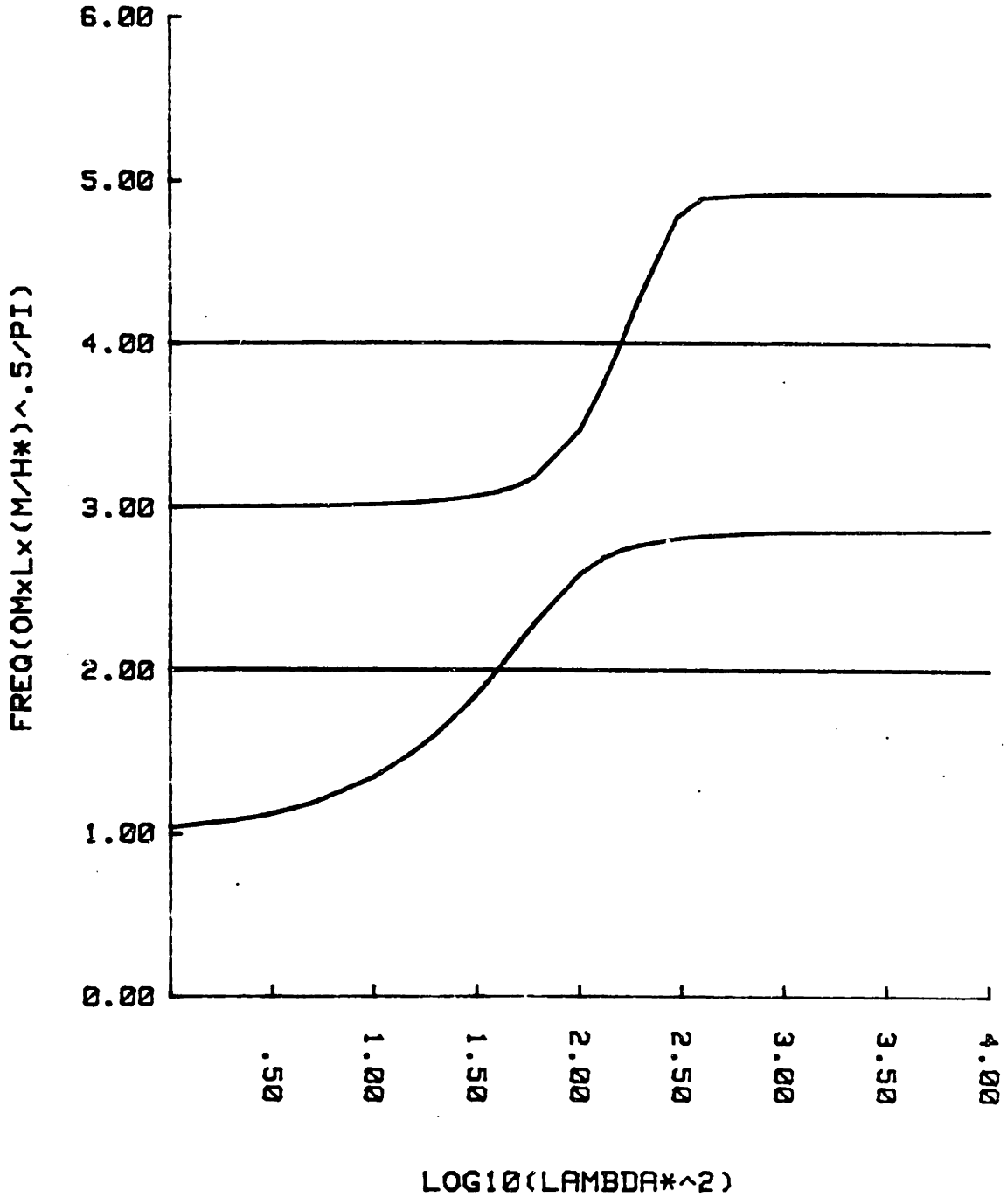

Figure 4-11: Eigenfrequencies for Shallow Sag Extensible Cables, Generalised for Inclination Angles

4.4 Terminal Impedances

The concept of termination impedances has been widely used in the design of guyed masts (See for example [Davenport 65]). In mooring line design, the termination impedances can also be useful. The upper end of the cable is excited by an externally imposed motion. The mooring line termination impedances are defined in the following way:

$$\begin{bmatrix} S_{xx}(\omega) & S_{xy}(\omega) \\ S_{yx}(\omega) & S_{yy}(\omega) \end{bmatrix} \begin{bmatrix} x \\ y \end{bmatrix} = \begin{bmatrix} F_x \\ F_y \end{bmatrix} \tag{4.4}$$

where: x: complex amplitude motion, horizontal direction

y: complex amplitude motion, vertical direction

F_x: complex amplitude force, horizontal direction

F_y: complex amplitude force, vertical direction

The resonance frequencies are the poles of the impedance transfer functions. The mooring line admittance matrix can be calculated as the inverse of the impedance matrix. In practical applications, the above transfer matrices can be used to find body motions and dynamic tensions.

The undamped transfer functions for the guy[9] of a guyed tower were calculated using both the perturbation method and the finite difference scheme (100 discretisation points).

At the top of the cable, unit sinusoidal motions in the x direction and y

---

[9]The relevant data for the guy can be found in chapter 7, as well as the eigenfrequencies and eigenmodes.

direction are imposed. The dynamic tension and the dynamic angle at the top are obtained as:

$$S_{xx} = T_{11} \cdot \cos\phi_o - T_o \cdot \sin\phi_o \cdot \phi_{11}$$

$$S_{yx} = T_{11} \cdot \sin\phi_o + T_o \cdot \cos\phi_o \cdot \phi_{11} \qquad (4.5)$$

where: T_{11}, ϕ_{11} are the dynamic tension and the angle, respectively, caused by unit amplitude motion in the x direction

$$S_{yy} = T_{12} \cdot \cos\phi_o - T_o \cdot \sin\phi_o \cdot \phi_{12}$$

$$S_{xy} = T_{12} \cdot \sin\phi_o + T_o \cdot \cos\phi_o \cdot \phi_{12} \qquad (4.6)$$

where: T_{12}, ϕ_{12} are the dynamic tension and the angle, respectively, caused by unit amplitude motion in the y direction

In the perturbation theory, the zeroth order slow solution was used. To leading order the slow solution is generating the dynamic tension and the fast solution is generating the dynamic angle.

In figures 4-12 through 4-14 a comparison of the transfer functions of the perturbation theory and the numerical, finite difference scheme is given.

The peaks corresponding to the anti-symmetric modes are very narrow and do not contribute to the transfer functions (anti-symmetric modes $\omega_{1a} = 0.90$ and $\omega_{2a} = 1.82$). The symmetric modes are solely responsible for the resonance phenomena ($\omega_{1s} = 1.19$, $\omega_{2s} = 1.61$, $\omega_{3s} = 2.31$). (See chapter 7 for the mode shapes.) The agreement between perturbation and numerical

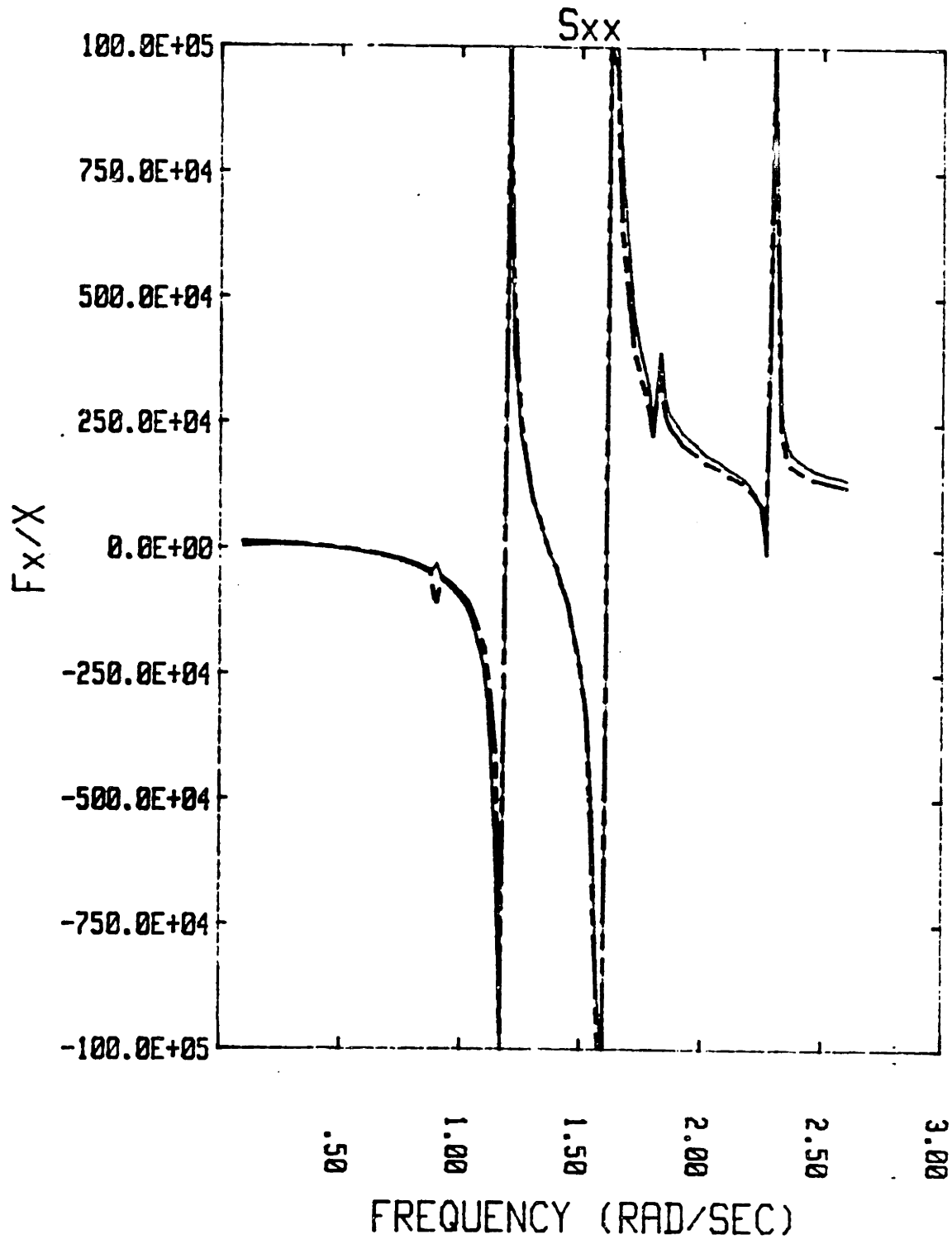

Figure 4-12: S_{xx} for a Guy of a Guyed Tower

(Solid line: perturbation theory)
(Dashed line: finite difference scheme)

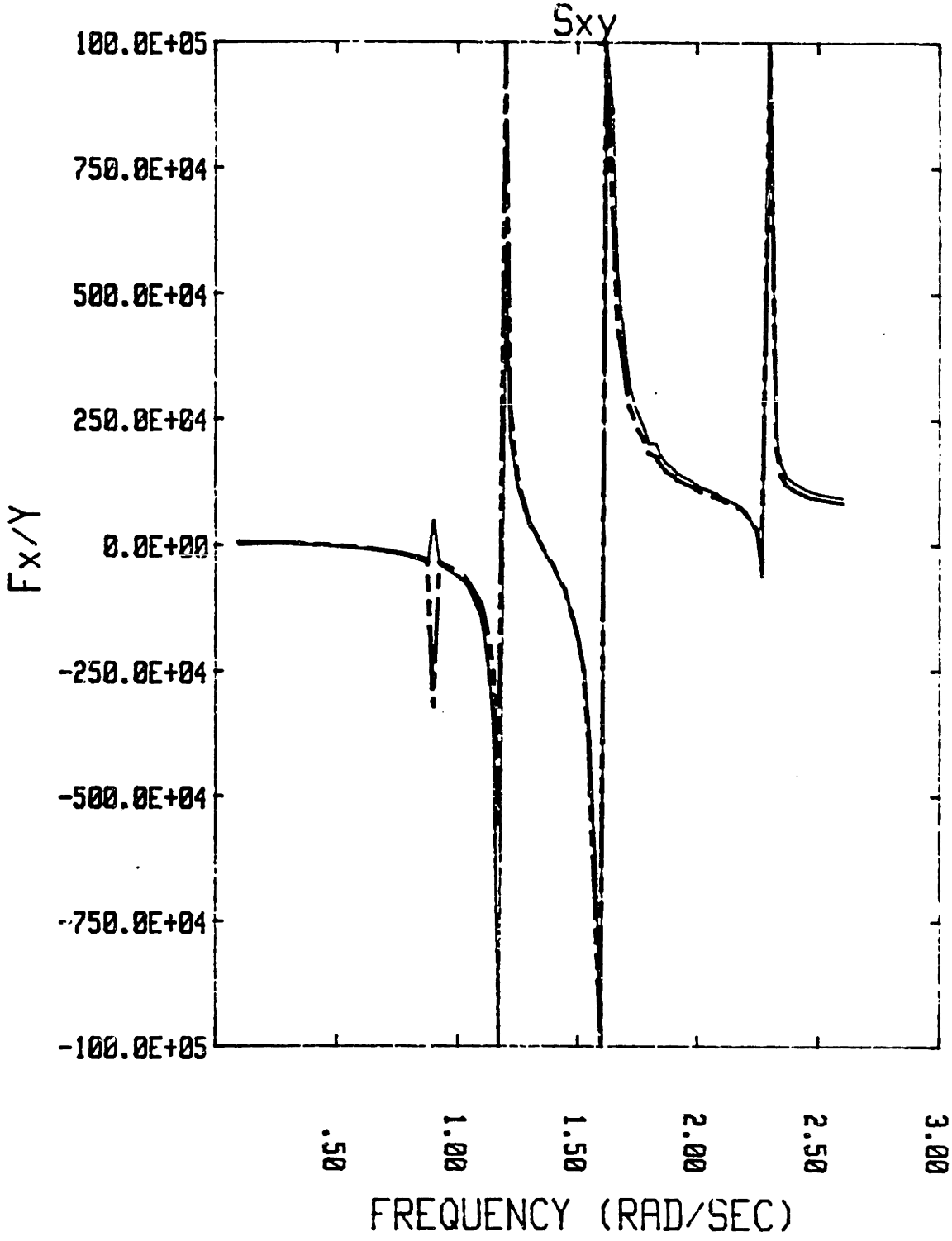

Figure 4-13: $S_{xy} = S_{yx}$ for a Guy of a Guyed Tower

(Solid line: perturbation theory)
(Dashed line: finite difference scheme)

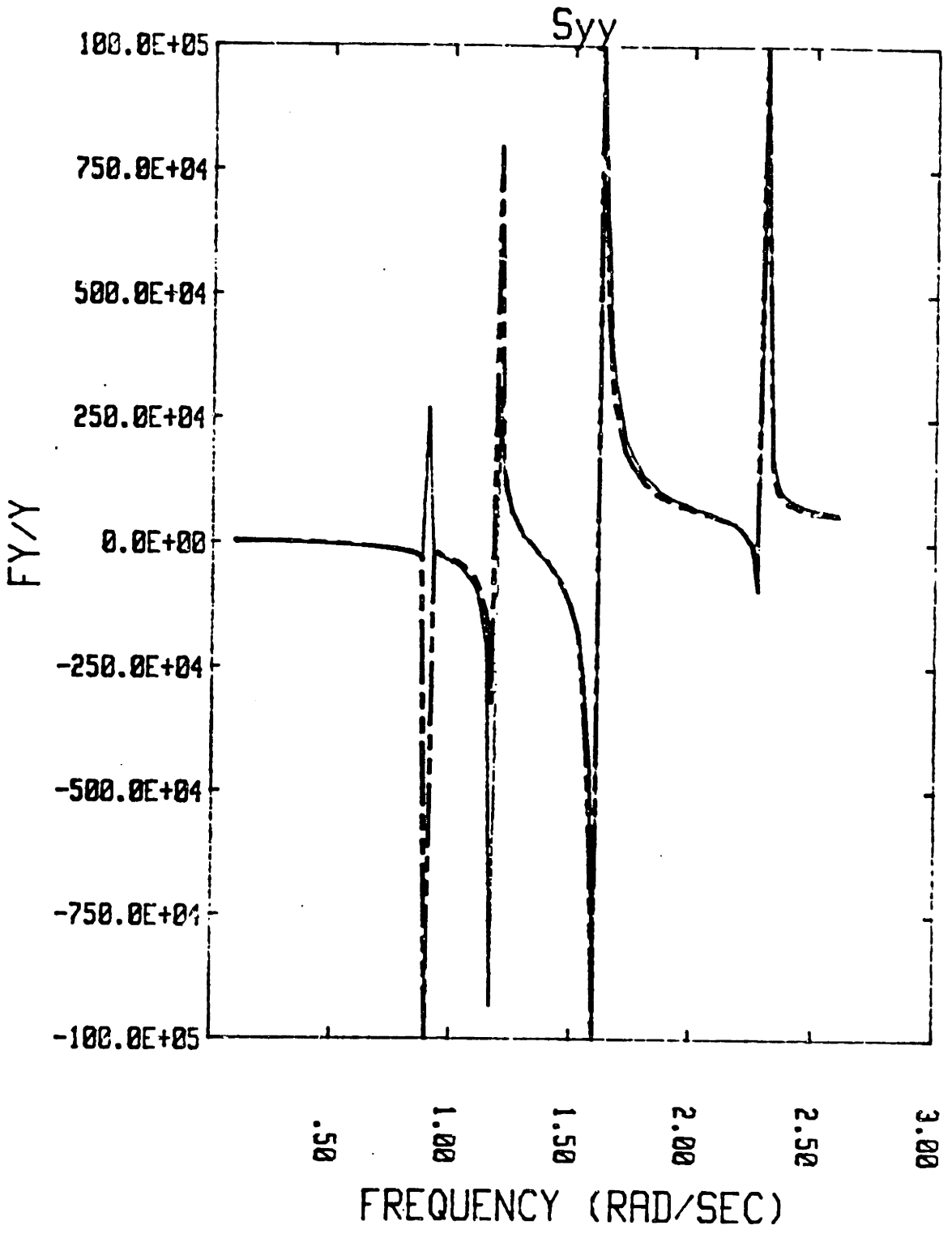

Figure 4-14: S_{yy} for a Guy of a Guyed Tower

(Solid line: perturbation theory)
(Dashed line: finite difference scheme)

solution, in the range considered, is very good.

4.5 References

[Bliek 84] Bliek, A. and Triantafyllou, M.S.
Determination of the Eigenfrequencies of Single Span Cables.
Technical Report, Design Lab. Department of Ocean Engineering MIT, 1984.
To appear.

[Davenport 65] Davenport, A. G. and Steels, G. N.
Dynamic Behavior of Massive Guy Cables.
Journal of the Structural Division, ASCE 91(ST2):43-76, April, 1965.

[Gambhir 77] Gambhir, M. L. and de Batchelor, B.
A Finite Element for 3D Prestressed Cable Nets.
International Journal for Numerical Methods in Engineering 2:1699-1718, 1977.

[Goodey 61] Goodey, W. J.
On the Natural Modes and Frequencies of a Suspended Chain.
Quarterly Journal of Mechanics and Applied Mathematics 14(1):118-127, 1961.

[Henghold 77] Henghold, W. M., Russell, J. J. and Morgan, J. D.
Free Vibrations of Cable in 3D.
Journal of the Structural Division, ASCE 103(ST5):1127-1136, May, 1977.

[Irvine 74] Irvine, H. M. and Caughey, T. K.
The Linear Theory of Free Vibrations of a Suspended Cable.
Proceedings of the Royal Society Series A 341:299-315, 1974.

[Kim 83] Kim, Y.C.
Nonlinear Vibrations of Long Slender Beams.
PhD thesis, MIT, 1983.

[Pugsley 49] Pugsley, A. G.
On the Natural Frequencies of Suspension Chains.
Quarterly Journal of Mechanics and Applied Mathematics 2(4):412-418, 1949.

[Ramberg 82] Rambert, S. E. and Bartholomew, C. L.
Vibrations of Inclined Slack Cables.
Journal of the Structural Division, ASCE 108(ST7):1662-1664, July, 1982.

[Saxon 53] Saxon, D. S. and Cahn, A. S. .
Modes of Vibration of Suspension Chain.
Quarterly Journal of Mechanics and Applied Mathematics 6:273-285, 1953.

[West 75] West, H. H., Geschwindner, L. F. and Suhoski, J. E.
Natural Vibrations of Suspended Bridges.
Journal of the Structural Division, ASCE 101(ST11):2277-2291, November, 1975.

[Yamaguchi 79] Yamaguchi, H. and Ito, H.
Linear Theory of Free Vibrations of an Inclined Cable in Three Dimensions.
Prcceedings Japanese Society of Civil Engineers (286):29-36, June, 1979.
In Japanese, Summary in English, Transactions Japanese Society of Civil Engineers 1979.

Chapter 5

NON-LINEAR STRINGS

5.1 Introduction

The study of non-linear strings has attracted since the 1940's a great deal of attention. The linear string equations are valid only for small motions, while, when the motions become large, the dynamic tension generated by the motion must be included in the governing equations. The popularity of the subject is mainly due to the fact that the governing equations can be solved using perturbation analysis.

Carrier formulated the equations of motion for a non-linear string and solved the problem by means of a perturbation expansion in terms of the amplitude of motion. See [Carrier 45] and [Carrier 49]. Oplinger [Oplinger 60] studied the planar motion of a non-linear string using the method of separation of variables. He studied the motions of a string subject to an imposed motion of the boundary and he derived the response in the middle of the string. The response curves he obtained both analytically and experimentally, show a hardening spring type of effect.

In figure 5-1 the response of a non-linear string subject to a forced motion of one of its ends is shown. The response of the midpoint is given as a function of the ratio of the frequency to the first resonance frequency.

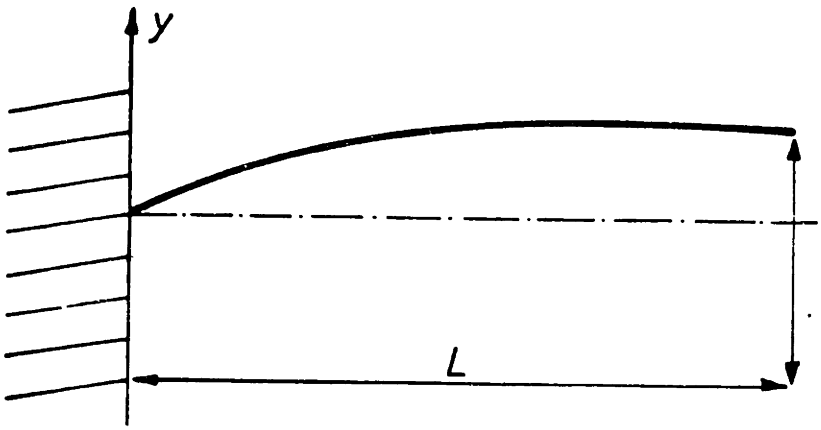

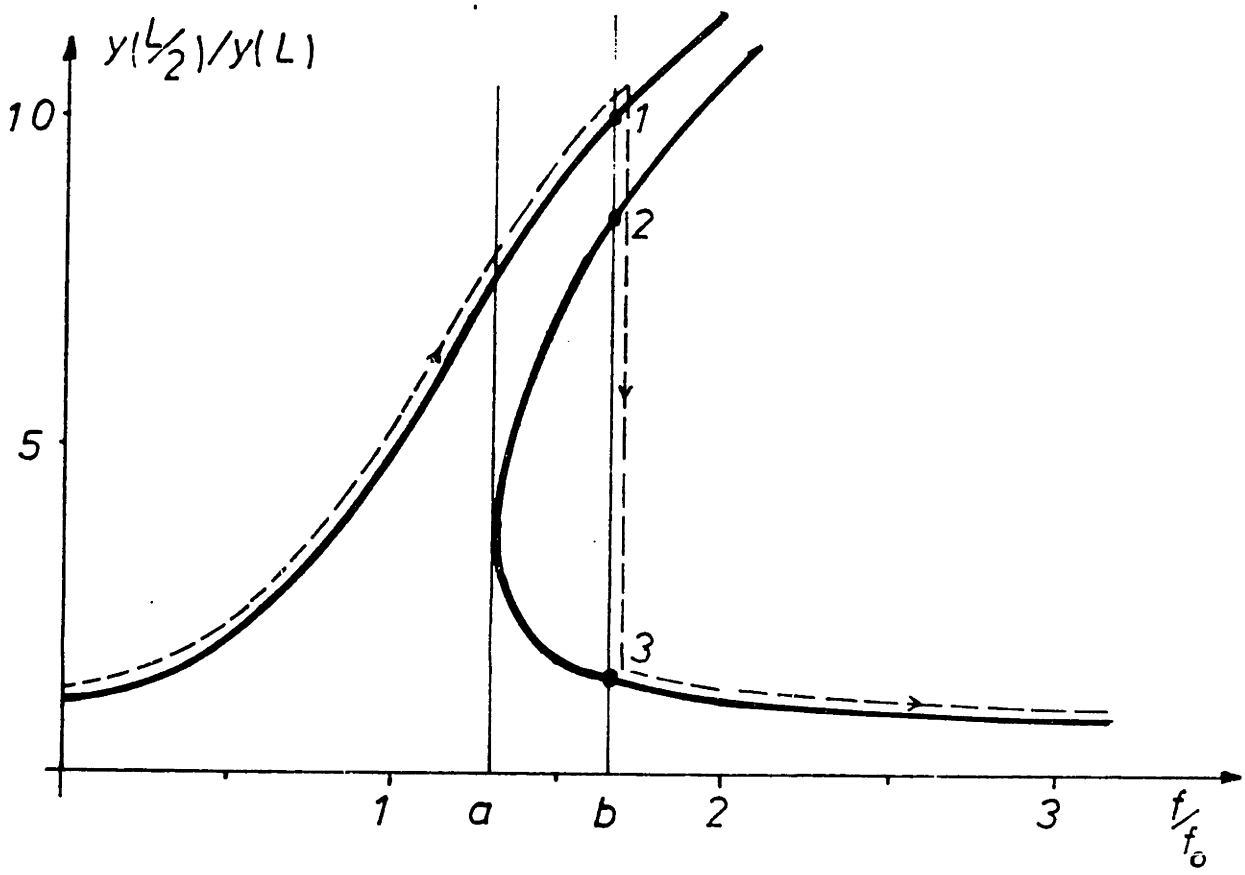

Figure 5-1: Response Curve for a Non-Linear String subject to Boundary Excitation

Taken from [Oplinger 60]

The parameter τ governs completely the non-linearity of the system. τ is given by:

$$\tau = \frac{E \cdot A}{T_o} \cdot \frac{(Ampl)^2}{2L^2} \tag{5.1}$$

The frequency response curve is bent to the right causing the resonance frequencies to shift to higher frequencies as the amplitude increases. True resonance is never obtained. Above a certain level, the response is multivalued and depends on how the exciting frequency was varied. Jump phenomena can occur, i.e. a sudden reduction in the amplitude of the response for a small increase in the frequency of excitation. Point 2 on the curve is an unstable point and cannot be achieved. When the excitation frequency is decreased an inverse jump (i.e. a sudden increase in amplitude) occurs.

Oplinger conducted also experiments to verify his results. The agreement of theory and experiments is remarkable. He also observed the spontaneous occurance of out-of-plane motion for high amplitudes.

The instabilities of the high-amplitude motion in a plane, and the resulting whirling motion, has been the focus of a major research effort. For a good review on this subject, see [Nayfeh 79].

Major contributions to the out-of-plane whirling motions can be found in [Murthy 65], [Miles 65], [Narasimha 68] and [Dickey 80]. Narasimha has also made in his paper an interesting derivation of the string equation, expressed in Eulerian coordinates.

Prediction of the accurate location of the jump phenomena can only be done when damping is included in the model. Anand [Anand 66] included viscous damping. A fluid drag type of damping was included by Hsu in his

study of parametric instabilities of a hanging string [Hsu 75]. This paper is particularly interesting as far as this study is concerned, because he uses the mode shapes directly in his solution method.

More recently, Richard and Anand studied the resonance phenomena caused by narrow band excitation [Richard 83]. Tagata [Tagata 83] studies the interesting subject of parametric excitation of a string of varying length.

In this work, we will only be concerned with the analysis of the in-plane motion of non-linear strings under excitation of one boundary. The main objective of the study is to illustrate the use of modal expansions to solve a non-linear problem. It should therefore not be considered as an in depth analysis of the subject.

5.2 Governing Equations

The string equation can be written in the transverse direction as:

$$M \frac{\partial^2 q}{\partial t^2} + b_d \frac{\partial q}{\partial t} \left| \frac{\partial q}{\partial t} \right| = \frac{\partial}{\partial x} \left[T(x,t) \frac{\partial q}{\partial x} \right] \tag{5.2}$$

q is the motion in the transverse direction, and x is the cartesian coordinate along the string in rest. In the above equation use was made of the fact that:

$$\frac{\partial x}{\partial s} \cong 1 \tag{5.3}$$

A quadratic damping of the Morison type was introduced, where b_d can be set in the form:

$$b_d = \frac{1}{2} \rho_w C_D D \tag{5.4}$$

It is convenient for further manipulation to write (5.2) as:

$$\frac{\partial^2 \eta}{\partial t^2} + \frac{b_d}{M} \frac{\partial \eta}{\partial t} \left| \frac{\partial \eta}{\partial t} \right| = \frac{1}{ML^2} \frac{\partial}{\partial \sigma} \left[T(\sigma,t) \frac{\partial \eta}{\partial \sigma} \right] \tag{5.5}$$

where: η: the non-dimensional displacement q/L

σ: the non-dimensional length s/L

This equation is subject to boundary conditions:

$$\eta(0) = 0$$

$$\eta(1) = F(t) \tag{5.6}$$

A stress-strain relation for moderately large transverse displacements can be formulated as:

$$T = T_o(\sigma) + E \cdot A \cdot e$$

The compatibility relation, derived in chapter 1, can be written as:

$$e = \frac{\partial \xi}{\partial \sigma} + \frac{1}{2(1+e_o)} \left\{ \left[\frac{\partial \xi}{\partial \sigma} \right]^2 + \left[\frac{\partial \eta}{\partial \sigma} \right]^2 \right\} \tag{5.7}$$

Even for moderately large motions, the tangential motion is an order of magnitude smaller than the transverse motion. Therefore:

$$e \cong \frac{\partial \xi}{\partial \sigma} + \frac{1}{2} \left[\frac{\partial \eta}{\partial \sigma} \right]^2 \tag{5.8}$$

The strain can be assumed to be constant over the string length. This assumption is valid for excitation frequencies well below the first elastic eigenfrequency. Therefore:

$$e = \int_0^1 e \, d\sigma$$

$$= u(1) - u(0) + \frac{1}{2} \int_0^1 \eta_{\sigma(\sigma} \, d\sigma \tag{5.9}$$

The governing equation can, therefore, be written as:

$$\frac{\partial^2 \eta}{\partial t^2} + \frac{b_d}{M} \frac{\partial \eta}{\partial t} \left| \frac{\partial \eta}{\partial t} \right| = \frac{1}{ML^2} \frac{\partial}{\partial \sigma} \left[T_o(\sigma) \frac{\partial \eta}{\partial \sigma} \right]$$

$$+ \frac{E \cdot A}{ML^2} e \frac{\partial^2 \eta}{\partial \sigma^2} \tag{5.10}$$

in which e is given by (5.9). This governing equation is subject to the boundary conditions (5.6). In equation (5.10) the static tension is allowed to vary along the length, which makes it more general than the case of a string under constant tension.

5.3 Expansions in Orthogonal Functions

We propose to expand the solution of the problem in the following form:

$$\eta(\sigma,t) = \eta_o(\sigma) \, f(t) + \sum_{i=1}^{n} \eta_i(\sigma) \, C_i(t) \tag{5.11}$$

where: $\eta_o(\sigma)$: the quasi-static solution, to take care of the inhomogeneous boundary conditions.

$\eta_i(\sigma)$: the modes, obtained from the linear eigenvalue problem with homogeneous boundary conditions.

The boundary condition is directly taken care of by introducing the quasi-static solution. The main advantage of using this technique is that for low frequency excitation only a very limited number of modes needs to be

included.

5.4 The Quasi-Static Problem

The quasi-static problem consists of finding the solution to the following equation:

$$\frac{\partial}{\partial\sigma}\left[\, T_o\,(\sigma)\,\frac{\partial\eta}{\partial\sigma}\,\right] = 0 \tag{5.12}$$

$$\eta(0) = 0 \qquad \eta(1) = 1$$

The solution to this problem can be written as:

$$\eta_o\,(\sigma) = C_1 \int_0^{\sigma} \frac{1}{T_o\,(\sigma)}\, d\sigma \tag{5.13}$$

$$\text{where: } C_1 = \left\{ \int_0^1 \frac{1}{T_o\,(\sigma)}\, d\sigma \right\}^{-1}$$

For a string under constant tension the solution is simply:

$$\eta_o\,(\sigma) = \sigma$$

5.5 The Eigenproblem

The linear eigenproblem associated with (5.10) can also be solved easily. The case of a string with varying static tension is a classical Sturm-Liouville problem:

$$\frac{1}{ML^2}\,\frac{\partial}{\partial\sigma}\left[\, T_o\,(\sigma)\,\frac{\partial\eta}{\partial\sigma}\,\right] = -\,\omega^2\,\eta \tag{5.14}$$

$$\eta(0) = 0 \qquad \eta(1) = 0$$

The eigenfunctions can be obtained using analytical, perturbation or numerical methods. The WKB method, as a solution to this problem, has been described in detail in chapter 3. The modes are orthogonal, with the following orthogonality condition: (η_i with $i \neq 0$ are the eigenmodes.)

$$\int_0^1 M\ \eta_i(\sigma)\ \eta_j(\sigma)\ d\sigma = 0 \qquad i \neq j \tag{5.15}$$

The eigenmodes are chosen to be orthonormal:

$$\int_0^1 M\ \eta_i^2(\sigma)\ d\sigma = 1 \tag{5.16}$$

5.6 Time Integration

The expansion (5.11) can be substituted in (5.10) where all of the space varying functions are known functions.

Substitution gives:

$$\eta_o \ddot{f} + \sum_{i=1}^{n} \eta_i \ddot{C}_i + \frac{b_d}{M} \left| \frac{\partial \eta}{\partial t} \right| \left[\eta_o \dot{f} + \sum_{i=1}^{n} \eta_i \dot{C}_i \right]$$

$$= -\sum_{i=1}^{n} \omega_i^2\ \eta_i\ C_i + \frac{E \cdot A}{ML^2}\, e \left[\eta_{o\sigma\sigma}\ f(t) + \sum_{i=1}^{n} \eta_{i\sigma\sigma}\ C_i(t) \right] \tag{5.17}$$

Multiplying with $M\eta_j$ and integrating over the domain gives the governing equation:

$$\ddot{C}_j + b_d \sum_{i=1}^{n} \int_0^1 \left| \frac{\partial \eta}{\partial t} \right| \eta_j \, \eta_i \, d\sigma \, \dot{C}_i$$

$$+ \sum_{i=1}^{n} \left[\delta_{ji} \, \omega_j^2 + \frac{E \cdot A}{L^2} \, e \int_0^1 \eta_{j\sigma} \, \eta_{i\sigma} \, d\sigma \right] C_i$$

$$= - \int_0^1 M \, \eta_o \, \eta_j \, d\sigma \, \ddot{f} - b \int_0^1 \left| \frac{\partial \eta}{\partial t} \right| \eta_o \, \eta_j \, d\sigma \, \dot{f}$$

$$- \frac{E \cdot A}{L^2} \, e \int_0^1 \eta_{o\sigma} \, \eta_{j\sigma} \, d\sigma \, f \qquad (5.18)$$

This sommation will be taken over a finite number n, so that a set of n non-linear differential equations with n unknown functions C_j is obtained. Several of the terms in the expansion are time varying. These are the coefficients involving $\partial\eta/\partial t$ and e, which are unknown.

Among the time integration schemes, which can be used to integrate (5.18) are: the explicit scheme, and the implicit scheme together with some iteration method. This will be discussed in great detail in chapter 6. Fortunately (5.18) has the characteristic that if the non-linearities are not dominant, the n equations are very weakly coupled. Even ignoring completely the coupling can lead to good practical results [Hsu 75].

In (5.18) integration by parts was used to reduce the order of spatial derivatives by one. This is a very important feature numerically and will be used in the more general cable dynamic problem extensively.

When a string with constant tension is simulated in time, the modes are simply sinuoidal functions and some of the cross-coupling terms between the equations disappear. An example of time simulation for a string with constant tension is discussed in chapter 7.

5.7 References

[Anand 66] Anand, G.V.
Non-Linear Resonance in Stretched Strings with Viscous Damping.
Journal Acoustical Society of America 40(6):1517-1528, 1966.

[Carrier 45] Carrier, G. F.
On the Non-Linear Vibration Problem of the Elastic String.
Quarterly Journal of Applied Mathematics 3(2):157-165, 1945.

[Carrier 49] Carrier, G. F.
A Note on the Vibrating String.
Quarterly Journal of Applied Mathematics 7(1):97-101, 1949.

[Dickey 80] Dickey,W.
Stability of Periodic Solutions of the Non-Linear String.
Quarterly of Applied Mathematics :253-259, July, 1980.

[Hsu 75] Hsu, C. S.
The Response of a Parametrically Excited String in Fluid.
Journal of Sound and Vibration 39(3):305-316, 1975.

[Miles 65] Miles, J. W.
Stability of Forced Oscillations of a Vibrating String.
Journal of the Acoustical Society of America 38:855-861, 1965.

[Murthy 65] Murthy, G.S.S. and Ramakrishna.
Nonlinear Character of Resonance in Stretched Strings.
Journal of the Acoustical Society of America 38:461-471, 1965.

[Narasimha 68] Narasimha, R.
Non-Linear Vibrations of an Elastic String.
Journal of Sound and Vibration 8:134-146, 1968.

[Nayfeh 79] Nayfeh, A. M. and Hook, D. T.
Non-Linear Oscillations.
John Wiley & Sons, New York, 1979, chapter Strings.

[Oplinger 60] Oplinger, D. W.
Frequency Response of a Nonlinear Stretched String.
Journal of the Acoustic Society of America 32(12):1529-1538, December, 1960.

[Richard 83] Richard, K. and Anand, G. V.
Non-Linear Resonance in Strings under Narrow-Band Random Excitation.
Journal of Sound and Vibration 86(1):85-98, 1983.

[Tagata 83] Tagata, G.
A Parametrically Driven Harmonic Analysis of a Non-Linear Stretched String with Time Varying Length.
Journal of Sound and Vibration 87(3):493-511, 1983.

Chapter 6

NON-LINEAR DYNAMICS USING GALERKIN'S METHOD

6.1 Introduction

The advantages of using modal decomposition in linear dynamic analysis of structures are well documented [Clough 75] and [Bathe 82]. The dynamic equations of motion become uncoupled and, what is even more important, in many cases the number of degrees of freedom can be reduced drastically, without losing accuracy.

Modal expansions in the analysis of non-linear dynamics is much less developed. Some structural examples have been solved; buckling problems [Nickell 76], contact problems and earthquake excitation [Bathe 81]. The results were very encouraging. Although the problems considered were highly non-linear, a very small number of modes gave reasonable accuracy.

In riser dynamics Galerkin's method has been used by several researchers. Kirk [Kirk 79] assumes the deflection as a series of sinusoids. Dareing [Dareing 79] solved the riser problem using a modal decomposition and he found that under regular wave excitation few modes are needed. To uncouple the equations he used a uniform equivalent damping over the riser. The full, non-linear drag term was used in the modal expansion of Y. C. Kim [Kim 83], who investigated, also, the effect of second order geometric terms. Fast convergence of the modal expansion is reported. Applications of modal expansions in non-linear strings have been described in chapter 5.

The use of modal analysis in linearised, small sag cable dynamics was developed by Irvine [Irvine 76]. He shows the influence of the ratio of elastic and geometric stiffness on the modal dynamic tension. See also [Veletsos 82]. Hagedorn [Hagedorn 80] includes non-linearities up to third order in the modal expansions of a small sag cable. The resulting equations were solved using a perturbation solution. In a very interesting paper, written in Japanese and therefore not well known in this continent, Yamaguchi [Yamaguchi 79] uses Galerkin's method with sinusoidal functions to solve the general linear cable problem. He uses this method to calculate eigenfrequencies and good agreement with previous results is reported. The use of modal expansion for a cable without using the small sag approximation has, to the author's knowledge, not been reported.

6.2 Galerkin's Method

The Galerkin method will be explained using a simple one-dimensional example, although the concept can be applied to problems in several dimensions. For more details, see [Gotlieb 77]. The problem considered is a mixed initial boundary value problem.

$$\frac{\partial u}{\partial t} = L(x,t)\, u(x,t) + f(x,t)$$

$$u(x_1,t) = 0 \qquad u(x_2,t) = 0 \qquad t > 0$$

$$u(x,o) = g(x) \qquad x_1 < x < x_2$$

The operator L is a linear differential operator in x. Only the homogeneous problem is considered, because the inhomogeneous problem can be rewritten as a homogeneous one by adding an appropriate, but otherwise

arbitrary function, satisfying the inhomogeneous boundary conditions.

The solution is expanded in the form of a truncated series:

$$u_n\ (x,t) = \sum_{i=0}^{n} a_i\ (t)\ \phi_i\ (x)$$

where ϕ_i are assumed to be linearly independent space functions, satisfying the homogeneous boundary conditions.

The residual error, by substituting the truncated series in the governing equation, is:

$$R_n = \frac{\partial u_n}{\partial t} - L_n - f$$

Several methods can be used to minimize this error over the solution domain. In Galerkin's method the error is weighted with the trial functions and the averaged value is required to be 0. This gives:

$$\sum_{i=0}^{n} \int \phi_j\ \phi_i\ dx\ \frac{\partial a_i}{\partial t} = \sum_{i=0}^{n} \int \phi_j\ L\ \phi_i\ dx\ a_i + \int \phi_j\ f\ dx \qquad j=1...n$$

Several types of functions can be used in the expansions. If the eigenfunctions of the problem are used, the above equations become uncoupled, resulting in a significant simplification of the time integration scheme.

6.3 Linearised Dynamics using Modal Expansions

The modal expansions can be applied directly to the linearised dynamic equations. The external forces can be of arbitrary form and they are a function of time. Because the static forces are in equilibrium (see chapter 2) only dynamic forces must be considered. The governing dynamic equations are:

$$m \frac{\partial^2 p}{\partial t^2} = \frac{\partial T_1}{\partial s} - T_o \frac{\partial \phi_o}{\partial s} \phi_1 + F_t(t)$$

$$M \frac{\partial^2 q}{\partial t^2} = \frac{\partial \phi_o}{\partial s} T_1 + \frac{\partial T_o}{\partial s} \phi_1 + T_o \frac{\partial \phi_1}{\partial s} + F_n(t)$$

$$\frac{\partial p}{\partial s} - q \frac{\partial \phi_o}{\partial s} = e_1 \qquad (6.1)$$

$$\frac{\partial q}{\partial s} + p \frac{\partial \phi_o}{\partial s} = \phi_1 (1+e_o)$$

These equations are supplemented with the linear tension-strain relation:

$$T_1 = E \cdot A \cdot e_1 \qquad (6.2)$$

To be able to use modal expansions, it is more convenient to eliminate the dynamic tension out of the relations (6.1) and (6.2):

$$m \frac{\partial^2 p}{\partial t^2} - \frac{\partial}{\partial s}\left[E \cdot A \left(\frac{\partial p}{\partial s} - q \frac{\partial \phi_o}{\partial s}\right) \right]$$

$$+ T_o \frac{\partial \phi_o}{\partial s} \cdot \frac{1}{1+e_o} \left(\frac{\partial q}{\partial s} + p \frac{\partial \phi_o}{\partial s}\right) = F_t(t)$$

$$M \frac{\partial^2 q}{\partial t^2} - \frac{\partial \phi_o}{\partial s} E \cdot A \left(\frac{\partial p}{\partial s} - q \frac{\partial \phi_o}{\partial s}\right) - \frac{\partial T_o}{\partial s} \cdot \frac{1}{1+e_o} \left(\frac{\partial q}{\partial s} + p \frac{\partial \phi_o}{\partial s}\right) \qquad (6.3)$$

$$- T_o \frac{\partial}{\partial s}\left[\frac{1}{1+e_o} \left(\frac{\partial q}{\partial s} + p \frac{\partial \phi_o}{\partial s}\right)\right] = F_n(t)$$

To have a complete formulation of the dynamic problem, four boundary conditions are needed. In this work we will assume imposed top motions and a fixed end at the bottom. The boundary conditions are then:

$$p(0) = 0 \qquad p(L) = f(t)$$
$$q(0) = 0 \qquad q(L) = g(t) \tag{6.4}$$

we expand the solutions in the following form:

$$p(s,t) = \sum_{i=0}^{n} c_i(t)\, p_i(s)$$
$$q(s,t) = \sum_{i=0}^{n} c_i(t)\, q_i(s) \tag{6.5}$$

where the functions in (6.5) must be determined to satisfy the governing equations (6.3) and the boundary conditions (6.4).

6.3.1 Solution of the Linearised Quasi-Static Problem

The boundary conditions (6.4) will be satisfied by introducing the quasi-static solutions in the proposed expansions. The quasi-static solutions are obtained by neglecting the inertia and external forces in (6.1) or (6.3) and solving the resulting equations:

$$0 = \frac{\partial T_1}{\partial s} - T_o \frac{\partial \phi_o}{\partial s} \phi_1$$

$$0 = \frac{\partial \phi_o}{\partial s} T_1 + \frac{\partial T_o}{\partial s} \phi_1 + T_o \frac{\partial \phi_1}{\partial t}$$

$$\phi_1 = \frac{1}{1+e_o} \cdot \left[\frac{\partial q}{\partial s} + p \frac{\partial \phi_o}{\partial s} \right] \tag{6.6}$$

$$e_1 = \frac{\partial p}{\partial s} - q \frac{\partial \phi_o}{\partial s}$$

$$T_1 = E \cdot A \cdot e_1$$

with boundary conditions:

$$p(0) = 0 \qquad p(L) = f(t)$$

$$q(0) = 0 \qquad q(L) = g(t)$$

We can separate the time and space dependence by writing the solutions, making use of the linearity, in the following form:

$$p_{qs} = f(t)\, p_{qs1}(s) + g(t)\, p_{qs2}(s)$$

$$q_{qs} = f(t)\, q_{qs1}(s) + g(t)\, q_{qs2}(s) \tag{6.7}$$

where p_{qs1} , q_{qs1} must satisfy:

$$p_{qs1}(0) = 0 \qquad p_{qs1}(L) = 1$$

$$q_{qs1}(0) = 0 \qquad q_{qs1}(L) = 0$$

and p_{qs2} , q_{qs2} must satisfy:

$$p_{qs2}(0) = 0 \qquad p_{qs2}(L) = 0$$

$$q_{qs2}(0) = 0 \qquad q_{qs2}(L) = 1$$

The quantities p_{qs},q_{qs} above are the solution to the very slow motion of a cable forced to move with unit amplitude in the tangential and normal direction, respectively. They are the zero frequency limit of the linear dynamic problem. The solution can be obtained by using methods similar to the ones described in chapter 3, because the equations are in the same form as the equations providing the mode shapes. In this work, numerical central differences were used to obtain quasi-static solutions.

We can now try expansions of the solutions in the following form:

$$p(s,t) = f(t)\, p_{qs1}(s) + g(t)\, p_{qs2}(s) + \sum_{i=1}^{n} C_i(t)\, p_i(s)$$

$$q(s,t) = f(t)\, q_{qs1}(s) + g(t)\, q_{qs2}(s) + \sum_{i=1}^{n} C_i(t)\, q_i(s) \qquad (6.8)$$

where $p_i(s)$, $q_i(s)$ are the compcnents of the i th mode with fixed end conditions.

6.3.2 Solution of the Eigenvalue Problem

The eigenmodes of the cable are obtained by solving the following eigenvalue problem.

$$-m\omega^2 p - \frac{\partial}{\partial s}\left[E \cdot A \left(\frac{\partial p}{\partial s} - q \frac{\partial \phi_o}{\partial s}\right)\right] + T_o \frac{\partial \phi_o}{\partial s} \cdot \frac{1}{1+e_o}\left(\frac{\partial q}{\partial s} + p \frac{\partial \phi_o}{\partial s}\right) = 0$$

$$-M\omega^2 q - \frac{\partial \phi_o}{\partial s} E{\cdot}A \left(\frac{\partial p}{\partial s} - q \frac{\partial \phi_o}{\partial s}\right) - \frac{\partial T_o}{\partial s} \cdot \frac{1}{1+e_o} \cdot \left[\frac{\partial q}{\partial s} + p \frac{\partial \phi_o}{\partial s} \right] - T_o \frac{\partial}{\partial s}\left[\frac{1}{1+e_o}\left(\frac{\partial q}{\partial s} + p \frac{\partial \phi_o}{\partial s}\right)\right] = 0 \qquad (6.9)$$

with the following boundary conditions:

$$p(0) = q(0) = 0 \qquad\qquad p(L) = q(L) = 0$$

Again, the methods described in chapter 3 can be used to solve this

problem. The results of the analysis are the eigenfrequencies and the eigenmodes p_i , q_i, as well as the modal dynamic tension and the modal dynamic angle, T_i , ϕ_i respectively.

The eigenmodes are orthogonal to each other, in the following form:

$$\int_0^L (m\ p_i p_j + M\ q_i q_j\ )\ ds = 0 \qquad i \neq j \tag{6.10}$$

In the sequel, the modes are also assumed to be normalised so that:

$$\int_0^L (m\ p_i^2 + M\ q_i^2\ )\ ds = 1 \tag{6.11}$$

6.3.3 Substitution in the Solution

The proposed solution (6.8)

$$p(s,t) = f(t)\ p_{qs1}\ (s) + g(t)\ p_{qs2}\ (s) + \sum_{i=1}^{n} C_i\ (t)\ p_i\ (s)$$

$$q(s,t) = f(t)\ q_{qs1}\ (s) + g(t)\ q_{qs2}\ (s) + \sum_{i=1}^{n} C_i\ (t)\ q_i\ (s)$$

can now be substituted in (6.3), taking into account the quasi-static equations and the eigenvalue equations:

$$\begin{aligned} m \left[\ddot{f} p_{qs1} + \ddot{g} p_{qs2} + \sum_{i=1}^{n} p_i \ddot{C}_i \right] + \sum_{i=1}^{n} m\ \omega_i^2\ p_i\ C_i &= F_t\ (t) \\ M \left[\ddot{f} q_{qs1} + \ddot{g} q_{qs2} + \sum_{i=1}^{n} q_i \ddot{C}_i \right] + \sum_{i=1}^{n} M\ \omega_i^2\ q_i\ C_i &= F_n\ (t) \end{aligned} \tag{6.12}$$

Multiplying the first equation in (6.12) with p_i and the second equation in (6.12) with q_i and integrating over the length, we obtain:

$$\ddot{C}_i + \omega_i^2\ C_i = \mathcal{F}_i - \mathcal{A}_i\ \ddot{f} - \mathcal{B}_i\ \ddot{g} \tag{6.13}$$

where: $\mathcal{F}_i = \int (F_t\ p_i + F_n\ q_i)\ ds$

$\mathcal{A}_i = \int (m\ p_{qs1}\ p_i + M\ q_{qs1}\ q_i)\ ds$

$\mathcal{B}_i = \int (m\ p_{qs2}\ p_i + M\ q_{qs2}\ q_i)\ ds$

To make the description more complete, we introduce a linear modal damping. The equations (6.13) can then be written in its final form as:

$$\ddot{C}_i + 2\ \xi_i\ \omega_i\ \dot{C}_i + \omega_i^2\ C_i = \mathcal{F}_i - \mathcal{A}_i\ \ddot{f} - \mathcal{B}_i\ \ddot{g} \tag{6.14}$$

6.4 Time Integration

In this analysis Newmark's method was selected. It is an implicit time integration scheme which is unconditionally stable. In the case of a modal description, no additional computational effort is needed compared with an explicit scheme, so that it is unquestionably preferable to use an implicit scheme. Newmark's method was developed for direct time integration of very large systems of linear equations, where it gives excellent results. (see [Bathe 82])

The Newmark integration scheme evaluates the equilibrium equations at a time $t + \Delta t$ as follows:

$$\begin{aligned} {}^{t+\Delta t}\dot{x} &= {}^{t}\dot{x} + \left[(1 - \delta)\ {}^{t}\ddot{x} + \delta\ {}^{t+\Delta t}\ddot{x}\right] \Delta t \\ {}^{t+\Delta t}x &= {}^{t}x + {}^{t}\dot{x}\ \Delta t + \left[(1/2 - \alpha)\ {}^{t}\ddot{x} + \alpha\ {}^{t+\Delta t}\ddot{x}\right] \Delta t^2 \end{aligned} \tag{6.15}$$

where α and δ are parameters which can be selected to give an optimal

combination of accuracy and stability. Writing the velocity and acceleration in terms of displacement, we obtain, using the conventions in [Bathe 82]:

$$a_0 = \frac{1}{\alpha \Delta t^2}$$

$$a_1 = \frac{\delta}{\alpha \Delta t}$$

$$a_2 = \frac{1}{\alpha \Delta t}$$

$$a_3 = \frac{1}{2\alpha} - 1$$

$$a_4 = \frac{\delta}{\alpha} - 1$$

$$a_5 = \frac{\Delta t}{2} \left(\frac{\delta}{\alpha} - 2 \right)$$

$$a_6 = \Delta t \, (1-\delta)$$

$$a_7 = \delta \Delta t$$

$$\begin{aligned} {}^{t+\Delta t}\ddot{x} &= a_0 \left({}^{t+\Delta t}x - {}^{t}x \right) - a_2 \, {}^{t}\dot{x} - a_3 \, {}^{t}\ddot{x} \\ {}^{t+\Delta t}\dot{x} &= - a_1 \, {}^{t}x - a_4 \, {}^{t}\dot{x} - a_5 \, {}^{t}\ddot{x} \end{aligned} \qquad (6.16)$$

Evaluation of the equations of motion at time $t+\Delta t$ gives:

$$\ddot{C}_i^{t+\Delta t} + 2\xi_i \omega_i \dot{C}_i^{t+\Delta t} + \omega_i^2 C_i^{t+\Delta t}$$

$$= \mathcal{F}_i^{t+\Delta t} - \ddot{f}^{t+\Delta t} A_i - \ddot{g}^{t+\Delta t} B_i \qquad (6.17)$$

Substitution of (6.16) in (6.17) gives:

$$(a_0 + a_1 2\xi_i \omega_i + \omega_i^2) C_i^{t+\Delta t}$$

$$= (a_0 C_i^t + a_2 \dot{C}_i^t + a_3 \ddot{C}_i^t)$$

$$+ 2\xi_i \omega_i (a_1 C_i^t + a_4 \dot{C}_i^t + a_5 \dot{C}_i^t)$$

$$+ \mathcal{F}_i^{t+\Delta t} - \ddot{f}^{t+\Delta t} A_i - \ddot{g}^{t+\Delta t} B_i \qquad (6.18)$$

When the above equations (6.18) are solved for each time step, a time history of the modal displacements is obtained. A complete solution of the linearised cable problem can be constructed as follows:

$$p(s,t) = f(t)\, p_{qs1}(s) + g(t)\, p_{qs2}(s) + \sum_{i=1}^{n} p_i(s)\, C_i(t)$$

$$q(s,t) = f(t)\, q_{qs1}(s) + g(t)\, q_{qs2}(s) + \sum_{i=1}^{n} q_i(s)\, C_i(t)$$

$$\phi_1(s,t) = f(t)\, \phi_{qs1}(s) + g(t)\, p_{qs2}(s) + \sum_{i=1}^{n} \phi_i(s)\, C_i(t) \qquad (6.19)$$

$$T_1(s,t) = f(t)\, T_{qs1}(s) + g(t)\, T_{qs2}(s) + \sum_{i=1}^{n} T_i(s)\, C_i(t)$$

where p_i , q_i , ϕ_i , T_i are the modal components of the tangential displacement, normal displacement, dynamic angle and dynamic tension

respectively.

The Newmark integration scheme is unconditionally stable when $\delta \geq 0.5$ and $\alpha \geq 0.25(\delta+0.5)^2$, which means that the solution does not grow without bound for any initial condition and for any Δt. Newmark introduced his method originally with $\delta = 0.5$ and $\alpha = 0.25$. This method is called the constant average acceleration method (also trapezoidal rule). (See figure 6-1)

It can be shown [Bathe 82] that using this selection, an undamped system shows no amplitude decay and only a phase shift due to time integration errors appears, while no numerical damping is introduced by the scheme. If numerical damping is desired, the value of δ must be taken greater than 0.5 and the value of α should be varied accordingly. Due to its favorable characteristics, the constant average acceleration scheme will be used.

The following relations are obtained for (6.16) using $\delta = 0.5$ and $\alpha = 0.25$:

$$
\begin{aligned}
{}^{t+\Delta t}\ddot{x} &= (0.25\Delta^2 t)^{-1} \left({}^{t+\Delta t}x - {}^{t}x\right) - (0.25\Delta t)^{-1}\, {}^{t}\dot{x} - {}^{t}\ddot{x} \\
{}^{t+\Delta t}\dot{x} &= {}^{t}\dot{x} + 0.5\Delta t \left({}^{t}\ddot{x} + {}^{t+\Delta t}\ddot{x}\right)
\end{aligned}
\tag{6.20}
$$

6.5 Non-Linear External Forces

6.5.1 Description

A full description of all the external forces was given in chapter 1. In the linear problem only the dynamic component of these forces should be included.

The only important force for most applications is the hydrodynamic

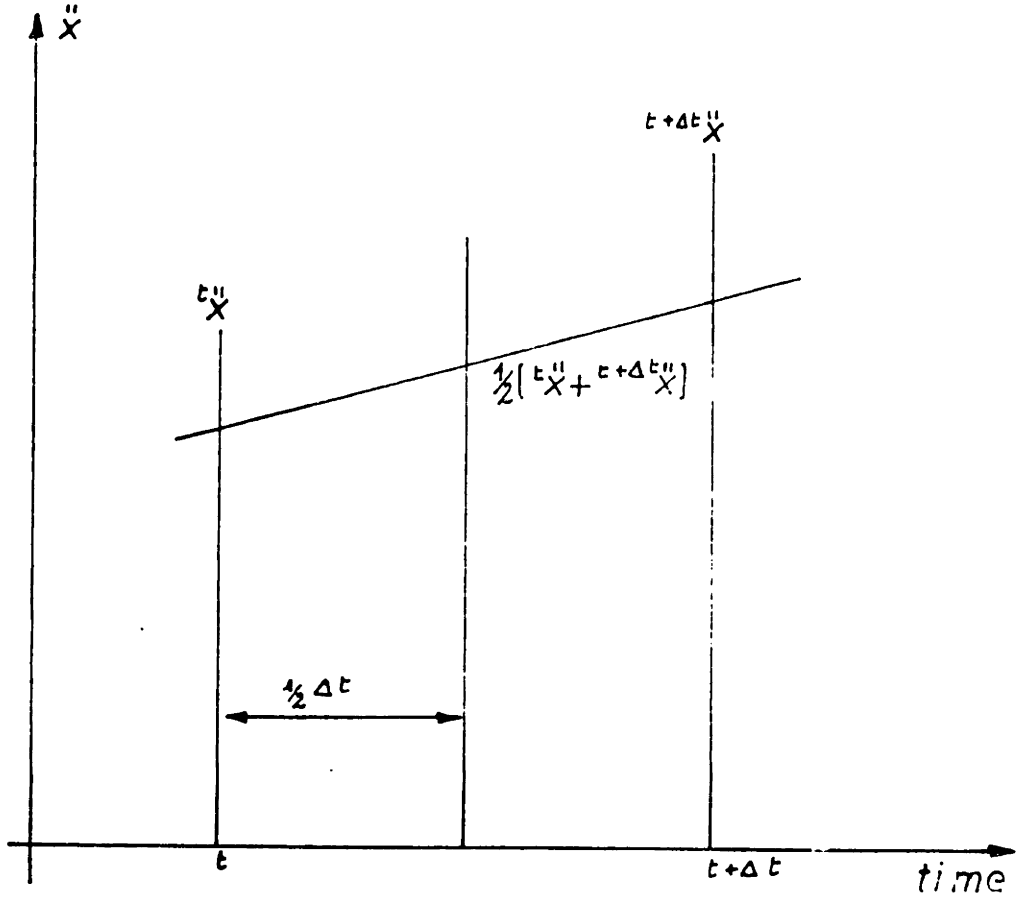

Figure 6-1: Newmark Constant Acceleration Scheme [Bathe 82]

loading. In this work, we use, apart from the added mass force, a quadratic drag force for the hydrodynamic loading, as described in chapter 1. Other forms of loading can easily be implemented. The dynamic component of the external force terms can be written as:

$$F_{dt} = 0.5\ \rho_w\ C_{Dt}\ (Re)\ D_o\ (U\ \cos\varphi - v_t)\ |U\ \cos\phi - v_t|\ (1+e/2)$$
$$- 0.5\ \rho_w\ C_{dt}\ (Re)\ D_o\ U \cdot \cos\phi_o\ |\ U \cdot \cos\phi_o\ |(1+e/2\ ) \qquad (6.21)$$

$$F_{dn} = -0.5\ \rho_w\ C_{Dn}\ (Re)\ D_o\ (U\ \sin\phi + v_n)|U\ \sin\phi + v_n|(1+e/2)$$
$$+ 0.5\ g[r]_w\ C_{dn}\ (Re)\ D_o\ U \cdot \sin\phi_o\ |\ U \cdot \sin\phi_o\ |(1+e/2\ )$$

6.5.2 Time Integration in the Presence of a Non-Linear Force

The equation of motion, using Newmark's method has been written as:

$$(\ a_0 + a_1\ 2\xi_i\ \omega_i + \omega_i^2\ )\ {}^{t+\Delta t}C_i$$

$$= (\ a_0\ {}^{t}C_i + a_2\ {}^{t}\dot{C}_i + a_3\ {}^{t}\ddot{C}_i\ )$$

$$+ 2\xi_i\ \omega_i\ (a_1\ {}^{t}C_i + a_4\ {}^{t}\dot{C}_i + a_5\ {}^{t}\dot{C}_i\ )$$

$$+\ {}^{t+\Delta t}\mathcal{F}_i - {}^{t+\Delta t}\ddot{f}\ \mathcal{A}_i - {}^{t+\Delta t}\ddot{g}\ \mathcal{B}_i$$

In the case of the hydrodynamic drag force, the modal force is given by:

$${}^{t+\Delta t}\mathcal{F}_i = \int_0^L ({}^{t+\Delta t}F_{dt}\ p_i + {}^{t+\Delta t}F_{dn}\ q_i\ )\ ds \qquad (6.22)$$

The forces are not known at time $t+\Delta t$, because they depend in a highly non-linear way on the relative velocities, therefore some approximation of the

hydrodynamic drag force is required.

$$ {}^{t+\Delta t}\hat{\mathcal{F}}_i = \int_0^L ({}^{t+\Delta t}\hat{F}_{dt}\ p_i + {}^{t+\Delta t}\hat{F}_{dn}\ q_i)\ ds \tag{6.23} $$

Several methods can be used to make estimations. The easiest approximation is simply to use the forces calculated at the previous time step. Therefore:

$$ {}^{t}\hat{\mathcal{F}}_i = \int_0^L ({}^{t}F_{dt}\ p_i + {}^{t}F_{dn}\ q_i)\ ds \tag{6.24} $$

Improvements on this first estimation can be achieved by using an iteration procedure to approximate the modal forces.

The complete governing equations for the modal components with equilibrium iterations can be written as:

$$ \begin{aligned} &(a_0 + a_1\ 2\xi_i\ \omega_i + \omega_i^2)\ {}^{t+\Delta t}C_i^k \\ &= (a_0\ {}^{t}C_i + a_2\ {}^{t}\dot{C}_i + a_3\ {}^{t}\ddot{C}_i) \\ &+ 2\xi_i\ \omega_i\ (a_1\ {}^{t}C_i + a_4\ {}^{t}\dot{C}_i + a_5\ {}^{t}\dot{C}_i) \\ &+ {}^{t+\Delta t}\mathcal{F}_i^{k-1} - {}^{t+\Delta t}\ddot{f}\ A_i - {}^{t+\Delta t}\ddot{g}\ B_i \end{aligned} \tag{6.25} $$

$$ \text{with:}\quad \mathcal{F}_i^{k-1} = \int_0^L ({}^{t+\Delta t}F_{dt}\ p_i + {}^{t+\Delta t}F_{dn}\ q_i)\ ds $$

$$ \text{with:}\quad \mathcal{F}_i^{o} = \int_0^L ({}^{t}F_{dt}\ p_i + {}^{t}F_{dn}\ q_i)\ ds $$

6.5.3 Discussion

Equation (6.25) describes completely the dynamics of a two-dimensional cable with a non-linear time varying force. The only restriction is the assumption of small motions, which means that the dynamic tension must be small compared to the static tension. The dynamic angle must also be small.

The complete solution procedure is described in table 6-I. The major advantage of the method is that a minimal number of modal components can be selected to represent the cable motions accurately.

It is the author's opinion that this procedure can also be used to solve the inverse problem. Knowing the cable motions, study the hydrodynamic forces in their modal components. This could enable us to make some progress in the understanding of the hydrodynamic loading of flexible structures.

6.6 Non-Linear Governing equations

The full non-linear equations of motion were derived in detail in chapter 2. The two dimensional equations of motion are written in a coordinate system fixed with respect to the equilibrium state. In our analysis we selected the static equilibrium as the reference coordinate of the system. (See figure 6-2)

p: tangential coordinate on static configuration

q: normal coordinate on static configuration

ϕ_1: angle between tangent on dynamic and static configuration

Solution Method

1. Evaluation of the Static Equilibrium

2. Calculation of quasi-static solution due to top motion

3. Calculation of eigenfrequencies and modes

4. Time simulation

   For each step ;

   Evaluation of the force

Iterative Evaluation of the modal force

Procedure Evaluation of the modal components

   Evaluation of the displacements.

Table 6-I: Time simulation using Modal Expansion

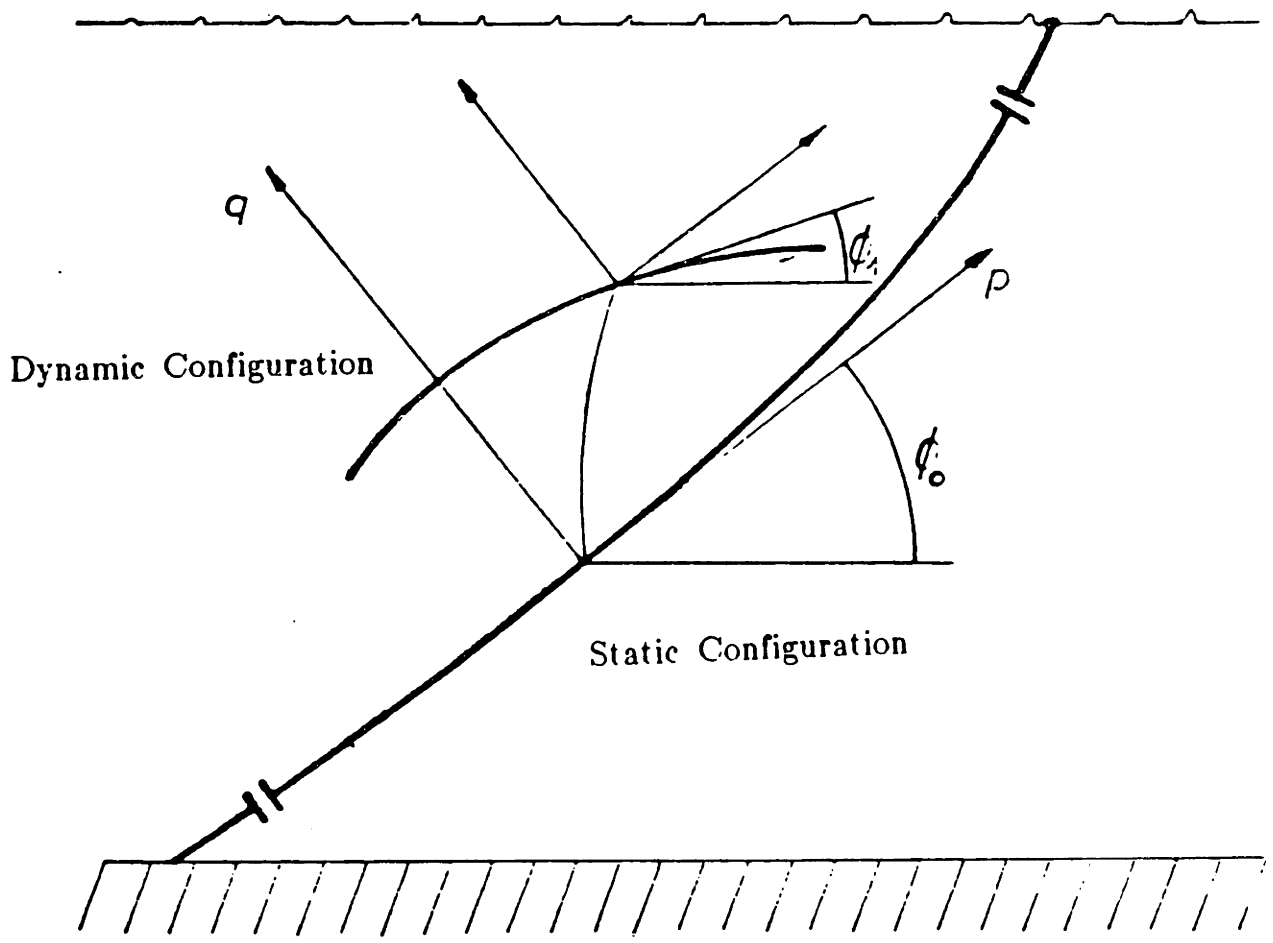

Figure 6-2: Coordinate System (p,q)

6.6.1 Dynamic Equations

The dynamic equilibrium, as outlined in chapter 2, can be used along the p and q directions to find the equations:

$$m \frac{\partial^2 p}{\partial t^2} = \frac{\partial T}{\partial s} \cdot \cos\phi_1 - T \frac{\partial \phi}{\partial s} \cdot \sin\phi_1 + \sum_{i=0}^{n} F_{ext,p,i}(1+e)$$

$$m \frac{\partial^2 p}{\partial t^2} = \frac{\partial T}{\partial s} \cdot \sin\phi_1 + T \frac{\partial \phi}{\partial s} \cdot \cos\phi_1 + \sum_{i=0}^{n} F_{ext,q,i}(1+e) \qquad (6.26)$$

These can be rewritten as:

$$m \frac{\partial^2 p}{\partial t^2} = \frac{\partial}{\partial s}(T\cos\phi_1) - T \frac{\partial \phi_o}{\partial s} \sin\phi_1 + \sum_{i=0}^{n} F_{ext,p,i}(1+e)$$

$$m \frac{\partial^2 p}{\partial t^2} = \frac{\partial}{\partial s}(T\sin\phi_1) + T \frac{\partial \phi_o}{\partial s} \cos\phi_1 + \sum_{i=0}^{n} F_{ext,q,i}(1+e) \qquad (6.27)$$

The external forces on the cable consist of the following components

- Gravity and buoyancy forces
- The added mass force
- The non-linear drag force

Gravity and buoyancy forces

The gravity and buoyancy forces act in the vertical direction when the effective tension concept is used. (See chapter 2) The net force acting on the cable is given by:

$$F_{ext,p}(1+e) = - w_o \cdot \sin\phi_o$$

$$F_{ext,q}(1+e) = - w_o \cdot \cos\phi_o \qquad (6.28)$$

where w_o is the net weight

The added mass force

The added mass force as derived in chapter 2, can be written in the p and q directions as:

$$F_{ext,p}\,(1+e) = -\,m_a\left[\frac{\partial^2 p}{\partial t^2}\cdot\sin^2\phi_1 - \frac{\partial^2 q}{\partial t^2}\cdot\cos\phi_1\cdot\sin\phi_1 + \frac{\partial p}{\partial t}\cdot\cos\phi_1\cdot\sin\phi_1\cdot\frac{\partial\phi_1}{\partial t} + \frac{\partial q}{\partial t}\cdot\sin^2\phi_1\cdot\frac{\partial\phi_1}{\partial t}\right]$$

$$F_{ext,q}\,(1+e) = -\,m_a\left[-\frac{\partial^2 p}{\partial t^2}\cdot\sin\phi_1\cdot\cos\phi_1 + \frac{\partial^2 q}{\partial t^2}\cdot\cos^2\phi_1 - \frac{\partial p}{\partial t}\cdot\cos^2\phi_1\cdot\frac{\partial\phi_1}{\partial t} - \frac{\partial q}{\partial t}\cdot\sin\phi_1\cdot\cos\phi_1\,\frac{\partial\phi_1}{\partial t}\right] \tag{6.29}$$

The added mass force, written in the reference coordinate system, is a complicated non-linear function of velocities, accelerations and angular orientation. This is mainly due to the appearance of Coriolis and centripetal terms. For small dynamic angles this force will be reduced to a normal component.

$$F_{2ext,q}\,(1+e) = -\,m_a\frac{\partial^2 q}{\partial t^2} \tag{6.30}$$

For a large dynamic angle, we rewrite the normal added mass force term as follows:

$$F_{2ext,q}\,(1+e) = -m_a\frac{\partial^2 q}{\partial t^2} - m_a\left[-\frac{\partial^2 p}{\partial t^2}\cdot\sin\phi_1\cdot\cos\phi_1 + \frac{\partial^2 q}{\partial t^2}\,(\cos^2\phi_1 - 1) - \frac{\partial p}{\partial t}\cdot\cos^2\phi_1\cdot\frac{\partial\phi_1}{\partial t} - \frac{\partial q}{\partial t}\,\sin\phi_1\cdot\cos\phi_1\cdot\frac{\partial\phi_1}{\partial t}\right] \tag{6.31}$$

The added mass can be considered to be the sum of a linear term in the q direction plus correction terms. The linear term can be included in the inertia term.

The added mass term is small compared with the mass term for chains and wires, therefore the influence of the additional added mass terms on the motion is believed to be minimal (see [Barr 74]).

The Non-linear Drag Force

The drag force, as described in chapter 2, can be written in the (p,q) coordinate system as:

$$\begin{aligned} F_{ext,p}\,(1+e) = {} & 0.5\ \rho_w\ C_{Dn}\ (Re)\ D_o\ (U\sin\phi + v_n\ )\ |\ U\sin\phi + v_n\ | \\ & (1+e/2)\ \cdot\ \sin\phi_1 \\ & +\ 0.5\ \rho_w\ C_{Dt}\ (Re)\ D_o\ (U\cos\phi - v_t)\ |U\cos\phi - v_t| \\ & (1+e/2)\ \cdot\ \cos\phi_1 \end{aligned} \tag{6.32}$$

$$\begin{aligned} F_{ext,q}(1+e) = {} & -\ 0.5\rho_w\ C_{Dn}\ (Re)\ D_o\ (U\ \sin\phi + v_n)\ |U\sin\phi + v_n| \\ & (1+e/2)\ \cdot\ \cos\phi_1 \\ & +\ 0.5\ \rho_w\ C_{Dt}\ (Re)\ D_o\ (U\ \cos\phi - v_t)\ |U\cos\phi - v_t| \\ & (1+e/2)\ \cdot\ \sin\phi_1 \end{aligned}$$

where: $\phi = \phi_o + \phi_1$

$$v_t = \frac{\partial p}{\partial t} \cdot \cos\phi_1 + \frac{\partial q}{\partial t} \cdot \sin\phi_1$$

$$v_n = - \frac{\partial p}{\partial t} \cdot \sin\phi_1 + \frac{\partial q}{\partial t} \cdot \cos\phi_1$$

6.6.2 The Compatibility Relations

The non-linear compatibility relations were derived in chapter 2 and are given as:

$$\begin{aligned} (1+e)\ \cos\phi_1 &= (1+e_o\ ) + \left[\ \frac{\partial p}{\partial s} - q\phi_{os}\ \right] \\ (1+e)\ \sin\phi_1 &= \left[\ \frac{\partial q}{\partial s} + p\phi_{os}\ \right] \end{aligned} \tag{6.33}$$

6.6.3 Summary

The equations in 6.6.1 and 6.6.2 give a complete description of the full non-linear two dimensional dynamic problem, with the external forces described in 6.6.1 A constitutive law, relating the strain and the tension and the boundary conditions must be added to make the formulation complete.

6.7 Newton-Raphson Method

The equations of motion of a cable are described by a set of non-linear partial differential equations of the hyperbolic type. In this work an incremental linearised description of the non-linear equations is used to solve the problem iteratively.

The partial differential equations are linearised in an incremental way. The result of the linearised problem is used to obtain an estimation of the solution of the non-linear problem, which is refined in succesive iterations until the error is below an acceptable bound. The linearisation of the partial differential equations is obtained by using a Taylor expansion in several variables.

The resulting linearised partial differential equations are solved by using the modal superposition technique described in sections 6.3 - 6.5.

The method of incremental linearisation of the partial differential equations is a suitable technique to solve a non-linear set of equations in several variables, as explained in the sequel.

In the Newton-Raphson method the non-linear set of equations is expanded in Taylor series [Dahlquist 74]. If we represent the set of non-linear equations as $\mathbf{f}(\mathbf{x})$, Taylor's formula gives:

$$\mathbf{f}(\mathbf{x}) = \mathbf{f}(\mathbf{x}^k) + \dot{\mathbf{f}}(\mathbf{x}^k)(\mathbf{x} - \mathbf{x}^k) + O(|\mathbf{x} - \mathbf{x}^k|)^2$$

where $\dot{\mathbf{f}}(\mathbf{x})$ is a $n \times n$ matrix, the Jacobian with element

$$\dot{f}_{ij}(x) = \frac{\partial f_i}{\partial x_i}(x) \qquad 1 \leq i, j \leq n$$

We try to find a solution to the problem $\mathbf{f(x)} = 0$. If $\mathbf{x}_k$ is close to the solution of $\mathbf{f(x)} = 0$, we obtain a better approximation as:

$$\mathbf{f}'(\mathbf{x}^k)(\mathbf{x}^{k+1} - \mathbf{x}^k) + \mathbf{f}(\mathbf{x}^k) = 0$$

which we can solve for $\mathbf{x}^{k+1}$, because in the case of non-linear functions, this is a set of n linear equations. In the case of non-linear partial differential equations, we obtain a set of linear partial differential equations as will be shown later.

The evaluation of the Jacobian of a $n \times n$ system can be quite complicated and time consuming. Therefore it can be advantageous to use the same Jacobian during several iterations. This method is known as the modified Newton-Raphson method and can be written as:

$$\mathbf{f}'(\mathbf{x}^p)(\mathbf{x}^{k+1} - \mathbf{x}^k) + \mathbf{f}(\mathbf{x}^k) = 0 \qquad k = p, p+m$$

In some cases it can be appropriate to evaluate the Jacobian only at the first iteration step. This can be done when the solution is close to the initial estimation and the non-linearities are not too severe. This can be written as:

$$\mathbf{f}'(\mathbf{x}^o)(\mathbf{x}^{k+1} - \mathbf{x}^k) + \mathbf{f}(\mathbf{x}^k) = 0$$

The selection of the most advantageous method depends strongly on the nature of the problem. An illustration of the modified Newton-Raphson scheme for a single function is shown in figure 6-3.

There can be a problem with the convergence of the Newton-Raphson scheme. This is especially true for concave curves, as for example in the case of stiffening systems. Also, if the initial estimate is not close to the root, the convergence can be very slow, as compared to the quadratic convergence of the

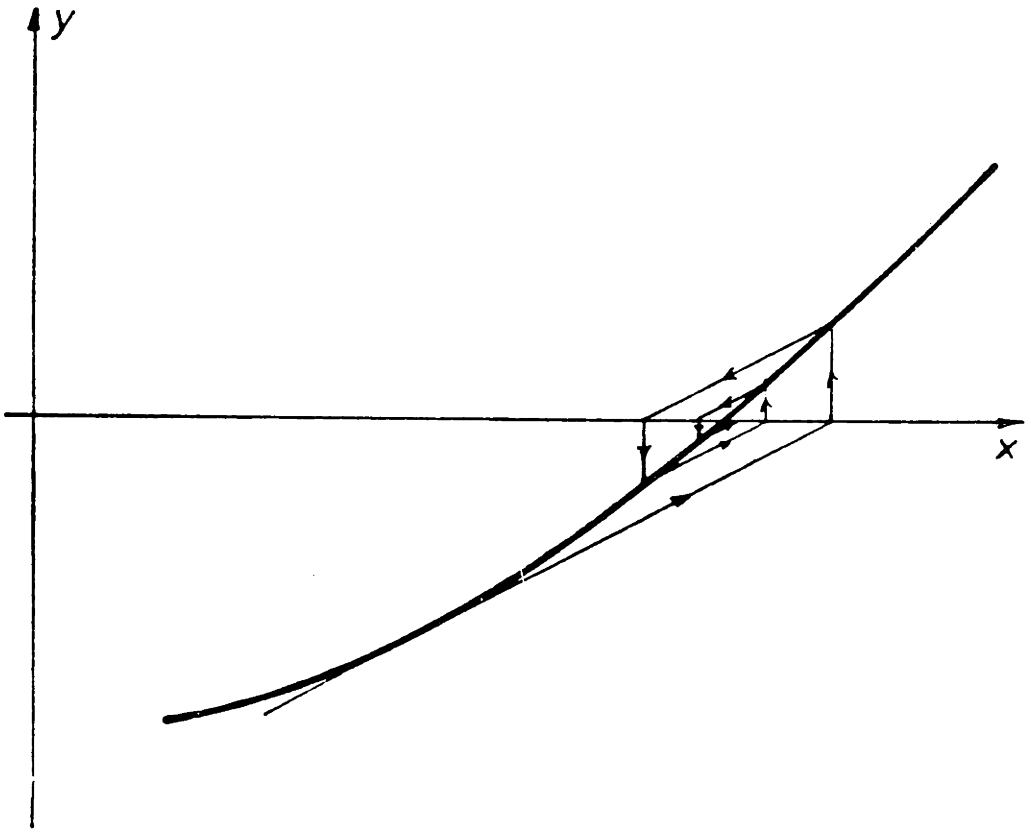

Figure 6-3: Convergence of Newton-Raphson Method

full Newton-Raphson method.

The modified Newton-Raphson method has been applied extensively to partial differential equations using non-linear finite element methods. When no updating of the Jacobian is performed, the method is known as the initial stiffness method [Bathe 80] and [Bathe 81].

In the case of time domain analysis, the initial stiffness method will always convergence for sufficiently small time steps [Bathe 82], although in some cases of severe non-linearities, time steps will be extremely small.

The initial stiffness method has been applied to cables with relative success [Larsen 82]. The method is espacially attractive for use with modal expansions, because no update of the modes is needed in the time simulation.

6.8 Incremental Formulation

We will use an incremental formulation of the governing equations, using a modified Newton-Raphson scheme. The Jacobian will be evaluated at a reference state, which was selected to be the static configuration of the cable. In this work no updating of the reference state will be performed. The formulation takes fully into account the non-linearities of the problem by using an iterative procedure to obtain the force balance.

6.8.1 Incremental Formulation of the Equations of Motion

The non-linear equations of motion can be written, including the added mass in the normal inertia term, as:

$$m \frac{\partial^2 p}{\partial t^2} = \frac{\partial}{\partial s} (T \cdot \cos\phi_1) + F_{ext,p}(1+e) - T \frac{\partial \phi_o}{\partial s} \cdot \sin\phi_1$$

$$M \frac{\partial^2 q}{\partial t^2} = \frac{\partial}{\partial s} (T \cdot \sin\phi_1) + F_{ext,q}(1+e) + T \frac{\partial \phi_o}{\partial s} \cdot \cos\phi_1 \qquad (6.34)$$

The only non-linear terms are the restoring force terms, which are:

$$F_{int,t} = \frac{\partial}{\partial s} (T \cdot \cos\phi_1) - T \cdot \frac{\partial \phi_o}{\partial s} \cdot \sin\phi_1$$

$$F_{int,n} = \frac{\partial}{\partial s} (T \cdot \sin\phi_1) + T \cdot \frac{\partial \phi_o}{\partial s} \cdot \cos\phi_1 \qquad (6.35)$$

We will linearise those terms, using the estimation of terms from a previous iteration plus a linearised part, while the Jacobian is evaluated in the reference state. This gives:

$$F_{int,t}^{k+1} = \frac{\partial \Delta T}{\partial s} - T_o \frac{\partial \phi_o}{\partial s} \Delta\phi_1 + \frac{\partial}{\partial s} (T^k \cdot \cos\phi_1^k) - T^k \frac{\partial \phi_o}{\partial s} \cdot \sin\phi_1^k$$

$$F_{int,n}^{k+1} = \frac{\partial \phi_o}{\partial s} \Delta T + \frac{\partial T_o}{\partial s} \Delta\phi_1 + T_o \frac{\partial \Delta\phi_1}{\partial s} + \frac{\partial}{\partial s} (T^k \cdot \sin\phi_1^k) + T^k \cdot \frac{\partial \phi_o}{\partial s} \cos\phi_1^k \qquad (6.36)$$

Therefore the incremental formulation of the equations of motion becomes:

$$m \left[\frac{\partial^2 p}{\partial t^2} \right]^{k+1} = \frac{\partial \Delta T}{\partial s} - T_o \frac{\partial \phi_o}{\partial s} \Delta\phi_1 + \frac{\partial}{\partial s} (T^k \cdot \cos\phi_1^k)$$

$$+ F_{ext,t}(1+e^k) - T^k \frac{\partial \phi_o}{\partial s} \cdot \sin\phi_1^k$$

$$M \left[\frac{\partial^2 q}{\partial t^2} \right]^{k+1} = \frac{\partial \phi_o}{\partial s} \Delta T + \frac{\partial T_o}{\partial s} \Delta \phi_1 + T_o \frac{\partial \Delta \phi_1}{\partial s}$$

$$+ \frac{\partial}{\partial s} (T^k \sin\phi_1^k) + F_{ext,n}(1+e^k) + T^k \frac{\partial \phi_o}{\partial s} \cos\phi_1^k \qquad (6.37)$$

6.8.2 Incremental Formulation of the Compatibility Relations

The non-linear compatibility relations are as given in 6.6.2

$$(1+e) \cos\phi_1 = (1+e_o) + \left[\frac{\partial p}{\partial s} - q\phi_{os} \right]$$

$$(1+e) \sin\phi_1 = \left[\frac{\partial q}{\partial s} + p\phi_{os} \right] \qquad (6.33)$$

The incremental form of the compatibility relations is:

$$\Delta e = \frac{\partial \Delta p}{\partial s} - \Delta q\phi_{os} + \left[\frac{\partial p^k}{\partial s} - q^k\phi_{os} \right] + (1+e_o) - (1+e^k) \cos\phi_1^k$$

$$(1+e_o)\Delta\phi_1 = \frac{\partial \Delta q}{\partial s} + \Delta p\phi_{os} + \left[\frac{\partial q^k}{\partial s} + p^k\phi_{os} \right] - (1+e^k) \sin\phi_1^k \qquad (6.38)$$

6.8.3 Incremental Formulation of the Force-Displacement Relation

The most frequently used force-displacement relations can be written as:

$$T = f(e)$$

This can be written incrementally as:

$$\Delta T = \left[\frac{\partial f}{\partial e} \right]_{e_o} \Delta e + \left[f(e^k) - T^k \right] \qquad (6.39)$$

To keep things relatively simple, we will use, without destroying the generality of the solution, a linear force-displacement relation.

$$\Delta T = A \cdot E \cdot \Delta e \tag{6.40}$$

6.8.4 Incremental Formulation of the Governing Equations

We can substitute (6.38) and (6.40) in (6.37) to obtain the incremental formulation of the governing equations. We obtain:

$$\begin{aligned} m \frac{\partial^2 p}{\partial t^2} - \frac{\partial}{\partial s}\left[EA\left(\frac{\partial \Delta p}{\partial s} - \Delta q \phi_{os}\right)\right] + T_o \frac{\partial \phi_o}{\partial s}\left[\frac{1}{1+e_o}\left(\frac{\partial \Delta q}{\partial s} + \Delta p \phi_{os}\right)\right] \\ = \frac{\partial}{\partial s}(T^k \cos\phi_1^k) + F^k_{ext,t}(1+e^k) - T^k \frac{\partial \phi_o}{\partial s}\sin\phi_1^k \\ + \frac{\partial}{\partial s}\left[EA\left[\frac{\partial^k p}{\partial s} - q^k \phi_{os} + (1+e_o) - (1+e^k)\cos\phi_1^k\right]\right] \\ - T_o \frac{\partial \phi_o}{\partial s}\left[\frac{1}{1+e_o}\left[\frac{\partial^k q}{\partial s} + p^k \phi_{os} - (1+e^k)\cdot \sin\phi_1^k\right]\right] \end{aligned} \tag{6.41}$$

$$\begin{aligned} M \frac{\partial^2 q}{\partial t^2} - \frac{\partial \phi_o}{\partial s}\left[EA\left(\frac{\partial \Delta p}{\partial s} - \Delta q \phi_{os}\right)\right] - \frac{\partial T_o}{\partial s}\left[\frac{1}{1+e_o}\left(\frac{\partial \Delta q}{\partial s} + \Delta p \phi_{os}\right)\right] \\ - T_o \frac{\partial}{\partial s}\left[\frac{1}{1+e_o}\left(\frac{\partial \Delta q}{\partial s} + \Delta p \phi_{os}\right)\right] \\ = \frac{\partial}{\partial s}(T^k \sin\phi_1^k) + F^k_{ext,n}(1+e^k) + T^k \frac{\partial \phi_o}{\partial s}\cos\phi_1^k \\ + \frac{\partial \phi_o}{\partial s}\left[EA\left[\frac{\partial^k p}{\partial s} - q^k \phi_{os} + (1+e_o) - (1+e^k)\cos\phi_1^k\right]\right] \\ + \frac{\partial}{\partial s}\left[T_o \frac{1}{1+e_o}\left[\frac{\partial^k q}{\partial s} + p^k \phi_{os} - (1+e^k)\cdot \sin\phi_1^k\right]\right] \end{aligned}$$

These are the complete incremental equations using the modified Newton-Raphson method. Note that in the left hand side are the linearised dynamic equations. To obtain the linearisation around the reference state we did not make any assumption about the reference state, so this can be any dynamic equilibrium position.

6.9 Solution using the Modes

As in the case of the linear dynamic problem, we look for a solution.

$$p(s,t) = f(t)\ p_{qs1}(s) + g(t)\ p_{qs2}(s) + \sum_{i=1}^{n} C_i(t)\ p_i(s)$$

$$q(s,t) = f(t)\ q_{qs1}(s) + g(t)\ q_{qs2}(s) + \sum_{i=1}^{n} C_i(t)\ q_i(s) \qquad (6.42)$$

where p_{qs1} , q_{qs2} and p_{qs1} , q_{qs2} are the two quasi-static solutions for the reference state and p_i , q_i are mode shapes for the reference state. As discussed previously the reference state was chosen to be the static equilibrium configuration.

Because the quasi-static solution and the mode shapes satisfy the compatibility relations, the following relations are valid:

$$e^k_{lin} - e_o = \frac{\partial p^k}{\partial s} - q^k \frac{\partial \phi_o}{\partial s}$$

$$\phi^k_{1\ lin} = \frac{\partial q^k}{\partial s} + p^k \frac{\partial \phi_o}{\partial s} \qquad (6.43)$$

where e^k_{lin} , $\phi^k_{1\ lin}$ are the strain and the dynamic tension obtained by linear superposition.

We can now obtain the modal equations of motion by multiplying equations (6.41) with the modal shapes, adding them up and integrating. The following relations are used to simplify the equations:

$$\int_0^L p_i \frac{\partial A}{\partial s}\, ds = - \int_0^L A \frac{\partial p_i}{\partial s}\, ds$$

$$\int_0^L q_i \frac{\partial A}{\partial s}\, ds = - \int_0^L A \frac{\partial q_i}{\partial s}\, ds \qquad (6.44)$$

$$e_i = \frac{\partial p_i}{\partial s} - q_i \frac{\partial \phi_o}{\partial s}$$

$$\phi_{1i} = \frac{\partial q_i}{\partial s} + p_i \frac{\partial \phi_o}{\partial s}$$

After some manipulation, the following modal equations are obtained:

$$\ddot{C}_i^{k+1} + 2\xi\,\omega_i\,\dot{C}_i^{k+1} + \omega_i^2\,\Delta C_i = - A_i\,\ddot{f} - B_i\,\ddot{g}$$

$$+ \int_0^L \left\{ \left[F_{ext,t}^k (1+e^k) + \frac{\partial T_o}{\partial s} \right] p_i + \left[F_{ext,n}^k (1+e^k) + T_o \frac{\partial \phi_o}{\partial s} \right] q_i \right\} ds$$

$$- \int_0^L e_i \,(T^k \cos\phi_1^k - T_o)\, ds - \int_0^L \phi_{1i} \left[T^k \sin\phi_1^k (1+e_o) \right] ds$$

$$- \int_0^L e_i \left[EA[(e_{lin}^k + 1) - (1+e^k)\cos\phi_1^k] \right] ds$$

$$- \int_0^L \phi_{1i} \left[T_o \,[\phi_{1\,lin}^k (1+e_o) - (1+e^k)\sin\phi_1^k] \right] ds \qquad (6.45)$$

This equation is the full incremental representation of the non-linear, two-

dimensional cable problem using modal expansion. The right hand side of (6.45) contains known quantities at the iteration step k+1.

Explanation of terms:

Terms to take account of the boundary conditions:

$$- A_i \ddot{f} - B_i \ddot{g}$$

Dynamic modal force:

$$+ \int_0^L \left\{ \left[F^k_{ext,t} (1+e^k) + \frac{\partial T_o}{\partial s} \right] p_i \right.$$

$$+ \left[F^k_{ext,n} (1+e^k) + T_o \frac{\partial \phi_o}{\partial s} \right] q_i$$

Force terms to take care of the increments of the internal forces and the non-linearities in the tension terms:

$$- \int_0^L e_i \, (T^k \cos\phi_1^k - T_o) ds - \int_0^L \phi_{1i} \left[T^k \sin\phi_1^k (1+e_o) \right] ds$$

Force terms to take care of non-linearities in the compatibility equations:

$$- \int_0^L e_i \left[EA[(e^k_{lin} + 1) - (1+e^k)\cos\phi_1^k] \right] ds$$

$$- \int_0^L \phi_{1i} \left[T_o \, [\phi_{1\,lin}^k (1+e_o) - (1+e^k)\sin\phi_1^k] \right] ds$$

6.10 Time Integration of the Equations in Incremental Form

The time integration can be done as described in 6.4. Written in an incremental way, (6.16) become:

$$
\begin{aligned}
{}^{t+\Delta t}\ddot{C}_i &= a_o \left({}^{t+\Delta t}C_i^{k-1} + \Delta C_i - {}^{t}C_i\right) - a_2\, {}^{t}\dot{C}_i - a_3\, {}^{t}\ddot{C}_i \\
{}^{t+\Delta t}\dot{C}_i &= a_1 \left({}^{t+\Delta t}C_i^{k-1} + \Delta C_i - {}^{t}C_i\right) - a_4\, {}^{t}\dot{C}_i - a_5\, {}^{t}\ddot{C}_i
\end{aligned}
\qquad (6.46)
$$

When we substitute in (6.45), the equations can be solved directly for the modal increments ΔC_i.

6.11 References

[Barr 74] Barr, R.A.
The Non-Linear Dynamics of Cable Systems.
Technical Report UM-1MR 74-1, Sea Grant, University of California,. 1974.

[Bathe 80] Bathe, K.J. and Cimento, A.P.
Some Practical Procedures for the solution of Non-Linear Finite Element Equations.
Computer Methods in Applied Mechanics and Engineering 22:58-85, 1980.

[Bathe 81] Bathe, K.J. and Gracewski, S.
On Non-Linear Dynamic Analysis using Substructuring and Mode Superposition.
Computers and Structures 13:699-707, 1981.

[Bathe 82] Bathe K.J.
Finite Element Procedures in Engineering Analysis.
Prentice Hall, Englewood Cliffs N.J., 1982.

[Clough 75] Clough, R.W. and Penzien J.
Dynamics of Structures.
Mc Graw-Hill, New York, 1975.

[Dahlquist 74] Dahlquist, G. and Bjork, A.
Numerical Methods.
Prentice Hall, Englewood Cliffs N.J., 1974.

[Dareing 79] Dareing, D.W. and Huang T.
Marine Riser Vibration Response determined by Modal Analysis.
Journal of Energy Resources Technology, ASME 101:159-166, September, 1979.

[Gotlieb 77] Gotlieb, D. and Orszag S.A.
Regional Conference Series in Applied Mathematics: Numerical Analysis of Spectral Methods, Theory and Applications.
Society for Industrial and Applied Mathematics, Philadelphia, 1977.

[Hagedorn 80] Hagedorn, P. and Shafer, B. .
On Non-Linear Free Vibrations of an Elastic Cable.
International Journal Non-Linear Mechanics 15:333-340, 1980.

[Irvine 76] Irvine, H. M. and Griffin, J. H.
On the Dynamic Response of a Suspended Cable.
Earthquake Engineering and Structural Dynamics 4:389-402, 1976.

[Kim 83] Kim, Y.C.
Nonlinear Vibrations of Long Slender Beams.
PhD thesis, MIT, 1983.

[Kirk 79] Kirk, C.L., Etok, E.U. and Cooper, T.M.
Dynamic and Static Analysis of Marine Riser.
Applied Ocean Research 1, 1979.

[Larsen 82] Larsen, C. M. and Fylling, I. J.
Dynamic Behaviour of Anchor Lines.
Norwegian Maritime Research (3), 1982.

[Nickell 76] Nickell, R. E.
Non-Linear Dynamics by Mode Superposition.
Computer Methods in Applied Mechanics and Engineering 7:107-129, 1976.

[Veletsos 82] Veletsos, A. S. and Darbre, G. R.
Free Vibrations of Parabolic Cables.
Technical Report 23, Rice University, Department of Civil Engineering, March, 1982.

[Yamaguchi 79] Yamaguchi, H. and Ito, H.
Linear Theory of Free Vibrations of an Inclined Cable in Three Dimensions.
Proceedings Japanese Society of Civil Engineers (286):29-36, June, 1979.
In Japanese, Summary in English, Transactions Japanese Society of Civil Engineers 1979.

Chapter 7

NUMERICAL APPLICATIONS OF NON-LINEAR DYNAMICS

7.1 Introduction

In this chapter, a number of applications are provided, to demonstrate the practical implications of the theory presented in the preceding chapter, and to validate the theoretical predictions by comparing them with experimental data and previous solutions.

7.2 The Non-Linear String

The use of modal expansions was first tested on a non-linear string. First, some calculations were performed including non-linear drag, which introduces an amplitude dependent damping. The results obtained can be seen as a special case of the second numerical application presented in this chapter (drag forces on a cable) and are therefore omitted. The study of a string with geometric non-linearity, as discussed in chapter 5, was the second case considered, and is presented in the sequel.

The dimensions of a guy of a guyed tower were used for the taut string, for demonstration purposes.

String characteristics: $T = 1\ 000\ 000$ N
$M = 48.7$ kg/m
$L = 1\ 036.32$ m

The eigenfrequencies in air can be obtained as:

$$\omega = \frac{n\pi\ (T/M)^{1/2}}{L} \rightarrow 0.434,\ 0.861,\ \ldots$$

The string was subject at one end to a transverse sinusoidal excitation with frequency equal to the first natural frequency. The coefficient of the geometric non-linearity is selected as (see chapter 5):

$$\tau = \frac{E \cdot A}{T_o} \cdot \frac{1}{2} \frac{(Ampl)^2}{L^2} = 0.01$$

For a realistic strain in the string, of the order of 10^{-3}, this corresponds to an A/L ratio of approximately 4.5 10^{-3}. The case considered was selected because it can be compared with Oplinger's theoretical results. [Oplinger 60]

	Time step as a fraction of the exiting period	Damping	number of modes	τ
Fig.7-1–7-2	1/1000	–	3 - 6	0.01
Fig.7-3	1/20	0.05	1 -3 - 6	0
Fig.7-4–7-5	1/100	0.05	1 - 3 - 6	0.01
Fig.7-6	1/100	0.05	1 - 3 - 6	0-0.01

Table 7-I: Geometric Non-Linearity

Note: The time steps are the minimum required to ensure convergence and accurate response calculations. Except for the case with no damping, the expansion using one mode gave essentially the same result as the expansion with more modes.

Several time simulation runs were performed. A linear modal damping was

also introduced. The simulation results can be seen in Table 7-I. The amplitude of the imposed motion is taken as equal to 1 , and the amplitude at the middle of the cable is given in the graphs. Also the tension variation is calculated.

In figures 7-1 and 7-2 the effect of a pure geometric non-linearity is studied. Because no damping is present, a beating phenomenon, caused by the non-decaying transient solution, is obtained. The dynamic tension oscillates at double the exciting frequency as expected.

Figure 7-3 shows the response with linear damping only. Figures 7-4 and 7-5 show the effect of the geometric non-linearity with some damping included. Figure 7-6 presents a comparison between the motion without geometric non-linearity and the motion with geometric non-linearity. The geometric non-linearity is clearly limiting the amplitude of the motion. The final value of the response with geometric non-linearity is around 3 at resonance, which agrees well with Oplinger's theoretical and experimental investigation. (See figure 5-1)

7.3 Linear Cable Model with the Non-Linear Drag Force

In order to study the effect of the drag force on the motions of a cable, it was decided to use the linearised cable model, with the drag forces treated as external forces. In this example a guy of a guyed tower was excited in the normal direction, at the top.

The data for the guy are:

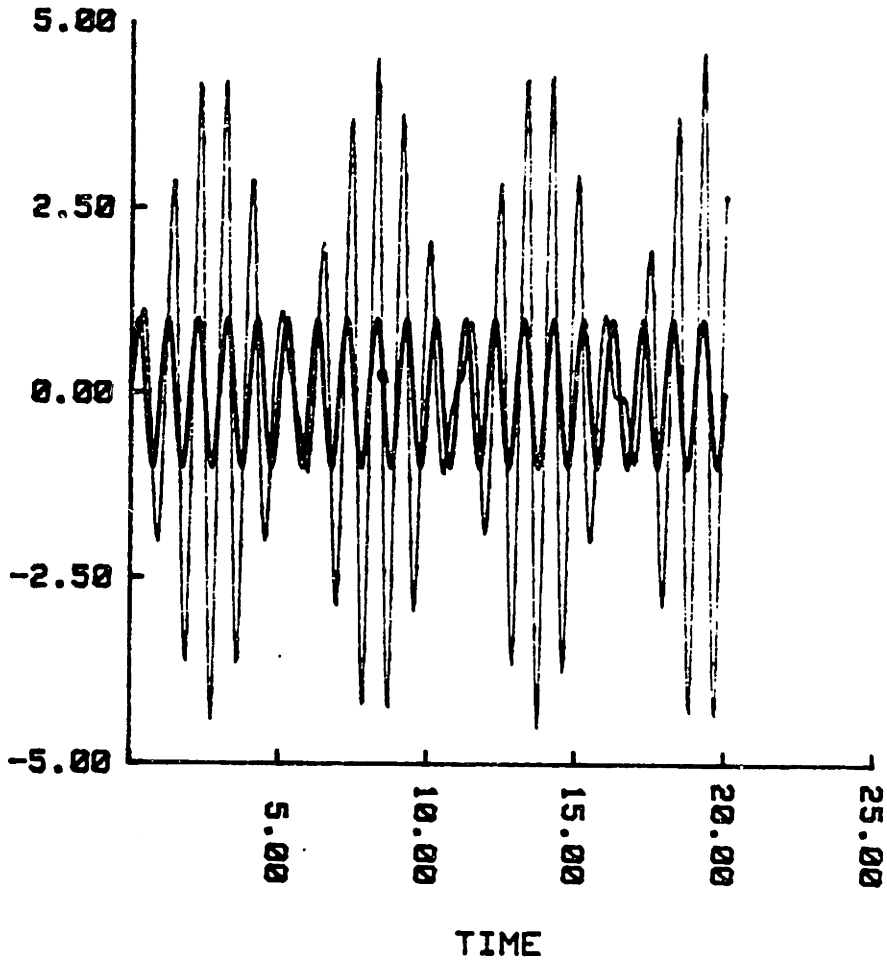

Figure 7-1: Non-Linear String; Motion at Midlength

Comparison with Unit Motion at the Top
$\tau = 0.01$
damping = 0
$\Delta T = 1/1000\ T_{per}$
3 modes

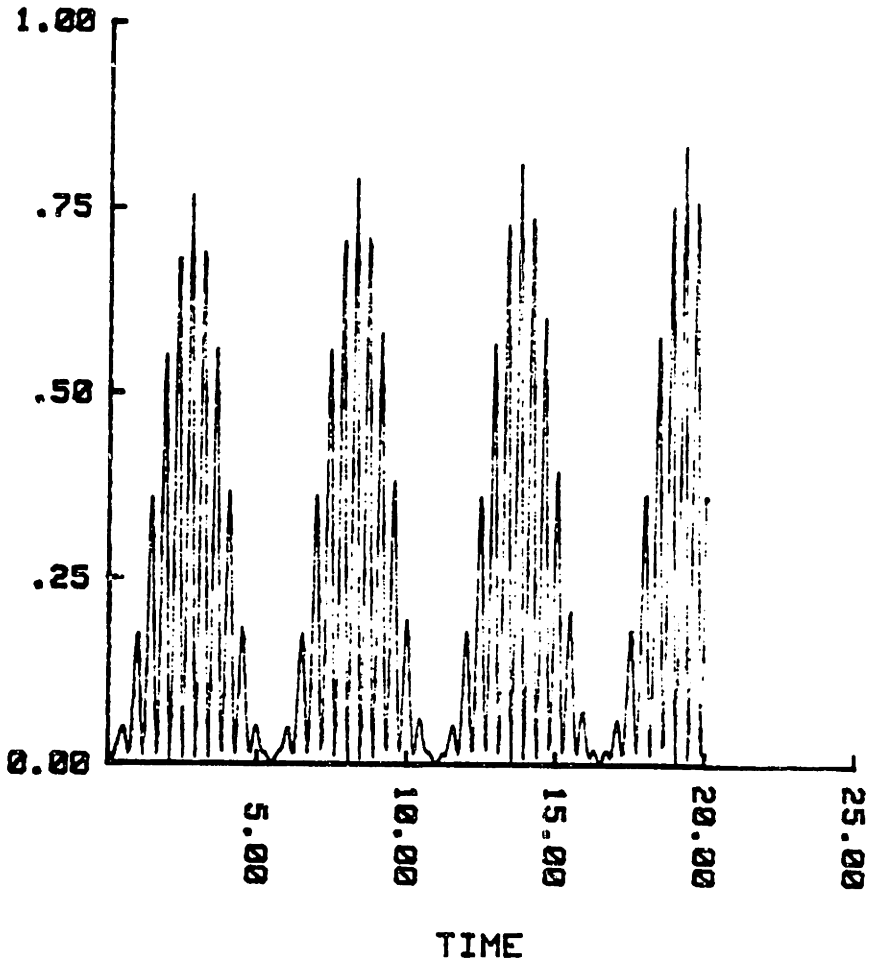

Figure 7-2: Non-Linear String; Dynamic Tension

(Dynamic Tension is given as fraction of Static Tension)
$\tau = 0.01$
damping = 0
$\Delta T = 1/1000\ T_{per}$
3 modes

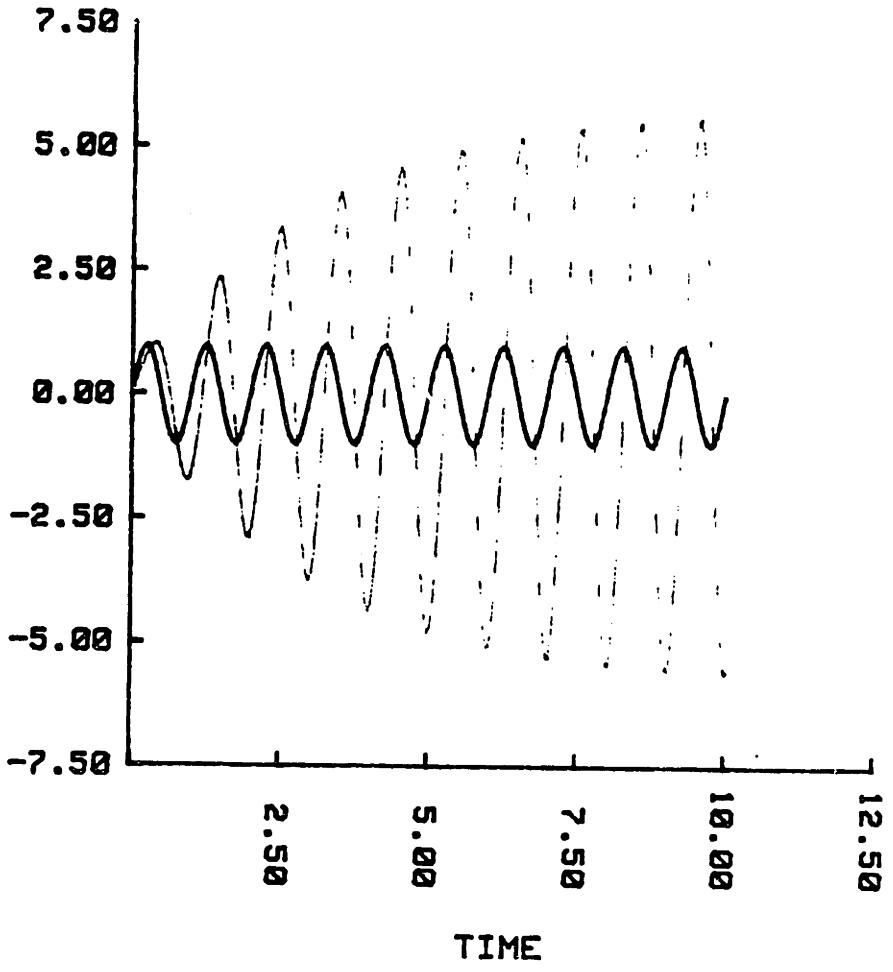

Figure 7-3: Non-Linear String; Motion at Midlength

Comparison with Unit Motion at the Top
$\tau = 0$
damping $= 0.05$
$\Delta T = 1/20\ T_{per}$
3 modes

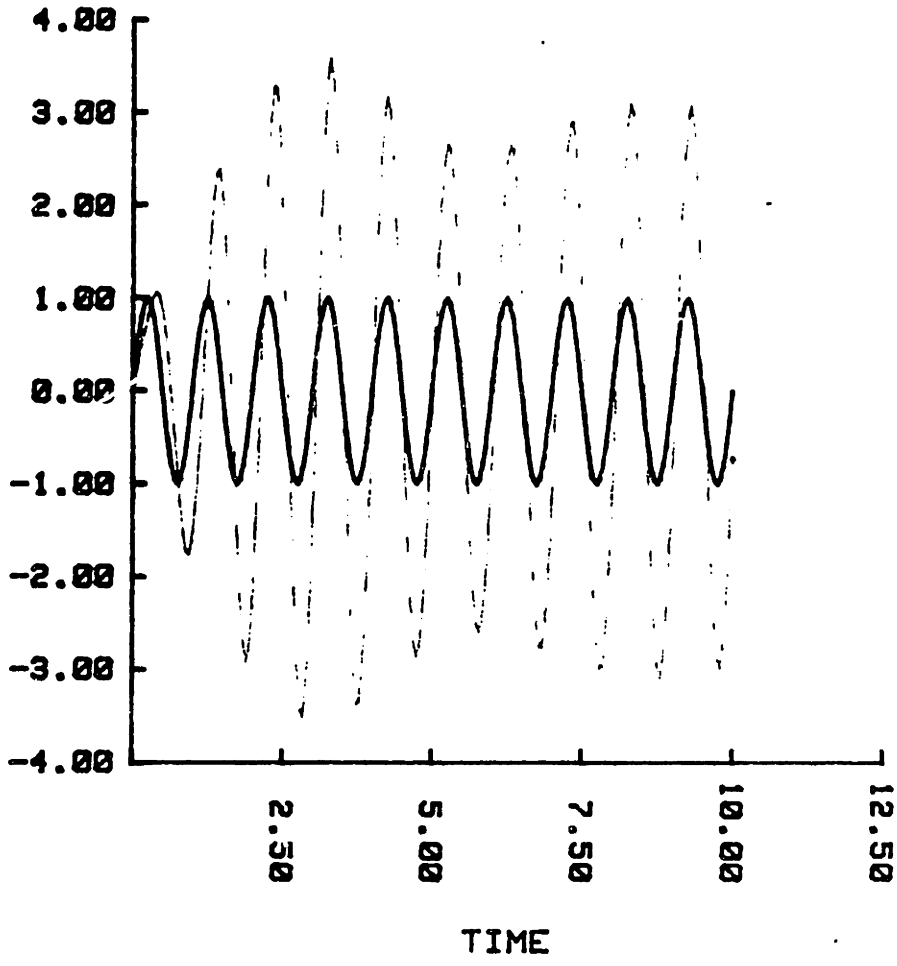

Figure 7-4: Non-Linear String; Motion at Midlength

Comparison with Unit Motion at the Top
$\tau = 0.01$
damping $= 0.05$
$\Delta T = 1/100\ T_{per}$
3 modes

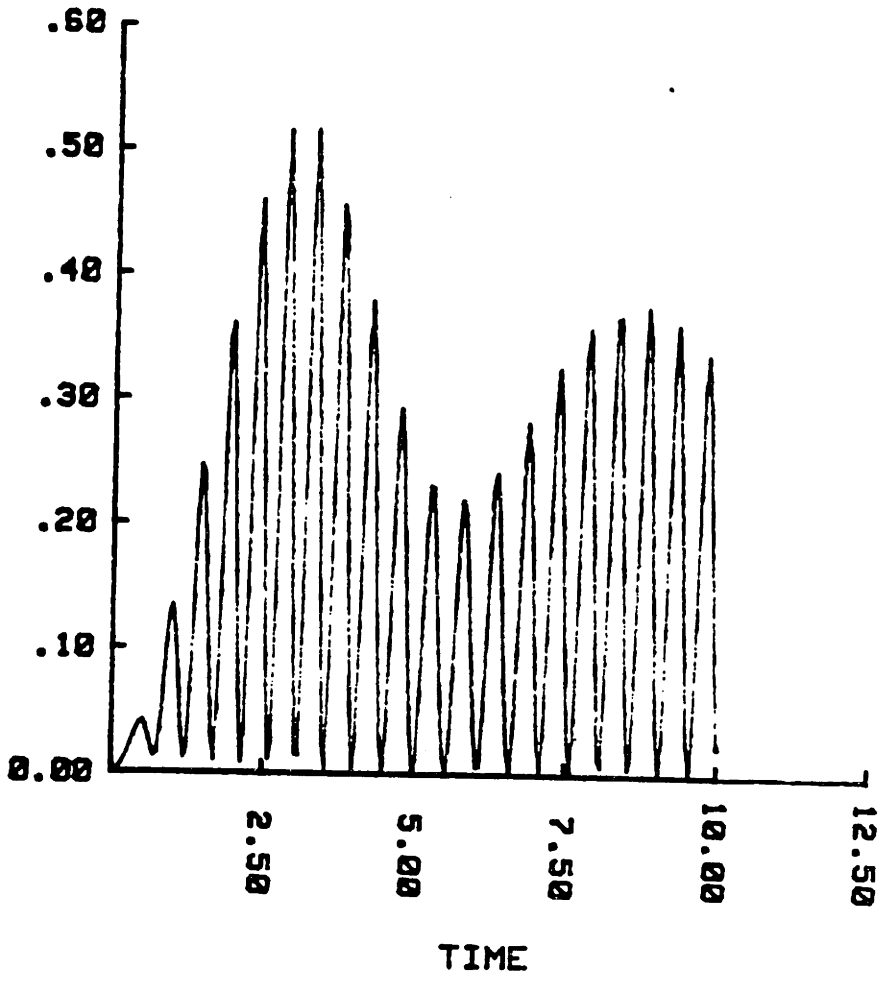

Figure 7-5: Non-Linear String; Dynamic Tension

(Dynamic Tension is given as a fraction of the Static Tension)
$\tau = 0.01$
damping = 0.05
$\Delta T = 1/100\ T_{per}$
3 modes

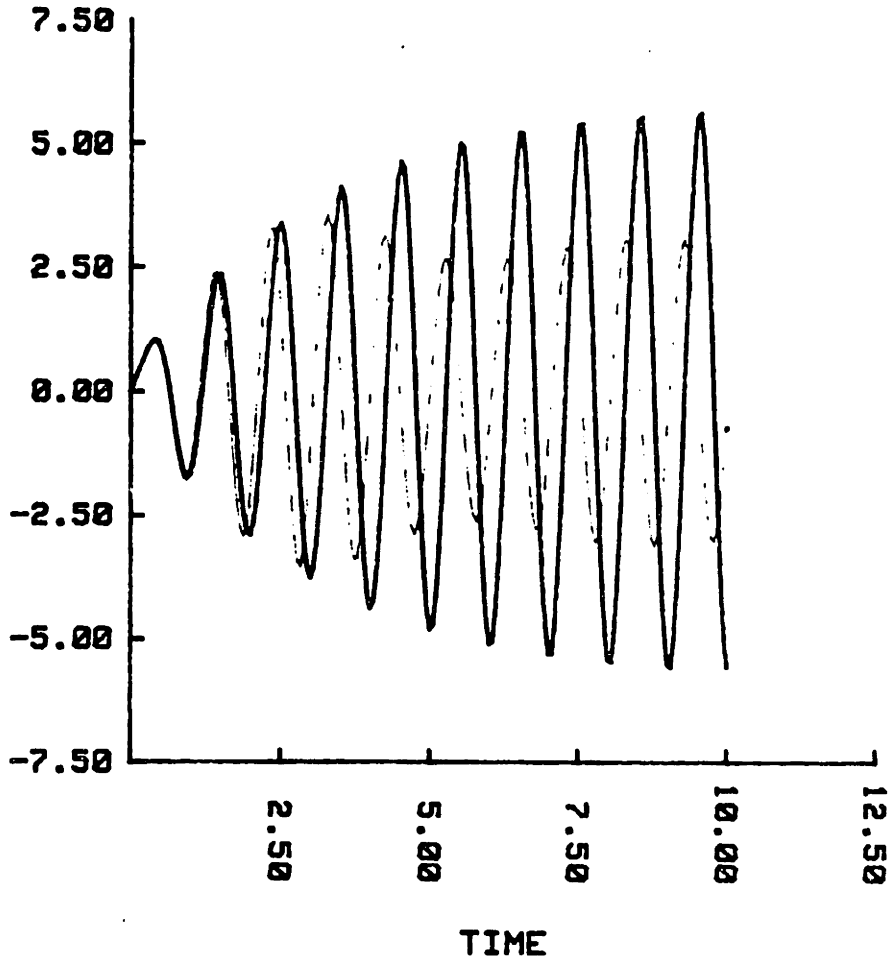

Figure 7-6: Non-Linear String; Motion at Midlength;
Comparison between responses with and without geometric non-linearity
(solid line)

$\tau = 0.01$
damping $= 0.05$
$\Delta T = 1/100\ T_{per}$
3 modes

T_{top}	=	1 332 000 N
T_{bot}	=	1 155 096 N
Mass	=	48.7 kg/m
Added mass	=	6.3 kg/m
Net weight	=	494.98 N/m
D_o	=	0.0889 m
E·A	=	1.30 10^9 N
Length	=	1 036 m
Depth	=	426.70 m
C_{Dn}	=	1.2
C_{Dt}	=	0.05

No external current

A static analysis of the problem gives the following results: (see figure 7-7)

$$\phi_{top} = 33.056^o$$

$$\phi_{bot} = 14.874^o$$

$$\Delta x = 940.68 \text{ m}$$

$$\phi_{av} = 24.399^o$$

ϕ_{av} is the angle formed between the cable chord and the horizontal.

The mode configuration is only approximately symmetric or anti-symmetric, because the inclination angle destroys the symmetry about the cable midpoint. The results above were calculated numerically, but the perturbation theory and even Irvine's inclined cable results, predict essentially the same values for the eigenfrequencies.

To give the reader a notion about the shape of the modes, some figures for the first four modes and for the quasi-static solution are presented. For the modes the solution has been normalised as described in chapter 6, but with the amplitude written in non-dimensional form (normalised amplitude ·

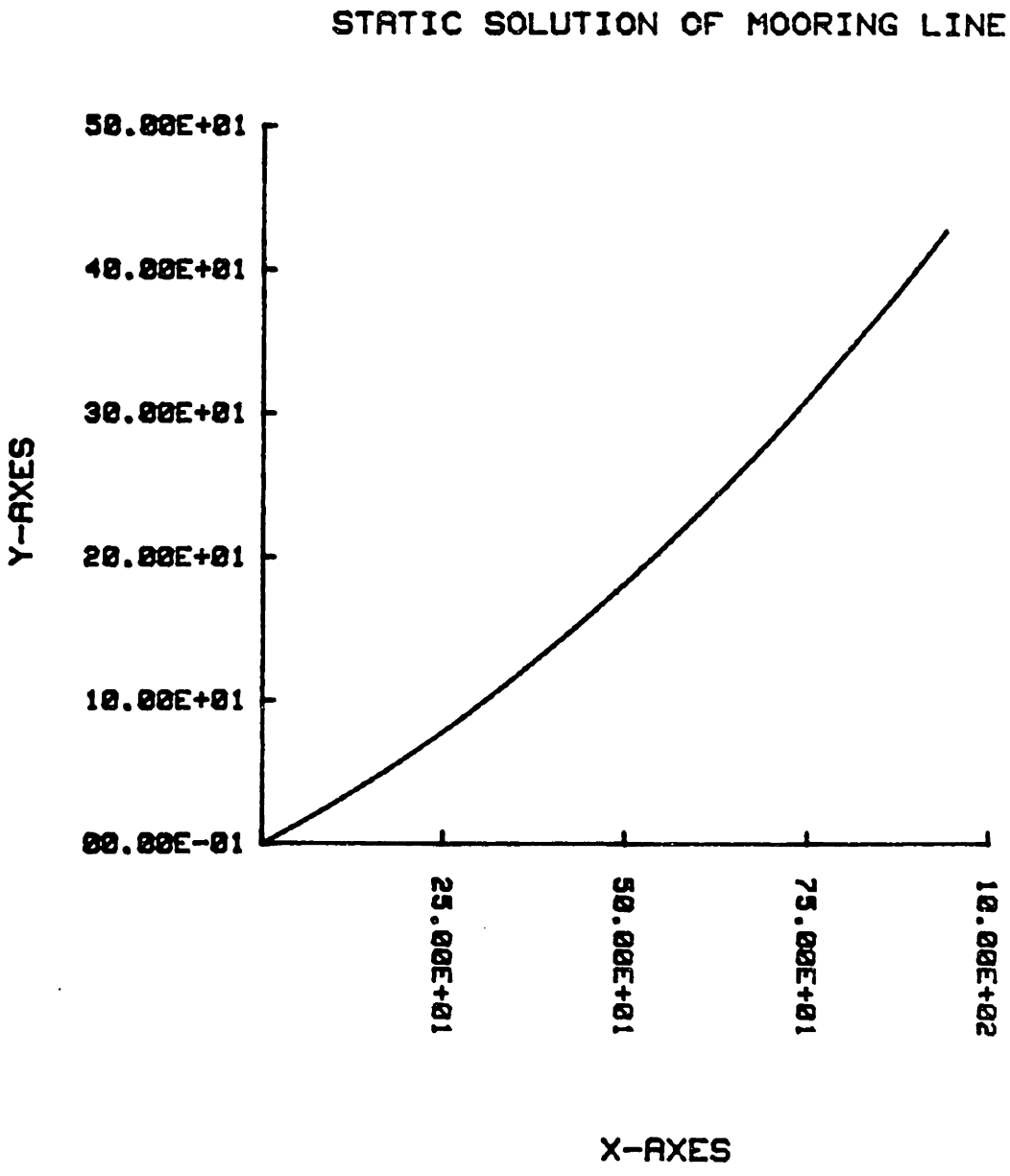

Figure 7-7: Static Shape of a Guy

The eigenfrequencies for this example are:

	ω(rad/sec)	T(period)	mode shape
1	0.9011	6.937	anti-symmetric
2	1.1949	5.258	symmetric
3	1.6086	3.906	symmetric
4	1.8228	3.447	anti-symmetric
5	2.3115	2.718	symmetric
6	2.7527	2.283	anti-symmetric
7	3.2335	1.943	symmetric
8	3.7059	1.695	anti-symmetric

Table 7-II: Eigenfrequencies

$(M)^{1/2}$ L). The four essential quantities for each mode are plotted, i.e. the tangential displacement, the normal displacement, the dynamic tension and the dynamic angle.

The second and third modes are symmetric, which is explained by the fact that the cable is in the region where the first symmetric mode has shifted to a higher value than a taut string mode, while the third symmetric mode has not. The dynamic tension is nearly constant or slowly varying for the low modes shown. The quasi-static solution is the solution to an imposed unit motion at the top in the normal and tangential direction at the limit of zero frequency.

Using the above modes, the influence of the drag forces was studied by exciting the cable with a top motion in the normal direction. The simulations

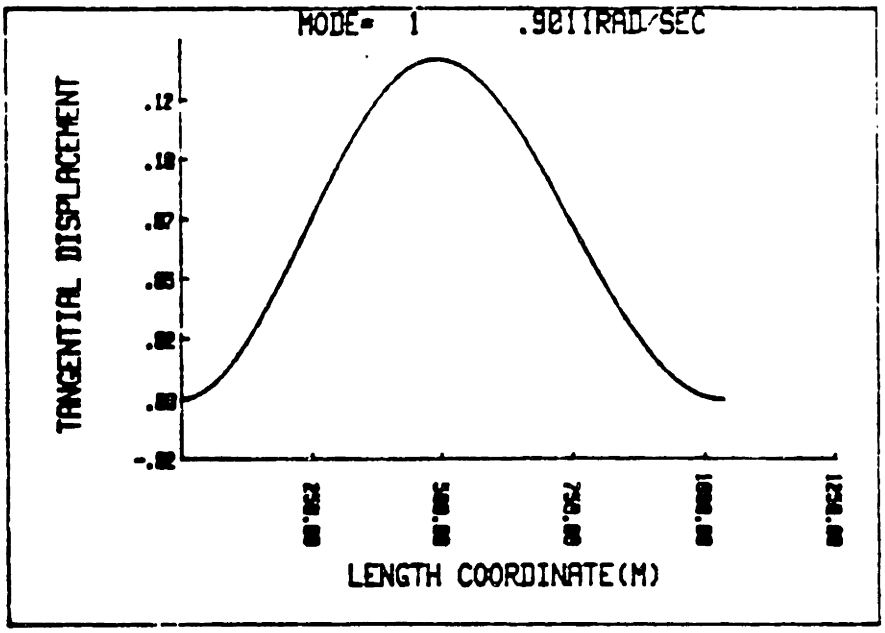

Figure 7-8: First Mode of a Guy: Tangential Displacement

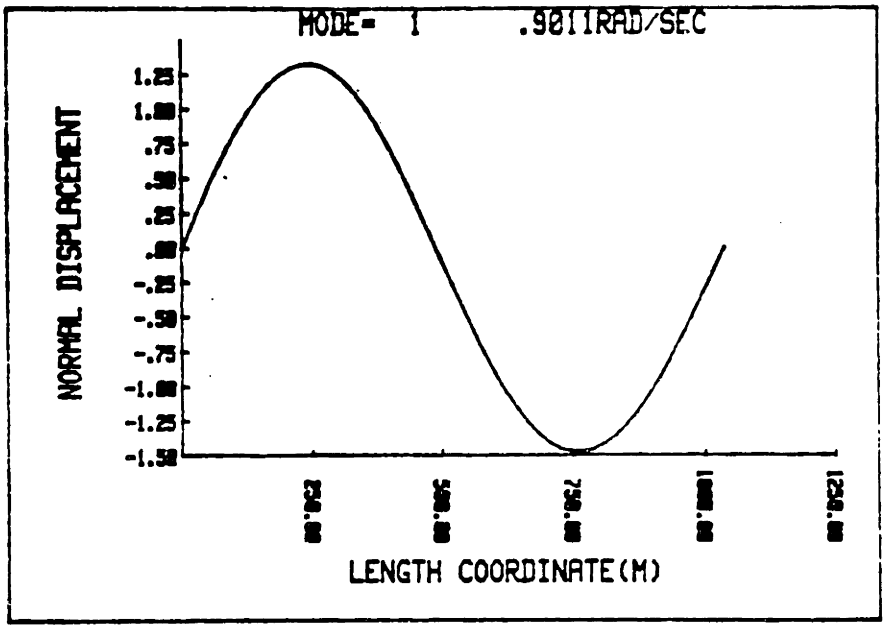

Figure 7-9: First Mode of a Guy: Normal Displacement

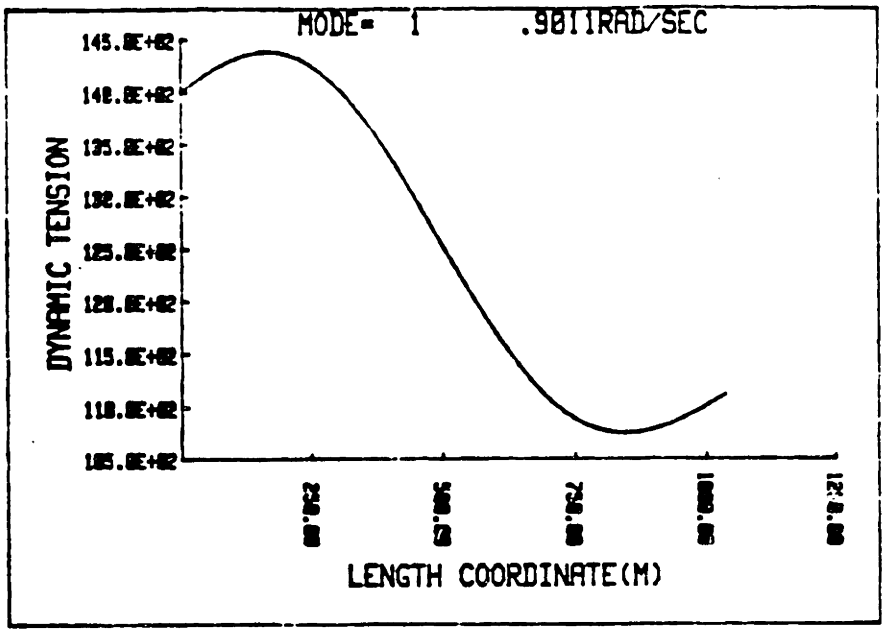

Figure 7-10: First Mode of a Guy: Dynamic Tension

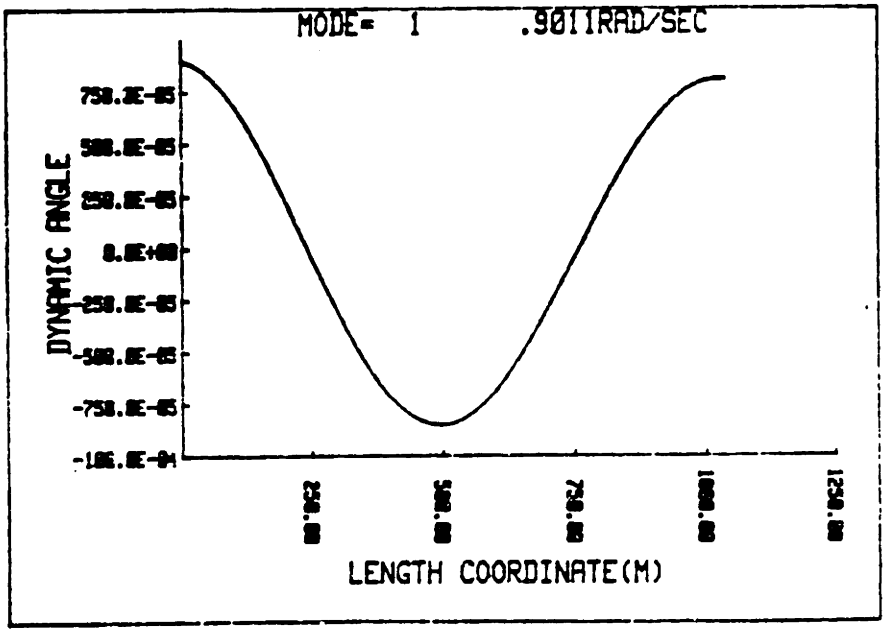

Figure 7-11: First Mode of a Guy: Dynamic Angle

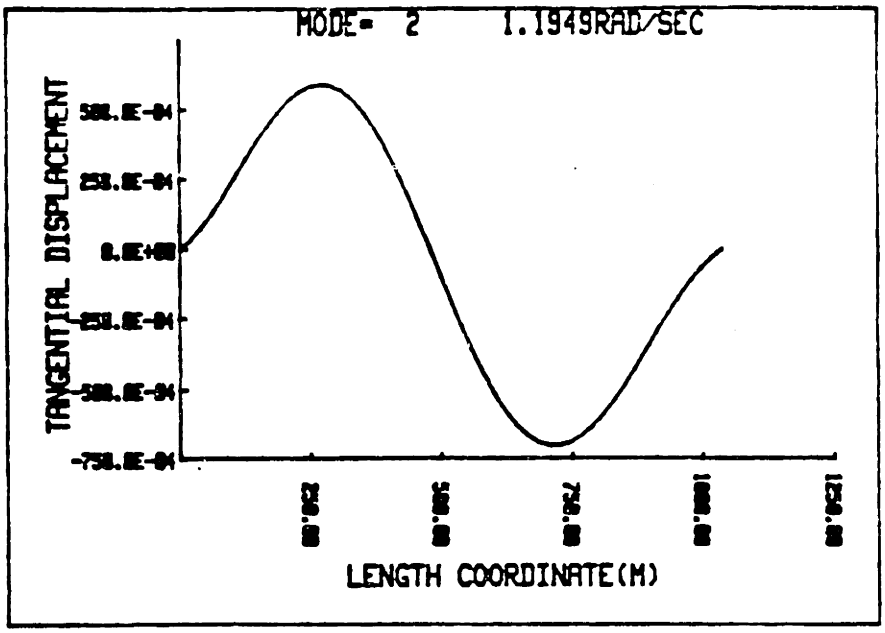

Figure 7-12: Second Mode of a Guy: Tangential Displacement

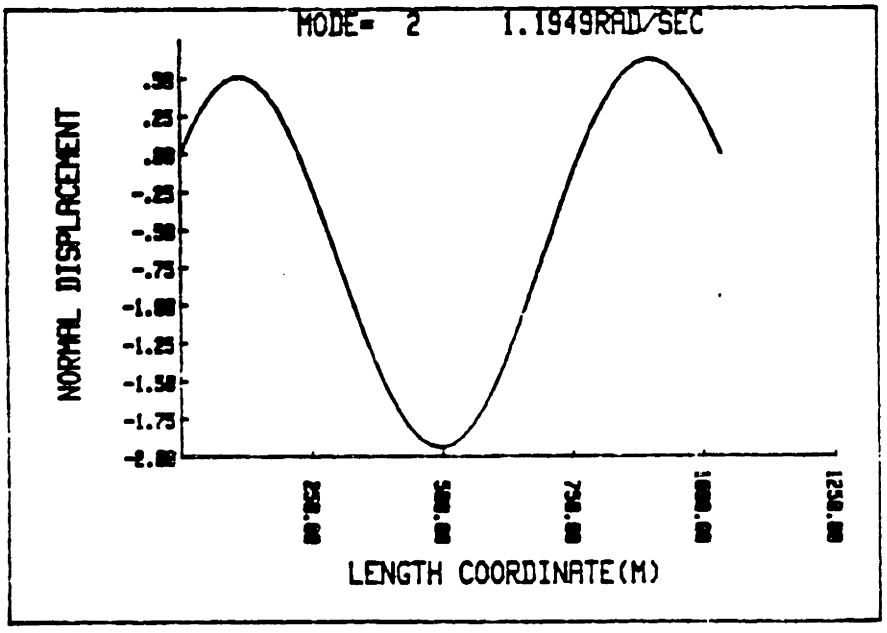

Figure 7-13: Second Mode of a Guy: Normal Displacement

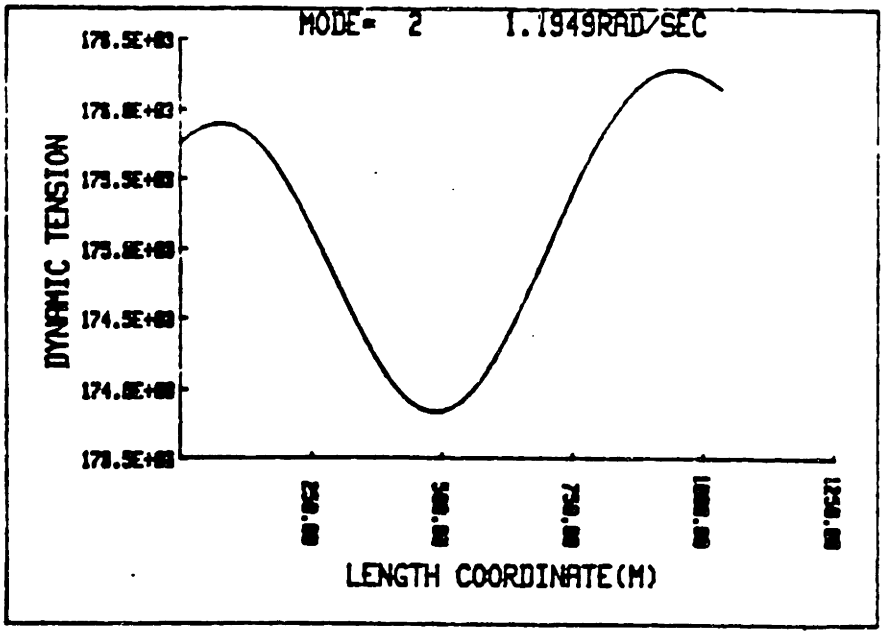

Figure 7-14: Second Mode of a Guy: Dynamic Tension

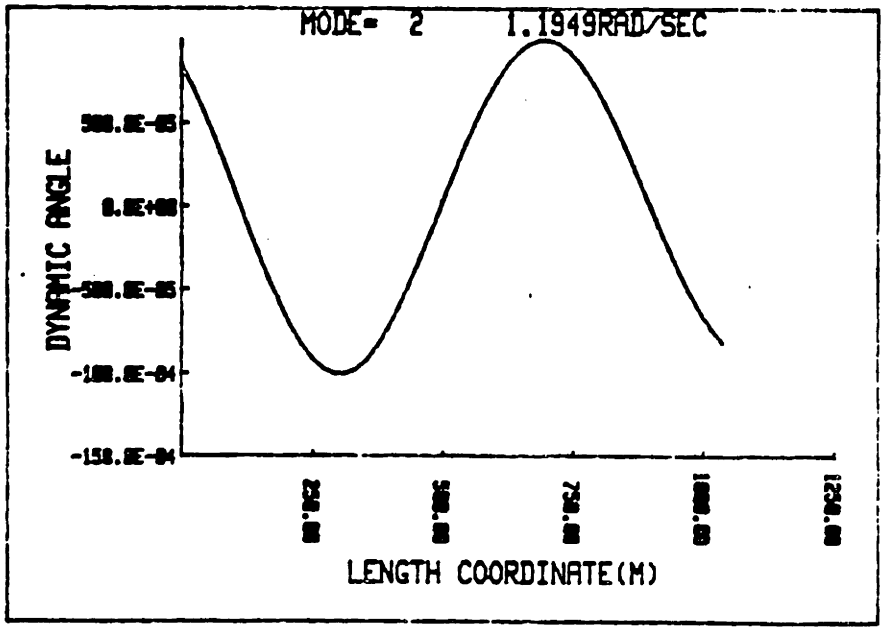

Figure 7-15: Second Mode of a Guy: Dynamic Angle

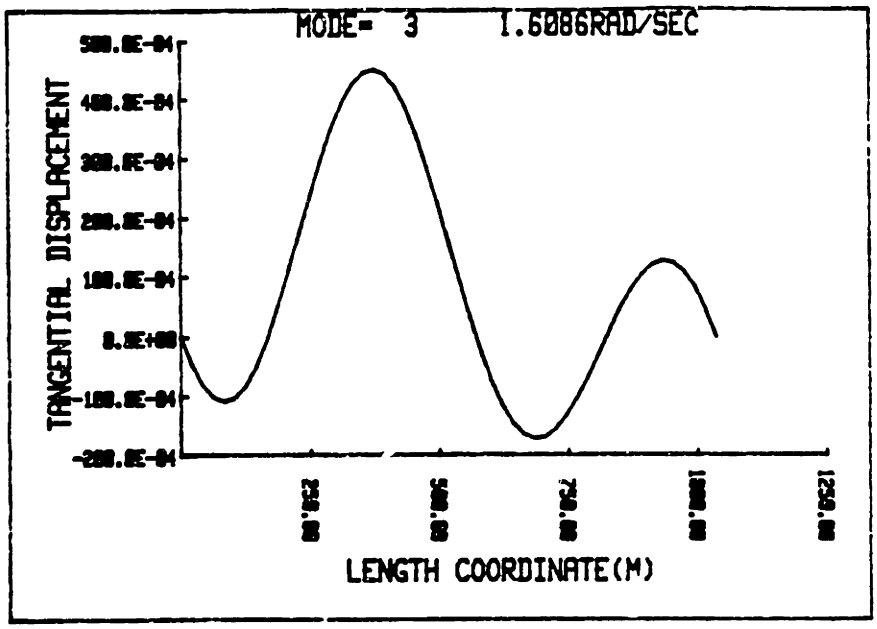

Figure 7-16: Third Mode of a Guy: Tangential Displacement

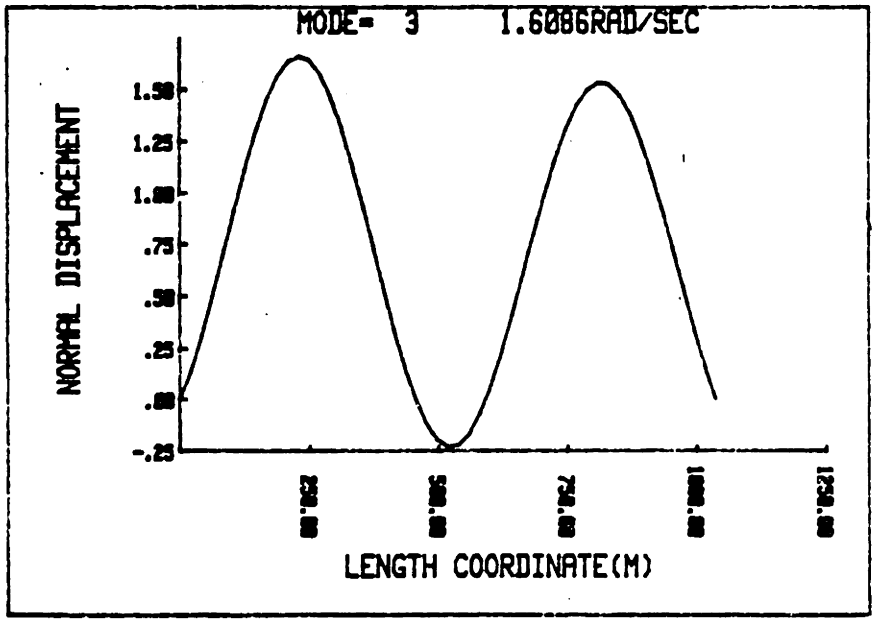

Figure 7-17: Third Mode of a Guy: Normal Displacement

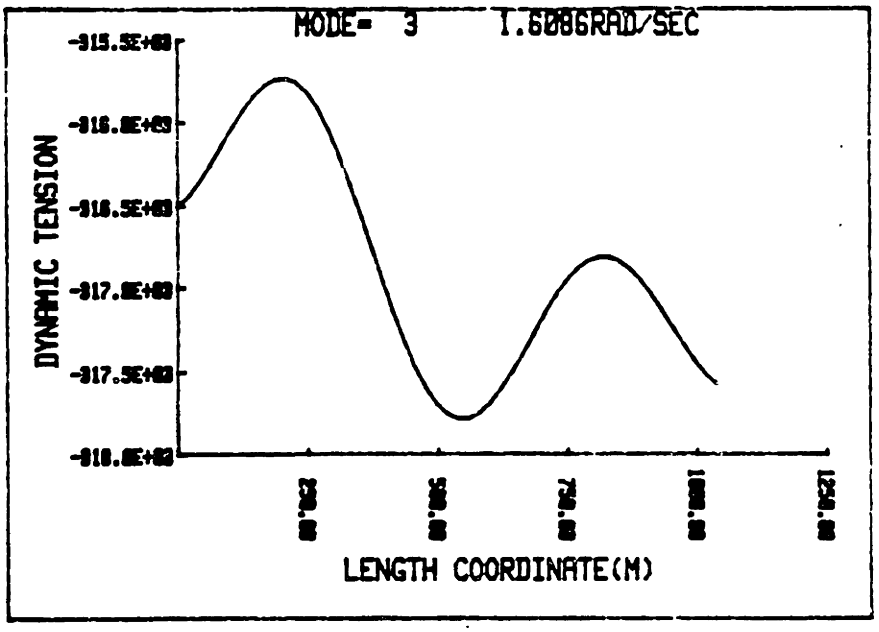

Figure 7-18: Third Mode of a Guy: Dynamic Tension

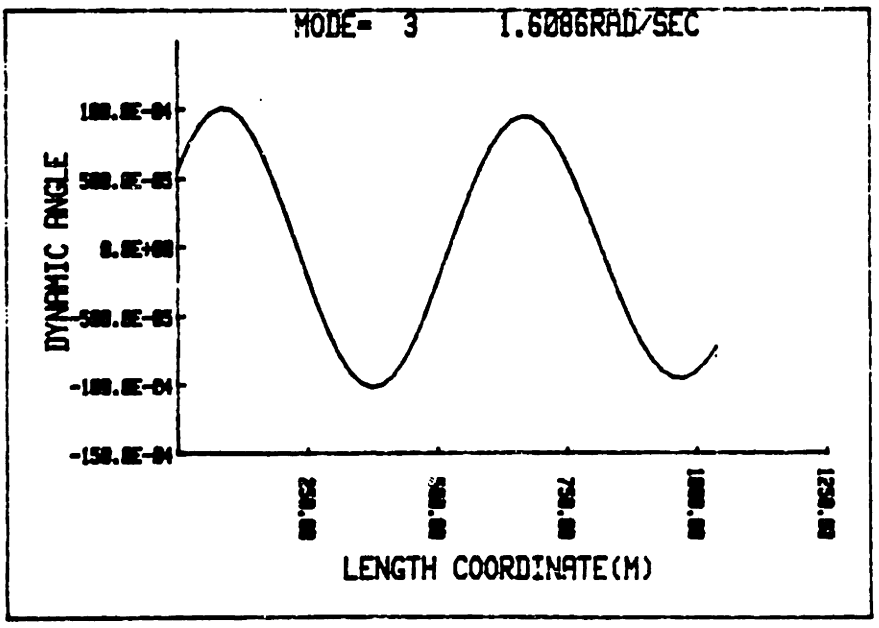

Figure 7-19: Third Mode of a Guy: Dynamic Angle

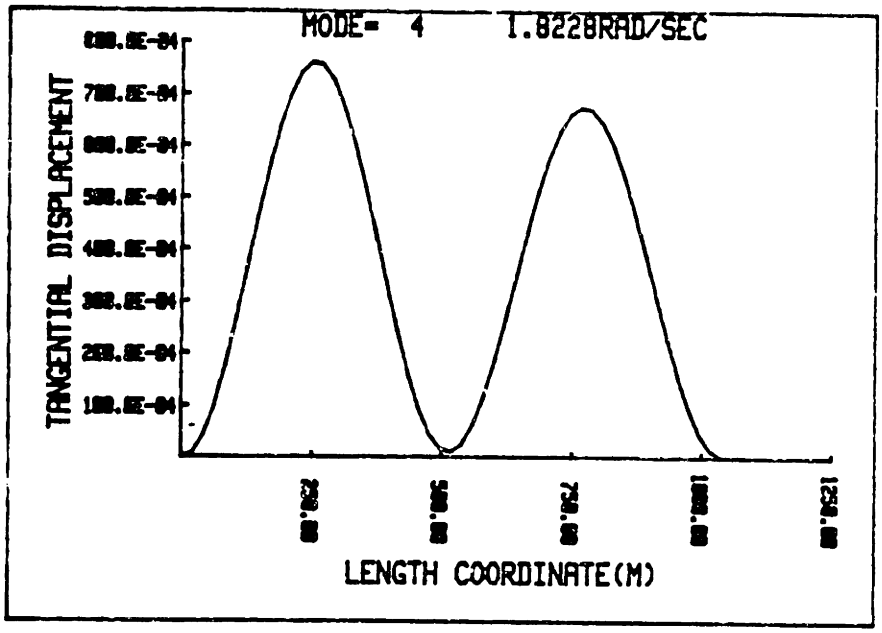

Figure 7-20: Fourth Mode of a Guy: Tangential Displacement

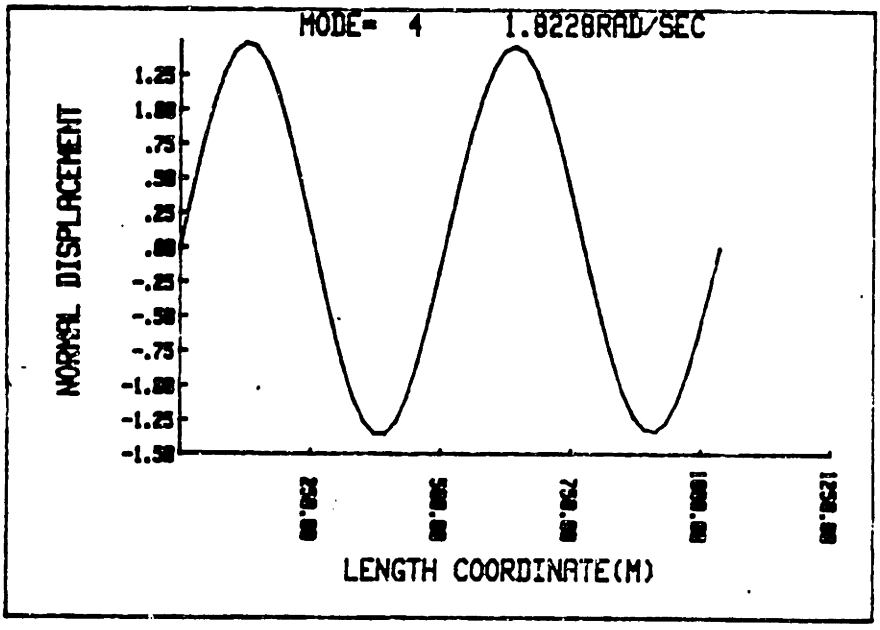

Figure 7-21: Fourth Mode of a Guy: Normal Displacement

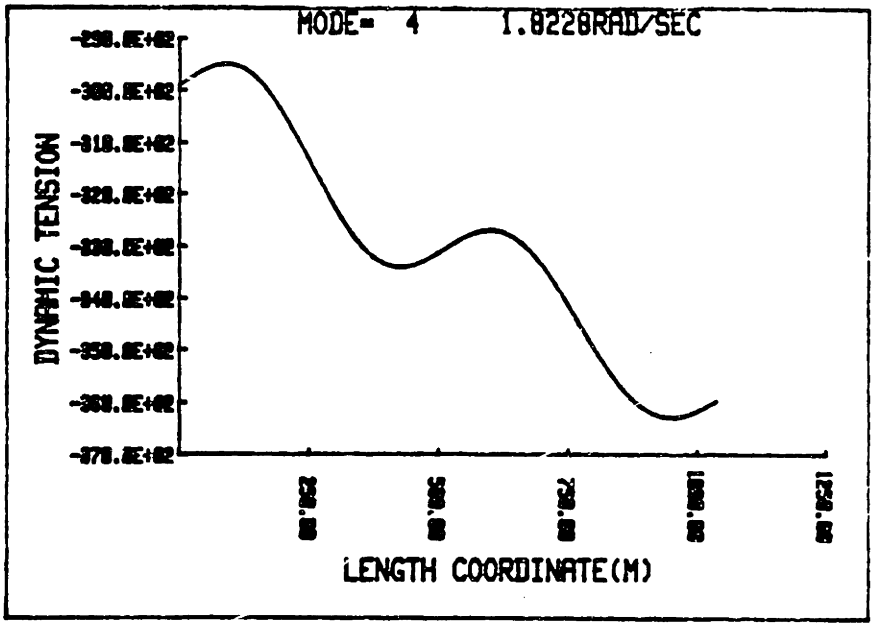

Figure 7-22: Fourth Mode of a Guy: Dynamic Tension

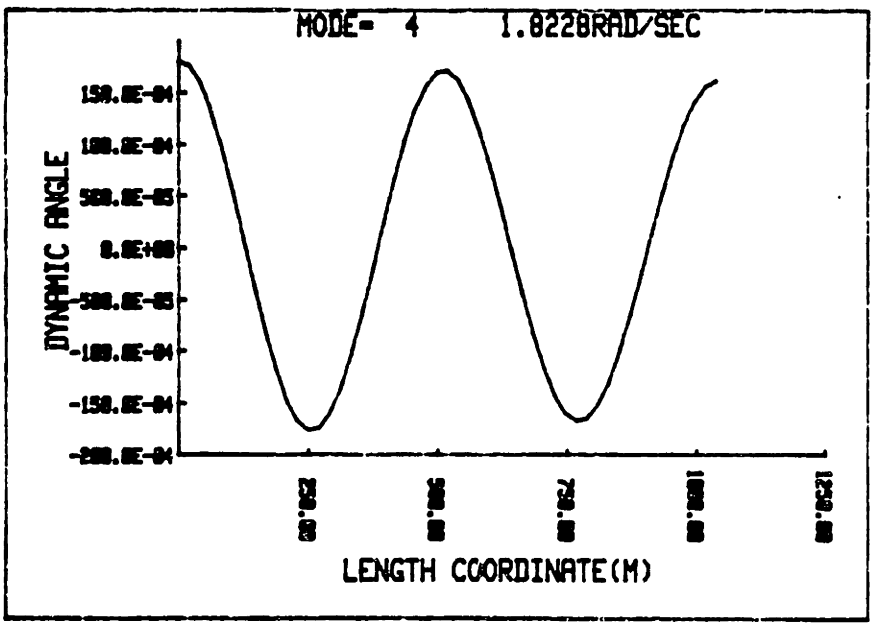

Figure 7-23: Fourth Mode of a Guy: Dynamic Angle

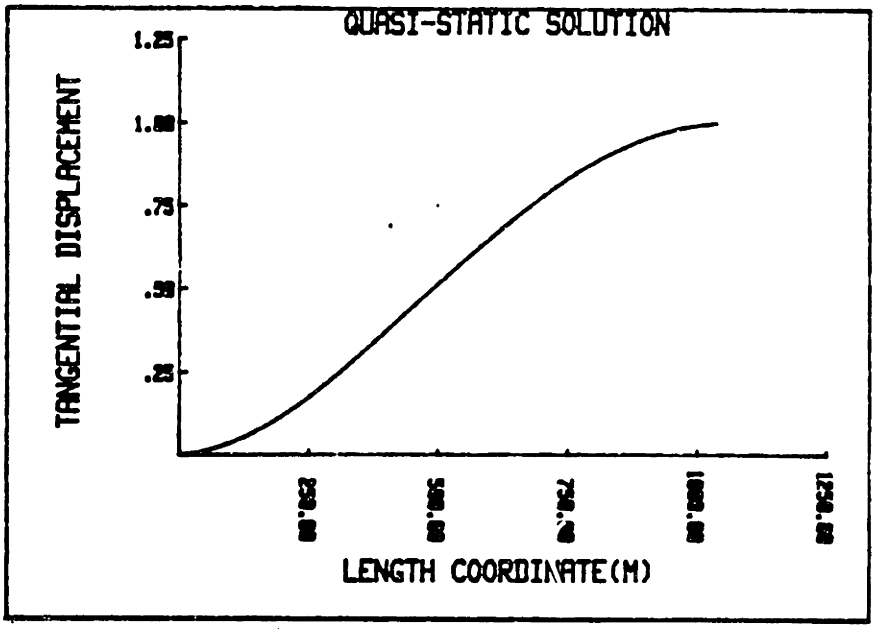

Figure 7-24: Tangential Quasi-Static Solution: Tangential Displacement

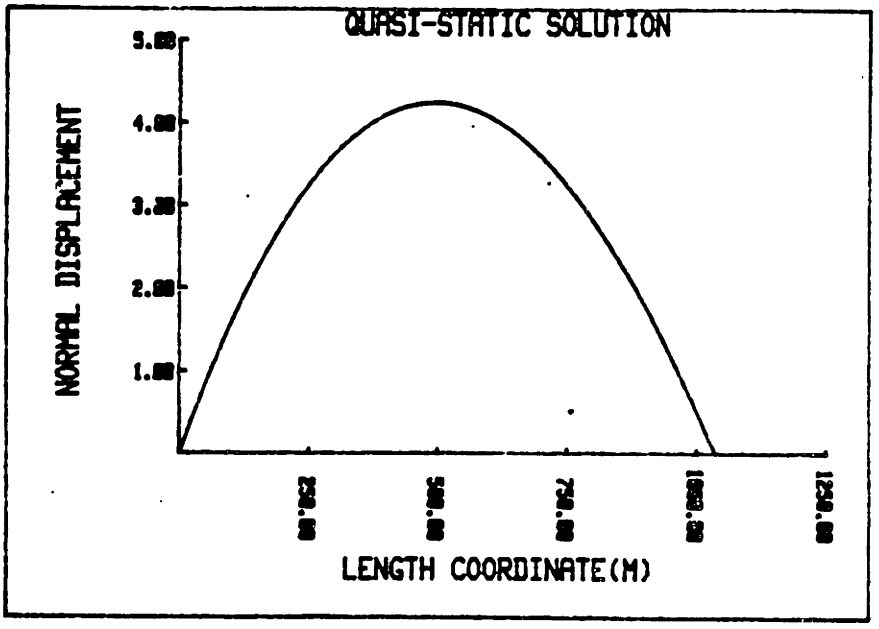

Figure 7-25: Tangential Quasi-Static Solution: Normal Displacement

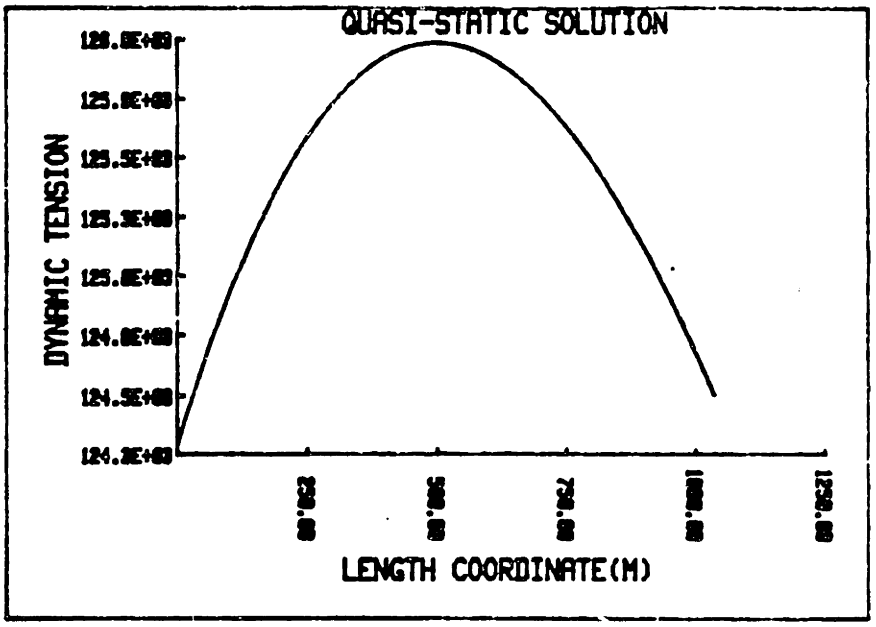

Figure 7-26: Tangential Quasi-Static Solution: Dynamic Tension

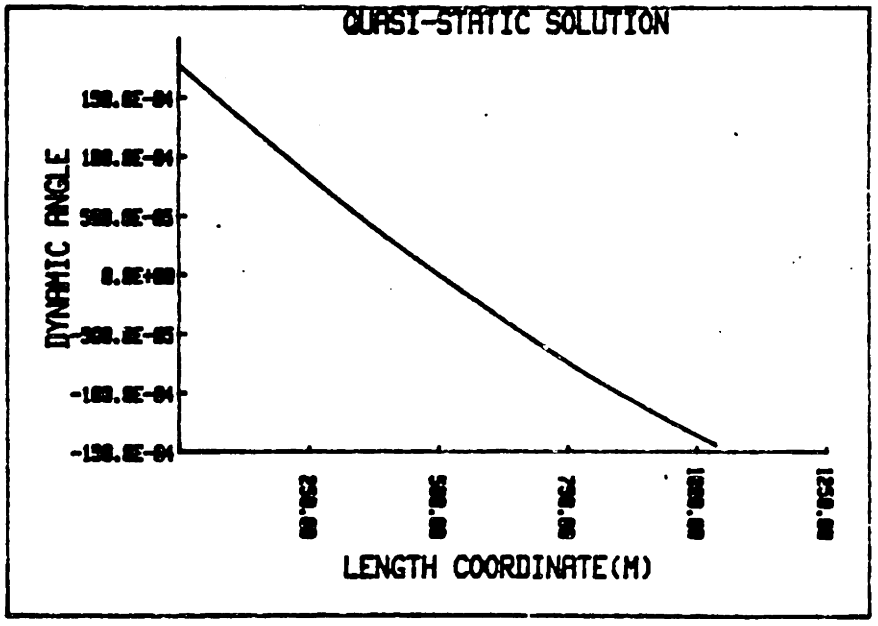

Figure 7-27: Tangential Quasi-Static Solution: Dynamic Angle

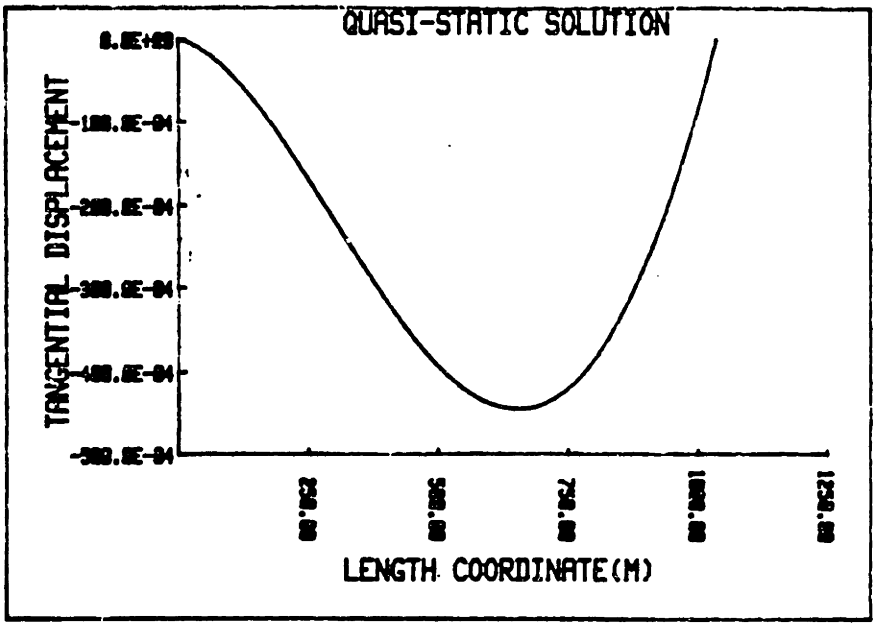

Figure 7-28: Normal Quasi-Static Solution: Tangential Displacement

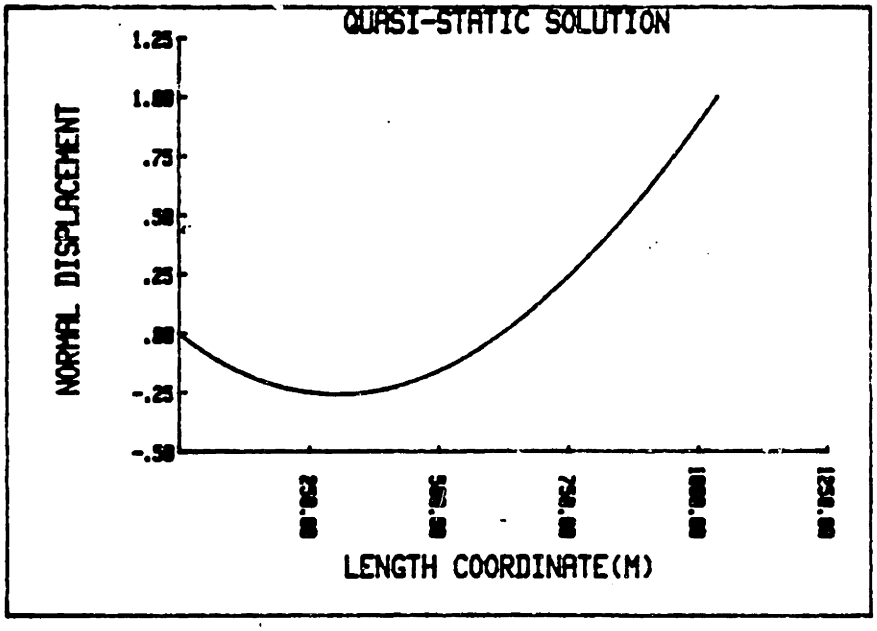

Figure 7-29: Normal Quasi-Static Solution: Normal Displacement

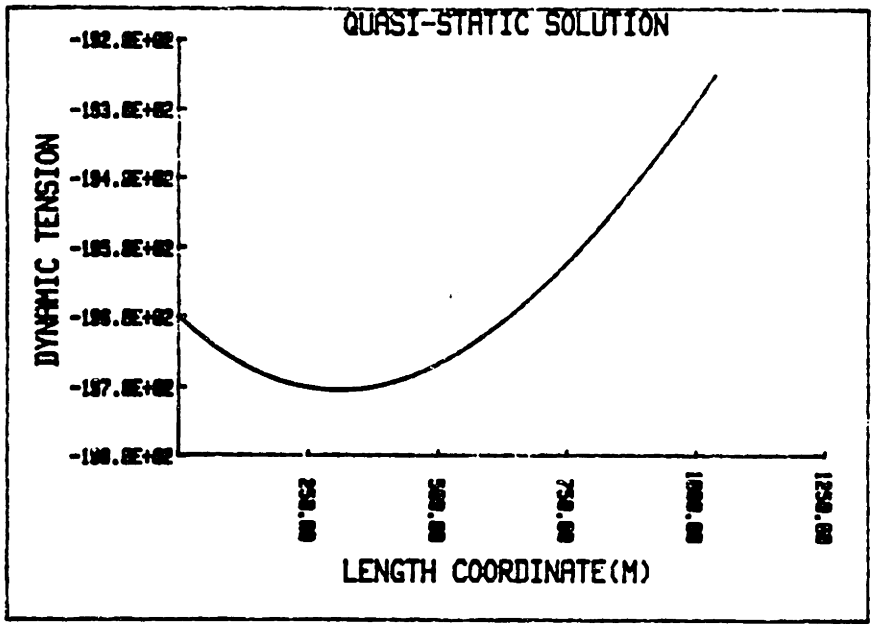

Figure 7-30: Normal Quasi-Static Solution: Dynamic Tension

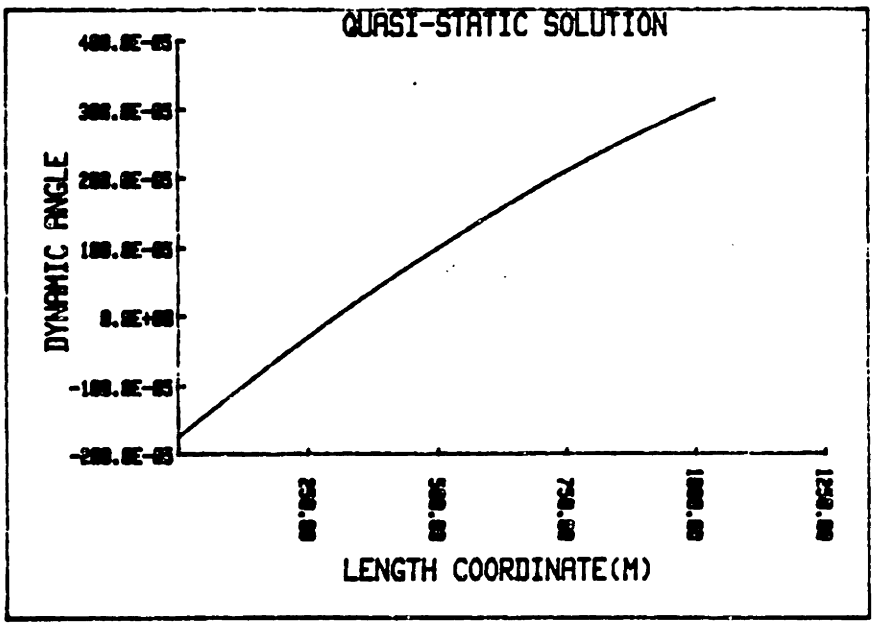

Figure 7-31: Normal Quasi-Static Solution: Dynamic Angle

List of Figures of Eigenmodes and Quasi-Static Shapes

	tangential	normal	dyn. tension	dyn. angle
first mode	7-8	7-9	7-10	7-11
second mode	7-12	7-13	7-14	7-15
third mode	7-16	7-17	7-18	7-19
fourth mode	7-20	7-21	7-22	7-23
tangential quasi-static	7-24	7-25	7-26	7-27
normal quasi-static	7-28	7-29	7-30	7-31

were done using 4 - 8 - 16 modes. The results for 8 modes are shown here. The simulation with four modes gave a similar envelope curve except for the high amplitude motions. The results are given in figures 7-32 through 7-35. The excitation frequency was equal to the first resonance frequency except for figure 7-32, for which excitation causes quasi-static motion. The plots represent the superposition of the shapes of the cable obtained at different time steps, so that an envelope of the transverse response of the cable is obtained. The plots give the motion normal to the static shape at each point expressed as a fraction of the A/D ratio, which was varied between 1.5 and 100. The dominant effect of the drag force at high amplitudes becomes clear.

The increasing importance of the drag force can simply be explained by looking at the ratio of inertia versus drag forces:

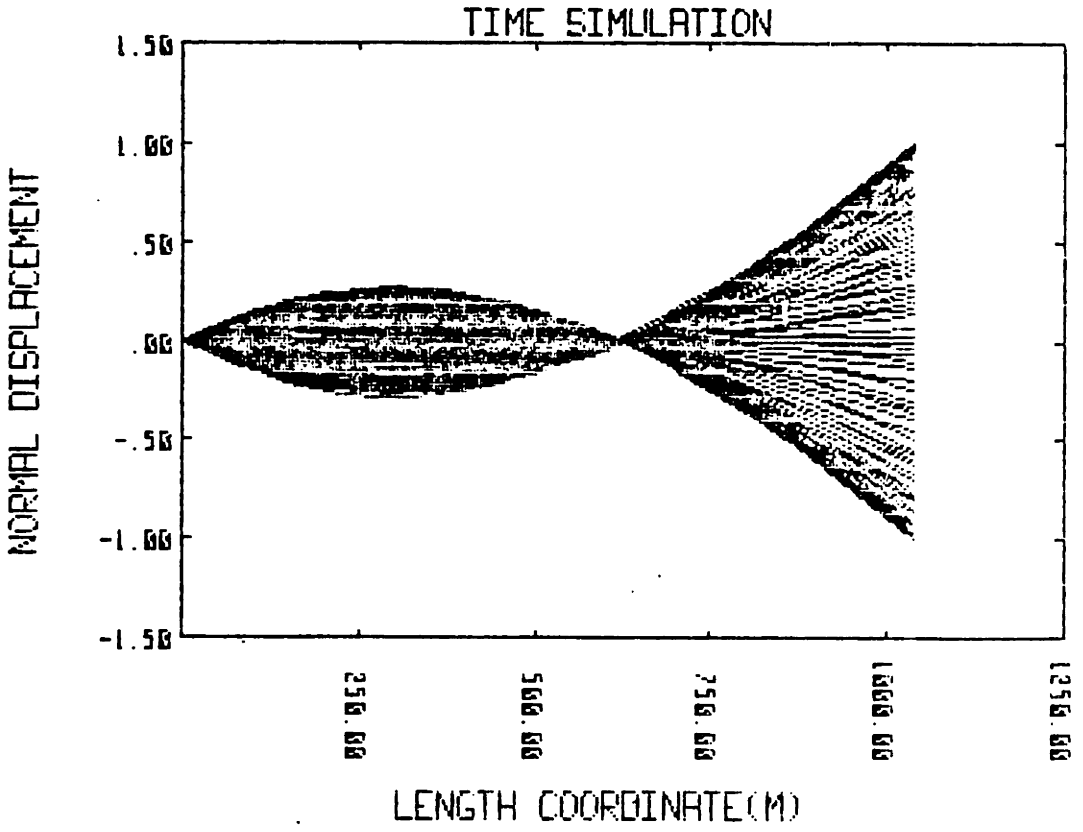

Figure 7-32: Quasi-Static Motion at very Low Frequency

Normal displacement along the guy.
Top motion has unit amplitude in the normal direction.
(A/D=1)
$\Delta T = 1/100\ T_{per}$

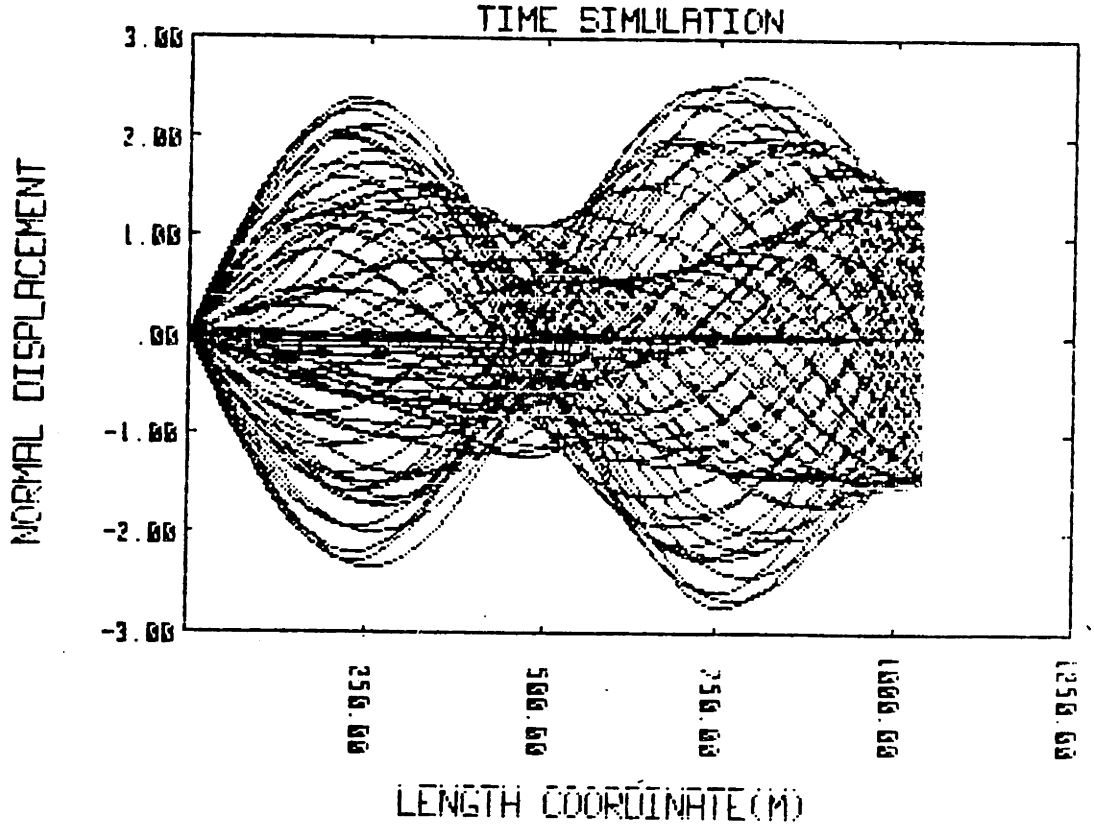

Figure 7-33: Response to Top Excitation at First Resonance Frequency, A/D = 1.5

Normal displacement along the guy.
Top motion A/D = 1.5 in the normal direction.
$\Delta T = 1/100\ T_{per}$

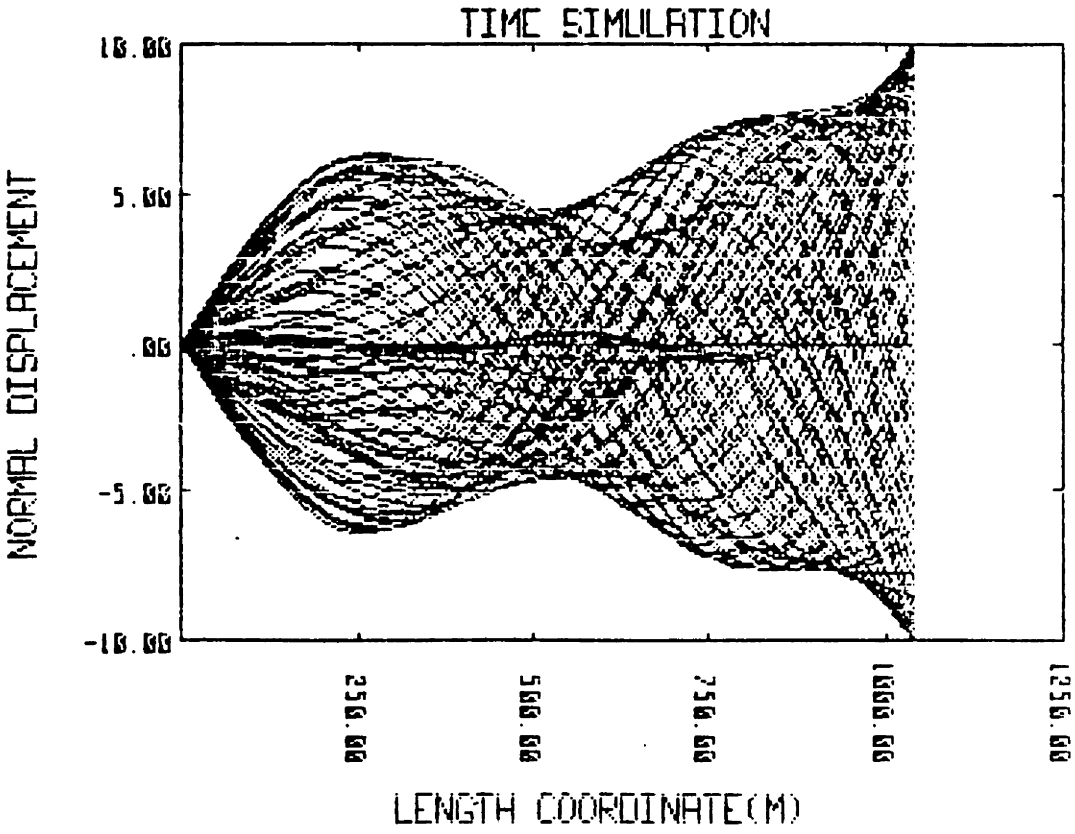

Figure 7-34: Response to Top Excitation at First Resonance Frequency, A/D = 10

Normal displacement along the guy.
Top motion A/D = 10 in the normal direction.
$\Delta T = 1/100\ T_{per}$

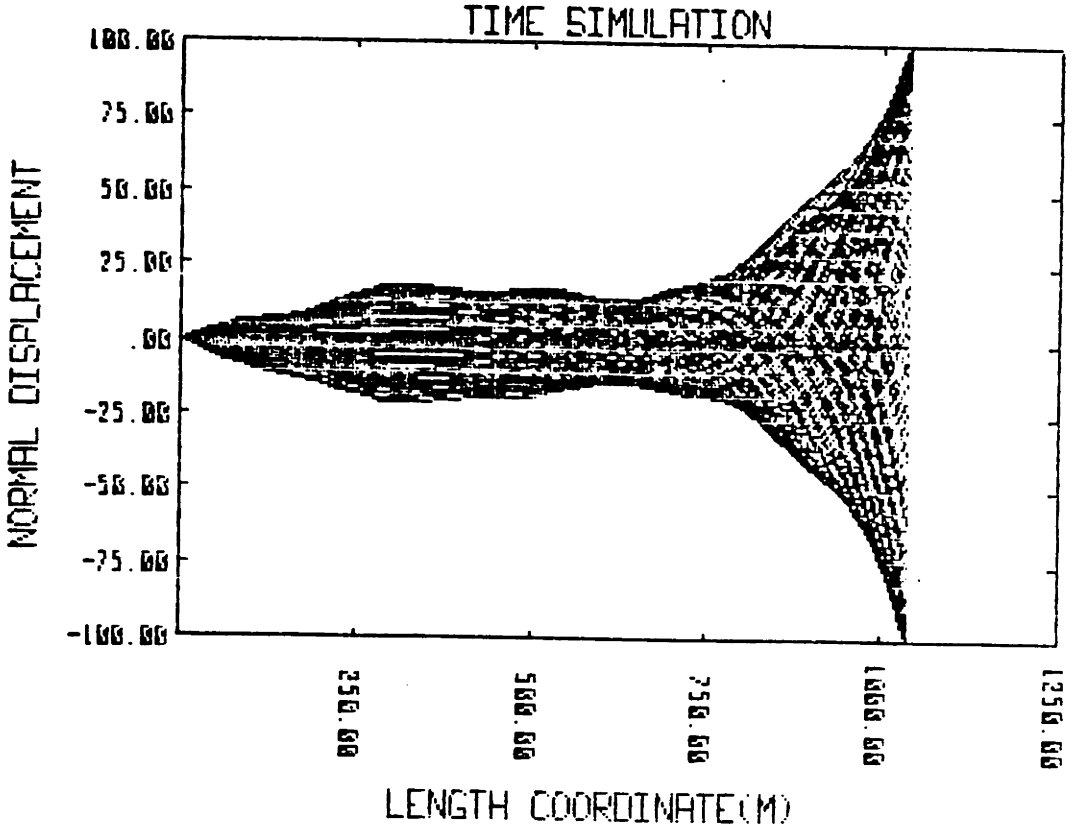

Figure 7-35: Response to Top Excitation at First Resonance Frequency A/D = 100

Normal displacement along the guy.
Top motion A/D = 100 in the normal direction.
$\Delta T = 1/100\ T_{per}$

$$\frac{F_{dr}}{F_{in}} = \frac{0.5\ \rho_w\ C_D\ D\ \omega^2\ A^2}{\rho_{tot}\ 1/4\ \pi\ D^2\ \omega^2\ A}$$

$$= \frac{2}{\pi}\ \frac{\rho_w}{\rho_{tot}}\ C_D\ \frac{A}{D}$$

7.4 Comparison of Non-Linear Cable Model Results with Davenport's Experiments

A computer code using the non-linear modal expansions, described in sections 6.8 - 6.10 was developed. The results of the code were compared with experimental data obtained by Davenport [Davenport 65].

Davenport's experiments consisted of moving the top of a guy cable sinusoidally in the horizontal direction through an excentric mechanism driven by an electric motor. The horizontal tension was measured by strain gauges. The horizontal motion at the top was also measured (See figure 7-36). The cable consisted of a piano wire of 0.026 inch diameter with cylindrical weights attached, to obtain the correct total weight to tension ratio. The cable was immersed in different liquids (oil or water) during the experiments to obtain different damping characteristics. Only one experiment (case 2.1 in water) was considered in this comparison.

The horizontal amplitude of excitation in the experiment was set at 0.01 inch. The data for the experiment are ;

$$L = 11\ ft$$

$$\phi_a = 41.06^o$$

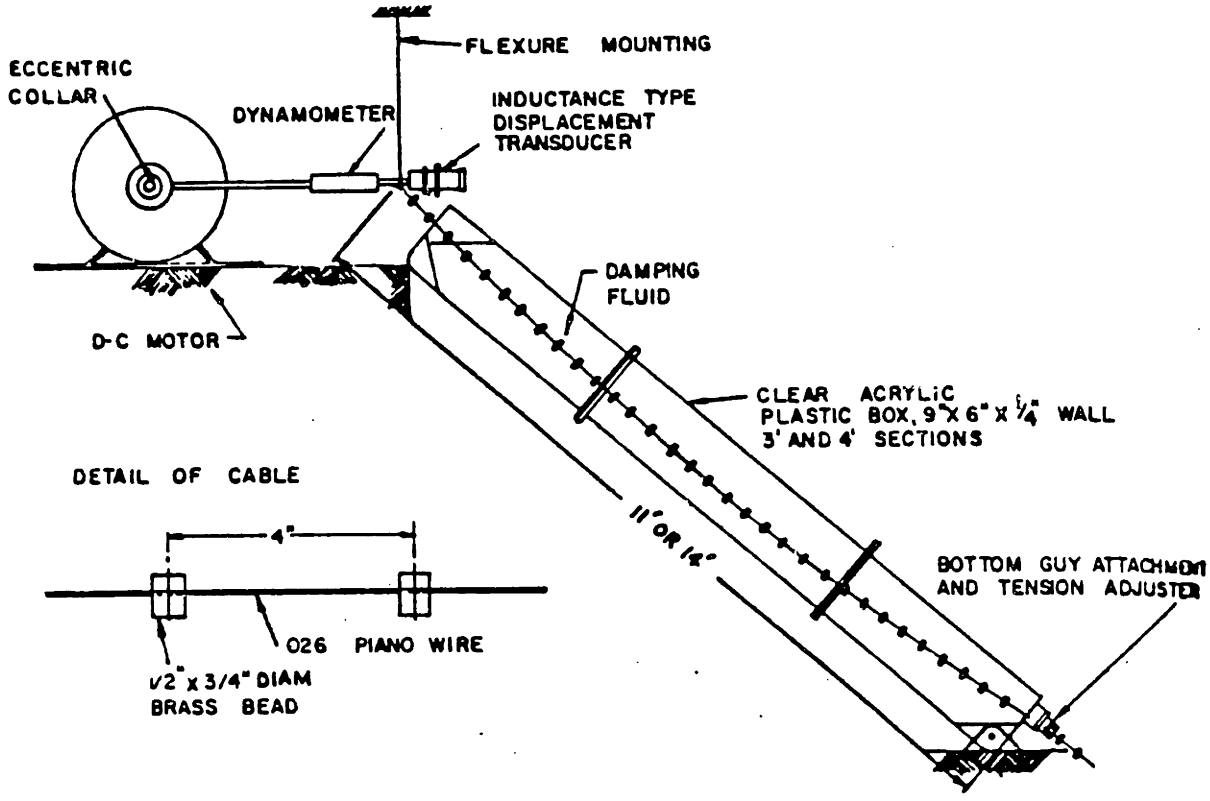

Figure 7-36: Experimental Arrangement for Dynamic tests

[Davenport 65]

$H_*/AE = 0.000671$

$WL/H_* = 0.202$ (W is weight in air)

Davenport measured the horizontal component of the dynamic tension caused by an imposed horizontal motion at the top for various frequencies. The amplitude of the motion was 0.01 inch. The measured tension can be viewed, apart from a scale factor, as the impedance function S_{xx} discussed in chapter 4. For the given amplitude, the geometric non-linear effects are not important and the damping forces are linear. The linear damping is due to the very low Reynolds number for both the oscillating cable and the attached cylindrical weights.

A number of time simulations, using the data of Davenport's experiment, were performed using the non-linear cable code. A linear modal damping was included in the code to simulate the linear damping of the cable. A damping coefficient of 4%, as suggested by Davenport, was used. This agrees approximately with the range of damping coefficients suggested by Ramberg and Griffin [Ramberg 77]. The selected damping coefficient should only be considered as a best estimate given the complicated configuration of the cable with the attached cylindrical weights. The time simulations were continued until a steady state was reached (10-20 periods).

The results are plotted on the graphs provided by Davenport. The frequency has been non-dimensionalised with respect to the first natural frequency of the equivalent string and the transfer function has been non-dimensionalised with respect to the horizontal dynamic stiffness coefficient of the equivalent string.

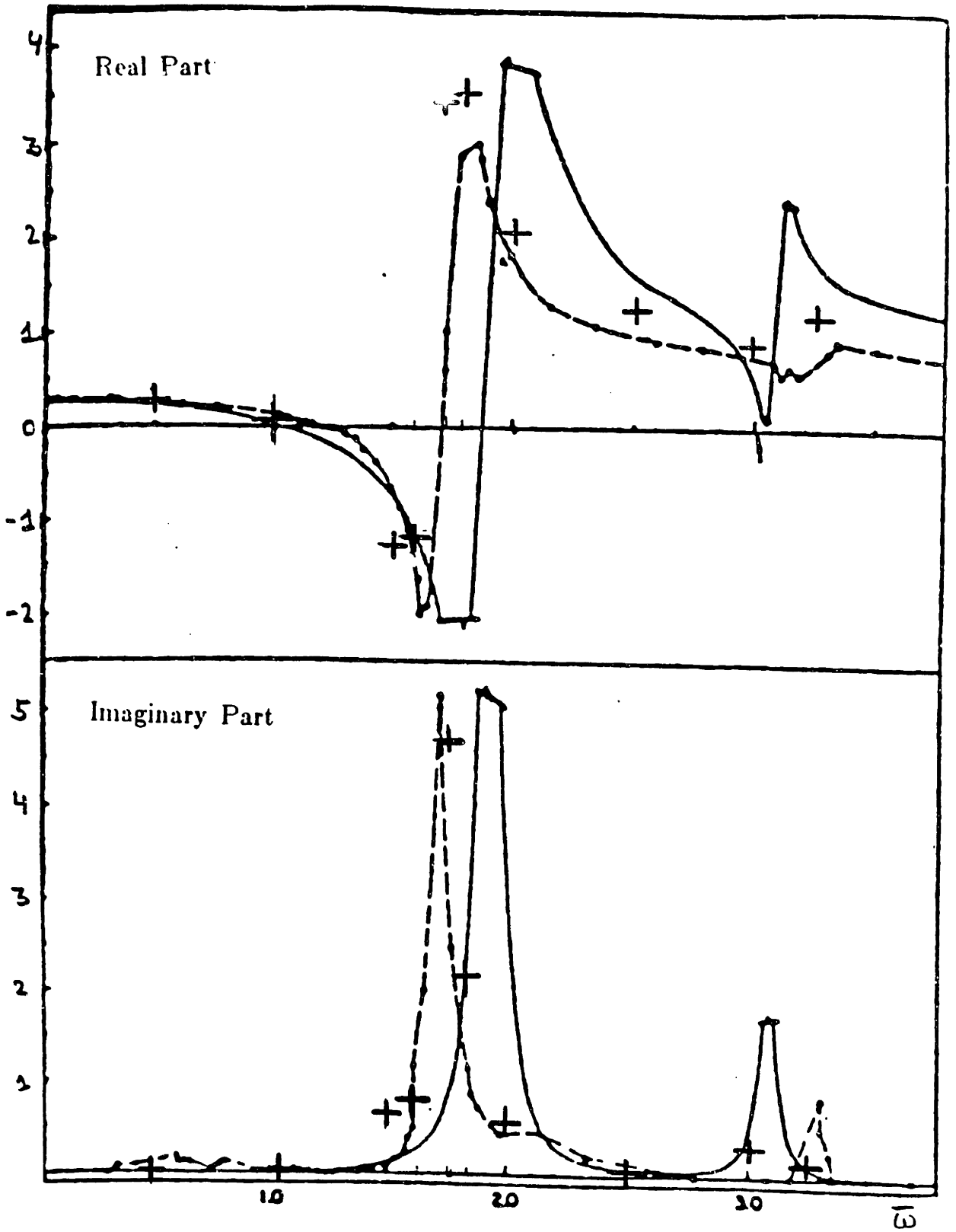

Figure 7-37: Impedance Function in the Horizontal Direction [Davenport 65]

——: Davenport's Theoretical Calculation
- - -: Experimental Data
+ : Time simulation Data

$$\bar{S}_{xx} = S_{xx}/k \quad \text{with } k = EA/L \cos^2\phi_a$$

$$\bar{\omega} = \omega/\omega_o \quad \text{with } \omega_o = \pi (H_*/M)^{1/2}/L$$

Using the linear cable theory the eigenfrequencies were calculated as (see chapter 3):

$\bar{\omega}_1 = 1.73$ symmetric

$\bar{\omega}_2 = 2.04$ anti-symmetric

$\bar{\omega}_3 = 3.06$ symmetric

$\bar{\omega}_4 = 4.02$ anti-symmetric

The transfer function obtained by the time simulations can be found in figure 7-37. The solid line represents Davenport's theoretical calculations. The dotted line shows the experimental results and the line annotated by plus(+) symbols shows the results obtained from the simulations. The simulation results agree fairly well with the experimental data considering the rough estimation of the damping coefficient. The location of the eigenfrequencies is predicted accurately using the linear cable theory outlined in this thesis. The symmetric modes are the only ones which contribute significantly to the transfer function, as expected. The time simulations predicted a steady state sinusoidal response, which was actually observed experimentally by Davenport.

7.5 A Comparison between the Non-linear Cable Model and Non-linear String Model

The results of the previous section were all within the linear regime. To test the code in the non-linear regime, the string example discussed in section

7.1 was simulated using the non-linear cable model. The data used can be found in section 7.1. The results can be found in figures 7-38 and 7-39, where it can be seen that the strings results are recovered. The major difference between the string and the cable analysis lies in the fact that in the string analysis the assumption is made, a priori, that the dynamic tension is constant over the length. If such an assumption is not made, the elastic modes seem to play an essential role in the redistribution of the dynamic tension over the cable, and they must be included to obtain a dynamic tension which is almost constant throughout the cable. This means that in the non-linear geometric regime elastic vibration modes must be included to get accurate results. The prediction of the motion in the middle, though, can be predicted accurately even when the elastic modes are left out of the response calculations.

To show the influence of sag on the geometric non-linearity, a cable weight term was added to the equations used in the previous example, which causes the cable to sag. This of course causes an asymmetric behavior of the cable: The dynamic tension when the cable is below its equilibrium position is larger for a cable than for a string, while the opposite is true when the cable moves above its equilibrium position. This can be seen in figures 7-40 and 7-41. The total cable weight to length ratio is still very small in this case ($WL/H_* = 0.021$). For a larger sag, the peak in the upward direction of the non-linear tension will disappear completely. Also, the linear component of the tension plays a significant role when the amplitude of the motion is small.

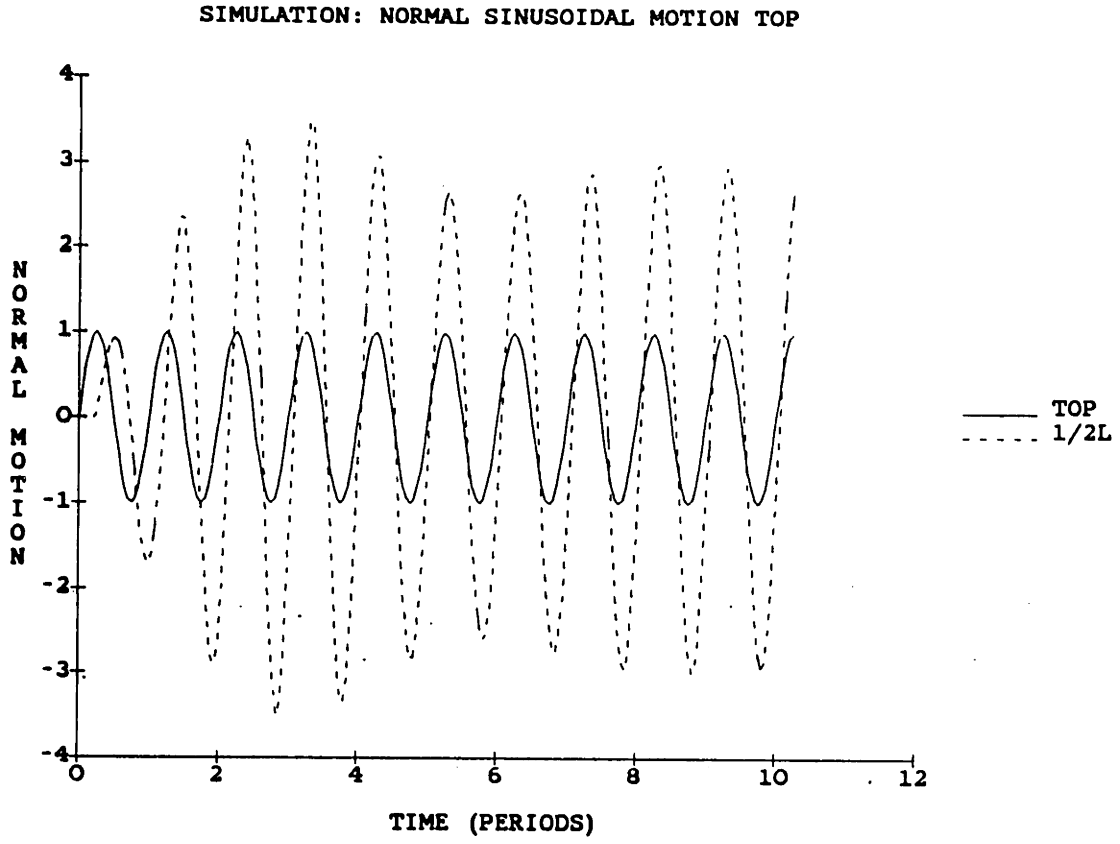

Figure 7-38: Non-linear String; Motion at midlength(cable model)

Comparison with unit motion at the top
$\tau = 0.01$
damping = 0.05
$\Delta T = 1/100\ T_{per}$
8 modes

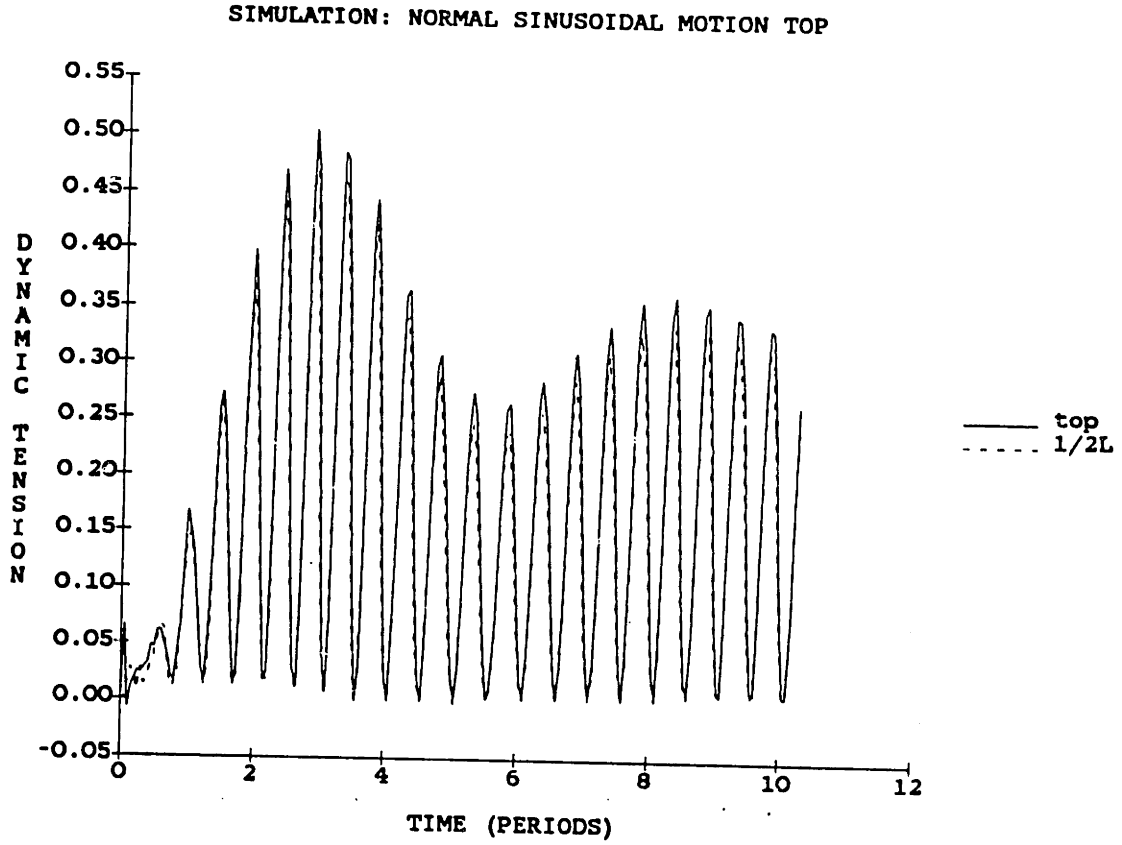

Figure 7-39: Non-linear String; Dynamic Tension (cable model)

(Dynamic Tension is given as fraction of the Static Tension)
$\tau = 0.01$
damping = 0.05
$\Delta T = 1/100\ T_{per}$
8 transverse modes, 3 elastic modes

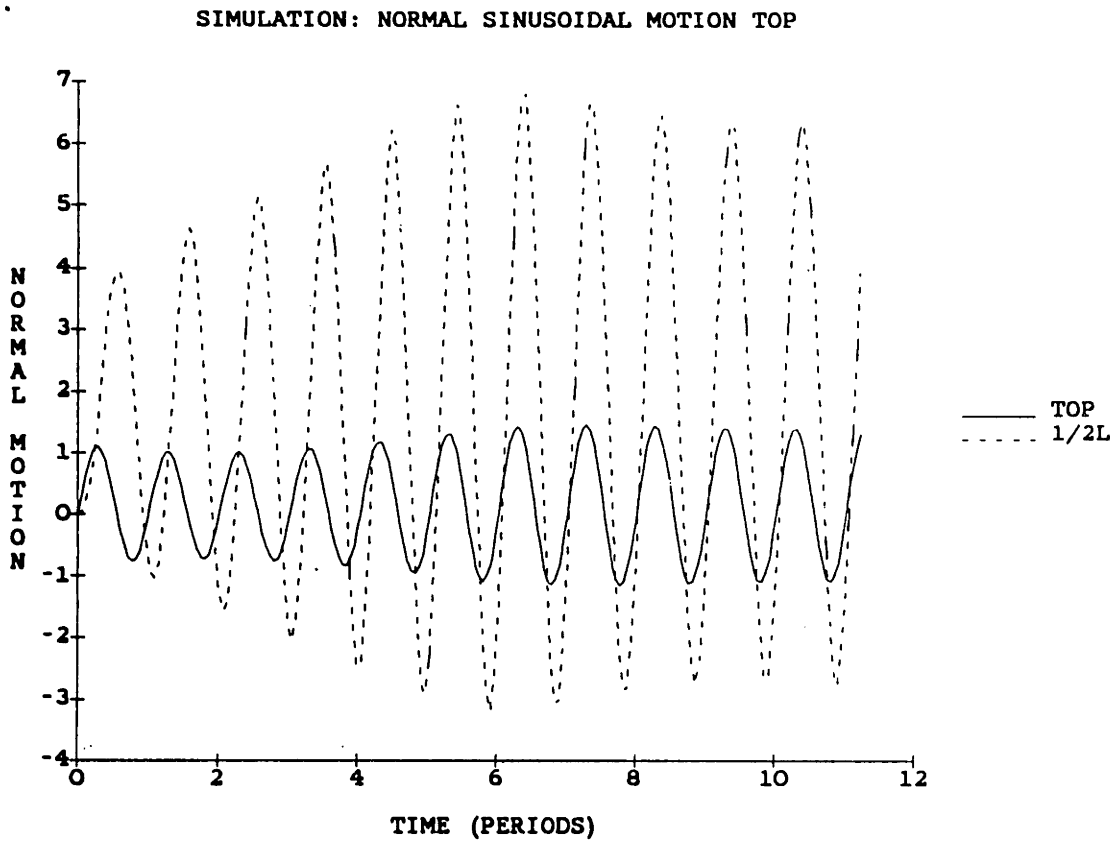

Figure 7-40: Non-linear Cable; Motion at midlength

Comparison with unit motion at the top
$\tau = 0.01$
damping = 0.05
$\Delta T = 1/100\ T_{per}$
8 modes

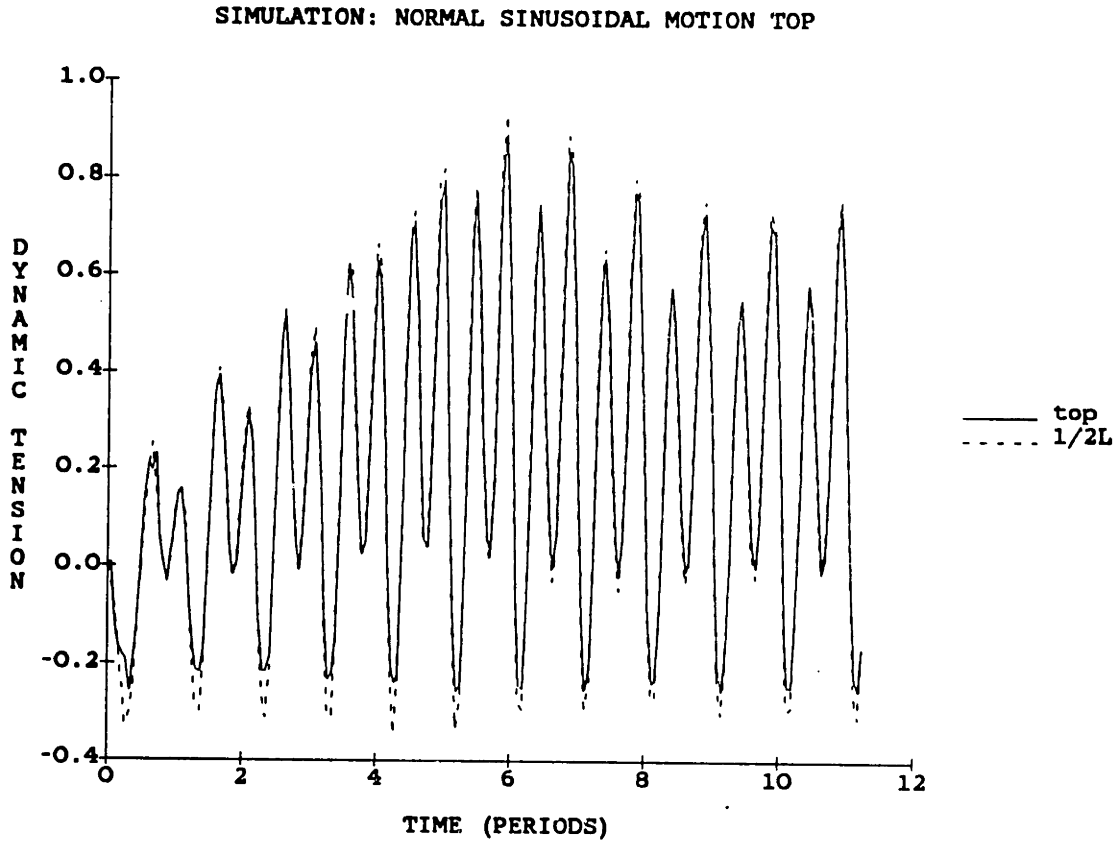

Figure 7-41: Non-linear Cable; Dynamic Tension

(Dynamic Tension is given as fraction of the Static Tension)
$\tau = 0.01$
damping $= 0.05$
$\Delta T = 1/100\ T_{per}$
8 transverse modes,3 elastic modes

7.6 References

[Davenport 65] Davenport, A. G. and Steels, G. N.
Dynamic Behavior of Massive Guy Cables.
Journal of the Structural Division, ASCE 91(ST2):43-70, April, 1965.

[Oplinger 60] Oplinger, D. W.
Frequency Response of a Nonlinear Stretched String.
Journal of the Acoustic Society of America 32(12):1529-1538, December, 1960.

[Ramberg 77] Ramberg, S. E. and Griffin, O. M.
Free Vibrations of Taut and Slack Marine Cables.
Journal of the Structural Division, ASCE 103(ST11):2079-2092, November, 1977.

Chapter 8

CONCLUSIONS AND RECOMMENDATIONS

The equations of motion and the compatibility relations derived in chapter 1 can readily be used to study the non-linear three-dimensional cable dynamics. The use of vector notation greatly simplifies and clarifies the derivation of the governing equations in the cable natural coordinates. It is certainly recommended to use this notation in future theoretical work on non-linear dynamics. Two different forms of the compatibility relations were derived, which are completely equivalent.

Explicit governing equations are obtained when the Euler angles are introduced. The two dimensional equations of motion can be considered as a special case of the previous results. The governing equations are, under weak restrictions, hyperbolic. The method of characteristics seems to have been abandoned, for the moment, for solving dynamic mooring problems. The author thinks that a renewed research attention in this domain is, considering the increase in computational speeds, certainly justifiable, especially when studying snap loads. In chapter 1 the author has put great emphasis on a rigorous derivation of the governing equations, without making any simplifying assumptions. A rigorous treatment is certainly required in the derivation of the governing equations (in whatever coordinate system desired) to avoid differences (which in most cases are fortunately very small) in the final form of the governing equations, obtained by different researchers.

The governing equations for the static shape as derived in chapter 2, can be directly implemented into efficient algorithms to calculate three-dimensional

static cable configurations.

The linearised, three-dimensional dynamic governing equations are the basis for the perturbation solutions. New perturbation solutions are formulated for inextensible and extensible cable dynamics. The orthogonality properties of the modes are also derived. The perturbation solutions contribute significantly to a better understanding of the parameters governing the linear cable dynamics. The simplicity of the solutions allows the prediction in the early design stage of the eigenfrequencies and eigenmodes of a cable system. Some application examples are given in chapter 4, but it is certain that further parametric studies, using the obtained solutions, on the variation of eigenfrequencies and the dynamic tension will produce more valuable information, directly usable in the design of mooring systems. The author believes that one unexplored area of theoretical research in linear dynamics is the investigation of possible interaction between high order transverse modes and the first elastic modes of the cables. The possibility of phenomena such as cross over and hybrid modes certainly exists in regions where the "elastic" modes are close to the "transverse" modes.

The use of modal expansions in studying non-linear cable dynamics is first demonstrated using taut strings. The use of modal expansions in cable problems, as discussed in chapter 6, leads to a new method for time simulations of dynamic mooring problems. The method makes use of the properties of the modes to obtain a compact numerical scheme. The scheme can be used as an alternative to the more classical finite difference or finite element schemes. As demonstrated in chapter 7, relatively accurate results can be obtained using only a few modes, which is a significant numerical advantage. A code implementing this scheme is presently under development

in the Design Laboratory of the department of Ocean Engineering. The use of alternative spectral methods in cable dynamic problems merits certainly further research.

Further work in comparing the non-linear scheme with other numerical and experimental data is certainly required. Unfortunately experimental data are very scarce. The author believes that further experiments in a controlled environment will be necessary. In the first phase these experiments should concentrate on the response caused by excitation at the top, in still water (Similar to Davenport's experiment described in chapter 7). This will allow a direct verification of the linear theory and an estimation of the importance of the non-linearities involved. The damping mechanisms should be studied very carefully in these experiments. One of the fundamental problems remaining, which has been studied inadequately until now, is the question of possible linearisation of the dampings mechanisms. In the author's view, these new experiments together with the increased understanding of the dynamic behavior of cables, could provide guidelines for the linearisation of the damping forces.

Appendix A

PROOF OF THE COMPATIBILITY RELATIONS IN TERMS OF VELOCITIES

Let $\vec{v}(t,p)$ denote the velocity of a material point of the cable. Then compatibility provides the following relation:

$$\frac{D\vec{v}}{Ds} = \frac{\partial e}{\partial t}\vec{t} + (1 + e)(\vec{\omega}\times\vec{t}) \tag{A.1}$$

We can prove this as follows: let $\vec{r}(p,t)$ denote the vector from the origin of a Cartesian system to a material point. Then, according to the definition of the tangential vector (see also [Hildebrand 48]):

$$\vec{t}\,(t,p) = \frac{D\vec{r}\,(t,p)}{Dp} \tag{A.2}$$

At time $t + \delta t$ the segment has stretched by a certain amount:

$$\delta p(s,\ t+\delta t) \simeq \delta s \left[\ 1 + e + \frac{\partial e}{\partial t}\,\delta t\ \right]$$

$$\simeq \frac{\delta p(s,t)}{1+e}\left[\ 1 + e + \frac{\partial e}{\partial t}\,\delta t\ \right]$$

$$\simeq \delta p(s,t)\left[\ 1 + \frac{\delta t}{1+e}\,\frac{\partial e}{\partial t}\ \right] \tag{A.3}$$

where relation (A.3) is exact in the limit as $\delta t \to 0$. Note also that it is convenient to revert to the Langrangian coordinate s, which is time invariant. At time $t+\delta t$ therefore, the tangential vector is:

$$\vec{t}\ (t+\delta t,s) = \frac{D\vec{r}(t+\delta t,s)}{Dp(t+\delta t,s)} \tag{A.4}$$

while:

$$\vec{r}(t+\delta t,s) \simeq \vec{r}(t,s) + \frac{\partial \vec{r}}{\partial t}(t,s) \cdot \delta t = \vec{r}(t,s) + \vec{v}(t,s) \cdot \delta t \tag{A.5}$$

a relation which is, again, exact as $\delta t \to 0$. So finally

$$\vec{t}\ (t+\delta t,\ s) \simeq \frac{1}{1 + \frac{\delta t}{1+e}\frac{\partial e}{\partial t}} \cdot \frac{D}{Dp}\left[\ \vec{r} + \vec{v} \cdot \delta t\ \right] \tag{A.6}$$

or:

$$\frac{D\vec{t}}{Dt} = \lim_{\delta t \to 0} \frac{1}{\delta t}\left[\ \vec{t}\,(t+\delta t,s) - \vec{t}\,(t,s)\ \right] = \frac{D\vec{v}}{Dp} - \frac{\partial e}{\partial t}\frac{\vec{t}}{1+e} \tag{A.7}$$

but from (1.8) we obtain that:

$$\frac{D\vec{t}}{Dt} = \vec{\omega} \times \vec{t} \tag{A.8}$$

therefore:

$$\frac{D\vec{v}}{Dp} = \frac{\vec{t}}{1+e} \cdot \frac{\partial e}{\partial t} + \vec{\omega} \times \vec{t} \tag{A.9}$$

When this is rewritten in the unstretched Lagrangian coordinate, (A.1) is obtained.

Appendix B

HIGHER ORDER WKB APPROXIMATION OF THE STRING EQUATION

The string equation with varying coeficients can be written as:

$$\frac{d}{ds}\left[T(\sigma) \frac{dq}{d\sigma} \right] + \omega^2 L^2 M(\sigma)\, q = 0 \qquad (B.1)$$

with: $M(\sigma)$ and $T(\sigma)$ slowly varying.

and/or: $\dfrac{\omega^2 M L^2}{T}$ large.

(σ is the non-dimensional length)

The WKB approximation is of the following form:

$$q = \frac{1}{(M \cdot T)^{1/4}} e^{\pm i\omega L(g_o + g_2/\omega^2)} \qquad (B.2)$$

where: $g_o = \int_0^\sigma (M/T)^{1/2}\, d\sigma$

$$g_2 = \int_0^\sigma \left[-\frac{1}{8} \frac{\ddot{T}}{(T \cdot M)^{1/2}} + \frac{1}{32} \frac{\dot{T}^2}{(M)^{1/2} \cdot T^{3/2}} \right.$$

$$- \frac{1}{16} \frac{\dot{M} \cdot \dot{T}}{M^{3/2} \cdot (T)^{1/2}}$$

$$\left. + \frac{5}{32} \frac{\dot{M}^2 \cdot (T)^{1/2}}{M^{5/2}} - \frac{1}{8} \frac{\ddot{M} \cdot (T)^{1/2}}{M^{3/2}} \right] d\sigma$$

Appendix C

ORTHOGONALITY OF THE MODES OF INEXTENSIBLE CABLES

The self-adjoint differential equation was obtained in subsection 3.6.4 as:

$$\left[\cos\phi_o \, \xi^{II} \right]^{II} + \left[2\cos\phi_o + \frac{\lambda^2}{\cos^2\phi_o} \, \xi^{I} \right]^{I} - \frac{h\lambda^2}{\cos^2\phi_o} \, \xi = 0 \qquad (C.1)$$

Assume ξ_i , ξ_j eigenmodes with eigenvalues λ_i , λ_j. We can write for mode i:

$$\left[\cos\phi_o \, \xi_i^{II} \right]^{II} + \left[2\cos\phi_o \, \xi_i^{I} \right]^{I}$$

$$= \lambda_i^2 \left\{ - \left[\frac{\xi_i^{I}}{\cos^2\phi_o} \right]^{I} + \frac{h}{\cos^2\phi_o} \, \xi_i \right\} \qquad (C.2)$$

Multiplication with ξ_j and integration over the domain gives:

$$\int_{\phi_{bot}}^{\phi_{top}} \xi_j \left\{ \left[\cos\phi_o \, \xi_i^{II} \right]^{II} + \left[2\cos\phi_o \, \xi_i^{I} \right]^{I} \right\} d\phi_o$$

$$= \lambda_i^2 \int_{\phi_{bot}}^{\phi_{top}} \left\{ - \xi_j \left[\frac{\xi_i^{I}}{\cos^2\phi_o} \right]^{I} + \frac{h\xi_i\xi_j}{\cos^2\phi_o} \right\} d\phi_o \qquad (C.3)$$

Using partial integration, this can be written as:

$$\int_{\phi_{bot}}^{\phi_{top}} \left[\cos\phi_o \, \xi_j^{II} \, \xi_i^{II} - 2\cos\phi_o \, \xi_j^{I} \, \xi_i^{I} \right] d\phi_o$$

$$= \lambda_i^2 \int_{\phi_{bot}}^{\phi_{top}} \left[\frac{\xi_j^{I} \, \xi_i^{I}}{\cos^2\phi_o} + h \, \frac{\xi_j \, \xi_i}{\cos^2\phi_o} \right] d\phi_o \qquad (C.4)$$

The same operation can be performed by multiplying ξ_i with the equation

for the mode ξ_j and integrating:

$$\int_{\phi_{bot}}^{\phi_{top}} \left[\cos\phi_o \; \xi_i^{II} \; \xi_j^{II} - 2\cos\phi_o \; \xi_i^{I} \; \xi_j^{I} \right] d\phi_o$$

$$= \lambda_j^2 \int_{\phi_{bot}}^{\phi_{top}} \left[\frac{\xi_i^I \; \xi_j^I}{\cos^2\phi_o} + h \; \frac{\xi_i \; \xi_j}{\cos^2\phi_o} \right] d\phi_o \qquad (C.5)$$

Substracting (C.4) from (C.5) gives:

$$\int_{\phi_{bot}}^{\phi_{top}} \left[\frac{\xi_i^I \; \xi_j^I}{\cos^2\phi_o} + h \; \frac{\xi_j \; \xi_i}{\cos^2\phi_o} \right] d\phi_o = 0 \qquad \text{for } i \neq j \qquad (C.6)$$

which was to be proved.

Using the relation that:

$$\xi_i^I = \eta_i \qquad\qquad \xi_j^I = \eta_j$$

and

$$\frac{d\phi_o}{d\sigma} = \alpha \cos^2\phi_o \qquad\qquad h = \frac{m}{M}$$

we obtain:

$$\int_0^1 (m \; \xi_i \; \xi_j + M \; \eta_i \; \eta_j \;) \; d\sigma = 0 \qquad \text{for } i \neq j \qquad (C.7)$$

Appendix D

ORTHOGONALITY OF THE MODES OF EXTENSIBLE CABLES

Using influence functions, the requirement for the modes of an extensible cable can be written as [Rosenthal 81]:

$$[\alpha_i\ (s)] = \int_0^L [H(s,r)]\ \omega_i^2\ [m(r)]\ [\alpha_i\ (r)]\ dr \tag{D.1}$$

where in the two dimensional case, with the components written in the tangential and normal direction, we have:

$$[\alpha_i\ (s)]^T = [p_i\ (s) \quad q_i\ (s)] \tag{D.2}$$

$$[H(s,r)] = \begin{bmatrix} H_{11}\ (s,r) & H_{12}\ (s,r) \\ H_{21}\ (s,r) & H_{22}\ (s,r) \end{bmatrix} \tag{D.3}$$

$$[m(r)] = \begin{bmatrix} m(r) & 0 \\ 0 & M(r) \end{bmatrix} \tag{D.4}$$

therefore: $[m(r)]^T = [m(r)]$

$$[H(s,r)]^T = [H(r,s)] \tag{D.5}$$

Multiplying (D.1) with the transpose of a the modal matrix of a different mode and the mass matrix, and integrating, we obtain:

$$\int_0^L [\alpha_j(s)]^T\ [m(s)]\ [\alpha_i(s)]\ ds$$

$$= \omega_i^2 \int_0^L [\alpha_j(s)]^T\ [m(s)]\ ds \int_0^L [H(s,r)]\ [m(r)]\ [\alpha_i(r)]\ dr \qquad (D.6)$$

Due to (D.5) this is equivalent to:

$$\int_0^L [\alpha_j(s)]^T\ [m(s)]\ [\alpha_i(s)]\ ds$$

$$= \omega_i^2 \int_0^L [\alpha_i(r)]^T\ [m(r)]\ dr \int_0^L [H(r,s)]\ [m(s)]\ [\alpha_j(s)]\ ds \qquad (D.7)$$

We can apply (D.6) also to the jth mode. Subtracting the result from (D.7) when ω_i is different from ω_j, then:

$$\int_0^L [\alpha_j(s)]^T\ [m(s)]\ [\alpha_i(s)]\ ds = 0 \qquad i \neq j$$

or, explicity in non-dimensional form:

$$\int_0^1 (m\ \xi_i\ \xi_j + M\ \eta_i\ \eta_j\ )\ d\sigma = 0 \qquad i \neq j \qquad (D.8)$$

Appendix E

BIBLIOGRAPHY

A bibliography of books and articles in the area of single span cable statics and dynamics, collected during the preparation of this thesis, is included in this appendix (The last update was in February 1984).

[Acaster 72] Acaster S.M.
Anchor Lines in the North Sea.
Offshore Technology Conference (OTC 1535), 1972.

[Afshari 73] Afshari, H. and Soler, A.I.
Cable Network using Galerkin's Method and Polynomial Approximation Functions.
Journal of Applied Mechanics, Series E 40(2):622-624, June, 1973.

[Afshari 74] Afshari, H. and Soler, A.I.
Vibration of cable Gridworks with Small Initial Deformation.
Journal of Applied Mechanics, Series E 41(1):131-136, March, 1974.

[Allen 49] Allen, H.J.
Estimation of Forces.
Technical Report RM A9126, NACA, November, 1949.

[Allen 51] Allen, H. J. and Perkins, E. W.
A Study of the Effects of Viscosity on Flow over Slender Bodies of Revolution.
Technical Report 1048, NACA, 1951.

[Anand 66] Anand, G.V.
Non-Linear Resonance in Stretched Strings with Viscous Damping.
Journal Acoustical Society of America 40(6):1517-1528, 1966.

[Anderson 78] Anderson, J.
Tension Leg Platforms.
In *North Sea Development*, pages 145-158. Heyden Publishers, Glasgow, 1978.

[Angrilli 77] Angrilli, F. and Bergamaschi, S.
On the Small Two Dimensional Oscillations of a Sea Line.
Meccanica 12(3):144-150, 1977.

[Barmina 73] Barmina, L.A.
Force Acting on a Deformable Contour in an Arbitrary Fluid Stream.
Izv. AN SSSR, Mekhanika Zhidkosti i Gaza (1):4-8, January, 1973.
In Russian, translation in *Fluid Dynamics* 1975.

[Barr 74] Barr, R.A.
The Non-Linear Dynamics of Cable Systems.
Technical Report UM-1MR 74-1, Sea Grant, University of California, 1974.

[Bleich 50] Bleich, F.
The Mathematical Theory of Vibration in Suspension Bridges.
Bureau of Public Roads, U.S. Department of Commerce, U.S. Government Printing Office, Washington, D.C., 1950.

[Blevins 77] Blevins, R. D.
Flow Induced Vibration.
Van Nostrand, Reinhold, New York, 1977.

[Blevins 79] Blevins, R. D.
Formulas for Natural Frequency and Mode Shape.
Van Nostrand Reinhold Co., New York, 1979.

[Bliek 82] Bliek, A.
Motion Analysis of an Ocean Mining Pipe.
Master's thesis, MIT, 1982.

[Bliek 84] Bliek, A. and Triantafyllou, M.S.
Determination of the Eigenfrequencies of Single Span Cables.
Technical Report, Design Lab. Department of Ocean Engineering MIT, 1984.
To appear.

[Bondarenko 73] Bondarenko, L. A. and Y. L. Yakimov.
The Force Produced by a Liquid Current on a Thin Curved Body of Circular Cross Section.
Izv. ANN SSSR, Mekhanika Zhidkosti i Gaza (1):9-12, January/February, 1973.
In Russian, translation Plenum Publishing Company 1975.

[Breslin 74] Breslin, J. P.
Dynamic Forces Exerted by Oscillating Cables.
Journal of Hydronautics 8(1):18-31, January, 1974.

[Calkins 79] Calkins, D. E.
Hydrodynamic Analysis of a High Speed Marine Towed System.
Journal of Hydronautics 13(1):10-19, January, 1979.

[Cannon 72a] Cannon, T. C. and Genin, J.
Three Dimensional Dynamical Behaviour of a Flexible Towed Cable.
Aeronautical Quarterly 25:201-210, August, 1972.

[Cannon 72b] Cannon, T. C.
Dynamical Behaviour of a Materially Damped Flexible Towed Cable.
Aeronautical Quarterly 23:109-120, May, 1972.

[Capanogly 78] Capanogly, C. C.
Tension-Leg Platform Design: Interaction of Naval Architecture and Structural Design Considerations.
Marine Technology 16(4):343-352, October, 1978.

[Carrier 45] Carrier, G. F.
On the Non-Linear Vibration Problem of the Elastic String.
Quarterly Journal of Applied Mathematics 3(2):157-165, 1945.

[Carrier 49] Carrier, G. F.
A Note on the Vibrating String.
Quarterly Journal of Applied Mathematics 7(1):97-101, 1949.

[Casarella 70] Casarella, M. J. and Parsons, M.
A Survey of Investigations and Motions of Cable Systems under Hydrodynamic Loading.
Marine Technology Society Journal 4(4), July-August, 1970.

[Chakrabarti 82] Chakrabarti, S. and Frampton, R. E.
Review of Riser Analysis Techniques.
Applied Ocean Research (4), 1982.

[Chang 73] Chang, P. Y. and Pilkey, W. D.
Static and Dynamic Analysis of Mooring Lines.
Journal of Hydronautics 7(1):29-34, January, 1973.

[Charnews 71] Charnews, D.P.
Drag Coefficients of Vibrating Synthetic Ropes.
Master's thesis, Massachussetts Institute of Technology, 1971.

[Chen 76] Chen, S. S., Wambsgauss, M. W. and Gendrnejcryk, J. A.
Added Mass and Damping of a Vibrating Rod in a Viscous Fluid.
Journal of Applied Mechanics, ASME :325-329, June, 1976.

[Chhabra 79] Chhabra, N.K.
Dynamics of a Tethered Spar Buoy System - Validation using full-scale Ocean Data.
In *Civil Engineering in the Oceans*, pages 209-223. ASCE, 1979.

[Choo 71] Choo, Y. I. and Casarella, M. J.
Hydrodynamic Resistance of Towed Cables.
Journal of Hydronautics 5(4), October, 1971.

[Choo 72] Choo, Y. I. and Casarella, M. J.
Configuration of a Tow Line Attached to a Vehicle in a Circular Path.
Journal of Hydronautics 6(1):51-57, January, 1972.

[Choo 73] Choo, Y. I. and Casarella, M. J.
A Survey of Analytical Methods for Dynamic Simulation of Cable-Body Systems.
Journal of Hydronautics 7(4):137-144, October, 1973.

[Chu 83] Chu, T.C.
A Method to Characterize the Mechanical Properties of Undersea Cables.
The Bell System Technical Journal 62(3):703-715, March, 1983.

[Collier 72] Collier, M. L.
Dynamic Similarity Scaling Laws Applied to Cables.
Journal of Hydronautics 6(2):111-114, July, 1972.

[Costello 76] Costello, G. A. and Phillips, J. W.
Effective Modulus of Twisted Wire Cables.
Journal of the Engineering Mechanics Division ASCE 102(EM1):171-181, February, 1976.

[Costello 77a] Costello, G. A. and Sinha, S. K.
Static Behaviour of Wire Rope.
Journal of the Engineering Mechanics Division ASCE 103(EM6):1011-1022, December, 1977.

[Costello 77b] Costello, G. A. and Sinha, S. K.
Torsional Stiffness of Twisted Wire Cables.
Journal of the Engineering Mechanics Division ASCE 103(EM4):766-770, August, 1977.

[Costello 79] Costello, G. A. and Miller, R. E.
Lay Effect of Wire Rope.
Journal of the Engineering Mechanics Division ASCE 105(EM4):599-608, August, 1979.

[Crandall 56] Crandall, S.H.
Engineering Analysis.
McGraw-Hill, New York, 1956.

[Critescu 64] Critescu, N.
Rapid Motions of Extensible Strings.
J. Mech. Phys. Solids 12:268-278, 1964.

[Critescu 67] Critescu, N.
Dynamic Plasticity.
North Holland Publishing Company, Amsterdam, Holland, 1967, chapter Extensible Strings.

[Dahlquist 74] Dahlquist, G. and Bjork, A.
Numerical Methods.
Prentice Hall, Englewood Cliffs N.J., 1974.

[Dareing 79] Dareing, D.W. and Huang T.
Marine Riser Vibration Response determined by Modal Analysis.
Journal of Energy Resources Technology, ASME 101:159-166, September, 1979.

[Davenport 59] Davenport, A. G.
The Wind Induced Vibration of Guyed and Self-Supporting Cylindrical Columns.
Transactions Engineering Institute of Canada 3:119-141, 1959.

[Davenport 65] Davenport, A. G. and Steels, G. N.
Dynamic Behavior of Massive Guy Cables.
Journal of the Structural Division, ASCE 91(ST2):43-70, April, 1965.

[Dean 61] Dean, D. L.
Static and Dynamic Analysis of Guy Cables.
Journal of the Structural Division, ASCE 87(ST1):1-21, January, 1961.

[Delmer 83] Delmer, Th. N. and Stephens, Th.
Numerical Simulation of Towed Cables.
Ocean Engineering 10(2):119-132, 1983.

[Deruntz 69] Deruntz, J. A.
End Effect Bending Stresses in Cables.
Journal of Applied Mechanics, ASME :750-756, December, 1969.

[Dickey 80] Dickey,W.
Stability of Periodic Solutions of the Non-Linear String.
Quarterly of Applied Mathematics :253-259, July, 1980.

[Dillon 73] Dillon, D. B.
An Inventory of Current Models of Scientific Data-Gathering Moors.
Technical Report 45500001, HCI, 1973.

[Dillon 82] Dillon, D. B.
Validation of Computer Models of Cable System Dynamics.
Technical Report CR82.015, Naval Civil Engineering Laboratory, 1982.

[Dominguez 72] Dominguez, R. F. and Smith, C. E.
Dynamic Analysis of Cable Systems.
Journal of the Structural Division, ASCE 98(ST8):1817-1834, August, 1972.

[Dubey 78] Dubey, R. N.
Vibration of Overhead Transmission Lines.
Shock Vibration Digest 10(4):3-6, 1978.

[Every 82] Every, M. J., King, P. and Weaver, D. S.
Vortex-Excited Vibrations of Cylinders and Cables and their Suppression.
Ocean Engineering 9(2):135-157, 1982.

[Felippa 74] Felippa, C. A.
F. E. Analysis of 3D Cable Structures.
In *International Conference on Computer Methods in Non-Linear Mechanics*, pages 311-325. University of Texas, 1974.

[Firebaugh 72] Firebaugh, M. S.
An Analysis of the Dynamics of Towing Cables.
PhD thesis, M.I.T., Department of Ocean Engineering, 1972.

[Fried 79a] Fried, I.
Numerical Solutions of Differential Equations.
Academic Press, New York, 1979, chapter Wave Propagation.

[Fried 79b] Fried, I.
Accuracy of String Element Mass Matrix.
Comput. Methods Appl. Mech. Eng. 20(3):317-321, 1979.

[Fried 82] Fried, I.
Large Deformation Static and Dynamic Finite Element Analysis of Extensible Cables.
Computers and Structures 15(3):315-319, 1982.

[Frohrib 67] Frohrib, D. A. and Plunkett, R.
The Free Vibrations of Stiffened Drill Strings with Static Curvature.
Journal of Engineering for Industry, ASME :23-30, February, 1967.

[Frosali 79] Frosali, G. P.
On the Stability of the Dirichlet Problem for the Vibrating String Equation.
Ann. SC. Norm. Super. Pisa, C1. Sci. 6(4):719-728, 1979.

[Frost 65] Frost, M. A. III and Wilhoit, J. C. Jr.
Analysis of the Motion of Deep Water Drill Strings - Part 2: Forced Rolling Motion.
Journal of Engineering for Industry, ASME :145-149, May, 1965.

[Gale 83] Gale, J. G. and Smith, C. E.
Vibrations of Suspended Cables.
Journal of Applied Mechanics 50:687-689, September, 1983.

[Gambhir 77] Gambhir, M. L. and de Batchelor, B.
A Finite Element for 3D Prestressed Cable Nets.
International Journal for Numerical Methods in Engineering 2:1699-1718, 1977.

[Gambhir 78] Gambhir, M.L. and de Batchelor, B.
Parametric Study of Free Vibrations of Sagged Cables.
Computers and Structures 8:641-648, 1978.

[Goeller 70] Goeller, J. E.
Analytic and Experimental Study of the Dynamic Response of Cable Systems.
Technical Report 70-3, Catholic University of America, Washington, D.C., April, 1970.

[Goodey 61] Goodey, W. J.
On the Natural Modes and Frequencies of a Suspended Chain.
Quarterly Journal of Mechanics and Applied Mathematics 14(1):118-127, 1961.

[Goodman 76] Goodman, T. R. and Breslin, J. P.
Statics and Dynamics of Anchoring Cables in Waves.
Journal of Hydronautics 10(4):113-120, October, 1976.

[Goodman 79] Goodman, Th. R. and Valentine, D. T.
Effect of Hydrostatic Pressure of Underwater Towed Body Configurations.
Journal of Hydronautics, Engineering Notes 13, October, 1979.

[Gorban 78] Gorban, V. A. et al.
Forced Oscillations of a Cable in a Flow.
Gidromechanikha (38):113-118, 1978.
In Russian.

[Gotlieb 77] Gotlieb, D. and Orzag A.
Regional Conference Series in Applied Mathematics: Numerical Analysis of Spectral Methods, Theory and Applications.
Society for Industrial and Applied Mathematics, Philadelphia, 1977.

[Graham 65] Graham, R. D., Frost, M. A. III and Wilhoit, J. A. Jr.
Analysis of the Motion of Deep-Water Drill Strings - Part 1: Forced Lateral Motion.
Journal of Engineering for Industry, ASME :137-144, May, 1965.

[Griffin 73] Griffin, O. M., Skop, R. A. and Koopman, G. H.
The Vortex Excited Resonant Vibrations of Circular Cylinders.
Journal of Sound and Vibration 31(2):235-249, November, 1973.

[Griffin 80] Griffin, O. M., Pattison, J. H., Skop, R. A., Ramberg, S. E. and Meggitt, D. J.
Vortex Excited Vibrations of Marine Cables.
Journal of Waterways, Port, Coastal and Ocean Division, ASCE 106(WW2):183-204, May, 1980.

[Griffiths 73] Griffiths, J. A., Alzheimer, J. M. and Bampton, M. C. C.
Large Displacement Analysis of Cable Structures.
In Bathe (editor), *Nonlinear FEM Analysis and ADINA* . M.I.T., August, 1973.

[Hagedorn 80] Hagedorn, P. and Shafer, B. .
On Non-Linear Free Vibrations of an Elastic Cable.
International Journal Non-Linear Mechanics 15:333-340, 1980.

[Harichandran 82]
Harichandran, R. S. and Irvine, H. M.
A Static Analysis Technique for Multi-Leg Cable-Buoy Systems.
Technical Report SG 82-13, M.I.T., July, 1982.

[Henghold 76] Henghold, W. M. and Russell, J. J.
Equilibrium and Natural Frequencies of Cable Structures (a non-linear finite element approach).
Computers and Structures 6:267-271, 1976.

[Henghold 77] Henghold, W. M., Russell, J. J. and Morgan, J. D.
Free Vibrations of Cable in 3D.
Journal of the Structural Division, ASCE 103(ST5):1127-1136, May, 1977.

[Hildebrand 49] Hildebrand, F.B.
Advanced Calculus for Applications.
Prentice Hall, Englewood Cliffs N.J., 1949.

[Hogben 77] Hogben, N. N., Miller, B. L., Searle, W. J. and Ward, G.
Estimation of Fluid Loading on Offshore Structures.
Proc. Instn. Civ Engrs. 63:515-562, September, 1977.

[Hsu 75] Hsu, C. S.
The Response of a Parametrically Excited String in Fluid.
Journal of Sound and Vibration 39(3):305-316, 1975.

[Hsu 77] Hsu, C.S.
On Non-linear Parametric Excitation Problems.
In Yih, C.S. (editor), *Advances in Applied Mechanics*, pages 245-301. Academic Press, New York, 1977.

[Huddleston 81] Huddleston, J. V.
Computer Analysis of Extensible Cables.
Journal of Engineering Mechanics Division, ASCE :27-37, February, 1981.

[Huffman 71] Huffman, R. R. and Genin, J.
The Dynamical Behaviour of a Flexible Cable in a Uniform Flow Field.
Aeronautical Quarterly 22:183-185, May, 1971.

[Imlay 61] Imlay, F. H.
The Complete Expressions for 'Added Mass' of a Rigid Body Moving in an Ideal Fluid.
Technical Report 1528, DTMB, July, 1961.

[Irvine 74] Irvine, H. M. and Caughey, T. K.
The Linear Theory of Free Vibrations of a Suspended Cable.
Proceedings of the Royal Society Series A 341:299-315, 1974.

[Irvine 75] Irvine, H. M.
Statics of Suspended Cables.
Journal of Engineering, Mechanics Division, ASCE , June, 1975.

[Irvine 76] Irvine, H. M. and Griffin, J. H.
On the Dynamic Response of a Suspended Cable.
Earthquake Engineering and Structural Dynamics 4:389-402, 1976.

[Irvine 78] Irvine, H. M.
Free Vibrations of Inclined Cables.
Journal of the Structural Division, ASCE 104(ST2):343-347, February, 1978.

[Irvine 80a] Irvine, H. M.
The Estimation of Earthquake Generated Additional Tension in Suspension Bridge Cable.
Earthquake Engineering and Structural Dynamics 8:267-273, 1980.

[Irvine 80b] Irvine, H. M.
Energy Relations for Suspended Cables.
Quarterly Journal of Mechanics and Applied Mathematics 33:227-234, 1980.

[Irvine 81] Irvine, H. M.
Cable Structures.
MIT Press, Cambridge, MA and London, England, 1981.

[Jefferys 82a] Jefferys, E. R. and Patel, M. M.
Dynamic Analysis Models of Tension Leg Platforms.
Journal of Energy Resources Technology 104, September, 1982.

[Jefferys 82b] Jefferys, E.R. and Patel, M.M.
On the Dynamics of Taut Mooring Systems.
Engineering Structures 4:37-43, January, 1982.

[Johansson 76] Johansson, P.I.
A Finite Element Model for Dynamic Analysis of Mooring Cables.
PhD thesis, MIT, 1976.

[Jones 82] Jones, H. L. and Nelson, J. K.
Optimum Design of Spread Mooring Systems.
Journal of Energy Resource Technology, ASME 104, March, 1982.

[Judd 78] Judd, B. J. and Wheen, R. J.
Non-Linear Cable Behaviour.
Journal of Structural Division, ASCE :567-575, March, 1978.

[Kasper 73] Kasper, R. G.
Cable Design Guidelines Based on a Bending, Tension and Torsion Study of an Electromechanical Cable.
Technical Report AD769212, Naval Underwater Systems Center, Distributed by National Technical Information Service, 1973.

[Kern 77] Kern, E. C., Milgram, J. H. and Lincoln W. B.
Experimental Determination of the Dynamics of a Mooring System.
Journal of Hydronautics 11(4):113-120, October, 1977.

[Kerney 71] Kerney, K. P.
Small Perturbation Analysis of Oscillatory Tow-Cable Motion.
Technical Report 3430, NSRDC, November, 1971.

[Kim 83] Kim, Y.C.
Nonlinear Vibrations of Long Slender Beams.
PhD thesis, MIT, 1983.

[Kirk 79] Kirk, C.L., Etok, E.U. and Cooper, T.M.
Dynamic and Static Analysis of Marine Riser.
Applied Ocean Research 1, 1979.

[Kolousek 47] Kolousek, V.
Solution Statique et Dynamique des Pylones d'antenne Haubanes.
International Association of Bridge and Structural Engineers 8, 1947.

[Krolikowski 80] Krolikowski, L. P. and Gay, T. A.
An Improved Linearization Technique for Frequency Domain Riser Analysis.
Offshore Technology Conference (OTC 3777), 1980.

[Lang 79] Lang, J. R. and Hedley, C. J.
BP Development of Tethered Buoyant Platform Production System.
In *North Sea Development*, pages 133-144. Heyden Publisher, Glasgow, 1979.

[Larsen 82] Larsen, C. M. and Fylling, I. J.
Dynamic Behaviour of Anchor Lines.
Norwegian Maritime Research (3), 1982.

[Laura 69] Laura, P.A., Goeller J.
Dynamic Stresses and Displacements in a Buoy Cable System Subjected to Longitudinal Excitation using a Continuum Approach.
In *Acoustical Society Meeting.* Acoustical Society, Philadephia, April, 1969.

[Lehner 73] Lehner, J. R. and Batterman, S. C.
Static and Dynamic Finite Deformations of Cables using Rate Equations.
Computer Methods in Applied Mechanics and Engineering 2:343-366, 1973.

[Lenskii 78] Lenskii, E. V.
Motion of Flexible Strings in an Ideal Liquid.
Vestnik Moskovskogo Universiteta Mekhanika 33(1):116-127, 1978.
In Russian, translation Allerton Press 1978.

[Leonard 72a] Leonard, J. W.
Curved Finite Element Approximation to Non-Linear Cables.
Offshore Technology Conference (OTC 1533):225-233, 1972.

[Leonard 72b] Leonard, J. W. and Recker, W. W.
Nonlinear Dynamics of Cables with Low Initial Tension.
Journal of the Engineering Mechanics Division, ASCE 98(EM2):293-309, April, 1972.

[Leonard 73a] Leonard, J. W.
Nonlinear Dynamics of Curved Cable Elements.
Journal of the Engineering Mechanics Division, ASCE 99(EM3):616-621, June, 1973.

[Leonard 73b] Leonard, J. W.
Incremental Response of 3-D Cable Networks.
Journal of the Engineering Mechanics Division, ASCE 99(EM3):616-618, June, 1973.

[Leonard 79] Leonard, J.W.
Newton-Raphson Iterative Method applied to Circularly Towed Cable-body Systems.
Engineering Structures 1:73-80, January, 1979.

[Leonard 81] Leonard, J. W. and Nath, J. H.
Comparison of Finite Element and Lumped Parameter Methods for Oceanic Cables.
Engineering Structures 3(3):153-167, July, 1981.

[Lighthill 60] Lighthill, M. J.
Note on the Swimming of Slender Fish.
Journal of Fluid Mechanics 9:305-317, 1960.

[Liu 73] Liu, F. C.
Snap Loads in Lifting and Mooring Cable Systems Induced by Surface Wave Conditions.
Technical Report 1288, Naval Civil Engineering Lab., September, 1973.

[Liu 75] Liu, F. C.
Rotational and Kinking Characteristics of Electromechanical Cable.
Technical Report 1403, Naval Civil Engineering Lab., November, 1975.

[Liu 80] Liu, D. and Chen, C. Y.
Integrated Computational Procedure for Hydrodynamic Loads and Structural Response of a TLP.
In *Computational Methods for Offshore Structures.* Chicago, Illinois, November, 1980.

[Liu 82] Liu, F. C.
Computer Simulation of a Tethered Vehicle Cable System.
In *Proceedings of the 1st Offshore Mechanics/Arctic Engineering Deep Sea Systems*, pages 163-173. 1982.

[Lo 82] Lo, A and Leonard, J. W.
Dynamic Analysis of Underwater Cables.
Journal of the Engineering Mechanics Division, ASCE 108(EM4):605-621, August, 1982.

[Loken 79] Loken, A. E. and Olsen, O. A.
The Influence of Slowly Varying Wave Forces on Mooring Systems.
Offshore Technology Conference (OTC 3626), 1979.

[Lubinski 50] Lubinski, A.
A Study on the Buckling of Rotary Drilling Strings.
In *Drilling and Production Practice*, pages 178-. API, 1950.

[Lubkin 43] Lubkin, S. and Stoker, J. J.
Stability of Columns and Strings under Periodically Varying Forces
Quarterly Journal of Applied Mathematics 1:215-236, 1943.

[Ma 79] Ma, D., Leonard, J. and Chu, K. H.
Slack Elasto-Plastic Dynamics of Cable Systems.
Journal of the Engineering Mechanics Division, ASCE 105(EM2):207-222, April, 1979.

[Maier 75] Maier, G. and Goutro, R.
Energy Approach to an Inelastic Cable-Structure Analysis.
Journal of the Engineering Mechanics Division, ASCE , October, 1975.

[Marczyk 79] Marczyk, S. and Niziol, J.
Longitudinal-Transversal Vibrations of Ropes of Variable Lengths.
Rozpr. Inz. 27(32):403-415, 1979.

[Meggitt 80] Meggitt, D. J., Webster, R. L. and Migliore, S. J.
Dynamic Response of Cables Subject to Ocean Forces.
Offshore Technology Conference , 1980.

[Miles 65] Miles, J. W.
Stability of Forced Oscillations of a Vibrating String.
Journal of the Acoustical Society of America 38:855-861, 1965.

[Murthy 65] Murthy, G.S.S. and Ramakrishna.
Nonlinear Character of Resonance in Stretched Strings.
Journal of the Acoustical Society of America 38:461-471, 1965.

[Narasimha 68] Narasimha, R.
Non-Linear Vibrations of an Elastic String.
Journal of Sound and Vibration 8:134-146, 1968.

[Nath 69a] Nath, J. H.
Dynamics of a Single Point Ocean-Moorings of a Buoy - A Numerical Model for Solution by Computer.
Technical Report 69-10, Oregon State University, Department of Oceanography, July, 1969.

[Nath 69b] Nath, J. H. and Felix, H. P.
Dynamics of a Single Point Mooring in Deep Water.
In *Proceedings Conference on Civil Engineering in the Oceans.* Miami Beach, Florida, December, 1969.

[Nath 71] Nath, J. H.
Dynamic Response of Taut Lines for Buoys.
Marine Technology Society Journal 5, July-August, 1971.

[Nath 79] Nath, J. H. and Leonard, J. W.
Continum, Lumped Parameter and Finite Element Methods for Flexible Tether Analysis.
Technical Report F320-4, U.S. Department of Commerce, N.O.A.A., 1979.

[Nayfeh 73] Nayfeh, A.M.
Perturbation Methods.
John Wiley & Sons, New York, 1973.

[Nayfeh 79] Nayfeh, A. M. and Hook, D. T.
Non-Linear Oscillations.
John Wiley & Sons, New York, 1979, chapter Strings.

[Nordstrom 82] Nordstrom, P.E. and Ottsen, H.
Test Cases for Seadyn Verification.
Technical Report CR82.014, Navy Civil Engineering Laboratory, April, 1982.

[Nuckolls 77] Nuckolls, C. and Dominguez, R. F.
Large Displacement Mooring Dynamics.
Offshore Technology Conference (OTC 2880):19-24, 1977.

[Olsen 79] Olsen, O. A. and Loken, A. E.
On the Effect of Non-Linearities in Mooring System Design.
In G. S. T. Azmer and F. K. Gerres (editors), *Offshore Structures; The Use of Physical Models in their Design*, . Construction Press, 1979.

[Oplinger 60] Oplinger, D. W.
Frequency Response of a Nonlinear Stretched String.
Journal of the Acoustic Society of America 32(12):1529-1538, December, 1960.

[Ozdemir 79] Ozdemir, H.
A Finite Element Approach for Cable Problems.
International Journal Solids Structures 15:427-437, 1979.

[Paidoussis 68] Paidoussis, M. P.
Stability of Towed Totally Submerged Flexible Cylinders.
Journal of Fluid Mechanics 34(2):273-297, 1968.

[Paidoussis 70] Paidoussis, M. P.
Dynamics of Submerged Towed Cylinders.
In *Eight Symposium of Naval Hydrodynamics in an Ocean Environment.* 1970.

[Palo 79] Palo, P. A.
Small-Scale Cable Dynamics Comparison.
In *Civil Engineering Conference in the Oceans*, pages 293-309. 1979.

[Paquette 65] Paquette, R. G. and Henderson, B. E.
The Dynamics of a Simple Deep Sea Buoy Moorings.
Technical Report 65-79, General Motors Defense Reserve Laboratories, November, 1965.

[Parnell 80] Parnell, L. A.
Experimental Scale Modeling of Large Undersea Cable Structures.
In *Oceans '80*, pages 541-547. 1980.

[Patel 75] Patel, J. S.
Dynamic Response of a Line Cable with Variable Length End Segment due to Time Dependent Kinematic Constraints.
Technical Report EM-83-75, Naval Underwater System Center, October, 1975.

[Paulling 79a] Paulling, J.R.
Frequency Domain Analysis of OTEC CW Pipe and Platform Dynamics.
Offshore Technology Conference (OTC 3543), 1979.

[Paulling 79b] Paulling, J. R.
An Equivalent Linear Representation of the Forces Exerted on the OTEC CW Pipe by Combined Effects of Waves and Current.
In Griffin and Giannotti (editors), *Ocean Engineering for OTEC.* ASME, 1979.

[Pedersen 77] Pedersen, P.T.
Comment on Statics and Dynamics of Anchoring Cables in Waves.
Journal of Hydronautics 11(4):112, October, 1977.

[Peyrot 73] Peyrot, A. H. and Goulois, A. M.
Analysis of Cable Structures.
Computer and Structures 10:805-813, 1973.

[Peyrot 80] Peyrot, A. H.
Marine Cable Structures.
Journal of Structural Division, ASCE :2391-2404, December, 1980.

[Phillips 49] Phillips, W. R.
Theoretical Analysis of Oscillation of a Towed Cable.
Technical Report 1796, NACA, 1949.

[Plunkett 76] Plunkett, R.
Static Bending Stresses in Catenaries and Drill Strings.
Journal of Engineering for Industry, ASME :31-36, February, 1976.

[Polachek 63] Polachek, H, Walton, T. S., Mejia, R. and Dawson, C.
Transient Motion of an Elastic Cable Immersed in a Fluid.
Mathematics of Computation :60-63, January, 1963.

[Poskitt 64] Poskitt, T. J.
The Free Oscillations of Suspended Cables.
The Structural Engineer 42(10), October, 1964.

[Pugsley 49] Pugsley, A. G.
On the Natural Frequencies of Suspension Chains.
Quarterly Journal of Mechanics and Applied Mathematics 2(4):412-418, 1949.

[Pugsley 68] Pugsley, A.
The Theory of Suspension Bridges.
E. Arnold Ltd., London, 1968.

[Pugsley 83] Pugsley, A.
The Nonlinear Behavior of a Suspended Cable.
Quarterly Journal of Mechanics and Applied Mathematics 36(2):157-162, 1983.

[Ramberg 75] Ramberg, S. E., Griffin, O. M. and Skop, R. A.
Some Resonant Vibration Properties of Marine Cables with Application to the Prediction of Vortex-Induced Vibrations.
In *Ocean Engineering Mechanics.* Houston, Texas, December, 1975.

[Ramberg 77] Ramberg, S. E. and Griffin, O. M.
Free Vibrations of Taut and Slack Marine Cables.
Journal of the Structural Division, ASCE 103(ST11):2079-2092, November, 1977.

[Ramberg 81] Ramberg, S. E. and Griffin, O.M.
Hydroelastic Response of Marine Cables and Risers.
In *Hydrodynamics in Ocean Engineering,* pages 1223-1245. Norwegian Institute of Technology, 1981.

[Ramberg 82] Rambert, S. E. and Bartholomew, C. L.
Vibrations of Inclined Slack Cables.
Journal of the Structural Division, ASCE 108(ST7):1662-1664, July, 1982.

[Rannie 41] Rannie, W. D.
The Failure of the Tacoma Narrows Bridge.
Technical Report, Federal Works Agency, 1941.

[Relf 17] Relf, E. F. and Powell, C. H.
Tests on Smooth and Stranded Wires Inclined to the Wind Direction and a Comparison of Results on Stranded Wires in Air and Water.
Technical Report 307, British Aeronautical Research Committee, January, 1917.

[Richard 83] Richard, K. and Anand, G. V.
Non-Linear Resonance in Strings under Narrow-Band Random Excitation.
Journal of Sound and Vibration 86(1):85-93, 1983.

[Rohrs 51] Rohrs, J. H.
On the Oscillation of a Suspension Chain.
Transactions of the Cambridge Philosophical Society 9:397-398, 1851.

[Rosenthal 80] Rosenthal, F. and Skop, R. A.
Guyed Towers under Arbitrary Loads.
Journal of Structural Division, ASCE (ST3), March, 1980.

[Rosenthal 81] Rosenthal, F.
Vibrations of Slack Cables with Discrete Masses.
Journal of Sound and Vibration 78:573-583, 1981.

[Roussel 76] Roussel, P.
Numerical Solution of Static and Dynamic Equations of Cables.
Computer Methods in Applied Mechanics and Engineering 9:65-74, 1976.

[Routh 55] Routh, E. J.
Dynamics of a System of Rigid Bodies.
Dover, New York, New York, 1955.

[Russel 78] Russel, J. J., Morgan, J. D. and Henghold, W. M.
Cable Equilibrium and Stability in Steady Wind.
Journal of Structural Division, ASCE :301-312, February, 1978.

[Samras 73] Samras, R. K., Skop, R. A. and Milburn, D. A.
An Analysis of Coupled Extensional-Torsional Oscillations of Wire Rope.
In *Winter Annual Meeting.* ASME, Detroit, Michigan, November, 1973.

[Sander 74] Sander, G. et al.
Accuracy versus Computational Efficiency in N. L. Dynamics.
Computer Methods in Applied Mechanics and Engineering 17-18:315-340, 1974.

[Sarpkaya 76] Sarpkaya, T.
Vortex Shedding and Resistance in Harmonic Flow about Smooth Stationary and Transverse Oscillating Cylinders.
Technical Report NPS69SL79011, Naval Postgraduate School, February, 1976.

[Sarpkaya 78] Sarpkaya, T.
Fluid Forces on Oscillating Cylinders.
The Journal of Waterway, Port, Coastal and Ocean Division 104(WW4), August, 1978.

[Sarpkaya 81] Sarpkaya, T. and Isaacson, M.
Mechanics of Wave Forces on Offshore Structures.
Van Nostrand Reinhold, New York, 1981.

[Saxon 53] Saxon, D. S. and Cahn, A. S. .
Modes of Vibration of Suspension Chain.
Quarterly Journal of Mechanics and Applied Mathematics 6:273-283, 1953.

[Schram 68] Schram, J. W. and Reyle, S. P.
A 3-D Dynamic Analysis of a Towed System.
Journal of Hydronautics 2(4):213-220, October, 1968.

[Sidiripoulos 79] Sidiripoulos, E and Muga, B. J.
Response Statistics of Cable Array Systems in an Ocean Environment.
In *Civil Engineering in the Oceans*, pages 309-321. ASCE, 1979.

[Simpson 66] Simpson, A.
Determination of the In-Plane Natural Frequencies of Multispan Transmission Lines by a Transfer Matrix Method.
Proceedings IEE 113(5), May, 1966.

[Simpson 72a] Simpson, A.
On the Oscillatory Motions of Translating Elastic Cables.
Journal of Sound and Vibration 20(2):177-189, 1972.

[Simpson 72b] Simpson, A.
Determination of the Natural Frequencies of Multiconductor Overhead Transmission Lines.
Journal of Sound and Vibration 20(4):417-449, 1972.

[Skop 70] Skop, R. A. and O'Hara, G. J.
The Method of Imaginary Reactions.
Marine Technology Society Journal , January-February, 1970.

[Skop 72] Skop, R.A.
A Method for the Analysis of Internally Redundant Structural Cable Arrays.
Marine Technology Society Journal 6, January-February, 1972.

[Skop 77] Skop, R. A., Griffin, O. M. and Ramberg, S. E.
Strumming Predictions for the SeaCon II Experimental Mooring.
Offshore Technology Conference (OTC 2884), 1977.

[Skop 79] Skop, R. A.
Cable Spring Constants for Guyed Tower Analysis.
Journal of the Structural Division, ASCE 105(ST7):1307-1318, 1979.

[Smith 73] Smith, C. E. and Thompson, R. S.
The Small Oscillations of a Suspended Flexible Line.
Journal of Applied Mechanics 40:624-626, 1973.

[Smith 74] Smith, C. E., Yamamoto, T. and Nath, J.
Longitudinal Vibrations in Taut Line Moorings.
Marine Technology Society Journal 8(5), June, 1974.

[Soler 70a] Soler, A. I. and Afshari, H.
On Analysis of Cable Network Vibrations using Galerkin's Method.
Journal of Applied Mechanics, Series E 37(3):606-611, September, 1970.

[Soler 70b] Soler, A. I.
Dynamic Response of Single Cables with Initial Sag.
Journal of Franklin Institute 290(4):377-387, October, 1970.

[Spanos 80] Spanos, P. T. and Chen, T. W.
Vibrations of Marine Riser Systems.
Journal of Energy Resources Technology, ASME 102:203-213, December, 1980.

[Suhara 80] Suhara, T. et al.
Behavior and Tension of Oscillating Chain in Water.
Japanese Society of Naval Architects Japan 148:89-10., 1980.

[Suhara 81] Suhara, T. et al.
Dynamic Behavior and Tension of Oscillating Mooring Chain.
Offshore Technology Conference (OTC 4053):415-418, 1981.

[Sullivan 80] Sullivan, B. J. and Batterman, S. C.
Nonlinear Static and Dynamic Deformations of Viscoelastic Cables.
Journal of the Engineering Mechanics Division, ASCE 106(EM3):543, June, 1980.

[Syed 74] Syed, A. and Shore, S.
Forced N. L. Vibrations of Sagged Cables.
In *Computational Methods in N. L. Mechanics*, pages 325-337. University of Texas, 1974.

[Tabarrok 74] Tabarrok, B., Leech, C.M. and Kim, Y.I.
On the Dynamics of an Axially Moving Beam.
Journal of the Franklin Institute 297(3):201-220, March, 1974.

[Tagata 83] Tagata, G.
A Parametrically Driven Harmonic Analysis of a Non-Linear Stretched String with Time Varying Length.
Journal of Sound and Vibration 87(3):493-511, 1983.

[Triantafyllou 80a]
Triantafyllou, M. S.
Mooring Lines
1980.
Class Notes.

[Triantafyllou 80b]
Triantafyllou, M. S. and Salter, R.
The Design of the Mooring System for a Tethered Current Water.
Technical Report, Seagrant MIT, April, 1980.

[Triantafyllou 82a]
Triantafyllou, M. S.
Preliminary Design of Mooring Systems.
Journal of Ship Research 26(1):25-35, March, 1982.

[Triantafyllou 82b]
Triantafyllou, M. S. and Bliek, A.
Dynamic Analysis of Mooring Lines Using Perturbation Techniques.
In *Proceedings OCEANS '82*, pages 496-501. Washington, D.C., September, 1982.

[Triantafyllou 82c]
Triantafyllou, M. S., Kardomateas, G. and Bliek, A.
The Statics and Dynamics of the Mooring Lines of a Guyed Tower for Design Applications.
In C. Chryssostomidis and J. J. Connor (editors), *Proceedings of BOSS '82.* Hemisphere Publishing Company, Washington, August, 1982.

[Triantafyllou 83a]
Triantafyllou, M. S. and Bliek, A.
The Dynamics of Inclined Taut and Slack Marine Cables.
Proceedings Offshore Technology Conference (OTC 4498):469-476, 1983.

[Triantafyllou 83b]
Triantafyllou, M. S., Kim, Y. C. and Bliek, A.
The Dynamics of the Mooring Legs of a Tension Leg Platform.
In *Proceedings Second Offshore Mechanics and Arctic Engineering Symposium.* Houston, Texas, January-February, 1983.

[Triantafyllou 84]
Triantafyllou, M. S.
The Dynamics of Taut Inclined Cables.
Quarterly Journal of Mechanics and Applied Mathematics , 1984.
To Appear.

[Van Oortmerssen 76]
Van Oortmerssen, G.
The Motions of Moored Ships in Waves.
Technical Report 510, N.S.M.B., Wageningen, 1976.

[Vaughan 78] Vaughan, H.
Effect of Stretch on Wavespeed in Rubberlike Materials.
Quarterly Journal of Mechanics and Applied Mathematics :215-231, 1978.

[Veletsos 82] Veletsos, A. S. and Darbre, G. R.
Free Vibrations of Parabolic Cables.
Technical Report 23, Rice University, Department of Civil Engineering, March, 1982.

[Verley 82] Verley, R. L. P.
A Simple Model of Vortex Induced Forces in Waves and Oscillatory Currents.
Applied Ocean Research (4), 1982.

[Wadsworth 82] Wadsworth, J. F. III.
A compendium of Tension Member Properties for Input to Cable Structural Analysis.
Technical Report CR82.017, Navy Civil Engineering Laboratory, April, 1982.

[Walton 59] Walton, T. S. and Polachek, H.
Calculation of Nonlinear Transient Motion of Cables.
Technical Report 1279, David Taylor Basin Report, July, 1959.

[Walton 60] Walton, T. S. and Polachek, H.
Calculation of Transient Motion of Submerged Cables.
Mathematical Tables and Aids to Computation 14:27-60, 1960.

[Walton 69] Walton, T. S. and Polachek, H.
Calculation of Transient Motion of Submerged Cables.
Mathematics of Computation 14(69):27-46, 1969.

[Watts 81] Watts, A. M. and Frith, R. H.
Efficient Numerical Solution of the Dynamic Equations of Cables.
Computer Methods in Applied Mechanics and Engineering 25:1-9, 1981.

[Webster 75] Webster, R.L.
Non-Linear Static and Dynamic Response of Underwater Cable Structures using FEM.
Offshore Technology Conference (OTC 2322):754-762, 1975.

[Webster 79] Webster, R. L.
Analysis of Deep Sea Moor and Cable Structures.
Offshore Technology Conference (OTC 3623):2299-2306, 1979.

[Webster 82a] Webster, R. L. and Palo, P. A.
Seadyn User's Manual.
Technical Report TN 1630, Navy Civil Engineering Laboratory, April, 1982.

[Webster 82b] Webster, R. L.
Seadyn Mathematical Models.
Technical Report CR82.019, Navy Civil Engineering Laboratory, April, 1982.

[Webster 82c] Webster, R. L.
Seadyn: Programmer's Reference Manual.
Technical Report CR82.018, Navy Civil Engineering Laboratory, April, 1982.

[West 68] West, H. H. and Robinson, A. R.
Continuous Method of Suspension Bridge Analysis.
Journal of the Structural Division, ASCE 94:2861-2883, December, 1968.

[West 73] West, H. H. and Caramanico, D. L.
Initial Value Discrete Suspension Bridge Analysis.
International Journal of Solids and Structures 9:1087-1105, September, 1973.

[West 75] West, H. H., Geschwindner, L. F. and Suhoski, J. E.
Natural Vibrations of Suspended Bridges.
Journal of the Structural Division, ASCE 101(ST11):2277-2291, November, 1975.

[Whitham 74] Whitham, G.B.
Linear and Non-Linear Waves.
John Wiley & Sons, New York, 1974, chapter Hyperbolic Systems.

[Wilhelmy 81] Wilhelmy, Fjeld and Schneider.
Non-Linear Response Analysis of Anchorage Systems for Deep Water Platforms.
Offshore Technology Conference (OTC 4051), 1981.

[Wilson 67] Wilson, B. W.
Elastic Characteristics of Moorings.
Journal of the Waterways and Harbors Division, ASCE 93:27-56, November, 1967.

[Winget 76] Winget, J. M. and Huston, R. L.
Cable Dynamics - A Finite Segment Approach.
Computers and Structures 6:475-489, 1976.

[Yakimov 70] Yakimov, Y. L.
Motion of a Cylinder in Arbitrary Planar Ideal Incompressible Fluid Flow.
IZV. AN SSSR, Mekhanika Zhidkosti i Gaza 5(2):202-204, March-April, 1970.
In Russian, translation Plenum Publishing Company 1972.

[Yamaguchi 79] Yamaguchi, H. and Ito, H.
Linear Theory of Free Vibrations of an Inclined Cable in Three Dimensions.
Proceedings Japanese Society of Civil Engineers (286):29-36, June, 1979.
In Japanese, Summary in English, Transactions Japanese Society of Civil Engineers 1979.